

Promotiecommissie

Promotor: Prof.dr. P.D. Verdouw

Overige leden: Prof.dr. J. Baan
Prof.dr. J.M.J. Lamers
Dr. R. van Mastrigt

Co-promotor: Dr. R. Krams

Regional mechanics and energetics of stunned myocardium in vivo
Thesis: Erasmus University Rotterdam, Rotterdam, The Netherlands

ISBN: 90-9014782-9

NUGI: 742

© S.A.I.P. Trines, 2001

Printed by Optima Grafische Communicatie, Rotterdam

Financial support by the Netherlands Heart Foundation for the publication of this thesis is gratefully acknowledged.

**Regional mechanics and energetics of
stunned myocardium in vivo**

S.A.I.P. Trines

**Regional mechanics and energetics of
stunned myocardium in vivo**

Regionale mechanica en energieverbruik van gestunned
myocardweefsel in vivo

Proefschrift

ter verkrijging van de graad van doctor
aan de Erasmus Universiteit Rotterdam
op gezag van de Rector Magnificus
Prof.dr.ir. J.H. van Bommel
en volgens besluit van het College voor Promoties

De openbare verdediging zal plaatsvinden op
woensdag 6 juni 2001 om 11:45 uur

door

Serge Alexander Ivo Petrus Trines
geboren te Eindhoven

Contents

Chapter 1	1
Introduction	
Chapter 2	31
A decreased force-frequency effect in stunned myocardium	
Chapter 3	51
Calcium handling in stunned myocardium	
Chapter 4	67
Maximization of external work and efficiency of energy transfer	
Chapter 5	89
Oxygen wastage of stunned myocardium	
Chapter 6	105
Cardiovascular profile of EMD 57033	
Chapter 7	127
EMD 57033 and Ca ²⁺ -responsiveness	
Chapter 8	143
Comparison of calcium sensitization and adrenoreceptor stimulation	
Chapter 9	159
Geometry assessment of the left ventricle	
Chapter 10	173
Discussion and summary	
Nederlandse samenvatting	181
Dankwoord	189
Curriculum Vitae	191
Publications	192

Chapter 1

Introduction

Brief myocardial ischemia

There is still some controversy about the definition of ischemia, a term originally derived from *ischo haima* (to restrain blood) (58). In this thesis, I would like to follow the definition of Robert Kloner: "Myocardial ischemia is that state in which blood flow (oxygen and substrate delivery) to the myocardium has been reduced to the point where myocardial metabolism shifts from aerobic to anaerobic and the products of anoxic metabolism accumulate in the tissue. The reduction in blood flow may be absolute, as occurs with a total coronary artery occlusion or relative, as occurs when there is an increase in oxygen demand that outweighs oxygen supply (as in the case of a coronary stenosis in the setting of exercise or rapid pacing)" (58). The reason to choose this definition lies in the fact that an absolute reduction in blood flow is not necessary for ischemia, and that it clearly defines when blood flow is inadequate. Apart from myocardial stunning, which is defined below, several other ischemic syndromes have been described. In this section I will concisely discuss ischemic preconditioning, myocardial hibernation, and silent ischemia.

In 1986, Murry et al. showed that multiple brief periods of ischemia protected canine myocardium against a longer period of ischemia, in the sense that infarct size was reduced (94). This phenomenon was called "ischemic preconditioning" and was later confirmed for a single brief period of ischemia, for a partial coronary artery occlusion, and in numerous other species (66, 142). In addition, several features of ischemic preconditioning were identified. Firstly, the brief period of ischemia ("preconditioning stimulus") has a minimum duration of 2-5 min, depending on the species and the kind of anesthetics used. Secondly, the reperfusion interval between the preconditioning period of ischemia and the preconditioned period of ischemia should be at least 90-120 s but not more than 2 h. However, if this interval is increased to 24 h, the myocardium may again become preconditioned ("second window of protection"). Thirdly, the protection of the myocardium is lost if the period of ischemia is extended to more than 90 min. Finally, preconditioning is associated with preservation of high-energy phosphates and dramatic slowing of the rate of anaerobic glycolysis, a phenomenon best explained by a reduction of the demand for energy in the preconditioned heart during the sustained episode of

ischemia (66, 142). The exact mechanism of ischemic preconditioning is not fully elucidated, but may involve opening of (mitochondrial) ATP sensitive K^+ -channels (55).

The phenomenon of myocardial hibernation is more difficult to describe. Though first used in 1978 by Diamond et al. (34), it was more clearly defined by Rahimtoola: "The relatively uncommon response to reduced myocardial blood flow at rest whereby the heart downgrades its myocardial function to the extent that blood flow and function are once again in equilibrium, and as a result, neither myocardial necrosis nor ischemic symptoms are present." (109). Therefore, in contrast to ischemia, anaerobic metabolism is absent. Although this perfusion-contraction matching has been shown to occur in animal models of partial coronary occlusion lasting several hours, until now studies on longer periods of flow reduction have always shown a severe decrease in regional function associated with an unchanged or slightly reduced blood flow, thereby revealing a perfusion-contraction mismatch (141). This suggests that myocardial hibernation may be a transient state between short-term and long-term ischemia rather than a chronic adaptation to reduced blood flow. The important difference however between myocardial stunning, as described below, and myocardial hibernation, lies in the reduction of resting blood flow in hibernating myocardium in contrast to the normal blood flow in stunned myocardium.

The final concept I would like to define is silent ischemia. It is mostly a clinical term, signifying ischemia in the absence of patient-reported complaints. If blood flow is restored or energy demand decreased, silent ischemia will develop into myocardial stunning; if blood flow remains depressed the myocardium will either become necrotic or adapt itself and become hibernating. To discriminate silent ischemia from hibernation, changes in the electrocardiogram or markers of anaerobic metabolism, for example lactate production, should be determined.

Definition of myocardial stunning

In the early 1970's, Heyndrickx et al. studied the effect of brief periods of ischemia followed by complete reperfusion in the conscious dog (62). They expected that function should recover quickly, as necrosis was not presumed after a short ischemic period. However, after an initial restoration of the electrocardiogram, coronary blood flow and mechanical function during the hyperemic phase, function deteriorated again and remained depressed during at least 6 h in the case of a 15-min occlusion (Figure 1). Only measured at 24 h of reperfusion, function was completely restored. In addition, in a second study they indeed found no evidence of necrosis in histological sections (61). This syndrome of prolonged, postischemic myocardial dysfunction was termed "stunning" by Braunwald and Kloner in 1982 (20).

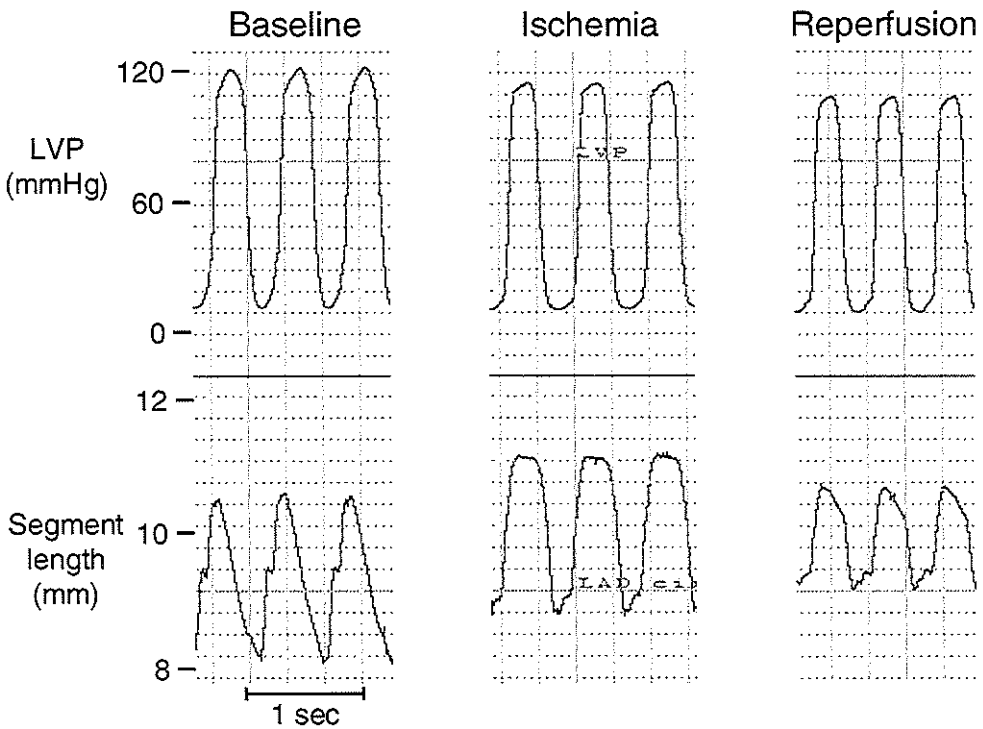


Fig. 1 Example of left ventricular pressure (LVP) and regional segment length signals during baseline, ischemia, and reperfusion (i.e. stunning). At baseline, normal contraction occurs (left panel), while during ischemia the myocardium does not contract in the systolic phase (middle panel). At reperfusion, contraction remains depressed (right panel).

In later studies, an positive relationship emerged between the time needed for recovery of mechanical function and the duration of ischemia (74). Furthermore, it was shown that the depressed function of the myocardium could be enhanced by means of inotropic drugs or postextrasystolic potentiation (38, 127). Moreover, it was shown that, although no necrosis was present, the reperfused myocardium did release creatine kinase (CK) and the specific myocardial subfraction (CK-MB) (60). Although both preconditioning and stunning are caused by a brief period of ischemia, their mechanisms are thought to be essentially different, as an ischemic period which is too short to induce stunning may already cause preconditioning, and the effect preconditioning of a preconditioning stimulus disappears after two hours of reperfusion while stunning is still undiminished (83).

In conclusion, myocardial stunning is defined as the prolonged decrease in myocardial function after a single or multiple brief periods of ischemia, followed by complete reperfusion with an intact flow reserve, i.e. a perfusion-contraction mismatch.

This decreased function occurs in the absence of necrosis, and is totally reversible. The myocardium exhibits contractile reserve, i.e. it can be stimulated by inotropic drugs, or postextrasystolic potentiation. Although necrosis is absent, myocardial enzymes are released, signifying the reversible myocardial damage.

Possible mechanisms underlying the pathogenesis of myocardial stunning

In the past, several mechanisms have been proposed for myocardial stunning, including generation of oxygen-derived free radicals, calcium overload, insufficient energy production by the mitochondria, impaired energy use by the myofibrils, impairment of sympathetic neural responsiveness and impairment of myocardial perfusion (12). Except for the first two mechanisms, all others have subsequently been refuted. Therefore, only these two hypotheses will be discussed below.

The oxyradical hypothesis

Abundant evidence is available that reactive oxygen species (for instance superoxide anion $\cdot\text{O}_2^-$, hydrogen peroxide H_2O_2 , and hydroxyl radical $\cdot\text{OH}$) play a role in the pathogenesis of myocardial stunning. In open chest dogs using spin trap α -phenyl-*N*-*tert*-butyl nitron (PBN), free radicals were detected after a 15 min coronary occlusion followed by reperfusion (17). In addition, these authors showed that pretreatment with antioxidants as superoxide dismutase plus catalase (which together catalyze the dismutation of $\cdot\text{O}_2^-$ to O_2 and H_2O), mercaptopropionyl glycine (a $\cdot\text{OH}$ scavenger) or desferrioxamine (which possibly prevents the iron-catalyzed formation of $\cdot\text{OH}$) suppressed both the formation of oxyradicals and attenuated the postischemic dysfunction, as determined by wall thickening fraction (14, 15, 18). More specifically, they showed that $\cdot\text{OH}$ radicals are present in the same model of myocardial stunning, using aromatic hydroxylation of phenylalanine (130). Other drugs that may exhibit free radical scavenging properties (prostacyclin mimetics, ACE inhibitors and ubiquinone) have also shown to attenuate stunning (36). Similar results were found in conscious dogs following 15 min of occlusion with subsequent reperfusion (121), in conscious pigs subjected to ten 2 min occlusions (131) and in isolated perfused rabbit hearts following 10 min of occlusion with successive reperfusion (160).

The exact mechanism through which reactive oxygen species depress myocardial function remains to be elucidated. Due to their highly reactive nature, oxygen radicals may attack non-specifically virtually all cellular components. For example, it has been shown that oxygen radicals may interfere with the sarcolemmal calcium ATPase (68, 69), the $\text{Na}^+/\text{Ca}^{2+}$ exchanger (110), and the Na^+/K^+ ATPase (71). In addition, oxyradicals may also cause a reduction in maximum calcium-activated force of the myofibrils (89) and sarcoplasmic reticulum dysfunction (116).

The calcium hypothesis

In 1982, Grinwald suggested the following hypothesis for calcium overload during reperfusion (54). Na^+ accumulates intracellularly during ischemia due to the energy depletion and increased influx through the Na^+/H^+ exchanger. However, because of the acidosis, $\text{Na}^+/\text{Ca}^{2+}$ exchange is inhibited. Upon reperfusion, the acidosis is rapidly reversed, while intracellular Na^+ is still high due to the sustained Na^+/H^+ exchange, leading to a reversed $\text{Na}^+/\text{Ca}^{2+}$ exchange and concomitant calcium overload. Later studies showed that decreasing calcium content of the perfusion fluid reduced stunning in isolated ferret hearts (81) and that transient calcium overload without ischemia caused a contractile dysfunction similar to stunning (73). Moreover, if acidosis was extended by perfusing the heart with an acidic solution, stunning was attenuated as well (72). Two years later, Pike et al. showed using $^{23}\text{Na}^+$ -NMR measurements, that indeed intracellular Na^+ remained elevated until 8-10 min after the beginning of reperfusion (107), while acidosis has been shown to resolve within 30 s of reflow (81). Furthermore, also the increased calcium concentration during reperfusion has been confirmed experimentally (26). Finally, pretreatment with calcium channel blockers may attenuate stunning (144).

If it seems reasonable to conclude that an increased intracellular calcium concentration during reperfusion is involved, the question arises by which mechanism this increased calcium undermines contractile function. There exists some evidence that the increased calcium concentration activates calpain-I, a calcium dependent protease. Calpain-I can proteolyze myofibrillar proteins (33), L-type calcium channels (115) and the skeletal SR calcium release channel (124). Calpain-I is activated by calcium concentrations of 2-75 μM (90), while the elevated calcium during reperfusion may reach these concentrations (26). Indeed, Urthaler et al. showed that the specific calpain inhibitor MDL 28170 could attenuate stunning in isolated ferret hearts (139), and Papp et al. showed that both ischemia/reperfusion and calpain-I caused similar degradation of desmin, a cytoskeletal protein (104), while Yoshida et al. showed caldesmon proteolysis in stunning which could be attenuated by calpain inhibitor I (157). However, in pilot experiments carried out in our laboratory, we could not detect any attenuating effect of MDL 28170 on the degree of stunning in vivo, following a single 15 min occlusion in open-chest pigs (unpublished data). In conclusion, definite evidence regarding the activation of calpain during the development of myocardial stunning in vivo is still lacking.

As described above, oxyradicals may cause dysfunction of sarcolemmal calcium channels and transporters and impair calcium transport of the sarcoplasmic reticulum. In addition, it has been shown that exposure of the heart to exogenous oxyradicals without ischemia produces calcium overload (28). This may be a second mechanism through which increased calcium influx during reperfusion may occur, synergistically acting with

the first. Therefore, the oxyradical hypothesis and the calcium hypothesis may be two sides of the same pathway, in which calcium plays a central role (16).

Localization of the culprit underlying the decreased contractile function

As mentioned above, either oxyradicals or calcium-dependent proteolysis can affect both calcium cycling proteins and myofibrillar proteins. But to what extent this actually takes place remains uncertain. For instance, in rat hearts it has been shown that the myofibrillar component troponin-I experiences proteolytic degradation (47). However, other laboratories (including ours, see chapter 3) found no detectable troponin-I degradation in porcine and canine myocardium which experienced myocardial dysfunction due to stunning (88, 123, 136). With respect to the mechanisms of calcium cycling, to the best of our knowledge no stunning-induced lysis of proteins underlying calcium cycling (sarcolemmal Ca^{2+} channel, $\text{Na}^+/\text{Ca}^{2+}$ exchanger and Ca^{2+} -ATPase, sarcoplasmic reticulum Ca^{2+} release channel, Ca^{2+} -ATPase, and phospholamban), has been shown until now. Regarding the ultrastructure of the myocyte, degradation of desmin (104), caldesmon (157), and ankyrin (156) has been detected.

With respect to the functional changes of stunned myocardium, both a decreased and unchanged calcium sensitivity of the myofibrillar apparatus have been shown (26, 35, 46, 50, 81). A decreased calcium sensitivity would cause the myofibrils to generate less force at any level of systolic calcium and may therefore very well explain the contractile dysfunction. Similarly, sarcoplasmic reticulum (SR) calcium uptake has been found to be decreased (29, 44, 78, 79, 86, 140, 153, 154), as well as unchanged (1, 70, 87, 92, 111, 158) or even slightly increased (84). A defect in the calcium release channel has also been described (140). It seems evident that SR dysfunction may cause a decrease in systolic calcium, which will also decrease contractile function. However, calcium transients have found to be unchanged in rat and ferret hearts (46, 80). Therefore, also changes in calcium cycling have not definitely been proven. Finally, degradation of cytoskeletal proteins is thought to cause fragility of the myocyte structure during force production. This has been detected in calpain-treated cells, which showed desmin degradation similar to degradation after ischemia and reperfusion (104). In conclusion, the exact mechanism(s) through which oxyradicals and/or calcium overload induce the dysfunction of the myocyte during stunning remain to be elucidated.

Myocardial stunning as an in vivo phenomenon

Although myocardial stunning has been studied extensively in in vitro preparations from numerous species, in this thesis we chose to study swine, as their coronary anatomy is similar to the human anatomy (relative absence of collaterals), and to restrict ourselves to the in vivo situation. A couple of reasons can be given to use an in vivo instead of an in

vitro model of stunning. At first, one of the most important parts of the definition of stunning is the full reversibility of the syndrome. In *in vitro* preparations, periods of ischemia lasting more than 5 min cause mechanical dysfunction longer than the preparation remains intact (3–4 h at most) (108). Therefore, the reversibility of the symptoms can never be proven, although the exclusion of necrosis and ultrastructural defects have been used as an alternative (98).

Secondly, most *in vitro* preparations apply global instead of regional ischemia. During global ischemia, developed pressure or tension drops to zero and the non-contracting tissue will not be stretched. This is in contrast to the *in vivo* situation, since in regional ischemia *in vivo* the ischemic myocardium is always stretched by the surrounding, contracting myocardium. This is important, as it has been shown that non-contracting myocardium has a much larger oxygen demand when it is stretched (48). Of course, also in the *in vitro* situation myocardium can be stunned regionally. However, even then, developed pressure (and therefore stretch of the ischemic segment) is not very well maintained, at approximately 40% of the baseline situation (30). Consequently, regionally stunned myocardium undergoes a larger ischemic burden than globally stunned hearts or muscle strips.

Thirdly, many isolated preparations are buffer-perfused. Due to the high flow rates necessary to maintain oxygenation of isolated hearts ($\pm 16 \text{ ml}\cdot\text{min}^{-1}\cdot\text{g}^{-1}$) and due to the low colloid osmotic pressure of the buffer, edema occurs, which causes the preparation to deteriorate over time (145, 146). This deterioration in function makes it difficult to separate the effect of the induction of stunning from the instability of the preparation. In addition to this, isolated muscle strips are usually not subjected to ischemia but to hypoxia (108). However, hypoxia still permits the tissue to exchange ions, proteins, and metabolites with its surroundings, making hypoxia essentially different from ischemia.

Finally, setting up the isolated heart or tissue model causes a time interval between removing the heart from the animal and fixation in the perfusion system. Since it has been shown that ATP and creatine phosphate start to decline within seconds after the heart is removed from the animal, and a period of 15 to 30 min after re-establishment of perfusion is usually necessary for stabilization and weaning of the hyperemia, the ischemia during the interval needed for the experimental setup might already cause some degree of stunning or preconditioning (143). Therefore, the duration of this time interval and the duration of the stabilization period could influence the outcome of such studies.

To sum up, although *in vitro* stunned myocardium may possess similar properties as *in vivo* stunned myocardium (108), because of the above-mentioned limitations it is preferable to study *in vivo* stunned myocardium.

Measurement of regional myocardial function in vivo

As discussed above, myocardial stunning is a syndrome preferably studied in the in vivo situation. This preamble causes several problems, however. It goes without saying that the experimental animal will not survive global left ventricular ischemia for more than a few minutes. Moreover, regional ischemia, rather than global ischemia, resembles best the clinical situation. Therefore, regional ischemia followed by regional myocardial stunning is usually applied in the in vivo situation. Because regional stunning causes the left ventricle to become heterogeneous, global parameters of left ventricular function will not adequately describe the function of the stunned myocardium. As a consequence, regional myocardial function has to be determined. In the past, segment length shortening and wall thickening were used to quantify regional function (61, 62, 129). However, as these parameters are regional variants on ejection fraction, they are highly load-dependent (4). Therefore, in analogy to the end-systolic pressure-volume relationship, Aversano et al. developed and validated end-systolic pressure-regional segment length and end-systolic pressure-regional wall thickness relations using ultrasound crystals (4, 5). The slope of these relations, the end-systolic elastance (E_{es}), is a measure of regional contractility. They showed that these relations could be determined without detectable baroreceptor reflexes and that both positive and negative inotropic interventions were reflected, while changes in loading condition were not.

However, although the area within the pressure-regional segment length loop was taken as a measure of regional work, it does not adequately reflect units of work (J), but work per surface area ($1 \text{ mmHg}\cdot\text{mm} = 1.333\cdot 10^{-4} \text{ J/mm}^2$). To overcome this problem, the group of Suga developed the wall tension-regional area relations (53). In this approach, wall tension was calculated from left ventricular pressure and anterior-posterior diameter, while area was determined from two perpendicularly oriented pairs of ultrasound crystals. The advantages of this approach are that the area within the tension-area loop adequately reflects units of work. Moreover, decreases in curvature of the region under study are taken into account, and by studying regional area instead of regional length, the position of the ultrasound crystals in relation to the transversal fiber direction becomes less crucial. Subsequently, they validated that in a heart with regional ischemia, integrated work from tension-area relations in the non-ischemic and ischemic regions together corresponded well to total left ventricular work (52). Therefore, the fact that a single diameter was applied to calculate work in different regions did not impair this calculation.

When we started to apply this approach, we encountered several limitations. First, since we have shown that different regions in the left ventricle influence each other, especially after induction of heterogeneity due to regional interventions (43), the need for a measure of regional afterload became clear. As end-systolic tension is a measure of global afterload, it did not meet this requirement. Secondly, because tension is force per

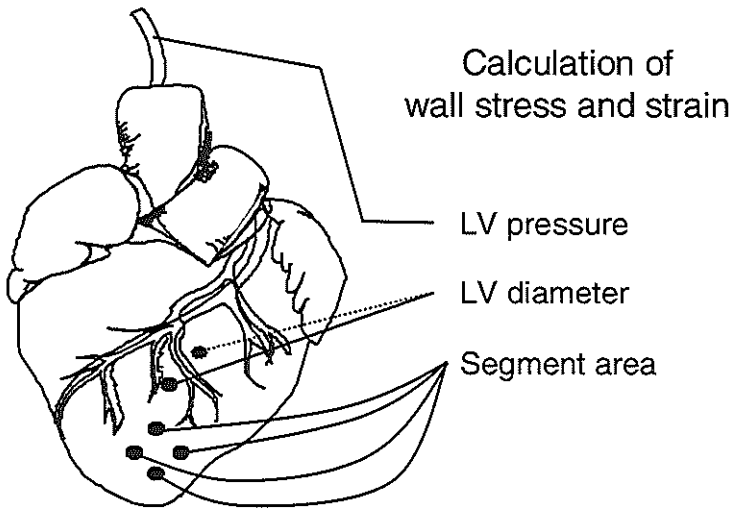


Fig. 2 Determination of regional wall stress and strain in the perfusion area of the left anterior descending coronary artery (LADCA). In addition, regional myocardial volume was measured at the end of the experiment.

length, wall thickness was not taken into account. Thirdly, in our data the relations appeared to be highly curvilinear in nature. While this has been reported for pressure-volume relations as well (22), it poses the difficulty of expressing contractility with a single number. Finally, large regional differences existed in contractility within the left ventricle. As the regional area depends on the individual distance between the regional area crystals, it was normalized. However, this did not eliminate these regional differences.

In an attempt to overcome these limitations at least partly, we adapted the tension-area approach using a single diameter and regional area measurements to regional midwall stress-strain relations. Using an adaptation from Laplace's law, we assumed a regional concentric spherical geometry, regional homogeneity of wall thickness, zero epicardial pressure (which is actually the case in open-chest animals), a constant stress from endocardium to epicardium and both a constant regional wall volume and a constant and equal number of muscle fibers in both transversal and longitudinal directions during the cardiac cycle. In the appendix to chapter 1, this approach has been described, while Figure 2 gives a graphical description.

We used global LV pressure in the calculation of regional stress, since pressure is equal for the whole left ventricle. We placed one pair of crystals in the left anterior descending coronary artery (LADCA) perfused region, the region which was subsequently occluded to produce stunning, and one pair in the left circumflex coronary artery (LCXCA) perfused region, the "control" region. Regional wall thickness as a

function of time was calculated from these regional area changes, and global transversal curvature was derived from the anterior-posterior diameter, assessed by a set of ultrasound crystals. As wall thickness was used in the calculation of stress and end-systolic stress is a measure of regional afterload, we assumed to have overcome the first two limitations. Because the end-systolic tension-area relations were usually concave to the area-axis, we expected the stress-strain relations to be less curvilinear, as strain was calculated from the square root of area. Finally, we hypothesized that overcoming the first three limitations would also decrease the regional differences in normal myocardium. Figure 3 shows a graphical description of the determination of regional stress-strain relationships.

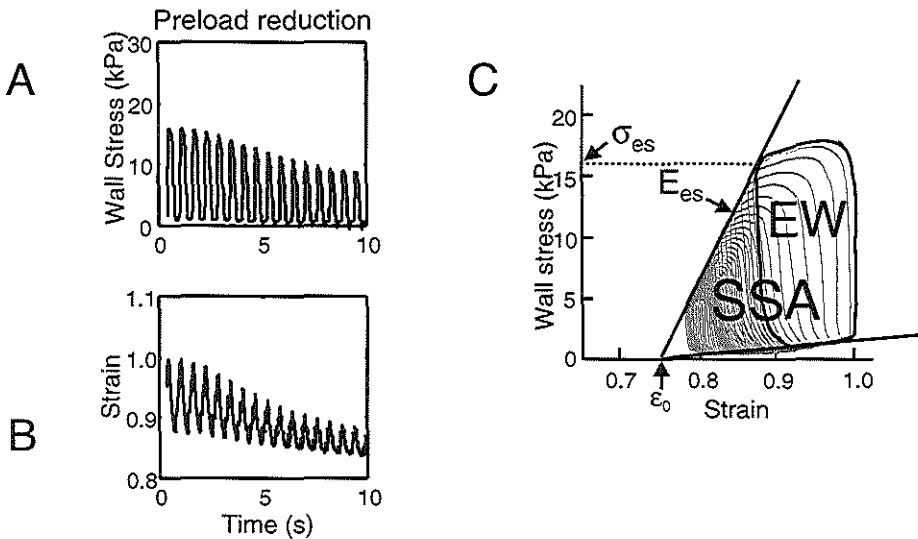


Fig. 3 Determination of regional stress-strain relationships. Reduction in left ventricular preload induces reductions in regional myocardial wall stress (A) and regional strain (B). After relating myocardial strain to myocardial stress during the reduction in preload, regional stress-strain relationships may be evaluated (C). σ_{es} , end-systolic stress; E_{es} , end-systolic elastance, the slope of the end-systolic stress-strain relationship; ϵ_0 , strain at zero stress; EW, external work; SSA, stress-strain area.

Measurement of regional myocardial energetics

Apart from the end-systolic elastance (E_{es} , Figure 3), which is a measure of regional myocardial contractility, two important energetic output parameters can be determined from the regional stress-strain relationship; total myocardial work (stress-strain area, SSA) and external work (EW). SSA is calculated in analogy to the pressure-volume area as the area between the end-diastolic and end-systolic stress-strain relations and the systolic trajectory of the stress-strain loop (Figure 3) (117). In our approach, SSA reflects regional myocardial work per unit of volume ($\text{kPa} = 10^3 \text{ N/m}^2 = \text{kJ/m}^3$). EW is the area within the regional stress-strain loop and reflects the part of the myocardial work which is performed onto the arterial system (Figure 3) (117). The difference between total work (SSA) and external work (EW) is the potential energy (PE), the internal work of the heart. Since the internal work is not actually performed due to closure of the aortic valve, this work is converted into heat (117). The percentage of external work over total work is called the efficiency of energy transfer ($\text{EET} = \text{EW}/\text{SSA} \cdot 100\%$).

As energetic input parameter, we chose to measure myocardial oxygen consumption (MVO_2). MVO_2 was calculated as the product of coronary (LADCA) blood flow and the arterial-venous oxygen difference. The venous blood samples were taken from the great cardiac vein, as it has been shown that this vein drains specifically from the LADCA perfusion area (10). As long as metabolism is aerobic, 1 ml of consumed O_2 equals approximately 20 J of consumed energy, relatively independent of the substrate (117). Although an existing anaerobic metabolism of stunned myocardium has been denied by several studies (51), a decreased efficiency of the mitochondria could also invalidate this assumption. This might interfere with our results, because we did not directly measure ATP production. However, it has been shown that the efficiency of the mitochondrial ATP production is undiminished in stunned myocardium (159). We therefore assumed that MVO_2 adequately reflects energy consumption, both in normal and in stunned myocardium.

Limitations of in vivo measurements

Although we state that myocardial stunning should be studied in the in vivo situation, several limitations are attached to this. Firstly, the direct measurement of intracellular processes is very limited. Therefore, derived parameters of these processes have to be applied. Consequently, the interpretation of these indirectly obtained functional parameters is complicated. Secondly, an intact animal needs anesthesia. In our model we used pentobarbital sodium, which is known to decrease contractility and to suppress baroreceptor reflexes (96, 125). While the latter may be an advantage during determination of stress-strain relations, due to the effect on contractility the need for

careful titration of pentobarbital is evident. However, as the need for pentobarbital may vary between animals, fixed doses can usually not be applied. Thirdly, variations in loading conditions exist between different animals and these loading conditions change within an animal due to inotropic interventions. Although the load-independence of E_{es} overcomes this problem, energetic parameters for example are highly load-dependent. Furthermore, since online calculation of E_{es} was not available during the course of the experiments, we depended on load-dependent parameters as mean arterial pressure and maximum rate of left ventricular pressure rise to assess contractile state. Finally, different regions within the myocardium may influence each other, especially as heterogeneity increases due to regional interventions (43). Because of this, loading conditions may vary between different regions of the heart, emphasizing the need for regional parameters to express loading. Differences in regional loading may still cause differences in regional energetics, however.

Treatment of myocardial stunning

Apart from prevention of stunning with antioxidant therapy (see the oxyradical hypothesis above) or with attenuation of ischemia using ACE inhibitors or calcium antagonists (36), stunning can be treated symptomatically. As mentioned in the first paragraph, stunning exhibits an inotropic reserve, i.e. it can be stimulated by different inotropic interventions (38, 127). In general, two mechanisms of inotropic interventions can be identified, increasing intracellular systolic calcium and increasing the sensitivity of the myofibrils to systolic calcium (40). Pharmacological increases in intracellular systolic calcium are usually obtained by β -adrenergic stimulation. Although increasing systolic calcium restores function in stunned myocardium (127), it also increases myocardial oxygen consumption needed for calcium cycling. Since, by definition, blood flow is restored, in theory sufficient additional oxygen should be available to prevent ischemia. Although some evidence is available that beta-adrenergic stimulation for 30-60 min indeed has no deleterious effects on stunned myocardium (7, 19), another study detected increased depletion of ATP and increased mitochondrial damage after stimulation by isoproterenol during 2 h (148). Moreover, stunning in patients is usually accompanied by hibernation and silent ischemia (97), rendering the use of drugs which increase oxygen consumption less preferable. In addition, beta-adrenergic drugs increase the occurrence of arrhythmias (85), preventing application outside the hospital, which for example could be useful in patients with angina-induced stunning.

To bypass these adverse effects, drugs developed to increase the sensitivity of the myofibrils to calcium, the so-called calcium sensitizers, seem more suitable (40). Although originally developed to treat cardiac failure, these drugs became interesting for stunning research because a decreased myofibrillar calcium sensitivity was detected in

stunned myocardium (26, 46). Whether this decreased calcium sensitivity is also present in humans remains to be elucidated, but as long as these drugs do not increase calcium cycling, they will not increase oxygen consumption for excitation-contraction coupling, and therefore have an energetic advantage over beta-adrenergic drugs. However, it needs to be kept in mind that enhancement of sensitivity of the myofibrils to calcium may increase myofibrillar cross-bridge cycling, which will inevitably increase oxygen consumption as well. Therefore, calcium sensitizers acting on the interaction between actin and myosin may be of particular interest, as it has been suggested that these drugs may slow down the dissociation of the actin-myosin cross-bridges or increase their force rather than increase the number of cross-bridges formed, which might increase force without additional energy consumption (135). A possible drawback of calcium sensitizers is their effect on diastolic function, as relaxation may be delayed due to the activation of the myofibrils at lower calcium concentrations (40, 76, 128). However, this diastolic dysfunction usually occurs at higher doses, while it has been shown that a lower dose even improves diastolic function (64). In conclusion, calcium sensitizers are potentially interesting in the treatment of myocardial stunning.

Clinical manifestations of myocardial stunning

In the clinical situation, stunning is likely to occur during reperfusion of the myocardium after a period of ischemia, which is short enough to prevent necrosis. This episode of ischemia can be absolute, e.g. after an attack of angina or after nontransmural myocardial infarction, or relative, e.g. after exercise which increases the oxygen demand above the level of maximum supply. The main problem in detecting myocardial stunning in the clinical situation is the differentiation between silent ischemia, hibernation and stunning, especially as they may often coexist in the same patient (97). This difficulty can only be overcome by measuring regional perfusion. As described in the first part of this Introduction, a normal perfusion points to stunned myocardium (i.e. a perfusion-contraction mismatch), while a reduced perfusion points to silent ischemia or hibernation (a perfusion-contraction match) (13). Since methods to assess regional perfusion became recently more widely available, the occurrence of stunning is more easily detected (2, 27, 49, 97, 106, 133). In addition, the increase in myocardial salvage due to the increase in successful restoration of coronary patency after myocardial infarction has also raised the prevalence of myocardial stunning (150).

Stunning following angioplasty

Usually, ischemia due to PTCA is too short to induce persistent systolic dysfunction (usually smaller than 2 min) (122). However, Wijns et al. showed that restoration of regional diastolic function was delayed after PTCA using 3-10 inflations, at a time that

systolic function had been restored (151). This suggests that diastolic function is more sensitive to brief periods of ischemia. However, another study showed that no decrease in global diastolic function was present after a single balloon inflation (82). Although the difference between these two studies may be explained by the application of a single versus multiple occlusions and the measurement of global versus regional function, Dupouy et al. confirmed the decrease in global left ventricular diastolic function after three 120 s balloon inflations (37). Therefore, although silent ischemia due to residual stenosis cannot be completely excluded, it seems likely that the decreased diastolic function compared to pre-inflation values is caused by some degree of myocardial stunning.

Exercise-induced stunning

Using bicycle exercise in patients with a history of stable angina pectoris, positive angiograms and no contractile abnormalities at rest, Ambrosio et al. showed that contractile abnormalities appeared during exercise, which were still present at 30 min and disappeared between 60 and 120 min of recovery (2). In contrast, no perfusion defects were detected at 30 min using technetium-99m sestamibi perfusion imaging. Another study showed that dobutamine stress also caused contractile dysfunction, similar to exercise (6). These findings underline that myocardial stunning may occur in patients with stable angina during exercise.

Stunning following unstable angina

Although unstable angina is possibly the clinical syndrome that meets the definition of myocardial stunning best (brief periods of severe ischemia, complete reperfusion, no necrosis), the problem of detecting myocardial stunning in unstable angina lies in the wide variety in severity of unstable angina and the differentiation from silent ischemia. However, a recent study in patients admitted to the coronary care unit for symptoms of unstable angina (class 2-3), showed persistence of regional dysfunction with normal myocardial blood flow and oxygen consumption following successful revascularization of the culprit lesion, thereby excluding hibernation and silent ischemia (49). Although the study population was limited (n=14) this study clearly suggests that myocardial stunning may occur after unstable angina.

Stunning in ischemic cardiomyopathy

In a group of 54 patients with angina or heart failure, but without unstable angina or recent acute myocardial infarction, Narula et al. showed that, based on gated single-photon emission tomography, from the 584 regional segments showing dysfunction, 22% was scarred, 30% was remodeled (perfusion-contraction mismatch without ischemia after dobutamine stress) 24% was hibernating and 23% was stunned (97). The lack of recently

recorded, major ischemic events implies the presence of unrecorded, minor ischemic events. Considering that the stunned regions showed ischemia after dobutamine stress, suggesting the absence of coronary flow reserve, these minor events may have taken place repetitively during daily life activities. Therefore, the dysfunction may very well be caused by repetitive stunning (see below). In another study using positron emission tomography, the existence of stunned myocardium without recent cardiac events was confirmed (133).

Stunning following acute myocardial infarction with early reperfusion

As reperfusion therapy is presently more successfully applied after myocardial infarction, more tissue is salvaged and may therefore become stunned. In 1990, Pierard et al. showed that regional function 7-9 days after myocardial infarction improved with dobutamine when perfusion with positron emission tomography was normal, improved less when perfusion was decreased and did not improve when perfusion was absent (106). In addition, only the group with normal perfusion showed late recovery of function after 9 months, thereby excluding the possibility that the late recovery of function was due to remodeling of the infarcted segment. Most likely, this group of patients exhibited myocardial stunning. Similar results were found with tissue plasminogen activator (3, 105, 138) and with direct PTCA (120). Moreover, in a group of patients of which some did not even receive reperfusion therapy, stunning could be predicted by comparing global left ventricular function with infarct size as determined by technetium-99m sestamibi perfusion imaging (27). Because this type of imaging differentiates between infarcted and stunned tissue, a mismatch between infarct size and function predicted the extent of the stunned myocardium and therefore the recovery of function.

Stunning following cardiac surgery

As the heart is exposed to global ischemia during aortic cross-clamping and subsequent reperfusion, stunning is likely to occur in cardiac surgery. To test this hypothesis, Breisblatt et al. studied LV global ejection fraction in 24 patients. In 23 patients ejection fraction decreased from an average of 58% to 37% at 4 h after surgery, and recovered completely within 24 to 48 h (21). Although perfusion was not determined, the occurrence of transient cardiac dysfunction after surgery makes the event of stunning likely. Moreover, since patients generally receive inotropic and/or afterload-reducing therapy in the post-operative period and have markedly elevated plasma catecholamines (113), the extent of stunning may even be underestimated.

Stunning in cardiac transplantation

Although a transplanted heart is always subjected to ischemia and reperfusion, the evidence regarding stunning in cardiac transplantation is scarce (11). In a recent study it

was shown that the type of preservation solution determined the amount of vasodilator and catecholamine therapy needed post-operatively (152). The authors suggested that the necessity for increased therapy in Celsior-preserved hearts suggested myocardial stunning. However, although stunning of transplanted hearts seems likely as ischemia is a certainty, it remains to be elucidated whether or not the ischemic burden is high enough to produce stunning.

Stunning after successful resuscitation

As homeostasis is impaired considerably in resuscitation (e.g. acidosis, high levels of catecholamines), the occurrence of stunning is difficult to ascertain. However, a severe depression of left ventricular function (ejection fraction below 30%) has been documented in three patients (32). This depression, which was initially diagnosed as idiopathic dilated cardiomyopathy, completely recovered within 2 weeks. Therefore, also cardiac arrest seems a possible cause for myocardial stunning.

Neurogenic stunned myocardium

Several case reports and a single study have been published regarding neurogenically-induced stunning. In a study of 12 patients, ST segment elevation and reversible wall motion abnormalities were described after subarachnoidal hemorrhage, while coronary angiograms were normal (75). Regional function was significantly improved after three weeks. Case reports described stunning after cerebral infarction (147), subdural hematoma (101), and an increase in sympathetic cardiovascular tone in Guillain-Barré syndrome (8). The mechanism of the neurogenic cause of stunning remains unclear, although a direct toxic effect of norepinephrine has been suggested (8, 75).

Hibernation versus repetitive stunning

By definition, stunning and hibernation are two different entities. Stunning occurs after a single or multiple brief periods of ischemia followed by reperfusion, while hibernation is the adaptation of the myocardium to chronically low blood flow. In the past, myocardial blood flow could often not be determined in patients, and chronic myocardial dysfunction which recovered after successful revascularization was usually diagnosed as hibernation. However, as mentioned above, stunning may take place following exercise in patients with stable angina and in patients without recent ischemic events (2, 97). Because exercise-induced attacks may often take place in these patients, stunning may occur repetitively. It is known that repetitive episodes of ischemia may lead to more profound and persistent postischemic dysfunction than a single episode of ischemia, if the interval between the episodes is long enough to prevent ischemic preconditioning (112). Additionally, it has recently been shown in a group of 30 patients

with hibernating myocardium that resting blood flow did not improve after revascularization, while coronary flow reserve improved greatly together with contractile function (23). The authors therefore suggested that a reduced coronary flow reserve rather than reduced resting blood flow may underlie chronic myocardial dysfunction. As, by definition, chronic dysfunction due to repetitive episodes of stunning with normal resting blood flow cannot be designated as hibernation, some of the cases of chronic dysfunction diagnosed as hibernation without measuring myocardial blood flow may actually be caused by repetitive stunning.

But misdiagnoses are not the only link between hibernation and repetitive stunning. A recent study with chronically instrumented pigs showed that a stenosis, which did not decrease resting blood flow, caused contractile dysfunction with normal resting flow after 1-2 months (i.e. stunning), while after three months resting flow was decreased (i.e. hibernation) (41). This temporal progression from chronic stunning to chronic hibernation in animals instrumented with a chronic flow-reserve reducing stenosis has recently been confirmed (24, 25, 45, 126). Moreover, although myocardial blood flow is reduced in human hibernating myocardium, this reduction is much less than that induced in animal models of short-term hibernation (25). More evidence against the hypothesis that hibernation is an adaptation to depressed blood flow comes from Elsasser et al, who showed that a chronically decreased blood flow in human myocardium will eventually lead to necrosis and apoptosis of the myocytes, demonstrating that hibernating myocardium is not adequately adapted to chronic underperfusion (39). Therefore, it seems likely that hibernation is not a simple adaptation to severely reduced blood flow, but may actually be the adaptive state that results from the injury-repair cycles associated with chronic myocardial stunning (23, 25). In this light, early revascularization of hibernating myocardium is warranted to prevent irreversible damage.

Importance of clinical manifestations of myocardial stunning

Among all of the clinical situations discussed above, acute myocardial infarction and cardiac surgery are the two situations in which stunning will have the most impact (11). In cardiac surgery, the whole heart may become stunned and left ventricular function may be severely impaired. However, stunning usually does not cause problems in cardiac surgery, except in patients with depressed baseline LV function, long aortic clamping time, repeated cardiac surgery, unstable angina, left main coronary disease, or concomitant valve replacement. In these situations stunning can have a major negative impact on prognosis. Although in many other cases of cardiac surgery prognosis is not impaired, stunning may still prolong the duration of the intensive care unit stay. Similar to cardiac surgery most patients with acute myocardial infarction, except the ones with significant co-morbidity, tolerate stunning well. Stunning may have significant

consequences in myocardial infarction, since the myocardial dysfunction caused by stunning is superimposed on the dysfunction caused by the infarction (11).

Apart from the influence of stunning on the clinical outcome, accurate diagnosis of stunning is clinically important. If myocardial stunning can be diagnosed adequately, reperfusion therapy can be applied with greater accuracy (11). The detection of stunned (and therefore viable) myocardium may help to decide whether or not to perform angioplasty or cardiac surgery. Even differentiating stunned from hibernating myocardium can be useful, although both are viable. Stunned myocardium can be stimulated with inotropics to treat severely impaired left ventricular function, while hibernation myocardium will show an initial response with inotropics, but will eventually deteriorate due to the increased ischemia (11). In addition, after acute myocardial infarction with impaired left ventricular function, the differentiation of stunning from necrosis may help to decide whether or not to continue aggressive life-supporting therapy. Finally, diagnosis of stunning following successful thrombolysis will help to predict the recovery of function more adequately, as stunning may take days to weeks to improve completely.

In conclusion, myocardial stunning is a common phenomenon in the clinical situation, diagnosis assists in decisions regarding both prognosis and therapy, and it may have severe impact on the clinical outcome.

Aims of the thesis

Chapter 2 and 3: Calcium cycling in stunned myocardium

In these chapters we will concentrate on a reduced calcium cycling as a possible cause for myocardial stunning. Due to the unchanged calcium transients found in stunned ferret and rat hearts in the past (46, 80), calcium cycling was generally considered to be unaffected by myocardial stunning. However, the calcium transients were measured at heart rates below physiological levels for these animals. As it is known that calcium transients increase with higher heart rates, the so-called “force-frequency effect”, stunning-induced decreases in calcium transients as reported in these studies may have been masked by the low heart rate. A decrease in the force-frequency effect in stunned myocardium has been shown before, but in atrial tissue (65), or applying load-dependent parameters (118). Therefore, in chapter 2 we will study the force-frequency effect before and after induction of myocardial stunning using end-systolic elastance (E_{es}), which is load-independent. In addition, since the central role of the sarcoplasmic reticulum calcium ATPase (SERCA2)-phospholamban interaction in the force-frequency effect was recently postulated (67, 93), we will also modulate this interaction before and after induction of stunning with dobutamine, which induces Ser¹⁶ phosphorylation of

phospholamban (56). We expect that a stunning-induced change in this interaction will be reflected in a different effect on the force-frequency effect before and after stunning.

In chapter 3 we will study the force-frequency effect of stunned myocardium in more detail. We ascribed the absence of the force-frequency effect in the previous chapter to changes in calcium cycling. However, the influence of a possibly decreased myofibrillar calcium sensitivity on the force-frequency effect could not be excluded. Therefore, in this chapter we will infuse the calcium sensitizer EMD 57033 after induction of myocardial stunning, and test the effect on the abolished force-frequency effect. Secondly, to distinguish between disturbances in SL Ca^{2+} fluxes and processes located in the interior of the cell, i.e. Ca^{2+} -induced Ca^{2+} -release (CICR), or SR Ca^{2+} -ATPase (SERCA2) function, we will also study the relationship between recirculation fraction (RF) and HR. The RF is a measure of the relative contribution of the internal Ca^{2+} cycling to total Ca^{2+} -cycling, and can be calculated from the exponential decay of contractility following a sudden decrease in stimulation frequency (57, 134, 149). A decreased RF in stunning will imply more directly a disturbed Ca^{2+} -handling located downstream of the SL. In addition, we will measure homogenate SR Ca^{2+} -uptake and phospholamban phosphorylation at Ser¹⁶ and Thr¹⁷ of the stunned and control region at two different heart rates. A heart rate-dependent inhibition of Ca^{2+} -uptake and/or phospholamban phosphorylation will provide strong evidence for a disturbance in the phospholamban regulation of SERCA2. Finally, we will infuse ryanodine, in a concentration known to partially open the SR Ca^{2+} -release channel (ryanodine receptor, RyR). If stunned myocardium exhibits a decreased opening of the RyR, as has been reported before (140), ryanodine should be able to partially counteract the stunning-induced changes.

Chapter 4: Maximization of external work and efficiency of energy transfer

In the past, it has been shown that myocardial stunning decreases both regional external work (EW) and efficiency of energy transfer (EET) (77, 155). Because these parameters are highly load-dependent, several studies have addressed the relationship between power, EW or EET and afterload in normal hearts and have found a maximum in power (95, 137), but not in EET (31). To the best of our knowledge, it is presently unknown whether relationships involving EW, EET and afterload display maxima in normal regional myocardium and whether regional myocardium operates at one of these maxima. In addition, as impairment of global left ventricular function causes the ventricle to deviate from the optimal situation (63, 99), we have shown in earlier work that, after myocardial stunning, both regional EW and regional EET decreased more than before stunning, when end-systolic pressure was increased (42). In view of the above-mentioned maxima in EW and EET, our previous findings may be explained either on the basis of a shift of these maxima to the left, or on a change of shape of the EW and EET

relationships. Therefore, in this chapter we will evaluate relationships of EW and EET versus regional afterload before and after producing regional myocardial stunning. In addition, we will study whether the myocardium operates at one of these maxima, and whether stunning influences this situation.

Chapter 5: Oxygen wastage of stunned myocardium

As discussed above, stunned myocardium displays decreased contractile function in combination with an unchanged oxygen consumption (oxygen wastage). In addition, unchanged calcium transients were found as well (26, 46). Since most of the VO_2 for excitation-contraction coupling is consumed by the SR Ca^{2+} -ATPase (132), unchanged calcium transients suggest an unchanged VO_2 for excitation-contraction coupling. Together with the decreased contractility, the unchanged VO_2 will cause an increased oxygen cost of contractility. This has indeed been shown in stunned dog hearts (100). Since VO_2 for excitation-contraction coupling comprises only 20-30% of total MVO_2 (103) and total MVO_2 is also unchanged by stunning, it seems likely that myofibrillar efficiency is decreased as well. However, studies on this efficiency are equivocal (100, 119). Moreover, as these studies were performed in isolated hearts lacking normal working conditions, the individual contribution of an increased oxygen cost of contractility and a decreased myofibrillar efficiency could not be determined. Therefore, in this chapter we will study both oxygen cost of contractility and myofibrillar efficiency in stunned myocardium *in vivo*, and calculate their relative contribution to the oxygen wastage. In addition, because calcium sensitizers are known to decrease oxygen cost of contractility (91, 102) and may even increase myofibrillar efficiency (135), we will test whether EMD 60263, a calcium sensitizer without phosphodiesterase III inhibiting properties, can indeed induce both these effects.

Chapter 6-8: Pharmacological modulation of myocardial stunning

If stunning affects a large region of the left ventricle, cardiac function will be impaired to a level that inotropic therapy is needed. As discussed above, calcium sensitizers may have energetic advantages above β -adrenergic drugs. A disadvantage may be impaired diastolic function, however (40, 76). Secondly, it has been shown that the inotropic and lusitropic response to calcium sensitizers may differ between normal and stunned myocardium (76, 129). However, these studies were performed *in vitro* (76), or *in vivo* using load-dependent parameters of systolic function (129). Therefore, in chapter 6 we will examine the effect of EMD 57033 on systolic and diastolic function of normal and stunned myocardium, using load-independent parameters. As a measure of contractility we will apply the end-systolic elastance (E_{es}), while early diastolic function will be assessed with the maximum rate of fall (dE/dt_{min}) and the time constant (τ_e) of the decay of elastance. Late diastolic function will be determined using the end-diastolic

elastance (E_{cd}). Since EMD 57033 exhibits phosphodiesterase III inhibiting properties, we will also study EMD 57033 in the presence of α - and β -adrenoreceptor blockade, to exclude any adrenergic dependence of this drug.

Although in vitro evidence is available that EMD 57033 increases myofibrillar calcium sensitivity (9), in vivo evidence is currently lacking. As calcium sensitivity cannot be measured directly in vivo, the response to intracoronary calcium may be determined. The possible drawback of this method however is that disturbances in calcium-induced calcium release are reflected as well. In the past, an unchanged response to intracoronary calcium was noted in stunned myocardium (59). However, in this study a load-dependent work index was applied. Additionally, the effect of a calcium sensitizer on this response in stunned myocardium has never been evaluated. Therefore, in chapter 7 we will evaluate the responsiveness to intracoronary calcium of stunned myocardium, in the absence and presence of EMD 57033, using end-systolic elastance as a load-independent parameter of contractility. Again, to minimize the phosphodiesterase III inhibiting properties, we will investigate the responsiveness to calcium in the presence of β -adrenoreceptor blockade.

In chapter 8 we will concentrate on the effect of EMD 57033 on regional energetics. Although we showed in chapter 4 and in earlier studies that stunning decreases EW, EET and mechanical efficiency (ME) (77), it is unclear whether these changes are secondary to the decreased contractility or that they primarily caused by a specific underlying mechanism of stunning. Moreover, as mentioned above, calcium sensitizers may have energetic advantages above drugs that increase calcium cycling. To evaluate these hypotheses, we will compare changes in external work (EW), efficiency of energy transfer (EET), and mechanical efficiency (ME), induced by this drug and by dobutamine, a specific β_1 -agonist. If the decreased contractility is the single underlying cause, both drugs will increase the energetic parameters similarly. Otherwise, the two drugs will have different effects. Because we expect the effects of these drugs to be dose-dependent, we will use contractility (end-systolic elastance) as a drug-independent parameter of increases in inotropy. Moreover, we will correct for the effect of afterload on EW and EET by studying the maxima in the EW- and EET-afterload relations, as they are afterload-independent.

Chapter 9: Geometry assessment of the left ventricle to estimate regional wall stress

In the final chapter we will introduce a new method to calculate regional myocardial wall stress. This method was developed to overcome some important limitations of the estimation of wall stress as applied in this thesis. First of all, due to the highly invasive nature of the placement of ultrasound crystals, application in the clinical situation is extremely limited. Secondly, the application of a single anterior-posterior diameter obliged us to assume regional spherical geometry of the myocardial region. However, it is

known that a three-dimensional (3D) curvature is comprised of at least two principal curvatures, which are perpendicular to each other (114). Finally, the invasive nature of the placement of ultrasound crystals limits the measurement of wall stress to 2 or 3 regions of the left ventricle. Therefore, we will apply the concept of 3D echocardiography with a rotating probe to reconstruct left ventricular 3D geometry, from which the required curvature and wall thickness parameters can be derived. To test this method first a left ventricular phantom will be generated using a real ventricular geometry. By computer simulation echo images will be generated. These virtual echo images will be traced and a new 3D image of the phantom will be constructed. Additionally, we will develop computer algorithms for the calculation of the two principal curvatures and wall thickness in 10 different regions of the left ventricle. Using these algorithms, we will compare the original phantom with the new 3D image of the phantom, to validate the accuracy of the algorithms for the reconstruction of a 3D image from 2D ultrasound images and the calculation of the two principal curvatures and wall thickness.

References

1. **Abdelmeguid, A. E., and J. J. Feher.** Effect of low perfusate $[Ca^{2+}]$ and diltiazem on cardiac sarcoplasmic reticulum in myocardial stunning. *Am J Physiol* 266: H406-414, 1994.
2. **Ambrosio, G., S. Betocchi, L. Pace, M. A. Losi, P. Perrone-Filardi, A. Soricelli, F. Piscione, J. Taube, F. Squame, M. Salvatore, J. L. Weiss, and M. Chiariello.** Prolonged impairment of regional contractile function after resolution of exercise-induced angina. Evidence of myocardial stunning in patients with coronary artery disease. *Circulation* 94: 2455-2464., 1996.
3. **Armstrong, P. W., R. S. Baigrie, P. A. Daly, A. Haq, M. Gent, R. S. Roberts, M. R. Freeman, R. Burns, P. Liu, and C. D. Morgan.** Tissue plasminogen activator: Toronto (TPAT) placebo-controlled randomized trial in acute myocardial infarction. *J Am Coll Cardiol* 13: 1469-1476, 1989.
4. **Aversano, T., W. L. Maughan, W. C. Hunter, D. Kass, and L. C. Becker.** End-systolic measures of regional ventricular performance. *Circulation* 73: 938-950, 1986.
5. **Aversano, T., W. L. Maughan, K. Sunagawa, and L. C. Becker.** Effect of afterload resistance on end-systolic pressure-thickness relationship. *Am J Physiol* 254: H658-663, 1988.
6. **Barnes, E., C. S. Baker, D. P. Dutka, O. Rimoldi, C. A. Rinaldi, P. Nihoyannopoulos, P. G. Camici, and R. J. Hall.** Prolonged left ventricular dysfunction occurs in patients with coronary artery disease after both dobutamine and exercise induced myocardial ischaemia. *Heart* 83: 283-289., 2000.
7. **Becker, L. C., J. H. Levine, A. F. DiPaula, T. Guarnieri, and T. Aversano.** Reversal of dysfunction in posts ischemic stunned myocardium by epinephrine and postextrasystolic potentiation. *J Am Coll Cardiol* 7: 580-589., 1986.
8. **Bernstein, R., S. A. Mayer, and A. Magnano.** Neurogenic stunned myocardium in Guillain-Barre syndrome. *Neurology* 54: 759-762., 2000.
9. **Bezstarosti, K., L. K. Soei, R. Krams, F. J. Ten Cate, P. D. Verdouw, and J. M. Lamers.** The effect of a thiadiazinone derived Ca^{2+} sensitizer on the responsiveness of Mg^{2+} -ATPase to Ca^{2+} in myofibrils isolated from stunned and nonstunned porcine and human myocardium. *Biochem Pharmacol* 51: 1211-1220, 1996.
10. **Bier, J., B. Sharaf, and H. Gewirtz.** Origin of anterior interventricular vein blood in domestic swine. *Am J Physiol* 260: H1732-1736, 1991.
11. **Bolli, R.** Basic and clinical aspects of myocardial stunning. *Prog Cardiovasc Dis* 40: 477-516., 1998.
12. **Bolli, R.** Mechanism of myocardial "stunning". *Circulation* 82: 723-738., 1990.
13. **Bolli, R.** Myocardial 'stunning' in man. *Circulation* 86: 1671-1691, 1992.

14. **Bolli, R., M. O. Jeroudi, B. S. Patel, O. I. Aruoma, B. Halliwell, E. K. Lai, and P. B. McCay.** Marked reduction of free radical generation and contractile dysfunction by antioxidant therapy begun at the time of reperfusion. Evidence that myocardial "stunning" is a manifestation of reperfusion injury. *Circ Res* 65: 607-622., 1989.
15. **Bolli, R., M. O. Jeroudi, B. S. Patel, C. M. DuBose, E. K. Lai, R. Roberts, and P. B. McCay.** Direct evidence that oxygen-derived free radicals contribute to postischemic myocardial dysfunction in the intact dog. *Proc Natl Acad Sci U S A* 86: 4695-4699., 1989.
16. **Bolli, R., and E. Marban.** Molecular and cellular mechanisms of myocardial stunning. *Physiol Rev* 79: 609-634., 1999.
17. **Bolli, R., B. S. Patel, M. O. Jeroudi, E. K. Lai, and P. B. McCay.** Demonstration of free radical generation in "stunned"; myocardium of intact dogs with the use of the spin trap alpha-phenyl N-tert-butyl nitron. *J Clin Invest* 82: 476-485., 1988.
18. **Bolli, R., B. S. Patel, M. O. Jeroudi, X. Y. Li, J. F. Triana, E. K. Lai, and P. B. McCay.** Iron-mediated radical reactions upon reperfusion contribute to myocardial "stunning". *Am J Physiol* 259: H1901-1911., 1990.
19. **Bolli, R., W. X. Zhu, M. L. Myers, C. J. Hartley, and R. Roberts.** Beta-adrenergic stimulation reverses postischemic myocardial dysfunction without producing subsequent functional deterioration. *Am J Cardiol* 56: 964-968., 1985.
20. **Braunwald, E., and R. A. Kloner.** The stunned myocardium: prolonged, postischemic ventricular dysfunction. *Circulation* 66: 1146-1149., 1982.
21. **Breisblatt, W. M., K. L. Stein, C. J. Wolfe, W. P. Follansbee, J. Capozzi, J. M. Armitage, and R. L. Hardesty.** Acute myocardial dysfunction and recovery: a common occurrence after coronary bypass surgery. *J Am Coll Cardiol* 15: 1261-1269., 1990.
22. **Burkhoff, D., S. Sugiura, D. T. Yue, and K. Sagawa.** Contractility-dependent curvilinearity of end-systolic pressure-volume relations. *Am J Physiol* 252: H1218-1227., 1987.
23. **Camici, P. G., and D. P. Dutka.** Repetitive stunning, hibernation, and heart failure: contribution of PET to establishing a link. *Am J Physiol Heart Circ Physiol* 280: H929-936., 2001.
24. **Canty, J. M., and J. A. Fallavollita.** Chronic hibernation and chronic stunning: a continuum. *J Nucl Cardiol* 7: 509-527., 2000.
25. **Canty, J. M., and J. A. Fallavollita.** Resting myocardial flow in hibernating myocardium: validating animal models of human pathophysiology. *Am J Physiol* 277: H417-422., 1999.
26. **Carrozza, J. P., Jr., L. A. Bentivegna, C. P. Williams, R. E. Kuntz, W. Grossman, and J. P. Morgan.** Decreased myofilament responsiveness in myocardial stunning follows transient calcium overload during ischemia and reperfusion. *Circ Res* 71: 1334-1340., 1992.
27. **Christian, T. F., M. J. Gitter, T. D. Miller, and R. J. Gibbons.** Prospective identification of myocardial stunning using technetium-99m sestamibi-based measurements of infarct size. *J Am Coll Cardiol* 30: 1633-1640., 1997.
28. **Corretti, M. C., Y. Koretsune, H. Kusuoka, V. P. Chacko, J. L. Zweier, and E. Marban.** Glycolytic inhibition and calcium overload as consequences of exogenously generated free radicals in rabbit hearts. *J Clin Invest* 88: 1014-1025., 1991.
29. **Davis, M. D., W. Lebolt, and J. J. Feher.** Reversibility of the effects of normothermic global ischemia on the ryanodine-sensitive and ryanodine-insensitive calcium uptake of cardiac sarcoplasmic reticulum. *Circ Res* 70: 163-171., 1992.
30. **De Graeff, P. A., W. H. Van Gilst, C. D. De Langen, J. H. Kingma, and H. Wesseling.** Concentration-dependent protection by captopril against ischemia-reperfusion injury in the isolated rat heart. *Arch Int Pharmacodyn Ther* 280: 181-193., 1986.
31. **De Tombe, P. P., S. Jones, D. Burkhoff, W. C. Hunter, and D. A. Kass.** Ventricular stroke work and efficiency both remain nearly optimal despite altered vascular loading. *Am J Physiol* 264: H1817-1824., 1993.
32. **Deantonio, H. J., S. Kaul, and B. B. Lerman.** Reversible myocardial depression in survivors of cardiac arrest. *Pacing Clin Electrophysiol* 13: 982-985., 1990.
33. **Di Lisa, F., R. De Tullio, F. Salamino, R. Barbato, E. Melloni, N. Siliprandi, S. Schiaffino, and S. Pontremoli.** Specific degradation of troponin T and I by mu-calpain and its modulation by substrate phosphorylation. *Biochem J* 308: 57-61., 1995.
34. **Diamond, G. A., J. S. Forrester, P. L. deLuz, H. L. Wyatt, and H. J. Swan.** Post-extrasystolic potentiation of ischemic myocardium by atrial stimulation. *Am Heart J* 95: 204-209., 1978.

35. Dietrich, D. L., G. R. van Leeuwen, G. J. Stienen, and G. Elzinga. Stunning does not change the relation between calcium and force in skinned rat trabeculae. *J Mol Cell Cardiol* 25: 541-549, 1993.
36. Dunker, D. J., L. K. Soei, and P. D. Verdouw. Pharmacologic Modulation of Myocardial Stunning. In: *Stunning, Hibernation, and Preconditioning: Clinical Pathophysiology of Myocardial Ischemia* (1st ed.), edited by G. R. Heyndrickx, S. F. Vatner and W. Wijns. Philadelphia: Lippincott-Raven Publishers, 1997, p. 229-251.
37. Dupouy, P., H. Geschwind, G. Pelle, E. Aptecar, L. Hittinger, A. El Ghalid, and J. L. Dubois-Rande. Repeated coronary artery occlusions during routine balloon angioplasty do not induce myocardial preconditioning in humans. *J Am Coll Cardiol* 27: 1374-1380, 1996.
38. Dyke, S. H., P. F. Cohn, R. Gorlin, and E. H. Sonnenblick. Detection of residual myocardial function in coronary artery disease using post-extra systolic potentiation. *Circulation* 50: 694-699, 1974.
39. Elsasser, A., M. Schlepper, W. P. Klovekorn, W. J. Cai, R. Zimmermann, K. D. Muller, R. Strasser, S. Kostin, C. Gagel, B. Munkel, W. Schaper, and J. Schaper. Hibernating myocardium: an incomplete adaptation to ischemia. *Circulation* 96: 2920-2931, 1997.
40. Endoh, M. Changes in intracellular Ca^{2+} mobilization and Ca^{2+} sensitization as mechanisms of action of physiological interventions and inotropic agents in intact myocardial cells. *Jpn Heart J* 39: 1-44, 1998.
41. Fallavollita, J. A., and J. M. Canty, Jr. Differential ^{18}F -2-deoxyglucose uptake in viable dysfunctional myocardium with normal resting perfusion: evidence for chronic stunning in pigs. *Circulation* 99: 2798-2805, 1999.
42. Fan, D., L. K. Soei, L. M. Sassen, R. Krams, and P. D. Verdouw. Mechanical efficiency of stunned myocardium is modulated by increased afterload dependency. *Cardiovasc Res* 29: 428-437, 1995.
43. Fan, D., L. K. Soei, R. Stubenitsky, E. Boersma, D. J. Duncker, P. D. Verdouw, and R. Krams. Contribution of asynchrony and nonuniformity to mechanical interaction in normal and stunned myocardium. *Am J Physiol* 273: H2146-2154, 1997.
44. Feher, J. J., W. R. LeBolt, and N. H. Manson. Differential effect of global ischemia on the ryanodine-sensitive and ryanodine-insensitive calcium uptake of cardiac sarcoplasmic reticulum. *Circ Res* 65: 1400-1408, 1989.
45. Firoozan, S., K. Wei, A. Linka, D. Skyba, N. C. Goodman, and S. Kaul. A canine model of chronic ischemic cardiomyopathy: characterization of regional flow-function relations. *Am J Physiol* 276: H446-455, 1999.
46. Gao, W. D., D. Atar, P. H. Backx, and E. Marban. Relationship between intracellular calcium and contractile force in stunned myocardium. Direct evidence for decreased myofilament Ca^{2+} responsiveness and altered diastolic function in intact ventricular muscle. *Circ Res* 76: 1036-1048, 1995.
47. Gao, W. D., D. Atar, Y. Liu, N. G. Perez, A. M. Murphy, and E. Marban. Role of troponin I proteolysis in the pathogenesis of stunned myocardium. *Circ Res* 80: 393-399, 1997.
48. Gayheart, P. A., J. Vinten-Johansen, W. E. Johnston, T. O. Hester, and A. R. Cordell. Oxygen requirements of the dyskinetic myocardial segment. *Am J Physiol* 257: H1184-1191, 1989.
49. Gerber, B. L., W. Wijns, J. L. Vanoverschelde, G. R. Heyndrickx, B. De Bruyne, J. Bartunek, and J. A. Melin. Myocardial perfusion and oxygen consumption in reperfused noninfarcted dysfunctional myocardium after unstable angina: direct evidence for myocardial stunning in humans. *J Am Coll Cardiol* 34: 1939-1946, 1999.
50. Geyer, M., J. D. Strauss, J. C. Ruegg, and H. Kogler. Ca^{2+} sensitivity of stunned myocardium after skinning using retrograde infusion of detergent. *Pflugers Arch* 438: 470-478, 1999.
51. Gorge, G., I. Papageorgiou, and R. Lerch. Epinephrine-stimulated contractile and metabolic reserve in postischemic rat myocardium. *Basic Res Cardiol* 85: 595-605, 1990.
52. Goto, Y., Y. Igarashi, Y. Yasumura, T. Nozawa, S. Futaki, K. Hiramori, and H. Suga. Integrated regional work equals total left ventricular work in regionally ischemic canine heart. *Am J Physiol* 254: H894-904, 1988.
53. Goto, Y., H. Suga, O. Yamada, Y. Igarashi, M. Saito, and K. Hiramori. Left ventricular regional work from wall tension-area loop in canine heart. *Am J Physiol* 250: H151-158, 1986.
54. Grinwald, P. M. Calcium uptake during post-ischemic reperfusion in the isolated rat heart: influence of extracellular sodium. *J Mol Cell Cardiol* 14: 359-365, 1982.

55. Gross, G. J. ATP-sensitive potassium channels and myocardial preconditioning. *Basic Res Cardiol* 90: 85-88., 1995.
56. Hagemann, D., M. Kuschel, T. Kuramochi, W. Zhu, H. Cheng, and R. P. Xiao. Frequency-encoding Thr17 phospholamban phosphorylation is independent of Ser16 phosphorylation in cardiac myocytes. *J Biol Chem* 275: 22532-22536, 2000.
57. Hata, Y., J. Shimizu, S. Hosogi, H. Matsubara, J. Araki, T. Ohe, M. Takaki, T. Takasago, T. W. Taylor, and H. Suga. Ryanodine decreases internal Ca^{2+} recirculation fraction of the canine heart as studied by postextrasystolic transient alternans. *Jpn J Physiol* 47: 521-530, 1997.
58. Hearse, D. J. Myocardial ischaemia: can we agree on a definition for the 21st century? [editorial] [see comments]. *Cardiovasc Res* 28: 1737-1744: discussion 1745-1736, 1994.
59. Heusch, G., J. Rose, A. Skyschally, H. Post, and R. Schulz. Calcium responsiveness in regional myocardial short-term hibernation and stunning in the in situ porcine heart. Inotropic responses to postextrasystolic potentiation and intracoronary calcium. *Circulation* 93: 1556-1566, 1996.
60. Heyndrickx, G. R., J. Amano, T. Kenna, J. T. Fallon, T. A. Patrick, W. T. Manders, G. G. Rogers, C. Rosendorff, and S. F. Vatner. Creatine kinase release not associated with myocardial necrosis after short periods of coronary artery occlusion in conscious baboons. *J Am Coll Cardiol* 6: 1299-1303, 1985.
61. Heyndrickx, G. R., H. Baig, P. Nellens, I. Leusen, M. C. Fishbein, and S. F. Vatner. Depression of regional blood flow and wall thickening after brief coronary occlusions. *Am J Physiol* 234: H653-659, 1978.
62. Heyndrickx, G. R., R. W. Millard, R. J. McRitchie, P. R. Maroko, and S. F. Vatner. Regional myocardial functional and electrophysiological alterations after brief coronary artery occlusion in conscious dogs. *J Clin Invest* 56: 978-985, 1975.
63. Ishihara, H., M. Yokota, T. Sobue, and H. Saito. Relation between ventriculoarterial coupling and myocardial energetics in patients with idiopathic dilated cardiomyopathy. *J Am Coll Cardiol* 23: 406-416, 1994.
64. Ishiki, R., T. Ishihara, H. Izawa, K. Nagata, M. Hirai, and M. Yokota. Acute effects of a single low oral dose of pimobendan on left ventricular systolic and diastolic function in patients with congestive heart failure. *J Cardiovasc Pharmacol* 35: 897-905., 2000.
65. Iwashiro, K., A. Criniti, R. Sinatra, A. A. Dawodu, G. d'Amati, F. Monti, L. Pannarale, P. Bernucci, G. L. Brancaccio, A. Vetusch, E. Gaudio, P. Gallo, and P. E. Puddu. Felodipine protects human atrial muscle from hypoxia-reoxygenation dysfunction: a force-frequency relationship study in an in vitro model of stunning. *Int J Cardiol* 62: 107-132, 1997.
66. Jennings, R. B., and K. A. Reimer. Discovery and Early History of Preconditioning. In: *Stunning, Hibernation, and Preconditioning: Clinical Pathophysiology of Myocardial Ischemia* (1st ed.), edited by G. R. Heyndrickx, S. F. Vatner and W. Wijns. Philadelphia: Lippincott-Raven Publishers, 1997, p. 83-104.
67. Kadambi, V. J., N. Ball, E. G. Kranias, R. A. Walsh, and B. D. Hoit. Modulation of force-frequency relation by phospholamban in genetically engineered mice. *Am J Physiol* 276: H2245-H2250, 1999.
68. Kaneko, M., R. E. Beamish, and N. S. Dhalla. Depression of heart sarcolemmal Ca^{2+} -pump activity by oxygen free radicals. *Am J Physiol* 256: H368-374., 1989.
69. Kaneko, M., V. Elimban, and N. S. Dhalla. Mechanism for depression of heart sarcolemmal Ca^{2+} pump by oxygen free radicals. *Am J Physiol* 257: H804-811., 1989.
70. Kaplan, P., M. Hendriks, M. Mattheussen, K. Mubagwa, and W. Flameng. Effect of ischemia and reperfusion on sarcoplasmic reticulum calcium uptake. *Circ Res* 71: 1123-1130, 1992.
71. Kim, M. S., and T. Akeru. O_2 free radicals: cause of ischemia-reperfusion injury to cardiac Na^+ - K^+ -ATPase. *Am J Physiol* 252: H252-257., 1987.
72. Kitakaze, M., M. L. Weisfeldt, and E. Marban. Acidosis during early reperfusion prevents myocardial stunning in perfused ferret hearts. *J Clin Invest* 82: 920-927., 1988.
73. Kitakaze, M., H. F. Weisman, and E. Marban. Contractile dysfunction and ATP depletion after transient calcium overload in perfused ferret hearts. *Circulation* 77: 685-695, 1988.
74. Kloner, R. A., S. G. Ellis, R. Lange, and E. Braunwald. Studies of experimental coronary artery reperfusion. Effects on infarct size, myocardial function, biochemistry, ultrastructure and microvascular damage. *Circulation* 68: 18-15, 1983.

75. Kono, T., H. Morita, T. Kuroiwa, H. Onaka, H. Takatsuka, and A. Fujiwara. Left ventricular wall motion abnormalities in patients with subarachnoid hemorrhage: neurogenic stunned myocardium. *J Am Coll Cardiol* 24: 636-640.. 1994.
76. Korbmacher, B., U. Sunderdiek, G. Selcan, G. Arnold, and J. D. Schipke. Different responses of non-ischemic and post-ischemic myocardium towards Ca²⁺ sensitization. *J Mol Cell Cardiol* 29: 2053-2066, 1997.
77. Krams, R., D. J. Duncker, E. O. McFalls, A. Hogendoorn, and P. D. Verdouw. Dobutamine restores the reduced efficiency of energy transfer from total mechanical work to external mechanical work in stunned porcine myocardium. *Cardiovasc Res* 27: 740-747, 1993.
78. Krause, S. M., W. E. Jacobus, and L. C. Becker. Alterations in cardiac sarcoplasmic reticulum calcium transport in the postischemic "stunned" myocardium. *Circ Res* 65: 526-530, 1989.
79. Krause, S. M., and D. Rozanski. Effects of an increase in intracellular free [Mg²⁺] after myocardial stunning on sarcoplasmic reticulum Ca²⁺ transport. *Circulation* 84: 1378-1383, 1991.
80. Kusuoka, H., Y. Koretsune, V. P. Chacko, M. L. Weisfeldt, and E. Marban. Excitation-contraction coupling in postischemic myocardium. Does failure of activator Ca²⁺ transients underlie stunning? *Circ Res* 66: 1268-1276, 1990.
81. Kusuoka, H., J. K. Porterfield, H. F. Weisman, M. L. Weisfeldt, and E. Marban. Pathophysiology and pathogenesis of stunned myocardium. Depressed Ca²⁺ activation of contraction as a consequence of reperfusion-induced cellular calcium overload in ferret hearts. *J Clin Invest* 79: 950-961, 1987.
82. Labovitz, A. J., M. K. Lewen, M. Kern, M. Vandormael, U. Deligonal, and H. L. Kennedy. Evaluation of left ventricular systolic and diastolic dysfunction during transient myocardial ischemia produced by angioplasty. *J Am Coll Cardiol* 10: 748-755.. 1987.
83. Lamers, J. M. Preconditioning and limitation of stunning: one step closer to the protected protein(s)? [editorial]. *Cardiovasc Res* 42: 571-575, 1999.
84. Lamers, J. M., D. J. Duncker, K. Bezstarosti, E. O. McFalls, L. M. Sassen, and P. D. Verdouw. Increased activity of the sarcoplasmic reticular calcium pump in porcine stunned myocardium. *Cardiovasc Res* 27: 520-524, 1993.
85. Leighton, K. M., and C. Bruce. Dobutamine and general anaesthesia: a study of the response of arterial pressure, heart rate and renal blood flow. *Can Anaesth Soc J* 23: 176-184, 1976.
86. Limbruno, U., R. Zucchi, S. Ronca-Testoni, P. Galbani, G. Ronca, and M. Mariani. Sarcoplasmic reticulum function in the "stunned" myocardium. *J Mol Cell Cardiol* 21: 1063-1072, 1989.
87. Liu, X., R. M. Engelman, Z. Wei, N. Maulik, J. A. Rousou, J. E. d. Flack, D. W. Deaton, and D. K. Das. Postischemic deterioration of sarcoplasmic reticulum: warm versus cold blood cardioplegia [see comments]. *Ann Thorac Surg* 56: 1154-1159, 1993.
88. Luss, H., A. Meissner, N. Rolf, H. Van Aken, P. Boknik, U. Kirchhefer, J. Knapp, S. Laer, B. Linck, I. Luss, F. U. Muller, J. Neumann, and W. Schmitz. Biochemical mechanism(s) of stunning in conscious dogs. *Am J Physiol Heart Circ Physiol* 279: H176-184, 2000.
89. MacFarlane, N. G., and D. J. Miller. Depression of peak force without altering calcium sensitivity by the superoxide anion in chemically skinned cardiac muscle of rat. *Circ Res* 70: 1217-1224.. 1992.
90. Mehdi, S. Cell-penetrating inhibitors of calpain. *Trends Biochem Sci* 16: 150-153, 1991.
91. Mori, M., M. Takeuchi, H. Takaoka, K. Hata, Y. Hayashi, H. Yamakawa, and M. Yokoyama. Oxygen-saving effect of a new cardioprotective agent, MCI-154, in diseased human hearts. *J Am Coll Cardiol* 29: 613-622, 1997.
92. Mubagwa, K., P. Kaplan, and W. Flameng. The effects of ryanodine on calcium uptake by the sarcoplasmic reticulum of ischemic and reperfused rat myocardium. *Fundam Clin Pharmacol* 11: 315-321, 1997.
93. Munch, G., B. Bolck, K. Brixius, H. Reuter, U. Mehlhorn, W. Bloch, and R. H. Schwinger. SERCA2a activity correlates with the force-frequency relationship in human myocardium. *Am J Physiol Heart Circ Physiol* 278: H1924-1932, 2000.
94. Murry, C. E., R. B. Jennings, and K. A. Reimer. Preconditioning with ischemia: a delay of lethal cell injury in ischemic myocardium. *Circulation* 74: 1124-1136.. 1986.
95. Myhre, E. S., A. Johansen, J. Bjornstad, and H. Piene. The effect of contractility and preload on matching between the canine left ventricle and afterload. *Circulation* 73: 161-171, 1986.

96. Namba, T., M. Takaki, J. Araki, K. Ishioka, and H. Suga. Energetics of the negative and positive inotropism of pentobarbitone sodium in the canine left ventricle. *Cardiovasc Res* 28: 557-564, 1994.
97. Narula, J., M. S. Dawson, B. K. Singh, A. Amanullah, E. R. Acio, F. A. Chaudhry, R. B. Arani, and A. E. Iskandrian. Noninvasive characterization of stunned, hibernating, remodeled and nonviable myocardium in ischemic cardiomyopathy. *J Am Coll Cardiol* 36: 1913-1919., 2000.
98. Nayler, W. G., J. S. Elz, and D. J. Buckley. The stunned myocardium: effect of electrical and mechanical arrest and osmolarity. *Am J Physiol* 255: H60-69, 1988.
99. Nichols, W. W., and C. J. Pepine. Ventricular/vascular interaction in health and heart failure. *Compr Ther* 18: 12-19, 1992.
100. Ohgoshi, Y., Y. Goto, S. Futaki, H. Taku, O. Kawaguchi, and H. Suga. Increased oxygen cost of contractility in stunned myocardium of dog. *Circ Res* 69: 975-988, 1991.
101. Ohtsuka, T., M. Hamada, K. Kodama, O. Sasaki, M. Suzuki, Y. Hara, Y. Shigematsu, and K. Hiwada. Images in Cardiovascular Medicine. Neurogenic stunned myocardium. *Circulation* 101: 2122-2124., 2000.
102. Onishi, K., K. Sekioka, R. Ishisu, Y. Abe, H. Tanaka, M. Nakamura, Y. Ueda, and T. Nakano. MCI-154, a Ca²⁺ sensitizer, decreases the oxygen cost of contractility in isolated canine hearts. *Am J Physiol* 273: H1688-1695, 1997.
103. Opie, L. H. Energy for ion fluxes. In: *The Heart, physiology from cell to circulation* (3d ed.). Philadelphia: Lippincot-Raven Publishers, 1998, p. 110.
104. Papp, Z., J. van der Velden, and G. J. Stienen. Calpain-I induced alterations in the cytoskeletal structure and impaired mechanical properties of single myocytes of rat heart [see comments]. *Cardiovasc Res* 45: 981-993, 2000.
105. Pfisterer, M., M. Zuber, R. Wenzel, and F. Burkart. Prolonged myocardial stunning after thrombolysis: can left ventricular function be assessed definitely at hospital discharge? *Eur Heart J* 12: 214-217, 1991.
106. Pierard, L. A., C. M. De Landsheere, C. Berthe, P. Rigo, and H. E. Kulbertus. Identification of viable myocardium by echocardiography during dobutamine infusion in patients with myocardial infarction after thrombolytic therapy: comparison with positron emission tomography. *J Am Coll Cardiol* 15: 1021-1031., 1990.
107. Pike, M. M., M. Kitakaze, and E. Marban. ²³Na-NMR measurements of intracellular sodium in intact perfused ferret hearts during ischemia and reperfusion. *Am J Physiol* 259: H1767-1773., 1990.
108. Przyklenk, K., and P. Whittaker. Stunned Myocardium in the Isolated Perfused Heart Preparation. In: *Stunned Myocardium. Properties, Mechanisms, and Clinical Manifestations* (1 ed.), edited by R. A. Kloner and K. Przyklenk. New York: Marcel Dekker, Inc., 1993, p. 109-134.
109. Rahimtoola, S. H. A perspective on the three large multicenter randomized clinical trials of coronary bypass surgery for chronic stable angina. *Circulation* 72: V123-135., 1985.
110. Reeves, J. P., C. A. Bailey, and C. C. Hale. Redox modification of sodium-calcium exchange activity in cardiac sarcolemmal vesicles. *J Biol Chem* 261: 4948-4955., 1986.
111. Rehr, R. B., B. E. Fuhs, J. I. Hirsch, and J. J. Feher. Effect of brief regional ischemia followed by reperfusion with or without superoxide dismutase and catalase administration on myocardial sarcoplasmic reticulum and contractile function. *Am Heart J* 122: 1257-1269, 1991.
112. Rinaldi, C. A., N. D. Masani, A. Z. Linka, and R. J. Hall. Effect of repetitive episodes of exercise induced myocardial ischaemia on left ventricular function in patients with chronic stable angina: evidence for cumulative stunning or ischaemic preconditioning? *Heart* 81: 404-411., 1999.
113. Roberts, A. J., A. P. Niarchos, V. A. Subramanian, R. M. Abel, S. D. Herman, J. E. Sealey, D. B. Case, R. P. White, G. A. Johnson, J. H. Laragh, and W. A. Gay. Systemic hypertension associated with coronary artery bypass surgery. Predisposing factors, hemodynamic characteristics, humoral profile, and treatment. *J Thorac Cardiovasc Surg* 74: 846-859., 1977.
114. Rogers, D. F., and J. A. Adams. Ruled and developed surfaces. In: *Mathematical Elements for Computer Graphics* (2nd ed.). New York: McGraw-Hill, Inc., 1990, p. 417-422.
115. Romanin, C., P. Grosswagen, and H. Schindler. Calpastatin and nucleotides stabilize cardiac calcium channel activity in excised patches. *Pflugers Arch* 418: 86-92., 1991.

116. Rowe, G. T., N. H. Manson, M. Caplan, and M. L. Hess. Hydrogen peroxide and hydroxyl radical mediation of activated leukocyte depression of cardiac sarcoplasmic reticulum. Participation of the cyclooxygenase pathway. *Circ Res* 53: 584-591., 1983.
117. Sagawa, K., L. Maughan, H. Suga, and K. Sunagawa. Energetics of the heart. In: *Cardiac contraction and the pressure-volume relationship*. New York: Oxford University Press. 1988. p. 171-231.
118. Schad, H., W. Heimisch, G. P. Eising, and N. Mendler. Effect of milrinone and atrial pacing on stunned myocardium. *Eur J Cardiothorac Surg* 11: 1125-1132, 1997.
119. Schipke, J. D., U. Sunderdiek, B. Korbmacher, U. Schwanke, and G. Arnold. Utilization of oxygen by the contractile apparatus is disturbed during reperfusion of post-ischaemic myocardium. *Eur Heart J* 16: 1476-1481, 1995.
120. Sciaga, R., L. Bolognese, D. Rovai, S. Sestini, G. M. Santoro, G. Cerisano, C. Marini, P. Buonamici, D. Antonucci, and P. F. Fazzini. Detecting myocardial salvage after primary PTCA: early myocardial contrast echocardiography versus delayed sestamibi perfusion imaging. *J Nucl Med* 40: 363-370., 1999.
121. Sekili, S., P. B. McCay, X. Y. Li, M. Zughuib, J. Z. Sun, L. Tang, J. I. Thornby, and R. Bolli. Direct evidence that the hydroxyl radical plays a pathogenetic role in myocardial "stunning" in the conscious dog and demonstration that stunning can be markedly attenuated without subsequent adverse effects. *Circ Res* 73: 705-723., 1993.
122. Serruys, P. W., W. Wijns, M. van den Brand, S. Meij, C. Slager, J. C. Schuurbijs, P. G. Hugenholtz, and R. W. Brower. Left ventricular performance, regional blood flow, wall motion, and lactate metabolism during transluminal angioplasty. *Circulation* 70: 25-36., 1984.
123. Sherman, A. J., F. J. Klocke, R. S. Decker, M. L. Decker, K. A. Kozlowski, K. R. Harris, S. Hedjbeli, Y. Yaroshenko, S. Nakamura, M. A. Parker, P. A. Checchia, and D. B. Evans. Myofibrillar disruption in hypocontractile myocardium showing perfusion-contraction matches and mismatches. *Am J Physiol Heart Circ Physiol* 278: H1320-1334, 2000.
124. Shevchenko, S., W. Feng, M. Varsanyi, and V. Shoshan-Barmatz. Identification, characterization and partial purification of a thiol-protease which cleaves specifically the skeletal muscle ryanodine receptor/Ca²⁺ release channel. *J Membr Biol* 161: 33-43., 1998.
125. Shimokawa, A., T. Kunitake, M. Takasaki, and H. Kannan. Differential effects of anesthetics on sympathetic nerve activity and arterial baroreceptor reflex in chronically instrumented rats. *J Auton Nerv Syst* 72: 46-54, 1998.
126. Shivalkar, B., W. Flameng, M. Szilard, S. Pislaru, M. Borgers, and J. Vanhaecke. Repeated stunning precedes myocardial hibernation in progressive multiple coronary artery obstruction. *J Am Coll Cardiol* 34: 2126-2136., 1999.
127. Smith, H. J. Depressed contractile function in reperfused canine myocardium: metabolism and response to pharmacological agents. *Cardiovasc Res* 14: 458-468, 1980.
128. Soei, L. K., S. de Zeeuw, R. Krams, D. J. Duncker, and P. D. Verdouw. Ca²⁺ sensitization and diastolic function of normal and stunned porcine myocardium. *Eur J Pharmacol* 386: 55-67., 1999.
129. Soei, L. K., L. M. Sassen, D. S. Fan, T. van Veen, R. Krams, and P. D. Verdouw. Myofibrillar Ca²⁺ sensitization predominantly enhances function and mechanical efficiency of stunned myocardium. *Circulation* 90: 959-969, 1994.
130. Sun, J. Z., H. Kaur, B. Halliwell, X. Y. Li, and R. Bolli. Use of aromatic hydroxylation of phenylalanine to measure production of hydroxyl radicals after myocardial ischemia in vivo. Direct evidence for a pathogenetic role of the hydroxyl radical in myocardial stunning. *Circ Res* 73: 534-549., 1993.
131. Sun, J. Z., X. L. Tang, S. W. Park, Y. Qiu, J. F. Turrens, and R. Bolli. Evidence for an essential role of reactive oxygen species in the genesis of late preconditioning against myocardial stunning in conscious pigs. *J Clin Invest* 97: 562-576., 1996.
132. Takaki, M., H. Kohzaki, Y. Kawatani, A. Yoshida, H. Ishidate, and H. Suga. Sarcoplasmic reticulum Ca²⁺ pump blockade decreases O₂ use of unloaded contracting rat heart slices: thapsigargin and cyclopiazonic acid. *J Mol Cell Cardiol* 30: 649-659, 1998.
133. Tawakol, A., H. A. Skopicki, S. A. Abraham, N. M. Alpert, A. J. Fischman, M. H. Picard, and H. Gewirtz. Evidence of reduced resting blood flow in viable myocardial regions with chronic asynergy. *J Am Coll Cardiol* 36: 2146-2153., 2000.

134. Ter Keurs, H. E., W. D. Gao, H. Bosker, A. J. Drake-Holland, and M. I. Noble. Characterisation of decay of frequency induced potentiation and post- extrasystolic potentiation. *Cardiovasc Res* 24: 903-910, 1990.
135. Teramura, S., and T. Yamakado. Calcium sensitizers in chronic heart failure: inotropic interventions-reservation to preservation. *Cardiologia* 43: 375-385, 1998.
136. Thomas, S. A., J. A. Fallavollita, T. C. Lee, J. Feng, and J. M. Canty, Jr. Absence of troponin I degradation or altered sarcoplasmic reticulum uptake protein expression after reversible ischemia in swine [see comments]. *Circ Res* 85: 446-456, 1999.
137. Toorop, G. P., G. J. Van den Horn, G. Elzinga, and N. Westerhof. Matching between feline left ventricle and arterial load: optimal external power or efficiency. *Am J Physiol* 254: H279-285, 1988.
138. Topol, E. J., J. L. Weiss, J. A. Brinker, K. P. Brin, S. O. Gottlieb, L. C. Becker, B. H. Bulkley, N. Chandra, J. T. Flaherty, G. Gerstenblith, and et al. Regional wall motion improvement after coronary thrombolysis with recombinant tissue plasminogen activator: importance of coronary angioplasty. *J Am Coll Cardiol* 6: 426-433., 1985.
139. Urthaler, F., P. E. Wolkowicz, S. B. Digerness, K. D. Harris, and A. A. Walker. MDL-28170, a membrane-permeant calpain inhibitor, attenuates stunning and PKC epsilon proteolysis in reperfused ferret hearts. *Cardiovasc Res* 35: 60-67, 1997.
140. Valdivia, C., J. O. Hegge, R. D. Lasley, H. H. Valdivia, and R. Mentzer. Ryanodine receptor dysfunction in porcine stunned myocardium. *Am J Physiol* 273: H796-804, 1997.
141. Vanoverschelde, J. L., and W. J. Flameng. Chronic Myocardial Hibernation in Humans. In: *Stunning, Hibernation, and Preconditioning: Clinical Pathophysiology of Myocardial Ischemia* (1st ed.), edited by G. R. Heyndrickx, S. F. Vatner and W. Wijns. Philadelphia: Lippincott-Raven Publishers, 1997, p. 273-286.
142. Verdouw, P. D., B. C. Gho, and D. J. Duncker. Ischaemic preconditioning: is it clinically relevant? *Eur Heart J* 16: 1169-1176., 1995.
143. Verdouw, P. D., M. A. van den Doel, S. de Zeeuw, and D. J. Duncker. Animal models in the study of myocardial ischaemia and ischaemic syndromes. *Cardiovasc Res* 39: 121-135, 1998.
144. Verdouw, P. D., B. H. Wolffenbuttel, and F. J. ten Cate. Nifedipine with and without propranolol in the treatment of myocardial ischemia: effect on ventricular arrhythmias and recovery of regional wall function. *Eur Heart J* 4 Suppl C: 101-108., 1983.
145. Vogel, W. M., and C. S. Apstein. Effects of alloxan-induced diabetes on ischemia-reperfusion injury in rabbit hearts. *Circ Res* 62: 975-982, 1988.
146. Vogel, W. M., A. W. Cerel, and C. S. Apstein. Post-ischemic cardiac chamber stiffness and coronary vasomotion: the role of edema and effects of dextran. *J Mol Cell Cardiol* 18: 1207-1218., 1986.
147. Wang, T. D., C. C. Wu, and Y. T. Lee. Myocardial stunning after cerebral infarction. *Int J Cardiol* 58: 308-311., 1997.
148. White, F. C., and G. Boss. Inotropic interventions during myocardial "stunning" in the pig. *Am J Cardiovasc Pathol* 3: 225-236, 1990.
149. Wier, W. G., and D. T. Yue. Intracellular calcium transients underlying the short-term force-interval relationship in ferret ventricular myocardium. *J Physiol (Lond)* 376: 507-530, 1986.
150. Wijns, W. Clinical Evidence of Myocardial Stunning. In: *Stunning, Hibernation, and Preconditioning: Clinical Pathophysiology of Myocardial Ischemia* (1st ed.), edited by G. R. Heyndrickx, S. F. Vatner and W. Wijns. Philadelphia: Lippincott-Raven Publishers, 1997, p. 253-272.
151. Wijns, W., P. W. Serruys, C. J. Slager, J. Grimm, H. P. Krayenbuehl, P. G. Hugenholtz, and O. M. Hess. Effect of coronary occlusion during percutaneous transluminal angioplasty in humans on left ventricular chamber stiffness and regional diastolic pressure-radius relations. *J Am Coll Cardiol* 7: 455-463., 1986.
152. Wildhirt, S. M., M. Weis, C. Schulze, N. Conrad, G. Rieder, G. Enders, K. Ihnken, W. von Scheidt, and B. Reichart. Effects of Celsior and University of Wisconsin preservation solutions on hemodynamics and endothelial function after cardiac transplantation in humans: a single-center, prospective, randomized trial. *Transpl Int* 13: S203-211., 2000.
153. Wu, Q. Y., and J. J. Feher. Ryanodine perfusion decreases cardiac mechanical function without affecting homogenate sarcoplasmic reticulum Ca²⁺ uptake: comparison with the stunned heart. *J Mol Cell Cardiol* 28: 943-955, 1996.

154. **Xu, K. Y., K. Vandegaer, and L. C. Becker.** The sarcoplasmic reticulum Ca^{2+} -ATPase is depressed in stunned myocardium after ischemia-reperfusion, but remains functionally coupled to sarcoplasmic reticulum-bound glycolytic enzymes. *Ann NY Acad Sci* 853: 376-379, 1998.
155. **Yokoyama, Y., D. Novitzky, M. T. Deal, and T. R. Snow.** Facilitated recovery of cardiac performance by triiodothyronine following a transient ischemic insult. *Cardiology* 81: 34-45, 1992.
156. **Yoshida, K., and K. Harada.** Proteolysis of erythrocyte-type and brain-type ankyrins in rat heart after postischemic reperfusion. *J Biochem (Tokyo)* 122: 279-285., 1997.
157. **Yoshida, K., M. Inui, K. Harada, T. C. Saido, Y. Sorimachi, T. Ishihara, S. Kawashima, and K. Sobue.** Reperfusion of rat heart after brief ischemia induces proteolysis of caldesmon (nonerythroid spectrin or fodrin) by calpain. *Circ Res* 77: 603-610., 1995.
158. **Zucchi, R., S. Ronca-Testoni, G. Yu, P. Galbani, G. Ronca, and M. Mariani.** Effect of ischemia and reperfusion on cardiac ryanodine receptors--sarcoplasmic reticulum Ca^{2+} channels. *Circ Res* 74: 271-280, 1994.
159. **Zuurbier, C. J., and J. H. van Beek.** Undiminished mitochondrial function during stunning in rabbit heart at 28 degrees C. *Cardiovasc Res* 35: 113-119, 1997.
160. **Zweier, J. L., P. Kuppusamy, R. Williams, B. K. Rayburn, D. Smith, M. L. Weisfeldt, and J. T. Flaherty.** Measurement and characterization of postischemic free radical generation in the isolated perfused heart. *J Biol Chem* 264: 18890-18895., 1989.

Chapter 2

A decreased force-frequency effect in stunned myocardium

Introduction - The precise localization of the disturbance in the chain of excitation to contraction in myocardial stunning is still under debate. Recently, the role of the sarcoplasmic reticulum Ca^{2+} -ATPase (SERCA2) – phospholamban interaction in the force-frequency effect has been reported. Consequently, we measured the response of the force-frequency effect before and after stunning, while altering SERCA2-phospholamban interaction by dobutamine.

Methods - Stunning was induced in open-chest pigs ($n=9$) by two LADCA occlusions (10 min) followed by 30 min of reperfusion. End-systolic elastance (E_{es}) was derived from regional stress-strain relationships at several heart rates (85, 100, 115, 130) from implanted crystals applying preload changes. The slope of E_{es} versus heart rate ($\alpha_{E_{es}}$) was evaluated after dobutamine, after stunning and after stunning with dobutamine.

Results - Stunning reduced E_{es} from 173 kPa to 87 kPa at 100 beats/min. $\alpha_{E_{es}}$ was abolished in myocardial stunning. Dobutamine increased $\alpha_{E_{es}}$, dose dependently before stunning (by 243%) and after stunning, but the effect was decreased by 47% compared to before stunning.

Conclusions - Myocardial stunning reduced the force-frequency effect and its regulation. These findings suggest that the contractile dysfunction underlying stunning is at least partially related to a disturbed regulation of SERCA2 function.

S.A.I.P. Trines, C.A.G. Smits, T.A.M. Onderwater, J.M.J. Lamers, P.D. Verdouw, C.J. Slager, and R. Krams. Myocardial Stunning is Associated with a Disturbed Regulation of the Force-Frequency Response. *Submitted*

Introduction

Contradictory experimental findings still exist regarding the mechanism of myocardial stunning. For instance, in rat and ferret hearts it has been shown that the sensitivity of the myofibrils to calcium was decreased, probably as a result of a proteolytic degradation of troponin-I (12, 25, 32). However, other laboratories have measured normal calcium sensitivity in skinned trabeculae (8, 13) and an absence of troponin-I degradation in stunned porcine and canine myocardium (29, 39, 43). Hence, at least in some species troponin-I degradation appears not to be mandatory for stunning, suggesting that additional factors, besides the decrease in myofibrillar calcium sensitivity, may be involved.

Development of contractile force not only depends on the function of the myofibrils, but also on the capacity of the sarcoplasmic reticulum (SR) to release and sequester calcium (33). Calcium transients measured in ferret and rat hearts did not show any alteration after induction of stunning (11, 24). However, in these two studies, calcium transients have been measured at heart rates far below the physiological heart rates for these species. As calcium transients, and therefore myocardial force, increase with increments in heart rate, the so-called "force-frequency effect" (4, 10, 16), the decreases in calcium transients in the stunned ferret and rat hearts may have been masked by the low heart rate (4, 10, 16). Recently, it has been reported that the sarcoplasmic reticulum Ca^{2+} -ATPase (SERCA2)-phospholamban interaction plays a role in the force-frequency effect in human myocardium (31). The force-frequency effect has been studied extensively in heart failure (16) but not in myocardial stunning (18, 37). In one study the response of atrial muscle was determined in vitro (18), while in another study load-sensitive parameters of force were used (37). In both studies a decrease in the force-frequency effect was observed, but the use of atrial rather than ventricular tissue and the use of load-sensitive parameters may have affected the outcomes. Hence, the first aim of the present study was to evaluate the effect of myocardial stunning on the force-frequency effect in an in vivo porcine model of regional stunning, using regional end-systolic elastance, a load-independent index of contractility (2, 14, 44).

Recent studies with transgenic mice indicate that the degree of inhibition of SERCA2 by phospholamban is inversely related with the force-frequency effect (4, 17, 19). Therefore, we modulated the interaction between SERCA2 and phospholamban with dobutamine and compared the effect of this modulation on the force-frequency effect in stunned and normal myocardium, to unmask alterations in the regulation of SERCA2. If stunning indeed affects the SERCA2-phospholamban interaction, we expect that the effect of dobutamine on the force-frequency effect will be attenuated. To this end, we also determined the effect of dobutamine on the force-frequency effect before and during myocardial stunning.

Methods

General

All experiments were performed in accordance with the 'Guiding principles for the care and use of animals' as approved by the Council of the American Physiological Society and under the regulations of the Animal Care Committee of the Erasmus Medical Center Rotterdam.

Instrumentation

After an overnight fast crossbred Yorkshire-Landrace pigs (25-39 kg, n=9, Oude Tonge, The Netherlands) were sedated with 20 mg·kg⁻¹ ketamine i.m. (Apharmo BV, Arnhem, The Netherlands), anesthetized with 15-20 mg·kg⁻¹ sodium pentobarbital i.v. (Apharmo BV, Arnhem, The Netherlands), intubated and connected to a ventilator for intermittent positive pressure ventilation with a mixture of O₂ and N₂ (1:2, vol/vol). Arterial oxygen content and blood gases were kept within the normal range (7.35 < pH < 7.45; 35 < pCO₂ (mmHg) < 45; 100 < pO₂ (mmHg) < 150) by adjusting the settings of the respirator (Bear 5 ventilator, Bear Medical Systems Inc., Riverside, Ca., USA). Three 7 French (F) fluid-filled catheters were placed in the superior caval veins for infusion of 10-15 mg·kg⁻¹·h⁻¹ sodium pentobarbital, saline or Haemaccel (Hoechst Marion Roussel B.V., Hoevelaken, the Netherlands), dobutamine (Dagra Pharma B.V., Diemen, The Netherlands) and the specific negative chronotropic agent zatebradine (1-2 mg·kg⁻¹, courtesy of Dr. J.W. Dämmgen, Dr. Karl Thomae, Biberach a/d Riss, Germany). Central aortic blood pressure (AoP) was monitored via an 8 F catheter positioned in the thoracic descending aorta. A 7 F micromanometer tipped catheter (B. Braun Medical B.V., Uden, The Netherlands) was inserted via the left carotid artery and advanced into the left ventricle for measurement of the left ventricular (LV) pressure and LVdP/dt. A latex balloon mounted on a 7 F fluid-filled catheter was positioned in the inferior caval vein above the diaphragm to transiently decrease LV preload. After administration of 4 mg pancuronium bromide (Organon Teknika B.V., Boxtel, The Netherlands), a midsternal thoracotomy was performed. The left mammarian artery and vein were ligated, a part of the second left rib was removed and the heart was suspended in a pericardial cradle. An electromagnetic flow probe (Skalar, Delft, The Netherlands) was placed around the ascending aorta to measure aortic flow (AoF). A small segment of the proximal part of the left anterior descending coronary artery (LADCA) was dissected free for later placement of an atraumatic clamp. Pacing wires were attached to the right atrial appendage and connected to a pacing stimulator (Grass S9, Quincy, Mass., USA). Rectal temperature was maintained between 37°C and 38°C using external heating pads, warming of the saline infusion and coverage of the animal with blankets.

To measure regional area changes over the cardiac cycle, two sets of ultrasonic crystals (diameter 2.5 mm; 7.5 MHz; Triton Technology Inc., San Diego, CA, USA) were implanted in the midmyocardium of the distribution area of the LADCA, at approximately one-third of the distance from apex to base. Two other pairs of crystals were implanted in the distribution area of the left circumflex coronary artery (LCXCA), at approximately half the distance between apex and base. Each pair of crystals was placed at an individual distance of 10 mm. One pair was positioned in the direction of the LV outflow tract (as determined visually) while the other pair was placed in the perpendicular direction. The position of the crystals was verified at the end of each experiment. To monitor LV diameter, ultrasonic crystals (diameter 6 mm; 5 MHz; Triton) were positioned in the midmyocardium of the anterior LV wall close to the segment length crystals and in the posterior wall at a position with optimal signal intensity.

Experimental protocol

After a 30-45 min stabilization period, steady-state recordings were made of systemic hemodynamic variables and parameters describing regional myocardial function. These recordings were followed by inflation of the balloon located in the inferior caval vein over a period of 15 s to create a series of 20-25 beats with a gradual reduction of end-systolic LV pressure of approximately 50-60 mmHg (2). The respirator was switched off during the inflation to avoid respiration-induced artifacts. This procedure is sufficiently short to prevent reflex-mediated changes in contractility (2, 44).

Subsequently, heart rate was lowered below 70 beats·min⁻¹ by infusion of zatebradine (36) and set at 85 beats·min⁻¹ with an external pacemaker. After all measurements were repeated, the heart rate was subsequently increased to 100, 115, and 130 beats·min⁻¹. After recovery from the pacing protocol, an infusion of 1 µg·kg⁻¹·min⁻¹ of dobutamine (low dose) was started and the pacing protocol was repeated. The infusion rate of dobutamine was then increased to 2 µg·kg⁻¹·min⁻¹ (high dose) and the pacing protocol was repeated. Myocardial stunning was then induced by occluding the LADCA twice for 10 min, separated by 10 min of reperfusion. Thirty min after the second occlusion, the pacing protocol was repeated in the absence and presence of the two doses of dobutamine. This model provides a stable degree of stunning for at least 3.5 hours (5).

At the end of each experiment, the myocardium inside the segment crystals in both LADCA and LCXCA regions was dissected and weighed.

Data acquisition and analysis

Hemodynamic signals, global LV diameter and the regional segment length signals were digitized (sample rate 125 Hz) with a 12 bit AD converter implemented in an AT-based personal computer (AT-CODAS, Keithley Instruments B.V., Gorinchem, The Netherlands) and stored on disk for off-line analysis. Mean arterial pressure (MAP),

maximal LV pressure rise ($LVdP/dt_{max}$), LV end-diastolic pressure (LVP_{ed}), cardiac output (CO), and systemic vascular resistance (SVR) were calculated following standard procedures. LV wall stress (σ , $N \cdot m^{-2}$) and strain (ϵ , dimensionless) were calculated off-line applying formulae as described before (44).

End-systolic stress-strain relationships were determined by fitting LV end-systolic stress-strain points using an iterative algorithm, as described before (46). In brief, elastance was defined as $\sigma/(\epsilon - \epsilon_0)$ in which ϵ_0 is the strain at zero wall stress. Firstly, ϵ_0 was set to zero and elastance was calculated. End-systolic stress-strain points were determined for each heart beat as the point at which elastance was maximal. A new ϵ_0 was calculated using an extrapolation from a linear least-squares fit to the above-determined end-systolic points. The new ϵ_0 value was used as a start for a new cycle as described above. This procedure was repeated until ϵ_0 did not change more than 1%, resulting in a series of end-systolic stress (σ_{es} , $N \cdot m^{-2}$) and end-systolic strain (ϵ_{es} , dimensionless) points.

As the end-systolic stress-strain relationships were often curvilinear, the end-systolic points were also fitted to second and third order polynomial regression equations: $\sigma = c_1 \cdot \epsilon^2 + c_2 \cdot \epsilon + c_3$ and $\sigma = c_4 \cdot \epsilon^3 + c_5 \cdot \epsilon^2 + c_6 \cdot \epsilon + c_7$, using a least-squares technique, and the best fit was selected as described before (44). The (local) slope of the end-systolic stress-strain relationship, called the end-systolic elastance (E_{es} , kPa) was used as an index of contractility. For each experiment at baseline condition, the stress at a LV pressure of 70 mmHg was calculated. If a non-linear stress-strain relationship was selected, E_{es} was calculated as the slope at this stress.

End-diastole was defined as the point at which $LVdP/dt$ decreased below 250 $mmHg \cdot sec^{-1}$ going backwards from peak $LVdP/dt_{max}$. The area inside the LV stress-strain loop during a single heartbeat was determined as the external work of the myocardial region (EW, $J \cdot m^{-3}$), normalized per unit of wall volume. External Power (EP, $J \cdot m^{-3} \cdot s^{-1}$) was calculated as $EW \cdot HR/60$. Stress-Strain Area (SSA, $J \cdot beat^{-1} \cdot m^{-3}$), the regional equivalent of the pressure-volume area, an index of total ventricular work, was calculated as the area enclosed by the end-systolic and end-diastolic relations and the systolic trajectory of stress-strain loop (21, 42). The regional efficiency of energy transfer (EET, %) was calculated as $(EW/SSA) \cdot 100\%$.

Statistics

To test the influence of heart rate, dobutamine and stunning on the hemodynamic parameters and on the regional contractile and energetic parameters, a three-way analysis of variance (ANOVA) for repeated measures was performed (SPSS, version 10, SPSS inc., Chicago, Illinois, USA). The regional contractile and energetic parameters were tested for the LADCA and LCXCA regions separately.

Next, regression analysis was performed on E_{es} and EP as a function of heart rate for the entire data set. The slope of the regression equation is a measure for the level of the force-

frequency effect. The effect of dobutamine, stunning and their interaction on the regression equation was evaluated with dummy variables for stunning, dobutamine dose, and their interaction. A two-step approach was used. In the first step, dummies signifying changes in offset and dummies signifying changes in slope were applied for each intervention. If both dummies resulted in an overspecified system, we selected in the second step one of the dummies depending on the highest absolute t-value. Furthermore, each animal was encoded with a dummy variable (40).

All data have been expressed as mean \pm SEM. Changes were tested for significance at the $P < 0.05$ level. In the RESULTS section only significant ($P < 0.05$) changes are mentioned.

Results

Systemic hemodynamics (Table 1)

Raising heart rate from 85 to 130 beats·min⁻¹ during baseline conditions increased MAP and CO up to 13% and decreased LVP_{ed} up to 35% at the highest heart rate, while LVdP/dt_{max} and SVR remained unchanged. The infusion of dobutamine increased, dose dependently, MAP (up to 14% for the highest dose), LVdP/dt_{max} (up to 152%), and CO (up to 28%). Due to the larger increase in CO compared to MAP, SVR decreased up to 15%.

Stunning of the LADCA region reduced MAP (9%), LVdP/dt_{max} (8%), and CO (15%). Furthermore, stunning completely counteracted the effect of dobutamine on MAP and attenuated the effect of dobutamine on LVdP/dt_{max} (62% of the increase before stunning).

Regional function and regional energetic parameters

LADCA perfusion area (Table 2)

Raising heart rate from 85 to 130 beats·min⁻¹ before stunning increased E_{cs} by a maximum of 41%, ($P = 0.08$ when the analysis was performed on the data before and after stunning). As we expected a different effect of heart rate on E_{cs} before and after stunning, we also tested the effect of heart rate and dobutamine on the data before and after stunning separately. Heart rate then increased E_{cs} ($P = 0.002$) before stunning. In addition, at the highest pacing rate SSA (19%) and EW (19%) both decreased. Infusion of dobutamine increased E_{cs} dose-dependently (111% for the highest dose), which was associated with increases in SSA (up to 39%) and EW (up to 51%).

Regional myocardial stunning reduced E_{cs} up to 51% and increased ϵ_0 up to 15%. If the influence of heart rate and dobutamine were tested on the data after stunning alone, heart rate did not affect E_{cs} ($P = 0.717$), while dobutamine did ($P < 0.001$). The decreased

Table 1. Systemic Hemodynamics during pacing and infusion of dobutamine in anesthetized pigs before and during stunning of the LADCA region (n=9).

	Pacing rate	Baseline			Stunning		
		Control run	Dobutamine low dose	Dobutamine high dose	Control run	Dobutamine low dose	Dobutamine high dose
MAP*†‡¶ (mmHg)	85	85±4	94±5	97±6	79±5	85±6	78±6
	100	92±4	100±5	101±5	86±5	85±5	86±5
	115	93±3	102±5	105±4	85±5	86±4	86±4
	130	96±5	103±5	103±5	87±4	89±4	90±9
LVdP/dt _{max} †‡¶ (mmHg/s)	85	1440±90	2460±220	3280±290	1360±140	1870±160	2300±200
	100	1460±80	2510±180	3320±250	1410±120	1840±190	2760±350
	115	1430±60	2460±170	3610±350	1320±120	1910±220	2680±310
	130	1420±60	2370±170	3380±230	1380±90	1970±270	2630±390
LVP _{ed} * (mmHg)	85	9.5±1.6	10.0±1.9	11.9±1.7	12.0±1.7	11.8±2.3	11.2±2.1
	100	8.9±1.6	9.2±1.9	11.0±1.6	11.3±1.9	10.2±2.0	10.1±2.0
	115	8.5±1.7	8.5±1.7	9.2±1.8	9.4±1.6	9.2±1.8	8.9±1.9
	130	7.6±1.5	7.4±1.7	7.7±1.8	8.8±1.5	8.6±1.8	7.5±2.3
CO*†‡ (l/min)	85	2.7±0.2	3.1±0.2	3.4±0.2	2.3±0.2	2.7±0.2	2.6±0.3
	100	2.9±0.2	3.3±0.2	3.7±0.3	2.5±0.2	2.8±0.2	2.9±0.2
	115	3.0±0.2	3.4±0.2	3.7±0.2	2.6±0.2	2.8±0.2	3.0±0.2
	130	3.0±0.3	3.5±0.2	3.7±0.3	2.8±0.3	2.9±0.2	3.2±0.2
SVR† (mmHg·min ⁻¹)	85	34±4	32±3	30±3	45±9	33±4	32±5
	100	34±4	32±3	29±3	37±4	32±3	31±3
	115	33±3	31±3	29±3	35±3	32±3	30±3
	130	34±3	30±3	29±3	34±3	32±3	31±3

MAP, mean arterial pressure; LVdPdt_{max}, maximum rate of left ventricular (LV) pressure rise; LVP_{ed}, LV end-diastolic pressure; CO, cardiac output; SVR, systemic vascular resistance. Dobutamine was infused intravenously at a rate of 0 (Control run), 1 (low dose) and 2 μg kg⁻¹min⁻¹ (high dose). * P < 0.05 heart rate effect; † P < 0.05 dobutamine effect. ‡ P < 0.05 stunning effect; § P < 0.05 interaction between heart rate effect and dobutamine effect; ¶ P < 0.05 interaction between heart rate effect and stunning effect; # P < 0.05 interaction between dobutamine effect and stunning effect; & P < 0.05 interaction between heart rate effect, dobutamine effect and stunning effect. Values are mean±SEM.

contractility was accompanied by a decrease in EW (up to 56%). Induction of stunning induced a diminishing effect of dobutamine on ε₀ (up to 5% for the highest dose) and σ_{es} (up to 19%).

Table 2. Regional function and energetic parameters of the LADCA region during pacing and infusion of dobutamine in anesthetized pigs before and during stunning of the LADCA region (n=9).

	Pacing rate	Baseline			Stunning		
		Control run	Dobutamine low dose	Dobutamine high dose	Control run	Dobutamine low dose	Dobutamine high dose
$E_{es} \dagger \ddagger$ (kPa)	85	151±20	257±31	319±42	103±20	118±20	184±61
	100	173±24	309±45	351±51	87±16	121±16	191±17
	115	201±28	336±45	391±39	82±18	118±14	180±19
	130	199±25	362±39	407±51	83±19	105±11	257±49
$\epsilon_0 \dagger \ddagger \S$ (dimensionless)	85	0.81±0.02	0.80±0.02	0.81±0.02	0.90±0.02	0.85±0.01	0.86±0.02
	100	0.81±0.02	0.81±0.02	0.81±0.02	0.92±0.03	0.88±0.03	0.87±0.03
	115	0.81±0.02	0.81±0.02	0.81±0.02	0.93±0.03	0.89±0.03	0.88±0.03
	130	0.82±0.02	0.81±0.02	0.80±0.03	0.94±0.04	0.89±0.03	0.89±0.03
$\sigma_{es} \parallel$ (10^3 N/m ²)	85	13.0±1.4	13.8±1.4	14.4±1.4	14.9±1.9	14.0±1.4	13.6±1.8
	100	13.8±1.4	14.4±1.5	15.0±1.7	16.5±1.8	15.0±1.7	14.0±1.7
	115	13.4±1.6	13.8±1.4	13.4±1.7	15.9±1.8	13.9±1.8	13.5±1.7
	130	14.0±1.7	13.7±1.4	14.5±1.6	16.2±1.8	14.5±1.8	13.2±1.8
SSA*†	85	20.8±3.0	24.0±3.6	28.1±4.0	13.1±2.1	18.1±2.4	18.6±3.1
(10^2 J/m ³)	100	20.0±3.1	23.4±3.4	27.8±4.4	14.2±2.2	17.0±2.4	19.4±3.2
	115	18.0±3.3	20.7±3.0	22.0±4.1	11.2±2.1	13.7±2.2	16.2±2.4
	130	18.5±3.5	19.5±3.0	24.3±4.9	9.6±1.4	13.2±2.0	13.7±2.5
EW*†‡	85	17.0±2.5	20.1±3.1	24.3±3.5	9.6±1.9	13.9±2.3	15.8±3.2
(10^2 J/m ³)	100	16.1±2.7	19.7±3.0	24.3±4.0	9.8±1.9	12.9±2.0	16.1±2.5
	115	13.9±2.7	16.8±2.5	19.1±3.7	7.4±1.6	9.8±1.8	13.7±2.1
	130	14.4±3.0	16.3±2.6	20.2±3.6	6.4±1.3	8.7±1.7	11.1±2.3
EP†‡§	85	24.1±3.6	28.4±4.4	34.5±5.0	13.6±2.8	19.6±3.3	22.4±4.5
(10^2 J·m ⁻³ ·s ⁻¹)	100	26.8±4.5	32.9±4.9	40.6±6.6	16.7±3.5	21.4±3.3	26.8±4.2
	115	26.6±5.3	32.2±4.7	36.6±7.0	14.8±3.4	18.9±3.5	26.3±4.1
	130	31.2±6.5	35.3±5.5	43.7±7.7	13.8±3.3	18.8±3.6	23.7±4.3
EET*	85	81±1	83±1	86±3	70±7	74±4	82±4
(%)	100	79±2	84±1	87±2	66±7	74±4	83±2
	115	76±2	81±2	86±2	63±8	70±6	84±3
	130	77±2	83±2	85±3	63±9	63±8	78±7

E_{es} , end systolic elastance; ϵ_0 , strain at zero wall stress; σ_{es} , end systolic stress; SSA, stress-strain area; EW, external work; EP, external power; EET, efficiency of energy transfer. Dobutamine was infused intravenously at a rate of 0 (Control run), 1 (low dose) and 2 $\mu\text{g kg}^{-1}\text{min}^{-1}$ (high dose). * $P < 0.05$ heart rate effect; † $P < 0.05$ dobutamine effect. ‡ $P < 0.05$ stunning effect; § $P < 0.05$ interaction between heart rate effect and dobutamine effect; || $P < 0.05$ interaction between heart rate effect and stunning effect; ¶ $P < 0.05$ interaction between dobutamine effect and stunning effect; # $P < 0.05$ interaction between heart rate effect, dobutamine effect and stunning effect. Values are mean±SEM.

Table 3. Regional function and energetic parameters of the LCXCA region during pacing and infusion of dobutamine in anesthetized pigs before and during stunning of the LADCA region (n=9).

	Pacing rate	Baseline			Stunning		
		Control run	Dobutamine low dose	Dobutamine high dose	Control run	Dobutamine low dose	Dobutamine high dose
E_{es}^* (kPa)	85	227±40	287±50	315±73	181±46	266±67	284±74
	100	244±43	302±64	343±80	211±49	281±66	319±78
	115	251±40	321±70	410±105	219±53	298±72	358±80
	130	267±40	336±64	390±95	214±52	329±82	356±93
$\epsilon_0^{*\dagger}$ (dimensionless)	85	0.85±0.02	0.84±0.02	0.84±0.02	0.86±0.03	0.84±0.02	0.85±0.03
	100	0.85±0.02	0.84±0.02	0.85±0.02	0.87±0.02	0.86±0.02	0.85±0.02
	115	0.85±0.02	0.85±0.02	0.83±0.02	0.87±0.02	0.86±0.02	0.85±0.02
	130	0.86±0.02	0.85±0.02	0.85±0.02	0.87±0.02	0.86±0.02	0.86±0.02
σ_{es} (10^3 N/m ²)	85	12.6±1.3	13.9±1.8	14.5±1.8	12.7±1.4	13.8±1.6	12.5±1.3
	100	13.6±1.6	14.2±1.8	15.0±1.7	13.9±1.4	13.3±1.4	12.6±1.4
	115	13.1±1.7	14.0±1.8	13.3±1.8	13.4±1.4	12.6±1.3	12.1±1.3
	130	13.9±1.9	13.9±1.8	14.7±1.8	13.6±1.4	13.2±1.4	10.9±1.3
SSA ^{*†‡§} (10^2 J/m ³)	85	14.1±1.8	17.5±2.5	20.2±3.2	11.6±3.1	13.5±2.3	13.3±3.4
	100	13.8±1.8	17.3±2.5	19.5±2.7	11.1±2.2	11.7±2.2	12.6±2.0
	115	11.2±1.5	15.3±2.3	16.0±2.4	9.5±1.8	10.1±1.8	11.1±1.7
	130	11.2±1.5	13.3±1.9	15.8±2.4	8.9±1.6	9.5±1.6	8.8±1.8
EW ^{*†‡§} (10^2 J/m ³)	85	10.1±1.5	14.0±2.0	16.9±2.9	7.7±2.2	10.4±2.1	10.9±3.0
	100	9.7±1.3	14.0±2.1	16.5±2.6	7.3±1.6	8.7±1.8	10.4±1.8
	115	7.5±1.1	12.2±1.8	13.3±2.1	6.1±1.3	7.3±1.5	9.1±1.6
	130	6.9±1.0	10.3±1.5	12.8±2.2	5.2±1.1	6.6±1.3	7.0±1.6
EP ^{*†‡} (10^2 J·m ⁻³ ·s ⁻¹)	85	14.3±2.1	19.9±2.9	24.0±4.1	10.9±3.2	14.8±2.9	15.4±4.3
	100	16.2±2.2	23.3±3.5	27.6±4.3	11.4±3.0	14.5±3.1	17.3±3.0
	115	14.4±2.1	23.4±3.5	25.6±4.1	11.1±2.7	14.0±2.9	17.5±3.0
	130	15.0±2.2	22.4±3.2	27.7±4.7	10.4±2.6	14.4±2.9	15.1±3.4
EET ^{*†‡} (%)	85	71±3	80±2	83±2	64±3	74±4	79±3
	100	70±2	80±3	84±2	63±4	71±3	81±2
	115	67±3	79±2	82±2	61±3	69±3	81±2
	130	61±4	78±3	80±3	54±4	67±4	76±3

E_{es} , end systolic elastance; ϵ_0 , strain at zero wall stress; σ_{es} , end systolic stress; SSA, stress-strain area; EW, external work; EP, external power; EET, efficiency of energy transfer. Dobutamine was infused intravenously at a rate of 0 (Control run), 1 (low dose) and 2 $\mu\text{g kg}^{-1}\text{min}^{-1}$ (high dose). * P < 0.05 heart rate effect; † P < 0.05 dobutamine effect. ‡ P < 0.05 stunning effect; § P < 0.05 interaction between heart rate effect and dobutamine effect; || P < 0.05 interaction between heart rate effect and stunning effect; ¶ P < 0.05 interaction between dobutamine effect and stunning effect; # P < 0.05 interaction between heart rate effect, dobutamine effect and stunning effect. Values are mean±SEM.

LCXCA perfusion area (Table 3)

In the LCXCA perfusion area, increasing heart rate increased E_{es} by a maximum of 24%. In addition, the decreased LV filling at increasing heart rate decreased SSA by 21% and EW by 32%. Again, the larger decrease in EW caused a decrease in EET (up to 14%). Infusion of dobutamine increased SSA (up to 43% for the highest dose), EW (up to 86%), and EET (up to 31%). Moreover, dobutamine attenuated the heart rate effect on EW (from 32% to 24%). Induction of LADCA stunning decreased EW (up to 25%) and EET (up to 11%).

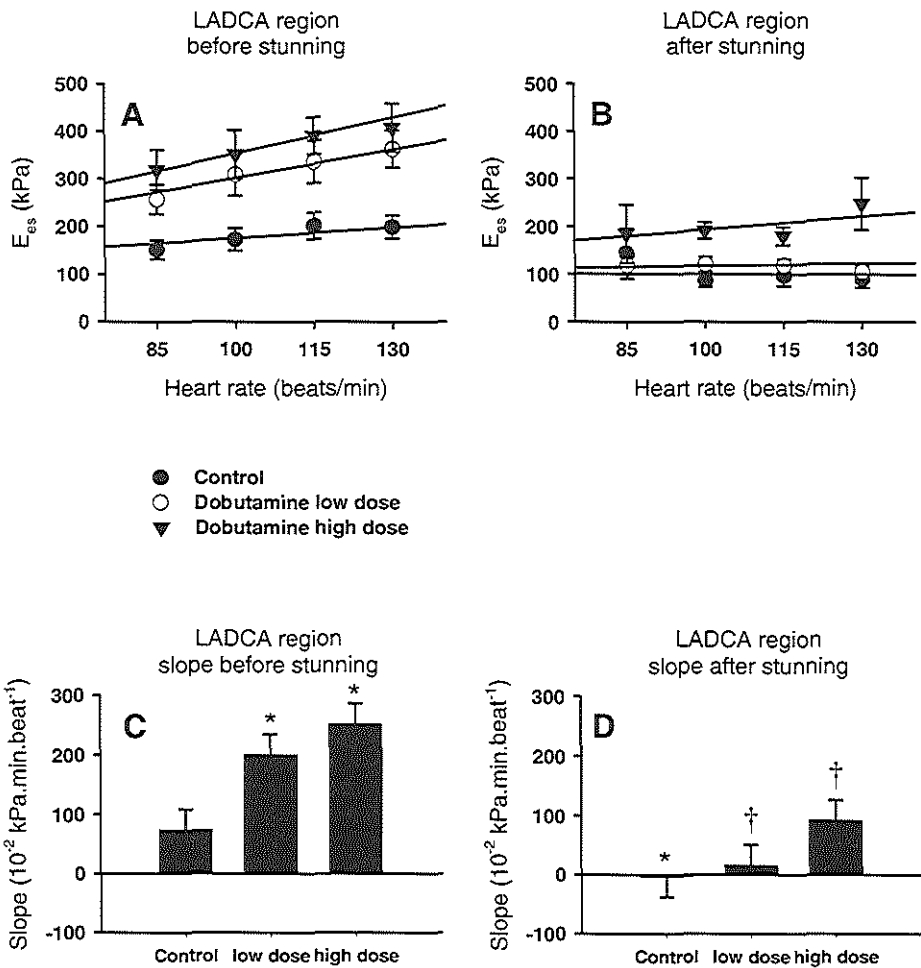


Fig. 1 Relationship between end-systolic elastance (E_{es}) and heart rate (HR) of the LADCA perfusion area. Before and after stunning (panels A and B) and the slopes of this relationship (panels C and D). * $P < 0.05$ vs. Control run before stunning, † $P < 0.05$ vs. Control run after stunning. Dobutamine low dose: $1 \mu\text{g}\cdot\text{kg}^{-1}\cdot\text{min}^{-1}$, high dose: $2 \mu\text{g}\cdot\text{kg}^{-1}\cdot\text{min}^{-1}$.

The influence of dobutamine and myocardial stunning on the force-frequency effect.

Contractility

Increasing heart rate caused a positive force-frequency response in the LADCA region during baseline conditions: $E_{cs} = 0.73 \cdot HR + 102$ ($r^2=0.72$, $P<0.001$; Figure 1A). Dobutamine increased the slope of the E_{cs} versus HR relationship dose-dependently by 172% and 243%, respectively (Figure 1). Stunning of the LADCA region not only abolished the positive force-frequency relationship (Figure 1B), but also significantly attenuated the dobutamine-induced increases in the slope of the E_{cs} versus HR relationship (14% and 53% of the original increases, respectively, $P=0.001$, Figure 1B and 1D).

In the LCXCA region, there was also a positive force-frequency relationship before stunning: $E_{cs} = 1.26 \cdot HR + 143$ ($r^2=0.83$, $P<0.001$). The slope of this relationship was not significantly different from the slope of the LADCA region ($P=0.569$), the intercept was significantly larger, however ($P<0.001$). Infusion of the two doses of dobutamine increased the force-frequency response, as the slope increased by 56% and 90%, respectively. Stunning the LADCA region had no effect on this relationship, while dobutamine again tended to increase the slope by 22% for the low dose and significantly increased the slope by 103% at the highest dose. These increases were not significantly different from before stunning.

External Power

External power displayed a positive force-frequency response in the LADCA region: $EP = 0.102 \cdot 10^2 \cdot HR + 16.4 \cdot 10^2$ ($r^2=0.82$, $P<0.001$, Figure 2A). During infusion of dobutamine the slope of the EP versus HR relation did not change while the intercept increased dose-dependently up to 59%. Stunning abolished the positive force-frequency relationship (Figure 2B), but infusion of dobutamine restored the positive relationship again, dose-dependently to 45% and 72% of the slope at baseline (Figure 2B and 2D).

In the LCXCA region, EP failed to show a positive relationship with heart rate before stunning. During the infusion of the low dose of dobutamine a positive relationship became apparent: $EP = 0.070 \cdot 10^2 \cdot HR + 14.7 \cdot 10^2$ ($r^2=0.83$, $P<0.001$), while during infusion of the high dose the intercept increased (by 75%). Stunning the LADCA region decreased the intercept of the EP-HR relation in the LCXCA region by 25%, while after stunning dobutamine increased the intercept dose-dependently by 27% and 48%, respectively.

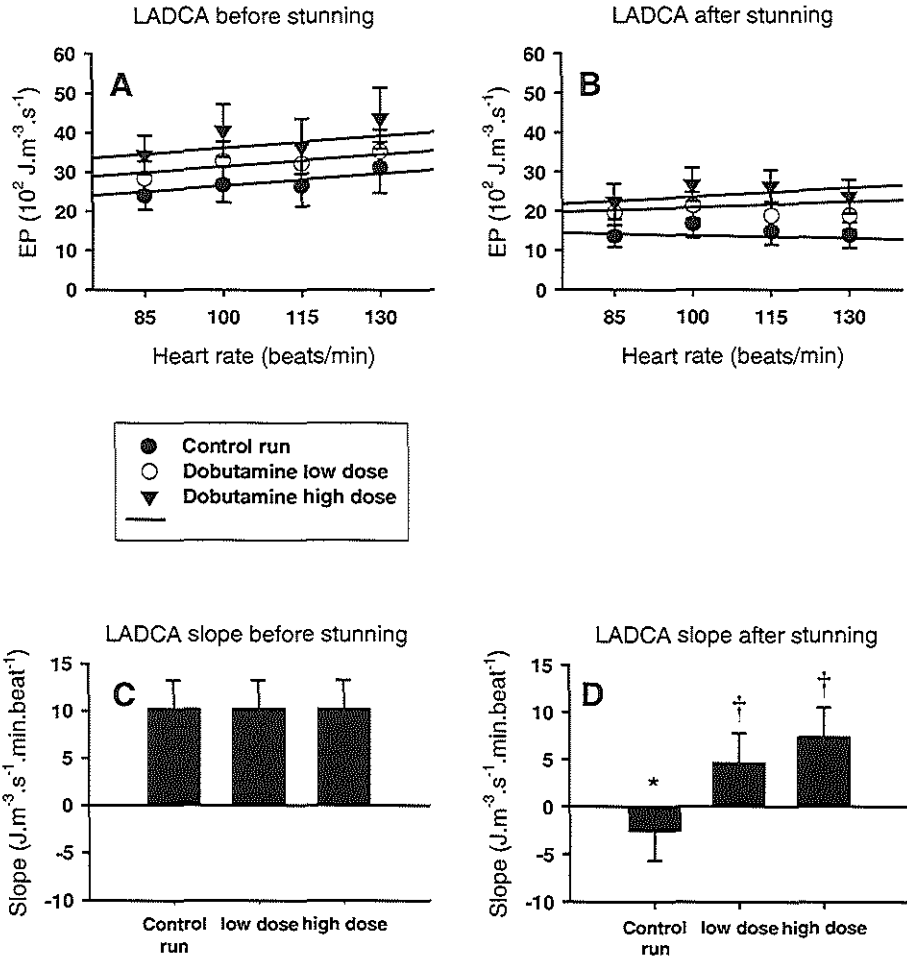


Fig. 2 Relationship between External Power (EP) and heart rate (HR) of the LADCA perfusion area. Before and after stunning (panels A and B) and the slopes of this relationship (panels C and D). * $P < 0.05$ vs. Control run before stunning, † $P < 0.05$ vs. Control run after stunning. Dobutamine low dose: $1 \mu\text{g}\cdot\text{kg}^{-1}\cdot\text{min}^{-1}$, high dose: $2 \mu\text{g}\cdot\text{kg}^{-1}\cdot\text{min}^{-1}$.

Discussion

The present study describes the influence of stunning on the (regulation of) the myocardial force-frequency effect. The major findings of the present study may be summarized as follows: (i) Regional contractile function (end-systolic elastance), increased by 41% with increasing heart rate from 85 to 130 beats/min ('positive force-frequency effect'). Dobutamine enhanced the positive force-frequency effect dose-

dependently. (ii) In stunned myocardium the positive force-frequency effect was abolished, and the response to dobutamine was attenuated compared to normal myocardium. The present findings will be discussed with respect to the literature and the underlying mechanism.

The force-frequency effect has been studied extensively in exercise and during heart failure, but only a few studies have focussed on the modulating effect of myocardial stunning (18, 37). One of these studies (18) was performed in atrial tissue *in vitro*, which is different from LV tissue in terms of SERCA2-activity and level of phospholamban phosphorylation (31). The other study (37) used external power to assess the force-frequency effect, which is dependent upon pre- and afterload. Changes in loading conditions are especially important in myocardial stunning, as several studies indicated that regional loading (stress and circumference) changes with regional myocardial stunning (3, 38). In a previous study we have shown that the afterload-dependency of EW (and therefore of EP) increases due to myocardial stunning (44). To show the difference between a regionally load-dependent and a regionally load-independent parameter in a single animal we evaluated the effect of heart rate on regional external power (EP). We indeed observed a difference in response of E_{cs} to heart rate and dobutamine compared to EP. In addition, in the LCXCA region EP failed to show a positive relationship with heart rate, while E_{cs} showed consistent results in response to heart rate and dobutamine for both the LADCA and LCXCA regions. Therefore, these data suggest that both the type of tissue under study and the load-dependency of the parameters may affect the stunning-induced changes in the force-frequency effect. As we used a load-independent parameter, the present findings are in accordance with an intrinsic myocardial dysfunction.

Underlying mechanism

Contractile function depends upon the calcium sensitivity of the myofibrils and the availability of the activator calcium. The former has been associated with the function of the actin-myosin complex (34) while the latter depends on the capacity of the SR to sequester and release calcium (33).

Myofibrillar calcium sensitivity

As we did not measure myofibrillar calcium sensitivity, we cannot exclude that part of the decrease in contractility was caused by a decrease in myofibrillar calcium sensitivity. Moreover, in the past we showed that drugs which increased the calcium sensitivity of the myofibrils, restored the contractile disturbances in stunned myocardium (7, 41). However, the force-frequency effect has repeatedly been related to calcium transients and SR function (4, 10, 16). Hence, the decrease in the force-frequency effect and the decreased responsiveness of the force-frequency effect to dobutamine can probably not be explained by a decreased calcium sensitivity.

Table 4. Overview of the literature concerning measurement of SR Ca²⁺-uptake in stunned myocardium.

Article	Ca ²⁺ -uptake	Ischemia (min)	Heart rate		Experimental protocol	Biochemical method
			Bl	Rep		
1. Feher, <i>Circ Res</i> , 1989, 65: 1400-1408	~88% of baseline	30	333	289?	Langendorff rat hearts	myocardial homogenate
2. Limbruno, <i>JMCC</i> , 1989, 21: 1063-1072	72% of baseline	10	296	309	Langendorff rat hearts	isolated SR vesicles
3. Rehr, <i>Am Heart J</i> , 1991, 122: 1257-1269	unchanged	15	114	115	open-chest dogs	myocardial homogenate
4. Davis, <i>Circ Res</i> , 1992, 70: 163-171	~66% of baseline	15	339	295	Langendorff rat hearts	myocardial homogenate
5. Kaplan, <i>Circ Res</i> , 1992, 71: 1123-1130	unchanged	15	143	123	Langendorff rabbit hearts	myocardial homogenate
6. Lamers, <i>Cardiovasc Res</i> , 1993, 27: 520-524	117% of baseline	2*10	109	115	open chest swine	isolated SR vesicles
7. Krause, <i>Circ Res</i> , 1989, 65: 526-530	83% of baseline	(8-12)*5	126	128	open chest dogs	isolated SR vesicles
8. Zucchi, <i>Circ Res</i> , 1994, 74: 271-280	unchanged	20+30	277	260	Langendorff rat hearts	myocardial homogenate
9. Abdelmeguid, <i>Am J Physiol</i> , 1994, 266: 406-414	unchanged	10+15	300	262	Langendorff rat hearts	myocardial homogenate
10. Valdivia, <i>Am J Physiol</i> , 1997, 273: H796-H804	63% of baseline	10	91	108	open chest swine	isolated SR vesicles
11. Liu, <i>Ann Thorac Surg</i> , 1993, 56: 1154-1159	unchanged	120 cardioplegia		120	in situ isolated pig hearts	isolated SR vesicles
12. Krause, <i>Circulation</i> , 1991, 84: 1378-1383	80% of baseline	15	161	148	Langendorff rabbit hearts	myocardial homogenate and isolated SR vesicles
13. Xu, <i>Ann NY Acad Sci</i> , 1998, 853: 376-379	52% of baseline	20	?	?	Langendorff rabbit hearts	isolated SR vesicles
14. Wu, <i>JMCC</i> , 1996, 28: 943-955	56% of baseline	20	?	?	Langendorff rat hearts	myocardial homogenate
15. Krause, <i>Am J Physiol</i> , 1991, 261: H229-H235	78-81% of baseline	15	?	?	Langendorff rabbit hearts	myocardial homogenate and isolated SR vesicles
16. Mubagwa, <i>Fund Clin Pharm</i> , 1997, 11: 315-321	unchanged	15	?	?	Langendorff rat hearts	myocardial homogenate
17. Flameng, <i>J Card Surg</i> , 1993, 8(suppl): 275-278	unchanged	15	?	?	Langendorff rabbit hearts	myocardial homogenate

Bl, baseline, Rep, reperfusion

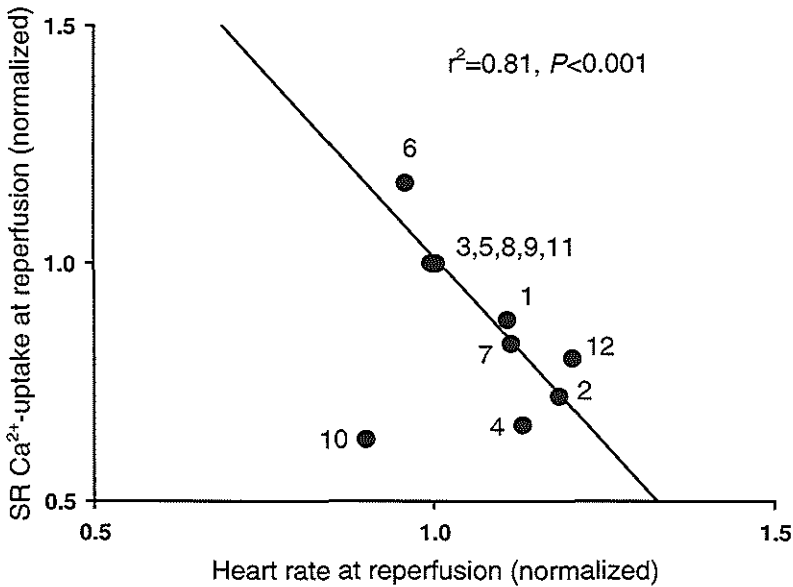


Fig. 3 Relationship between normalized Ca^{2+} -uptake of the sarcoplasmic reticulum and heart rate at reperfusion of the studies presented in Table 4 from which heart rate could be determined. For each species, unchanged SR Ca^{2+} -uptake and the heart rate at which unchanged SR Ca^{2+} -uptake occurred were set at 1. Numbers refer to the articles in Table 4.

Calcium cycling

To evaluate the possibility that decrements in calcium cycling underlie, at least partially, the decreased contractile function in stunned myocardium, we evaluated the effect of heart rate on SR Ca^{2+} -uptake of stunned myocardium from data published in the literature. A decreased SR Ca^{2+} uptake (6, 9, 22, 23, 27, 45, 48, 49), as well as an unchanged (1, 20, 28, 30, 35, 50) or even slightly increased Ca^{2+} -uptake (26) have been reported (Table 4). These equivocal findings were difficult to explain by differences in biochemical methods, species or protocols to produce stunning (Table 4). However, if we related the normalized stunning-induced changes in SR Ca^{2+} -uptake with the normalized heart rates at reperfusion (Figure 3, see legend for further explanation), a negative relationship was detected ($r^2 = 0.81$, $P < 0.001$). This finding may be explained by the hypothesis that stunning-induced changes in calcium transients are heart rate-dependent.

In previous studies, it has been shown that calcium transients were unaffected after induction of stunning. The authors argued that myofibrillar calcium sensitivity had to be decreased to explain the decrease of contractile function (11, 25). However, the calcium transients in those studies were measured at 48-84 beats/min in ferret hearts (25) and at 30 beats/min in rat myocardium (11), both far below the normal heart rates for these species. The unchanged systolic calcium transient found in these studies may have been

masked by these low heart rates. It has been shown in phospholamban knock-out and transgenic mice that the force-frequency effect is regulated by the SERCA2-phospholamban interaction (4, 17, 19), findings which have recently been confirmed in human tissue (31). Dobutamine changes the interaction between SERCA2 and phospholamban through a cyclic AMP-dependent relief of the phospholamban-inhibition on SERCA2 by inducing Ser¹⁶ phosphorylation of phospholamban (15, 36). Therefore, we modulated the interaction between SERCA2 and phospholamban with dobutamine and compared the effect on the force-frequency effect in stunned myocardium to that in normal myocardium. Indeed, dobutamine enhanced the force-frequency effect in normal myocardium, confirming its postulated biochemical effect. More importantly, its effect was significantly reduced in stunned myocardium, suggesting a stunning-induced alteration in the SERCA2-phospholamban interaction. A stunning-induced decrease in β -adrenoreceptor function would also attenuate the effect of dobutamine on the force-frequency effect. However, an increased rather than a decreased responsiveness to isoproterenol has been reported in stunned myocardium which was associated with an increased β -adrenoreceptor density and an unchanged adenylyl cyclase activity (47).

We can only speculate about the mechanism of the alteration in SERCA2-phospholamban interaction. Although the time-course and reversibility of myocardial stunning make proteolysis a possible cause, to the best of our knowledge there are no data available regarding proteolysis of SERCA2 or phospholamban. In contrast, a recent study showed that cAMP and phosphorylation of both phospholamban and troponin-I were decreased in stunned myocardium (29). A decreased phosphorylation of phospholamban increases SERCA2 inhibition, and therefore decreases the force-frequency effect (31). Therefore, decreased levels of cAMP may possibly underlie the present results.

Limitations

We used the posterior-anterior diameter to calculate regional stress in both the LADCA and LCXCA perfusion areas, which is not completely correct for the LCXCA perfusion area, especially after stunning. This diameter may increase after stunning, due to stretch of the LADCA perfusion-area. Consequently, applying the curvature-changes to the LCXCA perfusion area may not be fully correct. However, as induction of stunning increased the end-systolic diameter by less than 7% and did not affect σ_{es} and E_{cs} of the LCXCA perfusion-area, the error introduced was probably small.

Conclusions

In regional myocardial stunning in vivo, the force-frequency effect and the dobutamine-induced modulation of the force-frequency effect were disturbed. These findings, in concert with a survey of the literature, suggest that the stunning-induced

decrease in contractility is correlated with a decreased calcium cycling in addition to a decreased myofibrillar calcium sensitivity.

References

1. Abdelmeguid, A. E., and J. J. Feher. Effect of low perfusate $[Ca^{2+}]$ and diltiazem on cardiac sarcoplasmic reticulum in myocardial stunning. *Am J Physiol* 266: H406-414, 1994.
2. Aversano, T., W. L. Maughan, W. C. Hunter, D. Kass, and L. C. Becker. End-systolic measures of regional ventricular performance. *Circulation* 73: 938-950, 1986.
3. Bavaria, J. E., S. Furukawa, G. Kreiner, M. B. Ratcliffe, J. Streicher, D. K. Bogen, and L. H. Edmunds, Jr. Myocardial oxygen utilization after reversible global ischemia [see comments]. *J Thorac Cardiovasc Surg* 100: 210-220, 1990.
4. Bluhm, W. F., E. G. Kranias, W. H. Dillmann, and M. Meyer. Phospholamban: a major determinant of the cardiac force-frequency relationship. *Am J Physiol Heart Circ Physiol* 278: H249-H255, 2000.
5. Brand, T., H. S. Sharma, K. E. Fleischmann, D. J. Duncker, E. O. McFalls, P. D. Verdouw, and W. Schaper. Proto-oncogene expression in porcine myocardium subjected to ischemia and reperfusion. *Circ Res* 71: 1351-1360, 1992.
6. Davis, M. D., W. Lebolt, and J. J. Feher. Reversibility of the effects of normothermic global ischemia on the ryanodine-sensitive and ryanodine-insensitive calcium uptake of cardiac sarcoplasmic reticulum. *Circ Res* 70: 163-171, 1992.
7. de Zeeuw, S., S. A. Trines, R. Krams, D. J. Duncker, and P. D. Verdouw. In vivo evidence that EMD 57033 restores myocardial responsiveness to intracoronary Ca^{2+} in stunned myocardium. *Eur J Pharmacol* 403: 99-109., 2000.
8. Dietrich, D. L., G. R. van Leeuwen, G. J. Stienen, and G. Elzinga. Stunning does not change the relation between calcium and force in skinned rat trabeculae. *J Mol Cell Cardiol* 25: 541-549, 1993.
9. Feher, J. J., W. R. LeBolt, and N. H. Manson. Differential effect of global ischemia on the ryanodine-sensitive and ryanodine-insensitive calcium uptake of cardiac sarcoplasmic reticulum. *Circ Res* 65: 1400-1408, 1989.
10. Frank, K., B. Bolck, U. Bavendiek, and R. H. Schwinger. Frequency dependent force generation correlates with sarcoplasmic calcium ATPase activity in human myocardium. *Basic Res Cardiol* 93: 405-411, 1998.
11. Gao, W. D., D. Atar, P. H. Backx, and E. Marban. Relationship between intracellular calcium and contractile force in stunned myocardium. Direct evidence for decreased myofilament Ca^{2+} responsiveness and altered diastolic function in intact ventricular muscle. *Circ Res* 76: 1036-1048, 1995.
12. Gao, W. D., D. Atar, Y. Liu, N. G. Perez, A. M. Murphy, and E. Marban. Role of troponin I proteolysis in the pathogenesis of stunned myocardium. *Circ Res* 80: 393-399, 1997.
13. Geyer, M., J. D. Strauss, J. C. Ruegg, and H. Kogler. Ca^{2+} sensitivity of stunned myocardium after skinning using retrograde infusion of detergent. *Pflugers Arch* 438: 470-478, 1999.
14. Goto, Y., H. Suga, O. Yamada, Y. Igarashi, M. Saito, and K. Hiramori. Left ventricular regional work from wall tension-area loop in canine heart. *Am J Physiol* 250: H151-158, 1986.
15. Hagemann, D., M. Kuschel, T. Kuramochi, W. Zhu, H. Cheng, and R. P. Xiao. Frequency-encoding Thr17 phospholamban phosphorylation is independent of Ser16 phosphorylation in cardiac myocytes. *J Biol Chem* 275: 22532-22536, 2000.
16. Hasenfuss, G., H. Reinecke, R. Studer, B. Pieske, M. Meyer, H. Drexler, and H. Just. Calcium cycling proteins and force-frequency relationship in heart failure. *Basic Res Cardiol* 91: 17-22, 1996.
17. Hashimoto, K., N. G. Perez, H. Kusuoka, D. L. Baker, M. Periasamy, and E. Marban. Frequency-dependent changes in calcium cycling and contractile activation in SERCA2a transgenic mice. *Basic Res Cardiol* 95: 144-151, 2000.
18. Iwashiro, K., A. Criniti, R. Sinatra, A. A. Dawodu, G. d'Amati, F. Monti, L. Pannarale, P. Bernucci, G. L. Brancaccio, A. Vetuschchi, E. Gaudio, P. Gallo, and P. E. PuDDu. Felodipine

- protects human atrial muscle from hypoxia-reoxygenation dysfunction: a force-frequency relationship study in an in vitro model of stunning. *Int J Cardiol* 62: 107-132, 1997.
19. **Kadambi, V. J., N. Ball, E. G. Kranias, R. A. Walsh, and B. D. Hoit.** Modulation of force-frequency relation by phospholamban in genetically engineered mice. *Am J Physiol* 276: H2245-H2250, 1999.
 20. **Kaplan, P., M. Hendriks, M. Mattheussen, K. Mubagwa, and W. Flameng.** Effect of ischemia and reperfusion on sarcoplasmic reticulum calcium uptake. *Circ Res* 71: 1123-1130, 1992.
 21. **Krams, R., D. J. Duncker, E. O. McFalls, A. Hogendoorn, and P. D. Verdouw.** Dobutamine restores the reduced efficiency of energy transfer from total mechanical work to external mechanical work in stunned porcine myocardium. *Cardiovasc Res* 27: 740-747, 1993.
 22. **Krause, S. M., W. E. Jacobus, and L. C. Becker.** Alterations in cardiac sarcoplasmic reticulum calcium transport in the postischemic "stunned" myocardium. *Circ Res* 65: 526-530, 1989.
 23. **Krause, S. M., and D. Rozanski.** Effects of an increase in intracellular free $[Mg^{2+}]$ after myocardial stunning on sarcoplasmic reticulum Ca^{2+} transport. *Circulation* 84: 1378-1383, 1991.
 24. **Kusuoka, H., Y. Koretsune, V. P. Chacko, M. L. Weisfeldt, and E. Marban.** Excitation-contraction coupling in postischemic myocardium. Does failure of activator Ca^{2+} transients underlie stunning? *Circ Res* 66: 1268-1276, 1990.
 25. **Kusuoka, H., J. K. Porterfield, H. F. Weisman, M. L. Weisfeldt, and E. Marban.** Pathophysiology and pathogenesis of stunned myocardium. Depressed Ca^{2+} activation of contraction as a consequence of reperfusion-induced cellular calcium overload in ferret hearts. *J Clin Invest* 79: 950-961, 1987.
 26. **Lamers, J. M., D. J. Duncker, K. Bezstarosti, E. O. McFalls, L. M. Sassen, and P. D. Verdouw.** Increased activity of the sarcoplasmic reticular calcium pump in porcine stunned myocardium. *Cardiovasc Res* 27: 520-524, 1993.
 27. **Limbruno, U., R. Zucchi, S. Ronca-Testoni, P. Galbani, G. Ronca, and M. Mariani.** Sarcoplasmic reticulum function in the "stunned" myocardium. *J Mol Cell Cardiol* 21: 1063-1072, 1989.
 28. **Liu, X., R. M. Engelman, Z. Wei, N. Maulik, J. A. Rousou, J. E. d. Flack, D. W. Deaton, and D. K. Das.** Postischemic deterioration of sarcoplasmic reticulum: warm versus cold blood cardioplegia [see comments]. *Ann Thorac Surg* 56: 1154-1159, 1993.
 29. **Luss, H., A. Meissner, N. Rolf, H. Van Aken, P. Boknik, U. Kirchhefer, J. Knapp, S. Laer, B. Linck, I. Luss, F. U. Muller, J. Neumann, and W. Schmitz.** Biochemical mechanism(s) of stunning in conscious dogs. *Am J Physiol Heart Circ Physiol* 279: H176-184, 2000.
 30. **Mubagwa, K., P. Kaplan, and W. Flameng.** The effects of ryanodine on calcium uptake by the sarcoplasmic reticulum of ischemic and reperfused rat myocardium. *Fundam Clin Pharmacol* 11: 315-321, 1997.
 31. **Munch, G., B. Bolck, K. Brixius, H. Reuter, U. Mehlhorn, W. Bloch, and R. H. Schwinger.** SERCA2a activity correlates with the force-frequency relationship in human myocardium. *Am J Physiol Heart Circ Physiol* 278: H1924-1932, 2000.
 32. **Murphy, A. M., H. Kogler, D. Georgakopoulos, J. L. McDonough, D. A. Kass, J. E. Van Eyk, and E. Marban.** Transgenic mouse model of stunned myocardium. *Science* 287: 488-491, 2000.
 33. **Opie, L. H.** Excitation contraction coupling and calcium. In: *The Heart, physiology from cell to circulation* (3d ed.). Philadelphia: Lippincot-Raven Publishers, 1998, p. 149-171.
 34. **Opie, L. H.** Myocardial contraction and relaxation. In: *The Heart, physiology from cell to circulation* (3d ed.). Philadelphia: Lippincot-Raven Publishers, 1998, p. 209-231.
 35. **Rehr, R. B., B. E. Fuhs, J. I. Hirsch, and J. J. Feher.** Effect of brief regional ischemia followed by reperfusion with or without superoxide dismutase and catalase administration on myocardial sarcoplasmic reticulum and contractile function. *Am Heart J* 122: 1257-1269, 1991.
 36. **Ross, J., Jr., T. Miura, M. Kambayashi, G. P. Eising, and K. H. Ryu.** Adrenergic control of the force-frequency relation. *Circulation* 92: 2327-2332, 1995.
 37. **Schad, H., W. Heimisch, G. P. Eising, and N. Mendler.** Effect of milrinone and atrial pacing on stunned myocardium. *Eur J Cardiothorac Surg* 11: 1125-1132, 1997.
 38. **Schulz, R., J. Rose, H. Post, A. Skyschally, and G. Heusch.** Less afterload sensitivity in short-term hibernating than in acutely ischemic and stunned myocardium. *Am J Physiol Heart Circ Physiol* 279: H1106-1110, 2000.

39. Sherman, A. J., F. J. Klocke, R. S. Decker, M. L. Decker, K. A. Kozlowski, K. R. Harris, S. Hedjbeli, Y. Yaroshenko, S. Nakamura, M. A. Parker, P. A. Checchia, and D. B. Evans. Myofibrillar disruption in hypocontractile myocardium showing perfusion-contraction matches and mismatches. *Am J Physiol Heart Circ Physiol* 278: H1320-1334, 2000.
40. Slinker, B. K., and S. A. Glantz. Missing data in two-way analysis of variance. *Am J Physiol* 258: R291-297, 1990.
41. Soei, L. K., L. M. Sassen, D. S. Fan, T. van Veen, R. Krams, and P. D. Verdouw. Myofibrillar Ca^{2+} sensitization predominantly enhances function and mechanical efficiency of stunned myocardium. *Circulation* 90: 959-969, 1994.
42. Suga, H., R. Hisano, S. Hirata, T. Hayashi, O. Yamada, and I. Ninomiya. Heart rate-independent energetics and systolic pressure-volume area in dog heart. *Am J Physiol* 244: H206-214, 1983.
43. Thomas, S. A., J. A. Fallavollita, T. C. Lee, J. Feng, and J. M. Canty, Jr. Absence of troponin I degradation or altered sarcoplasmic reticulum uptake protein expression after reversible ischemia in swine [see comments]. *Circ Res* 85: 446-456, 1999.
44. Trines, S. A., C. J. Slager, J. van der Moer, P. D. Verdouw, and R. Krams. Efficiency of energy transfer, but not external work, is maximized in stunned myocardium. *Am J Physiol Heart Circ Physiol* 279: H1264-1273, 2000.
45. Valdivia, C., J. O. Hegge, R. D. Lasley, H. H. Valdivia, and R. Mentzer. Ryanodine receptor dysfunction in porcine stunned myocardium. *Am J Physiol* 273: H796-804, 1997.
46. van der Velde, E. T., D. Burkhoff, P. Steendijk, J. Karsdon, K. Sagawa, and J. Baan. Nonlinearity and load sensitivity of end-systolic pressure-volume relation of canine left ventricle in vivo. *Circulation* 83: 315-327, 1991.
47. Vatner, D. E., and S. F. Vatner. Physiological and biochemical adrenergic regulation of the stunned myocardium. *Mol Cell Biochem* 186: 131-137, 1998.
48. Wu, Q. Y., and J. J. Feher. Ryanodine perfusion decreases cardiac mechanical function without affecting homogenate sarcoplasmic reticulum Ca^{2+} uptake: comparison with the stunned heart. *J Mol Cell Cardiol* 28: 943-955, 1996.
49. Xu, K. Y., K. Vandegaer, and L. C. Becker. The sarcoplasmic reticulum Ca^{2+} -ATPase is depressed in stunned myocardium after ischemia-reperfusion, but remains functionally coupled to sarcoplasmic reticulum-bound glycolytic enzymes. *Ann N Y Acad Sci* 853: 376-379, 1998.
50. Zucchi, R., S. Ronca-Testoni, G. Yu, P. Galbani, G. Ronca, and M. Mariani. Effect of ischemia and reperfusion on cardiac ryanodine receptors--sarcoplasmic reticulum Ca^{2+} channels. *Circ Res* 74: 271-280, 1994.

Chapter 3

Calcium handling in stunned myocardium

Introduction - We investigated functional parameters of Ca^{2+} -handling in vivo and biochemical parameters in vitro in stunned and non-stunned myocardium, to demonstrate that stunning affects Ca^{2+} -handling in addition to myofibrillar Ca^{2+} -responsiveness.

Methods - Stunning was induced in open-chest pigs ($n=18$) by 15 min LADCA occlusion and 30 min reperfusion. End-systolic elastance (E_{es}) was derived from regional stress-strain relationships at 6 HR's (70-145 beats·min⁻¹). Recirculation fraction (RF, relative contribution of sarcoplasmic reticulum, SR, to total Ca^{2+} -cycling) was determined at 4 HR's (70-115). The force-frequency effect (FFE, slope of the E_{es} -HR relation) and RF ratio ($\text{RFR}_{\text{LCX/LAD}}$) versus HR were evaluated before and during stunning and during infusion of EMD 57033 (E_{es} only, 3.75 mg·kg⁻¹ + 0.03 mg·kg⁻¹·min⁻¹), or ryanodine (1 μg·kg⁻¹).

Results - Before stunning, E_{es} increased from 181 (HR=70) to 262 kPa (HR=145, positive FFE), while RF and $\text{RFR}_{\text{LCX/LAD}}$ were constant at 0.42 and 0.91. Stunning reduced E_{es} (34%, HR=100) and RF (42%), doubled $\text{RFR}_{\text{LCX/LAD}}$, and abolished the positive FFE. EMD 57033 increased E_{es} (36%) without restoring FFE. Ryanodine restored $\text{RFR}_{\text{LCX/LAD}}$ by decreasing non-stunned RF but had no effect on non-stunned FFE. Homogenate SR Ca^{2+} -uptake and Thr¹⁷-phosphorylation of phospholamban were unaffected by HR and stunning.

Conclusions - Stunning decreased FFE and RF, unrelated to a decreased myofibrillar Ca^{2+} -responsiveness, suggesting a disturbance in Ca^{2+} -handling. Because SERCA2 activity and its regulation by phospholamban were unaffected by HR and stunning, and ryanodine mimicked in non-stunned myocardium the stunning-induced decrease of RF but did not affect FFE, we suggest that Ca^{2+} -induced Ca^{2+} -release is disturbed, additional to the decreased myofibrillar Ca^{2+} -responsiveness.

S.A.I.P. Trines, K. Bezstarosti, C.A.G. Smits, J.M.J. Lamers, C.J. Slager, P.D. Verdouw, and R. Krams. Absence of the Force-Frequency Effect in Stunned Myocardium: Evidence for a Disturbed Ca^{2+} -handling. *Submitted*

Introduction

Myocardial stunning has been associated with disturbances in excitation-contraction coupling, but the precise localization of these disturbances remains unclear (1). While it has been demonstrated that a decreased myofibrillar Ca^{2+} -responsiveness explains the contractile dysfunction of stunned myocardium at least partly (3, 17), it was recently observed that also the force-frequency effect (FFE) had disappeared in myocardial stunning (8, 21). The FFE is thought to result from an interplay between a heart rate (HR)-dependent increase of sarcolemmal (SL) Ca^{2+} -influx and sarcoplasmic reticulum (SR) Ca^{2+} -cycling, the latter due to stimulation of the SR Ca^{2+} -release channel and Ca^{2+} -dependent phosphorylation of phospholamban (9, 14, 18, 19). Consequently, the absence of the FFE in stunning may be caused by one or more disturbances in Ca^{2+} -handling. However, the force developed by myocardial tissue does not only depend on the amount of systolic Ca^{2+} , but also on the sensitivity of the myofibrils to Ca^{2+} . Therefore, the FFE may decrease while the underlying heart rate (HR)-dependent increase in Ca^{2+} -cycling remains unchanged. To exclude this possibility *in vivo*, we studied the FFE in myocardial stunning before and after the application of a Ca^{2+} -sensitizer (EMD 57033). If a decreased Ca^{2+} -sensitivity of the myofibrils underlies the disappearance of the FFE in myocardial stunning, EMD 57033 should at least partly restore the FFE.

Subsequently, to distinguish between disturbances in SL Ca^{2+} fluxes and processes located in the interior of the cell, i.e. Ca^{2+} -induced Ca^{2+} -release (CICR) and SR Ca^{2+} -ATPase (SERCA2) function, we also studied the relationship between recirculation fraction (RF) and HR. The RF is a measure of the relative contribution of the internal Ca^{2+} cycling to total Ca^{2+} -cycling (7, 22, 26), and a decreased RF in stunning therefore implies more directly a disturbed Ca^{2+} -handling located downstream of the SL.

If a decrease in RF would be found, this decrease may be due to a disturbance in the CICR downstream of the SL (7), in SERCA2 function and/or in the interaction between SERCA2 and phospholamban (22, 26). Because it has been shown that stunning may decrease the opening-probability of the RyR (25), we administered ryanodine *in vivo* at a dose known to partially open the SR RyR in dogs (10, 20), in an attempt to counteract the effect of stunning. Additionally, to evaluate SERCA2 function and the interaction between SERCA2 and phospholamban, we measured SR Ca^{2+} -uptake at two different Ca^{2+} -concentrations and phosphorylation of phospholamban at Ser¹⁶ and Thr¹⁷ in cardiac homogenates prepared from biopsies taken from the stunned and non-stunned myocardium at two different HR's.

Methods

Instrumentation

In accordance with the "Guiding principles for the care and use of animals" of the American Physiological Society, Crossbred Yorkshire-Landrace pigs (30-41.5 kg, n=18) were anesthetized and ventilated with oxygen and nitrogen, and instrumented for infusion of 10-15 mg·kg⁻¹·h⁻¹ sodium pentobarbital, saline, EMD 57033 (courtesy of P. Schelling, E. Merck, Darmstadt, Germany), ryanodine (Sigma-Aldrich, Zwijndrecht, The Netherlands), and the negative chronotropic agent zatebradine (courtesy of Dr. J.W. Dämmgen, Dr. Karl Thomae, Boehringer Ingelheim KG, Biberach a/d Riss, Germany), and for measurement of aortic and left ventricular (LV) pressure (B. Braun Medical B.V., Uden, The Netherlands) (24). A balloon catheter was positioned in the inferior caval vein and a flow probe (Skalar, Delft, The Netherlands) was placed around the ascending aorta. The left anterior descending coronary artery (LADCA) was dissected for placement of an atraumatic clamp. A pacing stimulator (Grass S9, Quincy, Mass.) was connected to the right atrium. Rectal temperature was maintained between 37°C and 38°C. As described before (24), segment areas and LV diameter were measured using ultrasound crystals implanted in the LADCA and left circumflex coronary artery (LCXCA) regions and in the LV anterior and posterior wall.

Experimental protocol

After 30-45 min of stabilization, HR was lowered below 70 beats·min⁻¹ by zatebradine and measurements of hemodynamics and wall function were made at HR's of 85, 100, 115, 130 or 145 beats·min⁻¹ (in random order). At each HR with the ventilator turned off, LV preload was gradually reduced by inflating the balloon in the inferior caval vein (24). Stunning was produced by a 15 min LADCA occlusion. After 30 min reperfusion in 9 animals (EMD Group), we infused 0.5 mg·kg⁻¹ propranolol followed by 0.5 mg·kg⁻¹·h⁻¹ until the end of the experiment, to curtail the minor phosphodiesterase III inhibiting properties of EMD 57033 by minimizing cAMP availability (2). Subsequently, all measurements were repeated at each HR. Next, 0.25 mg·kg⁻¹·min⁻¹ EMD 57033 for 15 min was followed by 0.03 mg·kg⁻¹·min⁻¹, and measurements were repeated at each HR. In three pilot experiments, the stability of the increase in contractility by this dose was verified at 100 beats·min⁻¹ during 120 min (data not shown). In 9 other animals (Ryanodine group), after 30 min reperfusion, needle biopsies were taken from the LADCA and LCXCA regions at HR's of 70 and 145 beats·min⁻¹ after 5 min of stabilization, and N₂-frozen. Subsequently, measurements were repeated at each HR. Next, 1 µg·kg⁻¹ ryanodine was administered. After 30 min of stabilization, measurements were repeated at each HR. RF was determined according to Ter Keurs et al. (22) by a sudden decrease in HR from 145 to 70, 85, 100, or 115 beats·min⁻¹ (in random order).

After ryanodine, 70 beats·min⁻¹ could not be reached in 8 animals due to an increased intrinsic HR.

SR Ca²⁺-uptake

Oxalate-dependent and thapsigargin (1 μM)-sensitive Ca²⁺-uptake activity was measured by homogenizing liquid N₂-frozen ventricular tissue in 300 μl 0.3 M sucrose, 40 mM imidazole (pH 7.8), 5 mM DTT, 1 mM β-Glycerophosphate and a mixture of protease inhibitors (Boehringer) with a microdismembrator (Braun). Protein (100 μg) was preincubated at 37°C for 2 min in 198 μl 5 mM ATP, 3 mM CrP, 100 mM KCl, 20 mM imidazole (pH 7.0), 5 mM MgCl₂, 10 mM potassium oxalate, and 10 μM ruthenium red. Reactions were started by adding 22 μl ⁴⁵Ca²⁺ (0.2 Ci/mmol)-EGTA (1 mM) buffers (pCa's 5.5 and 4.5). Free Ca²⁺ concentrations were calculated using WinMAXC (C. Patton, Stanford University) with the dissociation constants: Ca²⁺-EGTA, 3.88·10⁻⁷ M; Ca²⁺-ATP, 8.16·10⁻⁵ M; Mg²⁺-EGTA, 3.10·10⁻² M and Mg²⁺-ATP, 6.86·10⁻⁵ M. Aliquots (50 μl) were filtered after 1, 2, and 4 min through 0.45-μm Millipore filters, and ⁴⁵Ca²⁺ was measured by liquid scintillation counting. SR Ca²⁺-uptake ratio was calculated as (Ca²⁺-uptake pCa=5.5)/(Ca²⁺-uptake pCa=4.5), to obtain a parameter for SERCA2 Ca²⁺-affinity independent of its maximal activity.

Phospholamban phosphorylation

Immunoblots of total phospholamban and phospholamban phosphorylated at Ser¹⁶ and Thr¹⁷ were quantified as follows. Protein (30 μg) in SDS sample buffer was separated with an SDS-PAGE 7.5% to 15% gradient gel and blotted onto PVDF (Boehringer). Blots were incubated overnight at 4°C in TTBS with primary antibodies raised against phospholamban (PLB, monoclonal, clone 2D12, Affinity Bioreagents, 1:2000 dilution), PLB-PS16 or PLB-PT17 (polyclonal, Cyclacel Dundee, UK, 1:4000) or troponin-I (monoclonal, clone 19C7, Research Diagnostic Inc., 1:2000). Secondary antibody was either ¹²⁵I-Labeled goat antimouse IgG or ¹²⁵I-labeled donkey antirabbit IgG both from Amersham Pharmacia Biotech. After washing blots were quantified in the molecular imager (Bio-Rad).

Data acquisition and analysis

Hemodynamic and ultrasound crystal signals were digitized at 125 Hz. Regional wall stress (σ , N·m⁻²) and strain (ϵ , dimensionless) were calculated off-line (24) and end-systolic stress-strain (σ_{es} - ϵ_{es}) relationships were determined from the preload changes. The slope of this relationship, E_{es} (end-systolic elastance) was calculated at a constant stress corresponding to a LV pressure of 70 mmHg at baseline and taken as a measure of contractility (24). The area enclosed by the LV stress-strain loop during a single heartbeat was determined as regional external myocardial work (EW, J·m⁻³) (4). The stress-strain

area (SSA, $J \cdot m^{-3}$, total regional myocardial work), was calculated as the area enclosed by the end-systolic and end-diastolic relations and the systolic trajectory of the stress-strain loop (24). For RF calculation, a single-beat E_{es} was calculated by a line from the ϵ_0 at 145 $beats \cdot min^{-1}$ to the point of the stress-strain loop at maximal elastance. Subsequently, an exponential decay-curve was determined for E_{es} and beat number (n): $E_{es} = a \cdot e^{-(n-1)/\tau} + b \cdot n + c$; τ is the constant of the exponential decay. RF was calculated as $RF = e^{-1/\tau}$ (7). RF ratio ($RFR_{LAD/LAD}$) was calculated as (RF baseline)/(RF stunning), while $RFR_{LCX/LAD}$ was calculated as (RF LCXCA)/(RF LADCA).

Statistics

Changes in contractile and energetic parameters and in SR Ca^{2+} -uptake and the SR Ca^{2+} -uptake ratio were evaluated using two-way and three-way analyses of variance for repeated measures followed by Dunnet's test (Sigmastat, SPSS). Regression was performed on E_{es} , $RFR_{LAD/LAD}$ and $RFR_{LCX/LAD}$ as a function of HR for the entire data set, encoding animals with dummy variables (SPSS). The effect of stunning, stunning with propranolol, EMD 57033 and ryanodine on the regression equation was evaluated with dummy variables. A two-step approach was used. In the first step, dummies signifying changes in offset and dummies signifying changes in slope were applied for each intervention. If both dummies resulted in an overspecified system, we selected in the second step one of the dummies depending on the highest absolute t-value. Furthermore, each animal was encoded with a dummy variable. All data are expressed as mean \pm SEM. In the Results-section only significant changes ($P < 0.05$) are mentioned.

Results

Systemic Hemodynamics (Table 1)

Raising HR from 85 to 145 $beats \cdot min^{-1}$ before stunning increased $LVdP/dt_{max}$ (by 12%), while MAP, CO and SVR showed biphasic responses. LVP_{ed} decreased by 34%. Induction of stunning in the LADCA region with infusion of saline decreased MAP (by 20% at 100 $beats \cdot min^{-1}$) $LVdP/dt_{max}$ (19%), and CO (29%). Induction of stunning with subsequent infusion of propranolol decreased MAP (21%), $LVdP/dt_{max}$ (35%), and CO (14%). Infusion of EMD 57033 following propranolol increased MAP (9%) and $LVdP/dt_{max}$ (15%). Administration of ryanodine following stunning with saline decreased MAP (18%), $LVdP/dt_{max}$ (48%), and CO (16%).

Table 1. Systemic Hemodynamics (n=18).

	Before LADCA-stunning						After LADCA-stunning				
	85	100	115	130	145		85	100	115	130	145
Heart rate											
MAP*†‡§ (mmHg)	91±2	97±2	98±2	97±2	96±2	Saline	73±3	77±3	82±4	80±4	76±5
						Prop	71±2	76±2	80±2	81±2	75±2
						Prop+EMD	79±2	83±2	83±3	82±2	77±3
						Ryanodine	58±5	63±5	62±6	64±6	64±5
LvPd/dt _{max} *†‡§ (mmHg·s ⁻¹)	1410±110	1500±100	1500±90	1520±90	1580±90	Saline	1170±180	1220±150	1230±160	1230±130	1260±130
						Prop	900±30	970±50	1010±50	1120±60	1220±60
						Prop+EMD	1110±60	1120±70	1160±70	1250±50	1290±40
						Ryanodine	590±140	640±120	690±100	740±120	840±130
LVP _{ed} * (mmHg)	13±1	12±1	10±1	9±1	9±1	Saline	13±1	13±1	11±1	10±1	10±1
						Prop	12±2	11±1	10±1	8±1	7±1
						Prop+EMD	12±2	11±2	10±1	9±1	7±1
						Ryanodine	14±1	13±1	12±1	11±1	11±1
CO*†‡ (l·min ⁻¹)	3.1±0.3	3.5±0.3	3.5±0.3	3.3±0.3	3.2±0.2	Saline	2.4±0.3	2.5±0.3	2.6±0.3	2.6±0.3	2.5±0.4
						Prop	2.6±0.2	3.0±0.2	3.1±0.2	2.9±0.2	2.8±0.2
						Prop+EMD	3.2±0.2	3.3±0.2	3.3±0.3	3.2±0.2	2.8±0.3
						Ryanodine	2.1±0.4	2.1±0.4	2.1±0.5	2.1±0.4	2.1±0.5
SVR* (mmHg·min·l ⁻¹)	34±4	30±2	31±2	33±3	34±3	Saline	34±3	33±3	34±3	34±3	34±3
						Prop	28±2	27±2	27±2	29±2	28±2
						Prop+EMD	25±2	26±2	26±2	26±2	29±2
						Ryanodine	31±6	35±4	35±4	37±6	36±5

Heart rate (beats·min⁻¹); MAP, mean arterial pressure; LvdPdt_{max}, maximum rate of left ventricular (LV) pressure rise; LVP_{ed}, LV end-diastolic pressure; CO, cardiac output; SVR, systemic vascular resistance. Prop, propranolol 0.5 mg·kg⁻¹+0.5 mg·kg⁻¹·h⁻¹, EMD, EMD 57033 0.25 mg·kg⁻¹·min⁻¹ for 15 min+0.03 mg·kg⁻¹·min⁻¹, Ryanodine 1 µg·kg⁻¹. * Effect of heart rate $P < 0.05$; † Effect of stunning + saline vs. baseline $P < 0.05$; ‡ Effect of stunning + propranolol vs. baseline $P < 0.05$; § Effect of EMD 57033 vs. stunning + propranolol $P < 0.05$; || Effect of stunning + ryanodine vs. stunning + saline $P < 0.05$. Values are mean±SEM.

Table 2. Regional contractile and energetic parameters of the LADCA perfusion area (n=18).

	Before LADCA-stunning						After LADCA-stunning					
	70	85	100	115	130	145	70	85	100	115	130	145
Heart rate												
$E_{es}^{*\dagger\ddagger\§}$ ($10^4 \text{ N}\cdot\text{m}^{-2}$)		18±3	19±2	20±2	20±2	26±3	Saline	15±4	13±3	14±4	14±3	13±3
							Prop	13±2	12±2	12±2	12±2	12±1
							Prop+EMD	17±3	17±3	16±3	19±4	16±2
							Ryanodine	26±4	25±2	18±3	14±2	14±1
$\sigma_{es}^{*\parallel}$ ($10^3 \text{ N}\cdot\text{m}^{-2}$)		18±1	19±1	19±1	18±1	17±1	Saline	18±2	18±2	19±2	19±2	18±2
							Prop	16±2	17±2	17±2	17±2	16±2
							Prop+EMD	16±2	17±2	16±2	16±2	15±1
							Ryanodine	14±1	15±2	15±2	15±2	14±2
$SSA^{*\dagger\ddagger}$ ($10^2 \text{ J}\cdot\text{m}^{-3}$)		32±5	32±5	30±5	25±4	20±4	Saline	19±7	18±6	18±6	16±6	12±4
							Prop	11±2	12±2	11±2	11±2	8±1
							Prop+EMD	16±3	14±2	12±2	10±2	9±2
							Ryanodine	4±2	10±4	10±4	10±4	9±3
$EW^{*\dagger\ddagger\§}$ ($10^2 \text{ J}\cdot\text{m}^{-3}$)		24±5	24±5	21±5	17±3	14±4	Saline	12±6	11±5	9±5	7±4	5±3
							Prop	4±1	3±1	2±1	1±1	-1±1
							Prop+EMD	10±2	7±1	5±1	5±1	3±1
							Ryanodine	3±2	7±4	8±4	7±4	6±3
$RF^{*\dagger}$ (dimensionless)	0.42±0.02	0.42±0.03	0.43±0.02	0.40±0.03			Saline	0.31±0.04	0.23±0.04	0.25±0.03	0.16±0.04	
							Ryanodine		0.20±0.05	0.33±0.10	0.19±0.06	

Heart rate (beats·min⁻¹); E_{es} , end systolic elastance; σ_{es} , end systolic stress; SSA, stress-strain area; EW, external work; RF recirculation fraction. For explanation of symbols see Table 1.

Table 3. Regional contractile and energetic parameters of the LCXCA perfusion area (n=18).

Heart rate	Before LADCA-stunning							After LADCA-stunning					
	70	85	100	115	130	145		70	85	100	115	130	145
$E_{es}^{*\ddagger}$ ($10^4 \text{ N}\cdot\text{m}^{-2}$)		20±3	22±3	24±4	22±3	27±4	Saline	24±3	26±4	25±5	36±7	36±6	
							Prop	20±3	22±3	24±4	25±4	28±4	
							Prop+EMD	28±4	27±4	29±4	31±4	32±4	
							Ryanodine	27±8	31±4	35±6	35±7	36±7	
$\sigma_{es}^{*\ddagger\ddagger}$ ($10^3 \text{ N}\cdot\text{m}^{-2}$)		18±2	19±2	19±2	18±2	17±1	Saline	14±2	14±2	14±2	14±2	13±2	
							Prop	16±2	17±2	17±2	17±2	16±2	
							Prop+EMD	17±2	18±2	18±2	17±2	15±2	
							Ryanodine	11±1	13±2	12±2	11±1	11±2	
$SSA^{*\ddagger\ddagger\parallel}$ ($10^2 \text{ J}\cdot\text{m}^{-3}$)		25±3	24±3	22±3	19±2	14±2	Saline	15±3	14±3	13±3	11±2	9±2	
							Prop	16±3	16±3	16±3	14±2	11±2	
							Prop+EMD	19±3	17±3	15±3	13±2	10±2	
							Ryanodine	8±2	9±3	9±3	5±1	7±2	
$EW^{*\ddagger\ddagger\parallel}$ ($10^2 \text{ J}\cdot\text{m}^{-3}$)		18±2	16±2	15±2	11±2	8±1	Saline	12±3	10±2	10±2	7±2	6±1	
							Prop	11±2	11±2	10±2	8±1	6±1	
							Prop+EMD	14±2	12±2	10±2	8±2	6±1	
							Ryanodine	6±1	7±2	7±2	4±1	5±2	
RF* (dimensionless)	0.38±0.03	0.38±0.05	0.39±0.05	0.41±0.04			Saline	0.37±0.04	0.39±0.04	0.36±0.05	0.31±0.05		
							Ryanodine		0.26±0.04	0.32±0.10	0.24±0.06		

Heart rate (beats·min⁻¹); E_{es} , end systolic elastance; σ_{es} , end systolic stress; SSA, stress-strain area; EW, external work; RF, recirculation fraction. For explanation of symbols see Table I.

LADCA perfusion area (Table 2)

Increasing HR from 85 to 145 beats·min⁻¹ increased E_{es} (by 45%), and decreased σ_{es} (by 6%), SSA (by 38%), and EW (by 43%). Induction of stunning decreased E_{es} (by 34% at 100 beats·min⁻¹), SSA (44%), EW (55%), and RF (42%). Stunning with infusion of propranolol had a slightly more profound effect, as E_{es} decreased by 36%, SSA by 63%, and EW by 88%. Infusion of EMD 57033 in addition to propranolol increased E_{es} (41%) and EW (145%). Administration of ryanodine decreased σ_{es} (17%).

LCXCA perfusion area (Table 3)

E_{es} of the LCXCA region increased by 34% when HR was raised from 85 to 145 beats·min⁻¹. In addition, σ_{es} decreased by 8%, SSA by 44%, and EW by 54%. Induction of LADCA-stunning with saline decreased σ_{es} (26%), SSA (41%), and EW (36%) because of their load-dependency. Induction of stunning followed by propranolol decreased σ_{es} (10%), SSA (32%), and EW (33%). Infusion of EMD 57033 following propranolol increased E_{es} (22%), while the other mechanical and energetical parameters remained unchanged. Administration of ryanodine only decreased SSA (34%) and EW (36%).

Relationship between E_{es} and HR

In the LADCA perfusion area before stunning, E_{es} increased with increasing HR: $E_{es}=1147 \cdot HR+75.9 \cdot 10^3$ ($r^2=0.60$, $P<0.001$, Fig. 1A). Both induction of stunning followed by saline and stunning followed by propranolol completely abolished this relationship. Infusion of EMD 57033 in addition to propranolol increased the intercept of the relationship by 31%, without affecting the slope (i.e. the force-frequency effect; Fig. 1B). Ryanodine, in contrast, strongly decreased the slope and increased the intercept by 153%, changing the relationship in a negative one (Fig. 1C).

E_{es} of the LCXCA region also increased with HR: $E_{es}=1045 \cdot HR+107 \cdot 10^3$ ($r^2=0.63$, $P<0.001$, Fig. 2A). In contrast to the LADCA region, stunning increased the slope of this relationship by 46%, while stunning with propranolol had no effect. Comparable to the LADCA perfusion area, EMD 57033 increased the intercept by 50%, without changing the slope (Fig. 2B). In contrast to the stunned myocardium, ryanodine had no effect on this relationship (Fig. 2C).

Relationship between RFR and HR

Before stunning, $RFR_{LCX/LAD}$ was independent of HR (Fig. 3B). Because of the stunning-induced, HR-dependent decrease in RF in the LADCA region, $RFR_{LAD/LAD}$ displayed an increase with increasing HR ($RFR_{LAD/LAD}=0.032 \cdot HR - 0.70$, $r^2=0.84$, $P<0.001$), to a similar degree as $RFR_{LCX/LAD}$ during stunning ($RFR_{LCX/LAD}=0.024 \cdot HR - 0.39$, $r^2=0.56$, $P<0.001$, Fig. 3A). After administration of ryanodine, $RFR_{LCX/LAD}$ became

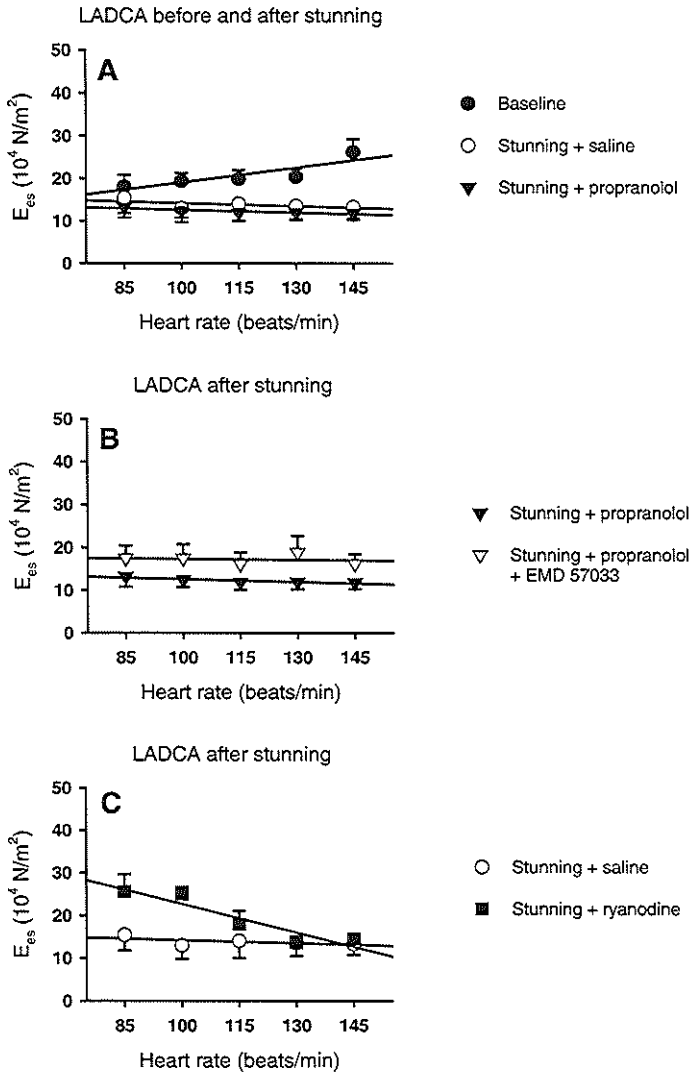


Fig. 1 Relationship between end-systolic elastance (E_{es}) of the LADCA region and heart rate (force-frequency effect). Panel A: effect of stunning with subsequent infusion of saline or propranolol, panel B: effect of EMD 57033, panel C: effect of ryanodine.

again independent of HR (Fig. 3B), while the intercept was not significantly different from unity ($P=0.50$).

SR Ca^{2+} -uptake and phospholamban phosphorylation

SR Ca^{2+} -uptake at 70 beats·min⁻¹ in the non-stunned region was 10.1 ± 0.8 and 13.8 ± 0.9 nmol·mg⁻¹·min⁻¹, at a pCa of 5.5 and 4.5, respectively. Neither stunning nor HR

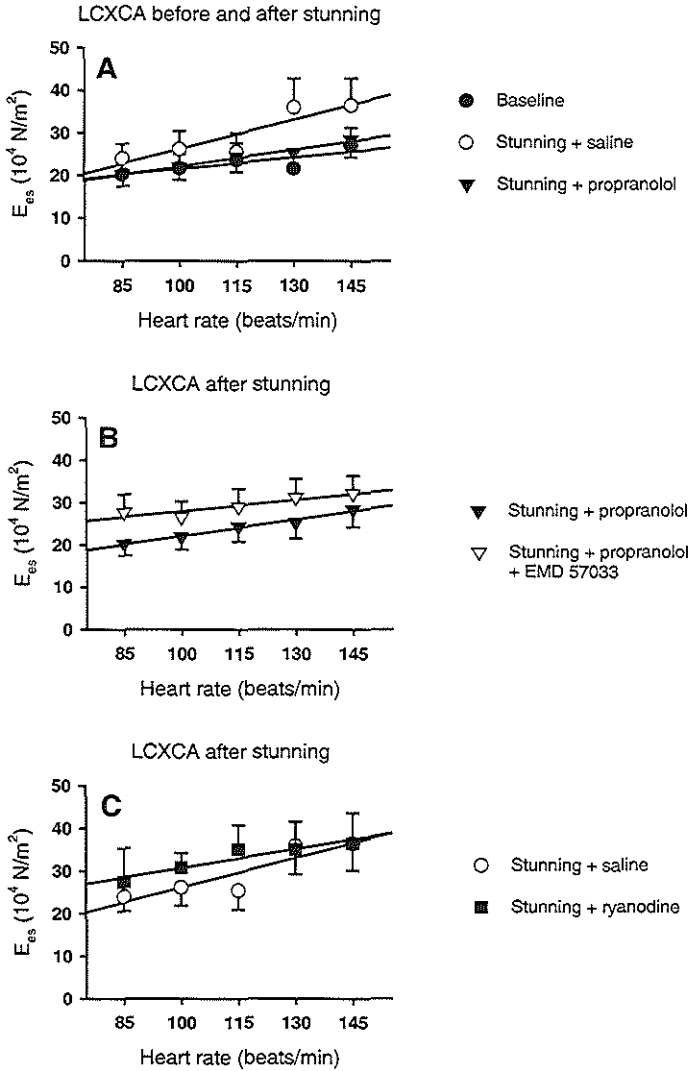


Fig. 2 Relationship between end-systolic elastance (E_{es}) of the LCXCA region and heart rate (force-frequency effect). Panel A: effect of LADCA-stunning with subsequent infusion of saline or propranolol, panel B: effect of EMD 57033, panel C: effect of ryanodine.

had an effect on SR Ca^{2+} -uptake or on the Ca^{2+} -uptake ratio (definition see Methods). Fig. 4 shows a representative gelpattern of site-specific phosphorylation of phospholamban. The mean phospholamban-Thr¹⁷-phospholevels of stunned vs. non-stunned myocardium or low vs. high HR were not significantly different (values not shown). Phospholamban-Ser¹⁶-phospholevels were in most of the pigs very low. To study troponin-I (cTnI) breakdown we applied the antibody against an epitope common to the phosphorylated,

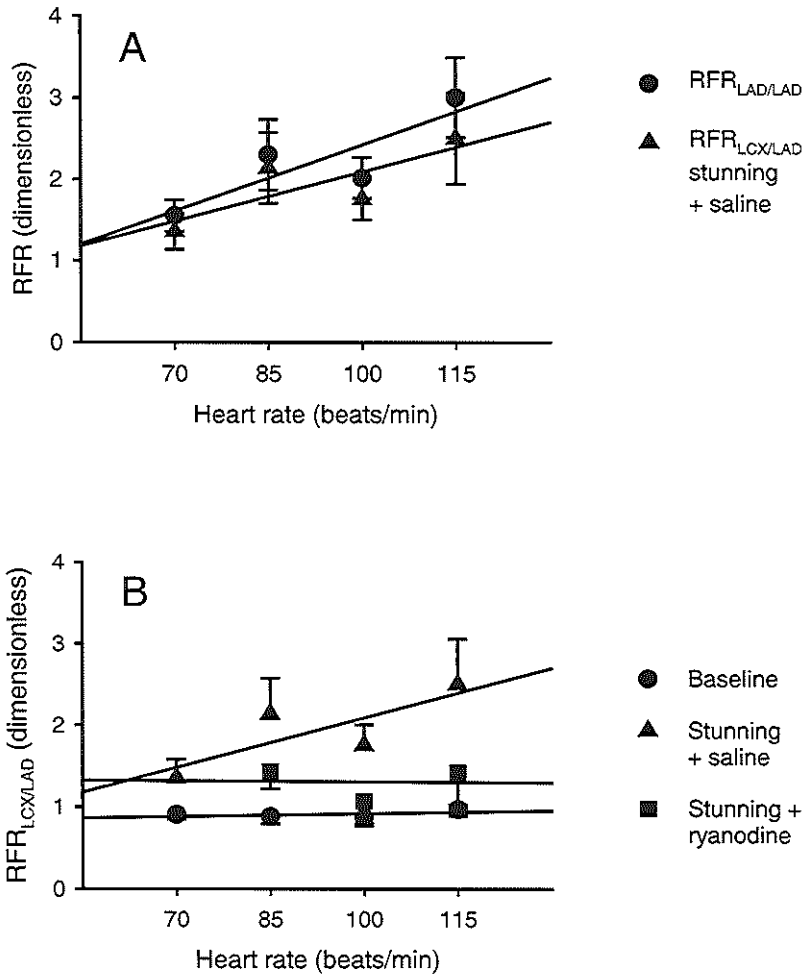


Fig. 3 Relationship between recirculation fraction ratio (RFR) and heart rate. Panel A: comparison of RFR baseline/stunning ($RFR_{LAD/LAD}$) with RFR LCXCA/LADCA ($RFR_{LCX/LAD}$) in stunning. Panel B: comparison of $RFR_{LCX/LAD}$ between baseline, stunning with subsequent infusion of saline, and stunning with subsequent infusion of ryanodine.

the unphosphorylated cTnI form and the earlier described 22 kDa cTnI degradation product (15). In accordance with the study of Thomas et al. (23), no detectable TnI breakdown product was present in the stunned porcine myocardium.

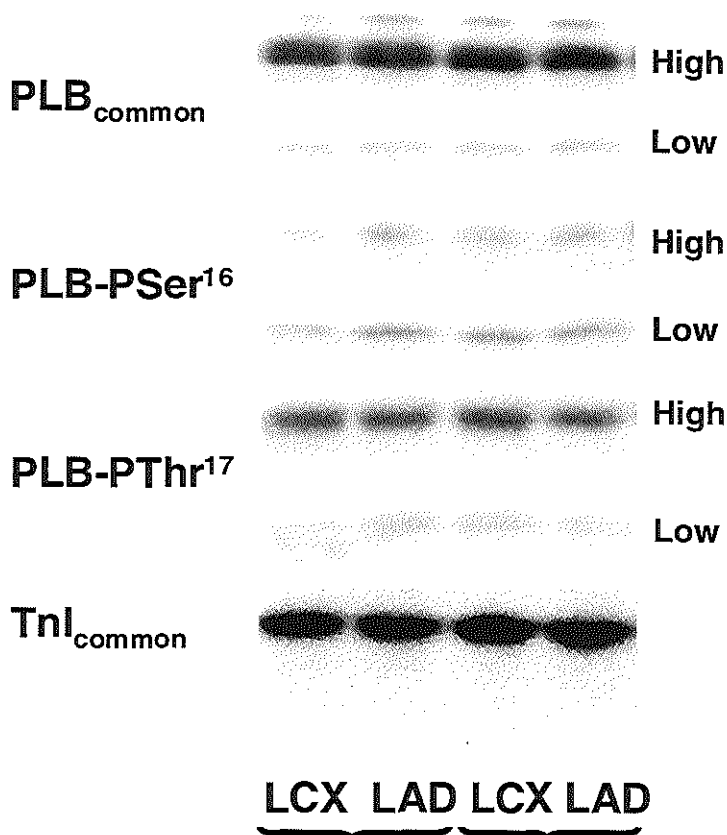


Fig. 4 Representative patterns of site-specific phosphorylation of phospholamban (PLB) at serine-16 (PLB-PSer¹⁶) and threonine-17 (PLB-PThr¹⁷) in homogenates (30 $\mu\text{g}/\text{well}$) prepared from small needle biopsies (10-20 mg) taken from non-stunned (LCX-perfused) and stunned (LAD-perfused) myocardium of one of the pigs at low (70 min^{-1}) and high (145 min^{-1}) pacing rate. PLB_{common} is the signal obtained using an antibody against an epitope of PLB which is common to all PLB forms. In each gel both the Low (monomeric) or High (pentameric) molecular weight forms are shown. The bottom gelpattern shows the signal of an antibody against an epitope of TnI which is common to the unphosphorylated and phosphorylated TnI forms.

Discussion

The results of this study can be summarized as follows: (i) In in-vivo stunned myocardium the FFE was abolished. (ii) In both stunned and normal myocardium, Ca^{2+} -sensitization increased contractility without affecting the FFE. (iii) A HR-dependent decrease in the RF, causing a HR-dependent increase in $\text{RFR}_{\text{LCX/LAD}}$, was measured in stunning. (iv) Ryanodine did not restore the RF in the stunned region, but mimicked the stunning-induced changes in RF in the normal myocardium, thereby restoring

RFR_{LCX/LAD}. (v) Ryanodine did not abolish the FFE of the normal myocardium. (vi) Neither stunning nor raising HR from 70 to 145 beats·min⁻¹ influenced the affinity of SERCA2 for Ca²⁺ or the Thr¹⁷ phosphorylation level of phospholamban.

The first issue we studied was whether the absence of the FFE in stunned myocardium could solely be explained by a decreased Ca²⁺-sensitivity of the myofibrils. We argued that if a decreased myofibrillar Ca²⁺-sensitivity would underlie the absence of the FFE, the Ca²⁺-sensitizing properties of EMD 57033 (5) should at least partly restore the FFE. However, infusion of EMD 57033 did not increase the FFE while it increased E_{cs}. Theoretically, a decreased myofibrillar Ca²⁺-sensitivity could still explain the absent FFE, if the increase in Ca²⁺-sensitivity by EMD 57033 would be accompanied by a concomitant decrease of the Ca²⁺-transient. However, this seems unlikely, as EMD 57033 should then have a different effect on the unchanged myofibrillar Ca²⁺-sensitivity of the non-stunned region, affecting the FFE differently. However, as can be seen in Figs. 1 and 2, Ca²⁺-sensitization had similar effects on the FFE of the stunned and the non-stunned region. Thus it is likely that the decrease of the FFE in stunned myocardium is not caused by a decrease in myofibrillar Ca²⁺-responsiveness but by a disturbance in myocyte Ca²⁺-handling. The latter is in accordance with observations performed in failing hearts (6, 12).

We also addressed the question which of the Ca²⁺-handling systems is (are) involved in the decrease of the FFE in stunned myocardium. To this end, we specifically studied the combined processes of CICR and SERCA2 function *in vivo* by calculating RF, which has been shown to present the relative contribution of the internal Ca²⁺-cycling to total Ca²⁺-cycling (7, 22, 26). In accordance with excised cross-circulated hearts (13), RF was decreased in stunned myocardium. Moreover, the decrease in RF was HR-dependent, which implies that at higher HR's CICR and/or SERCA2 function deteriorated with respect to the SL Ca²⁺-fluxes. To further separate these two possible disturbances, we studied SERCA2 function and the interaction between SERCA2 and phospholamban *in vitro*.

We did not detect a difference in the Ca²⁺-affinity of SERCA2 between the stunned and the non-stunned region at the lowest and highest HR, which findings are in accordance with earlier studies (11). Because we considered the possibility that the change in Ca²⁺-affinity of SERCA2 was too small to be detected by the activity ratio of Ca²⁺-uptake at pCa 5.5 and 4.5, we additionally measured site-specific phosphorylation of phospholamban by immunoblotting. As expected, in most of the pigs a very low antibody signal of the Ser¹⁶ site was found. In contrast, Thr¹⁷ phosphorylation was already present to a large extent at the lowest HR and did not increase at the highest HR. Furthermore, Thr¹⁷ phosphorylation was also not affected by stunning, suggesting that disturbances in SERCA2 function as well as its HR-dependent regulation are not involved in the mechanism of stunning. Consequently, a disturbance in CICR probably underlies the absence of the FFE in stunning.

Since evidence is available in the literature pointing to a decreased opening of the RyR (25), we administered ryanodine *in vivo* in a concentration known to partially open the RyR (16). We reasoned that if a decreased opening-probability of the RyR was the underlying cause of the absence of the FFE, ryanodine should at least partially restore this. It could clearly be seen that ryanodine did not restore any stunning-induced changes, but mimicked in the non-stunned region the stunning-induced changes in the RF of the stunned region, thereby restoring RFR_{LCXLAD} to baseline values, implying that an increased rather than a decreased opening of the RyR may relate to myocardial stunning. However, it is unlikely that only an increased opening of the RyR underlies the stunning-induced absence of the FFE, as ryanodine (which also opens the RyR) did not affect the FFE of the LCXCA region. Therefore, the present findings suggest that a second disturbance in CICR, in addition to a possible RyR dysfunction, may underlie the absence of the FFE in stunning.

References

1. **Bolli, R., and E. Marban.** Molecular and cellular mechanisms of myocardial stunning. *Physiol Rev* 79: 609-634, 1999.
2. **de Zeeuw, S., S. A. Trines, R. Krams, P. D. Verdouw, and D. J. Duncker.** Cardiovascular profile of the calcium sensitizer EMD 57033 in open-chest anaesthetized pigs with regionally stunned myocardium. *Br J Pharmacol* 129: 1413-1422, 2000.
3. **Gao, W. D., D. Atar, P. H. Backx, and E. Marban.** Relationship between intracellular calcium and contractile force in stunned myocardium. Direct evidence for decreased myofilament Ca^{2+} responsiveness and altered diastolic function in intact ventricular muscle. *Circ Res* 76: 1036-1048, 1995.
4. **Goto, Y., Y. Igarashi, Y. Yasumura, T. Nozawa, S. Futaki, K. Hiramori, and H. Suga.** Integrated regional work equals total left ventricular work in regionally ischemic canine heart. *Am J Physiol* 254: H894-904, 1988.
5. **Gross, T., I. Lues, and J. Daut.** A new cardiotoxic drug reduces the energy cost of active tension in cardiac muscle. *J Mol Cell Cardiol* 25: 239-244, 1993.
6. **Hasenfuss, G., H. Reinecke, R. Studer, M. Meyer, B. Pieske, J. Holtz, C. Holubarsch, H. Posival, H. Just, and H. Drexler.** Relation between myocardial function and expression of sarcoplasmic reticulum $Ca(2+)$ -ATPase in failing and nonfailing human myocardium. *Circ Res* 75: 434-442, 1994.
7. **Hata, Y., J. Shimizu, S. Hosogi, H. Matsubara, J. Araki, T. Ohe, M. Takaki, T. Takasago, T. W. Taylor, and H. Suga.** Ryanodine decreases internal Ca^{2+} recirculation fraction of the canine heart as studied by postextrasystolic transient alternans. *Jpn J Physiol* 47: 521-530, 1997.
8. **Iwashiro, K., A. Criniti, R. Sinatra, A. A. Dawodu, G. d'Amati, F. Monti, L. Pannarale, P. Bernucci, G. L. Brancaccio, A. Vetuschi, E. Gaudio, P. Gallo, and P. E. Puddu.** Felodipine protects human atrial muscle from hypoxia-reoxygenation dysfunction: a force-frequency relationship study in an *in vitro* model of stunning. *Int J Cardiol* 62: 107-132, 1997.
9. **Kadambi, V. J., N. Ball, E. G. Kranias, R. A. Walsh, and B. D. Hoit.** Modulation of force-frequency relation by phospholamban in genetically engineered mice. *Am J Physiol* 276: H2245-H2250, 1999.
10. **Kalthof, B., N. Sato, M. Iwase, Y. T. Shen, I. Mirsky, T. A. Patrick, and S. F. Vatner.** Effects of ryanodine on cardiac contraction, excitation-contraction coupling and "Treppe" in the conscious dog. *J Mol Cell Cardiol* 27: 2111-2121, 1995.
11. **Kaplan, P., J. Lehotsky, and P. Racay.** Role of sarcoplasmic reticulum in the contractile dysfunction during myocardial ischaemia and reperfusion. *Physiol Res* 46: 333-339, 1997.

12. Kass, D. A. Force-frequency relation in patients with left ventricular hypertrophy and failure. *Basic Res Cardiol* 93: 108-116, 1998.
13. Lee, S., J. Araki, T. Imaoka, M. Maesako, G. Iribe, K. Miyaji, S. Mohri, J. Shimizu, M. Harada, T. Ohe, M. Hirakawa, and H. Suga. Energy-wasteful total Ca^{2+} handling underlies increased O_2 cost of contractility in canine stunned heart. *Am J Physiol Heart Circ Physiol* 278: H1464-1472, 2000.
14. Lemaire, S., C. Piot, F. Leclercq, V. Leuranguer, J. Nargeot, and S. Richard. Heart rate as a determinant of L-type Ca^{2+} channel activity: mechanisms and implication in force-frequency relation. *Basic Res Cardiol* 93: 51-59., 1998.
15. McDonough, J. L., D. K. Arrell, and J. E. Van Eyk. Troponin I degradation and covalent complex formation accompanies myocardial ischemia/reperfusion injury. *Circ Res* 84: 9-20., 1999.
16. Meissner, G. Ryanodine activation and inhibition of the Ca^{2+} release channel of sarcoplasmic reticulum. *J Biol Chem* 261: 6300-6306, 1986.
17. Miller, W. P., K. S. McDonald, and R. L. Moss. Onset of reduced Ca^{2+} sensitivity of tension during stunning in porcine myocardium. *J Mol Cell Cardiol* 28: 689-697, 1996.
18. Munch, G., B. Bolck, K. Brixius, H. Reuter, U. Mehlhorn, W. Bloch, and R. H. Schwinger. SERCA2a activity correlates with the force-frequency relationship in human myocardium. *Am J Physiol Heart Circ Physiol* 278: H1924-1932, 2000.
19. Negash, S., S. Huang, and T. C. Squier. Rearrangement of domain elements of the Ca-ATPase in cardiac sarcoplasmic reticulum membranes upon phospholamban phosphorylation. *Biochemistry* 38: 8150-8158, 1999.
20. Prabhu, S. D., M. M. Rozek, D. R. Murray, and G. L. Freeman. Ryanodine and left ventricular function in intact dogs: dissociation of force-based and velocity-based indexes. *Am J Physiol* 273: H1561-1568., 1997.
21. Schad, H., W. Heimisch, G. P. Eising, and N. Mendler. Effect of milrinone and atrial pacing on stunned myocardium. *Eur J Cardiothorac Surg* 11: 1125-1132, 1997.
22. Ter Keurs, H. E., W. D. Gao, H. Bosker, A. J. Drake-Holland, and M. I. Noble. Characterisation of decay of frequency induced potentiation and post- extrasystolic potentiation. *Cardiovasc Res* 24: 903-910, 1990.
23. Thomas, S. A., J. A. Fallavollita, T. C. Lee, J. Feng, and J. M. Canty, Jr. Absence of troponin I degradation or altered sarcoplasmic reticulum uptake protein expression after reversible ischemia in swine [see comments]. *Circ Res* 85: 446-456, 1999.
24. Trines, S. A., C. J. Slager, J. van der Moer, P. D. Verdouw, and R. Krams. Efficiency of energy transfer, but not external work, is maximized in stunned myocardium. *Am J Physiol Heart Circ Physiol* 279: H1264-1273, 2000.
25. Valdivia, C., J. O. Hegge, R. D. Lasley, H. H. Valdivia, and R. Mentzer. Ryanodine receptor dysfunction in porcine stunned myocardium. *Am J Physiol* 273: H796-804, 1997.
26. Wier, W. G., and D. T. Yue. Intracellular calcium transients underlying the short-term force-interval relationship in ferret ventricular myocardium. *J Physiol (Lond)* 376: 507-530, 1986.

Chapter 4

Maximization of external work and efficiency of energy transfer

Introduction and Methods - There is no evidence regarding the effect of stunning on maximization of regional myocardial external work (EW) or efficiency of energy transfer (EET) in relation to regional afterload (end-systolic stress, σ_{es}). To that end, we studied these relationships in both the left anterior descending coronary artery (LADCA) and left circumflex coronary artery regions in anesthetized, open-chest pigs before and after LADCA stunning.

Results - In normal myocardium, EET vs. σ_{es} was maximal at 75.4 (69.7–81.0)%, whereas EW vs. σ_{es} was submaximal at 12.0 (6.61–17.3)·10² J/m³. Increasing σ_{es} increased EW by 18 (10–27)%. Regional myocardial stunning decreased EET (27%) and EW (36%) and caused the myocardium to operate both at maximal EW (EW_{max}) and at maximal EET (EET_{max}). EET and EW became also more sensitive to changes in σ_{es} . In the nonstunned region the situation remained unchanged. Combining the data from before and after stunning, both EW_{max} and EET_{max} displayed a positive relationship with contractility.

Conclusions - The normal regional myocardium operated at maximal EET rather than at maximal EW. Therefore, additional EW could be recruited by increasing regional afterload. After myocardial stunning, the myocardium operated at both maximal EW and maximal EET, at the cost of increased afterload sensitivity. Contractility was a major determinant of this shift.

Serge A.I.P. Trines, Cornelis J. Slager, Joost van der Moer, Pieter D. Verdouw, and Rob Krams. Efficiency of energy transfer, but not external work, is maximized in stunned myocardium. *Am J Physiol Heart Circ Physiol* 279: H1264-H1273, 2000

Introduction

Left ventricular external work (EW) and left ventricular efficiency of energy transfer (EET) have been shown to depend on a complex interplay of afterload, preload and contractility (20). The individual contribution of these factors to EW and EET may be quantified using the time-varying elastance concept (23). According to this concept, the left ventricular elastance, measured by the instantaneous ratio of pressure over volume (minus the extrapolated volume at zero pressure), changes during a cardiac cycle from a minimal end-diastolic value to a maximal end-systolic value. The latter value (end-systolic elastance or E_{es}) is a measure of contractility (23). The area bounded by the end-diastolic and end-systolic pressure-volume relationships and the systolic trajectory of the pressure-volume loop is a measure of total left ventricular work, while the area within the pressure-volume loop is a measure of left ventricular EW. Left ventricular EET is defined as the ratio of external work over total work.

Several studies have addressed the relationship of power, EW or EET vs. afterload and have found a maximum in power (20, 25), but not in EET (7). Until now, these relationships have been derived for global heart function, while most of the cardiac pathophysiology is associated with regional dysfunction (27). However, to study the energy-afterload relationships during regional dysfunction, it is necessary to apply the physiological concepts on a regional basis. To the best of our knowledge, it is presently unknown whether relationships involving external work, efficiency of energy transfer and afterload derived for global hearts are applicable to regional myocardium. Hence, the first aim of the present study was to evaluate in open-chest anesthetized pigs whether maxima in external work and efficiency of energy transfer, as found in global hearts, are present in regional myocardium in open-chest pigs. As a measure for afterload we applied regional end-systolic stress (σ_{es}), as arterial properties, e.g. effective arterial elastance, cannot constitute afterload for regional myocardium.

Impairment of global left ventricular function causes the ventricle to deviate from the optimal situation (11, 21). In earlier work we have shown that, after myocardial stunning, both regional EW and regional EET decreased more than before stunning, when end-systolic pressure was increased (9). In view of the above-mentioned maximum in work our previous findings may be explained either on the basis of a shift of these maxima to the left, or on a change of shape of the EW and EET relationships. Therefore, the second aim of the present study was to evaluate relationships of EW and EET vs. regional afterload before and after producing regional myocardial stunning.

Apart from the question how regional EW- σ_{es} and EET- σ_{es} relationships are affected by regional stunning, it is presently unknown whether and how stunning of a region influences the nonstunned region. Hence, we evaluated the relationship of EW- σ_{es} and EET- σ_{es} for the nonstunned region after stunning another region. All of the above-

proposed studies were conducted in open-chest pigs with a well-accepted protocol to induce myocardial stunning.

Materials and methods

General

All experiments were performed in accordance with the "Guiding principles for the care and use of animals" as approved by the Council of the American Physiological Society and under the regulations of the Animal Care Committee of the Erasmus University Rotterdam.

Instrumentation

After an overnight fast crossbred Yorkshire-Landrace pigs (30-39 kg, n=9) were sedated with 20 mg/kg ketamine i.m. (Apharmo BV, Arnhem, The Netherlands), anesthetized with 15-20 mg/kg sodium pentobarbital i.v. (Apharmo BV, Arnhem, The Netherlands), intubated and connected to a ventilator for intermittent positive pressure ventilation with a mixture of oxygen and nitrogen (1:2, vol/vol). Arterial oxygen content and blood gases were kept within the normal range ($7.35 < \text{pH} < 7.45$; $35 < \text{pCO}_2(\text{mmHg}) < 45$; $100 < \text{pO}_2(\text{mmHg}) < 150$) by adjusting, when necessary, the respiratory rate and tidal volume. Three 7 French (F) fluid filled catheters were placed in the superior caval veins for the continuous infusion of $10\text{-}15 \text{ mg}\cdot\text{kg}^{-1}\cdot\text{h}^{-1}$ sodium pentobarbital, the continuous infusion of saline, the administration of 4 mg of the muscle relaxant pancuronium bromide (Organon Teknika B.V., Boxtel, The Netherlands) prior to thoracotomy and the administration of the specific negative chronotropic agent zatebradine (1-2 mg/kg, courtesy of Dr. J.W. Dämmgen; Dr. Karl Thomae, Boehringer Ingelheim KG, Biberach a/d Riss, Germany). Central aortic blood pressure was monitored via an 8 F catheter positioned in the thoracic descending aorta, while left ventricular pressure and its first derivative were obtained with a 7 F micromanometer-tipped catheter (Braun Medical B.V. Uden, The Netherlands), which was inserted via the left carotid artery. A latex balloon made in our laboratory was mounted on a 7 F fluid filled catheter and inserted via the right femoral vein and positioned in the inferior caval vein just above the diaphragm. Inflation of this balloon reduced the preload for the left ventricle. A 7 F latex Fogarty catheter (Baxter Healthcare, Irvine, CA, USA) was inserted via the right carotid artery and positioned in the ascending aorta. Inflation of this balloon gradually increased afterload for the left ventricle.

Following a midline sternotomy and after ligation of the left mammarian artery and vein, a part of the second left rib was removed and the heart was suspended in a pericardial cradle. An electromagnetic flow probe (Skalar, Delft, The Netherlands) was placed around the ascending aorta to measure aortic flow. A small segment of the

proximal part of the left anterior descending coronary artery (LADCA) was dissected free for placement of an electromagnetic flow probe (Skalar, Delft, The Netherlands) and an atraumatic clamp to occlude the LADCA. To obtain local coronary venous blood samples, a cannula was inserted into the great cardiac vein which drains specifically the LADCA perfusion area (2). Pacing leads were attached to the right atrial appendage and connected to a pacing stimulator (Grass S9, Quincy, Mass., USA). Rectal temperature was monitored throughout the experiment and was maintained between 37°C and 38°C using external heating pads, warming of the saline infusion and coverage of the animals with blankets.

Two ultrasonic crystals (Triton Technology Inc., San Diego, CA, USA) were positioned in the midmyocardium of both the anterior and posterior left ventricular wall to measure the diameter of the left ventricle. The diameter crystal in the anterior wall was positioned close to the LADCA segment length crystals. The diameter crystal in the posterior wall was positioned such as to optimize signal quality. Two pairs of ultrasonic crystals were implanted in the midmyocardium of the distribution area of the LADCA, each pair 10 mm apart, approximately at one-third of the distance from apex to base. One pair was positioned in the direction of the left ventricular outflow tract (as determined visually), while the other pair was placed perpendicular to this direction. The distance of 10 mm and the perpendicularity of the two pairs were assured using a homemade device consisting of two perpendicularly fixed pairs of needles. Similarly, two pairs of crystals were implanted in the midmyocardium of the distribution area of the left circumflex coronary artery (LCXCA), approximately at half the distance from apex to base. One pair was positioned in the direction of the left ventricular outflow tract and the other pair was placed in the perpendicular direction. The position of the crystals in the midmyocardium was verified at the end of the experiment.

Experimental protocol

After a 30-45 min stabilization period, steady-state recordings of hemodynamics and segment lengths in the two myocardial regions were made during 10 respiratory cycles and global arterial and regional myocardial venous blood samples were collected. After these baseline recordings were made, heart rate was lowered below 70 beats/min by infusion of zatebradine and set at 100 beats/min with the external pacemaker to exclude effects of alterations in heart rate. The baseline measurements were repeated and followed by inflation of the balloon located in the inferior caval vein over a period of 15 s to create a series of 20-25 beats with a gradual reduction of end-systolic left ventricular pressure of approximately 50-60 mmHg. During the inflation of the balloon the respirator was switched off. The period of 15 s is sufficiently short to prevent reflex-mediated changes in contractility (1). Moreover, before the heart was paced, systolic, diastolic and total heart cycle duration did not change in our experiments up to 18 s (for definition of systole

and diastole see below). After hemodynamic variables had resumed pre-inflation values (differences in mean arterial pressure and in maximum left ventricular pressure rise smaller than 4 mmHg and 100 mmHg/s, respectively), the balloon located in the ascending aorta was then gradually inflated over a period of 10 s to create 10-20 beats with an increase of end-systolic left ventricular pressure of approximately 30-40 mmHg. The respirator was again switched off during this procedure. The order of inflating the two balloons was randomized for each measurement.

Subsequently, myocardial stunning was produced in the LADCA region by two coronary (LADCA) occlusions of 10 min, separated by 10 min of reperfusion. The last occlusion was followed by 30 min of reperfusion. After this period, the steady-state measurements and the balloon inflations as mentioned above were repeated.

At the end of each experiment, methylene blue was infused into the LADCA, and the myocardium perfused by the LADCA was dissected and weighed. In addition, also the myocardium inside the segment crystals in both LADCA and LCXCA regions was dissected and weighed.

Data acquisition and analysis

Left ventricular pressure, its first derivative, central aortic pressure, aortic flow, coronary blood flow, left ventricular diameter and the regional segment length signals were digitized (sample rate 125 Hz) with a 12 bit AD converter connected to an AT-based personal computer (AT-CODAS, Keithley Instruments B.V., Gorinchem, The Netherlands) and stored on disk for off-line analysis. Mean arterial pressure, systolic arterial pressure, diastolic arterial pressure, maximum left ventricular pressure rise, left ventricular end-diastolic pressure, cardiac output, stroke volume and systemic vascular resistance were calculated following standard procedures. Myocardial oxygen consumption of the LADCA perfusion area (MVO_2 , in $J \cdot \text{beat}^{-1} \cdot \text{m}^{-3}$) was calculated as the product of coronary blood flow and the difference in arterial and coronary venous oxygen content divided by the heart rate and the mass of the LADCA perfusion area. The energy generated by 1 ml of O_2 was set equal to 20 J (22). Left ventricular wall stress (σ , in N/m^2) and strain (ϵ , dimensionless) were calculated off-line applying the formulae described in the appendix. End-systolic stress-strain relationships were determined from the combined pre- and afterload changes by determining left ventricular end-systolic stress-strain points using an iterative fitting algorithm, as described before (26). Briefly, to determine these points, a linear relationship was applied in which elastance was defined as $\sigma/(\epsilon - \epsilon_0)$, in which ϵ_0 is the strain at zero wall stress. To initiate the iteration, ϵ_0 was set to zero and elastance was calculated. End-systolic stress-strain points were determined for each heart beat as the point at which elastance was maximal. Subsequently, a new ϵ_0 was calculated using a linear least-squares fit through the end-systolic points. The new ϵ_0 value was used to start a new cycle as described above. This

procedure was repeated until ε_0 did not differ more than 1% from the ε_0 determined during the previous cycle. The stress and strain at these points were defined as end-systolic stress (σ_{es}) and end-systolic strain (ε_{es}).

As the end-systolic stress-strain relationship was often curvilinear, the end-systolic points were also fitted to a second order polynomial regression equation: $\sigma = c_3 \cdot \varepsilon^2 + c_2 \cdot \varepsilon + c_1$ (14, 26), using the least-squares technique. If the coefficient c_3 was not significantly different from zero ($p \geq 0.05$), the linear equation was selected. If c_3 was negative (concave to the strain-axis), the second order polynomial was selected. If c_3 was positive (convex to the strain-axis) and the fitted curve did not intersect the strain-axis, the data were fitted to the third order polynomial $\sigma = c_4 \cdot \varepsilon^3 + c_3 \cdot \varepsilon^2 + c_2 \cdot \varepsilon + c_1$. The slope of the end-systolic stress-strain relationship, called the end-systolic elastance (E_{es} , in N/m^2) was used as an index of contractility. As this slope is strain-dependent, E_{es} was calculated as the local slope at a stress, corresponding to a left ventricular pressure of 80 mmHg at baseline. This value was identical during the experiment for each pig.

The area enclosed by the left ventricular stress-strain loop during a single heart beat was calculated as the external work of the myocardial region (EW, in J/m^3), normalized per unit of volume (10, 19, 28). Stress-Strain Area (SSA, in J/m^3), the regional equivalent of the Pressure-Volume Area (PVA), an index of total ventricular work, was calculated as the area enclosed by the end-systolic and end-diastolic relations and the systolic trajectory of the stress-strain loop (14, 24). Potential Energy (PE, in J/m^3) was calculated by subtracting EW from SSA. The regional efficiency of energy transfer (EET, in %) was calculated as $(EW/SSA) \cdot 100\%$. The situation before pre- and afterload changes was called the working point, and σ_{es} , SSA, EW, PE, and EET at the working point were called $\sigma_{es,wp}$, SSA_{wp} , EW_{wp} , PE_{wp} , and EET_{wp} .

Subsequently, for each animal, EW and EET were plotted versus σ_{es} and the relationships were normalized such that EW_{wp} , EET_{wp} , and $\sigma_{es,wp}$ were equal to unity before stunning. To account for changes in the coordinates of the working point for σ_{es} , EW, and EET after stunning, the relationships were normalized such that the coordinates of the working point were equal to the ratio of the mean value after stunning and the mean value before stunning. Each relationship was linearly interpolated to obtain a range of equal σ_{es} -coordinates for each animal. Maximal EW (EW_{max}), maximal EET (EET_{max}) and their respective σ_{es} values ($\sigma_{es,EWmax}$ and $\sigma_{es,EETmax}$) were determined from the normalized curves. The respective differences between EW_{wp} , EET_{wp} , and $\sigma_{es,wp}$ and EW_{max} , EET_{max} , $\sigma_{es,EWmax}$, and $\sigma_{es,EETmax}$ (ΔEW , ΔEET , $\Delta \sigma_{EW}$, $\Delta \sigma_{EET}$) were determined. Finally, the intervals on the σ_{es} -axis (surrounding $\sigma_{es,wp}$) in which EW and EET did not decrease significantly from EW_{wp} and EET_{wp} , were determined using paired t-tests. The left and right borders of these intervals are referred to as left and right significance-borders. To determine the dependence of EW and EET on σ_{es} , the slopes of the EW- σ_{es} and EET- σ_{es} relationships at these significance-borders were calculated. The normalized

curves from different animals were averaged at each normalized σ_{es} -coordinate showing at least five EW or EET measuring values, and the average curve was filtered applying a moving average filter.

Statistics

For all hemodynamic, contractile, and energetic parameters, the effect of infusion of zatebradine and subsequent pacing at 100 beats/min and of LADCA stunning and, for the contractile and energetic parameters (except MVO_2), the difference between the LADCA and LCXCA regions, was tested by a two-way ANOVA for repeated measurements, followed by Student-Newman-Keuls post hoc tests for multiple comparisons. As MVO_2 was only measured in the LADCA perfusion area, a one-way ANOVA for repeated measurements was performed. Because we could not describe the EW- σ_{es} and EET- σ_{es} relationships with a regression equation, we could not perform an ANCOVA to test for changes in these relationships. To overcome this problem, we applied a three-way ANOVA for repeated measures, using σ_{es} , stunning and myocardial region as within-subject factors. Because within-subject factors have to be discrete, we divided the range of σ_{es} values in 6 equal ranges, using the mid- σ_{es} value of each range and the mean of the accompanying EW or EET values. Next, paired t-tests were employed for both perfusion areas to test whether ΔEW and ΔEET differed from zero. Paired t-tests were also performed to test the influence of LADCA stunning on the parameters of the EW- σ_{es} and EET- σ_{es} relationships.

The influence of E_{es} on the curve parameters EW_{max} , ΔEW , EET_{max} , and ΔEET was tested using linear regression on the pooled data of the LADCA and LCXCA perfusion areas before and after stunning. To validate pooling of the data, the two perfusion areas were encoded using a slope- and an intercept-dummy variable and significance of these dummies was tested using an F-test. For the regressions, one data-point with an E_{es} that was 3.7 standard deviations higher than the mean E_{es} was removed. No regression equations are given.

All data have been expressed as mean and 95% prediction interval. $P < 0.05$ was considered significant. Unless stated otherwise, only significant changes are mentioned in the Results.

Results

Systemic hemodynamics

Lowering heart rate by zatebradine from 109 (99-118) beats/min to below 70 beats/min and subsequent pacing to 100 beats/min did not affect any hemodynamic parameter significantly, except for the maximum left ventricular pressure rise, which decreased by 13%. (Table 1). Stunning of the LADCA perfusion area decreased diastolic arterial pressure (15%) and the maximum left ventricular pressure rise (18%). Cardiac

output and stroke volume both decreased by 23% and systemic vascular resistance increased by 17%.

Table 1. *Systemic hemodynamics before and after LADCA stunning*

	Baseline		
	109 (99–118) beats/min	Before stunning 100 beats/min	After stunning 100 beats/min
Mean arterial pressure, mmHg	92 (82–102)	89 (79–99)	78 (67–88)
Systolic arterial pressure, mmHg	108 (99–118)	106 (96–116)	96 (87–105)
Diastolic arterial pressure, mmHg	77 (68–85)	74 (64–84)	63 (53–73)†
Maximum left ventricular pressure rise, mmHg/s	1730 (1450–2010)	1510 (1350–1660)*	1240 (950–1530)†
End-diastolic left ventricular pressure, mmHg	9.8 (8.2–11.4)	9.0 (7.2–10.8)	10.8 (8.8–12.8)
Cardiac output, l/min	2.9 (2.3–3.5)	2.6 (2.3–3.0)	2.0 (1.5–2.4)†
Stroke volume, ml	27 (22–31)	26 (23–30)	20 (15–24)†
Systemic arterial resistance, mmHg·min ⁻¹	34 (26–41)	35 (28–41)	41 (35–48)†

Values are means, with 95% prediction-interval in parentheses; n=9 pigs. LADCA, left anterior descending coronary artery. * $P < 0.05$ vs. baseline, † $P < 0.05$ vs. before stunning at heart rate of 100 beats/min.

Regional contractile and energetic parameters

At baseline, all contractile and energetic parameters were the same between the LADCA and LCXCA regions, except for SSA_{wp} in the LCXCA region, which was 89% of SSA_{wp} in the LADCA region. Lowering heart rate from 109 to below 70 beats/min and pacing at 100 beats/min had no effect on E_{es} , ϵ_0 , $\sigma_{es,wp}$, EW_{wp} , PE_{wp} , and EET_{wp} in both the LADCA and the LCXCA perfusion area, except for SSA_{wp} of the LCXCA region, which decreased by 15% (Table 2). There was no difference between the LADCA and LCXCA region for any parameter, while MVO_2 of the LADCA perfusion area was also unaffected. In the LADCA perfusion area stunning reduced E_{es} by 38%, while ϵ_0 increased by 10%. EW_{wp} decreased by 36%, causing a decrease in EET_{wp} of 27%. SSA_{wp} and PE_{wp} remained unchanged, although PE_{wp} tended to increase. Stunning did not affect MVO_2 . Stunning the LADCA perfusion area had no effect on any of the contractile and energetic parameters of the LCXCA perfusion area, except for EW_{wp} , which decreased by 23%. Stunning also induced differences between the LADCA and LCXCA perfusion areas for E_{es} , ϵ_0 , PE and EET .

Table 2. Regional contractile and energetic parameters before and after LADCA stunning

		Baseline	Before stunning	After stunning
Heart rate (beats/min)		109 (99–118) beats/min	100 beats/min	100 beats/min
E_{es} , $\cdot 10^4$ N/m ²	LADCA	10.8 (7.17–14.4)	11.6 (8.84–14.3)	7.21 (5.16–9.26)†
	LCXCA	11.9 (8.55–15.2)	12.0 (8.43–15.5)	12.9 (8.12–17.7)‡
ϵ_0	LADCA	0.81 (0.78–0.83)	0.81 (0.77–0.84)	0.89 (0.86–0.92)†
	LCXCA	0.82 (0.78–0.85)	0.81 (0.77–0.86)	0.83 (0.78–0.89)‡
$\sigma_{es,wp}$, $\cdot 10^3$ N/m ²	LADCA	12.3 (7.83–16.8)	11.4 (7.45–15.4)	12.8 (7.90–17.7)
	LCXCA	11.8 (9.10–14.4)	11.0 (7.94–14.1)	10.2 (7.74–12.6)
SSA_{wp} , $\cdot 10^2$ J/m ³	LADCA	18.8 (10.6–27.0)	16.3 (8.70–23.8)	14.1 (5.98–22.2)
	LCXCA	16.7 (10.8–22.6)‡	14.2 (9.15–19.2)*	11.1 (6.04–16.1)
EW_{wp} , $\cdot 10^2$ J/m ³	LADCA	13.7 (8.00–19.4)	12.0 (6.61–17.3)	7.69 (2.86–12.5)†
	LCXCA	11.8 (7.35–16.2)	9.75 (6.51–13.0)	7.50 (4.01–11.0)†
PE_{wp} , $\cdot 10^2$ Jm ³	LADCA	5.10 (2.41–7.78)	4.28 (2.00–6.57)	6.38 (2.65–10.1)
	LCXCA	4.93 (3.05–6.82)	4.43 (2.38–6.47)	3.55 (1.95–5.16)‡
EET _{wp} %	LADCA	74.7 (69.1–80.4)	75.4 (69.7–81.0)	54.7 (41.3–68.2)†
	LCXCA	70.8 (65.6–75.5)	69.7 (65.1–74.2)	67.2 (61.4–73.0)‡
MVO_2 , $\cdot 10^2$ J·beat ⁻¹ ·m ⁻³	LADCA	112 (73.9–150)	169 (92.8–244)	157 (69.9–245)

Values are means, with 95% prediction-interval in parentheses; n=9 pigs. E_{es} , end systolic elastance; ϵ_0 , strain at zero stress; subscript “wp” indicates working point; σ_{es} , end-systolic stress; SSA, stress-strain area; EW, external work; PE, potential energy; EET, efficiency of energy transfer; MVO_2 , myocardial oxygen consumption; LCXCA, left circumflex coronary artery. * $P < 0.05$ vs. baseline, † $P < 0.05$ vs. before stunning at 100 beats/min, ‡ $P < 0.05$ vs. LADCA.

EW- σ_{es} relationships

Before stunning, the individual EW- σ_{es} relationships displayed a maximum in EW at $14.1 (7.8-20.4) \cdot 10^2$ J/m³ at an σ_{es} of $15.3 (10.1-20.6) \cdot 10^3$ N/m² (LADCA, before stunning, Fig. 1) and $11.9 (7.9-15.8) \cdot 10^2$ J/m³ at an σ_{es} of $15.9 (12.3-19.5) \cdot 10^3$ N/m² (LCXCA, before stunning). There was no significant difference between the two curves. The normalized average curves of both the LADCA and LCXCA regions displayed a steep descending relationship during σ_{es} reduction, the slopes of these curves at the left significance border were 3.46 (0.63–6.29) (LADCA) and 2.62 (-0.06–5.30) (LCXCA)

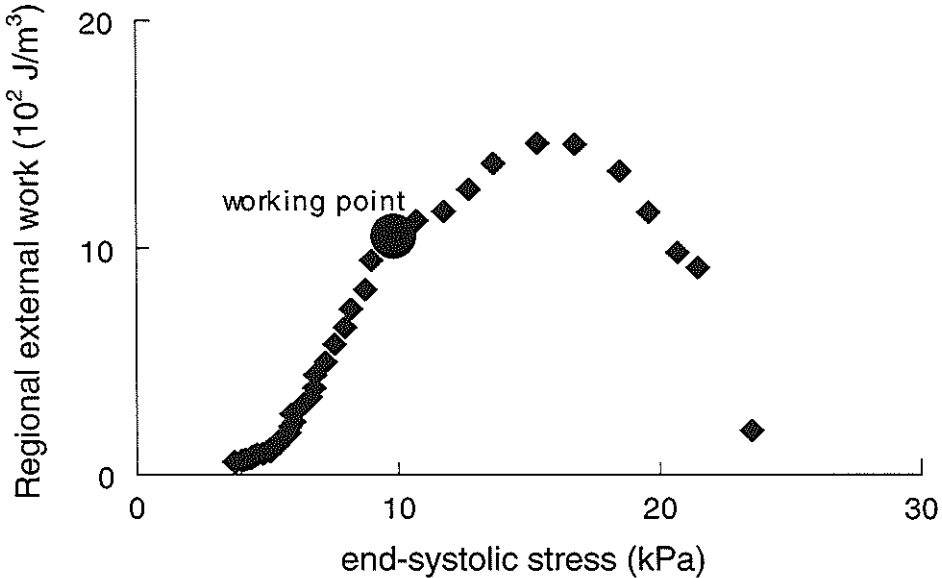


Fig. 1. Example of an $EW-\sigma_{es}$ relationship of the left anterior descending coronary artery (LADCA) perfusion area before stunning of the LADCA perfusion area. See text for details. EW, external work; σ_{es} , regional end-systolic stress.

(Fig. 2, A and C). However, they displayed a flat relationship during σ_{es} increments, the slopes of the curves at the right non-significant maxima were -0.68 (-1.61 – 0.26) (LADCA) and -0.83 (-1.84 – 0.19) (LCXCA). Consequently, a decrease in σ_{es} had a strong influence on EW, only a 2.8% (LADCA) or 1.3% (LCXCA) decrease in σ_{es} from the working point already resulted in a significant decrease in EW. In contrast, an increase in σ_{es} did firstly result in an increase in EW, but a further increase in σ_{es} did not result in a significant decrease in EW. Because of this increase in EW, both $\Delta\sigma_{EW}$ and ΔEW were different from zero; $\Delta\sigma_{EW}$ being 0.35 (0.26 – 0.45) and 0.39 (0.15 – 0.64) and ΔEW being 0.18 (0.10 – 0.27) and 0.21 (0.07 – 0.34) for the LADCA and LCXCA regions, respectively.

Stunning the LADCA region changed the shape of the $EW-\sigma_{es}$ curve and shifted it downward (Fig. 2B). Therefore, the curves became different between the LADCA and LCXCA regions. Now both a decrease (10%) and an increase (13%) in σ_{es} caused a significant reduction in EW in the LADCA region, while in the LCXCA region an 1.1% decrease in σ_{es} still caused a significant decrease in EW and an increase in σ_{es} did not cause a significant decrease in EW. The slopes at the left and right significance-border for the LADCA region did not change significantly, however, and remained at 1.86 (1.07 – 2.65) (left) and -1.06 (-2.03 to -0.09) (right). Furthermore, $\Delta\sigma_{EW}$ decreased to 0.08

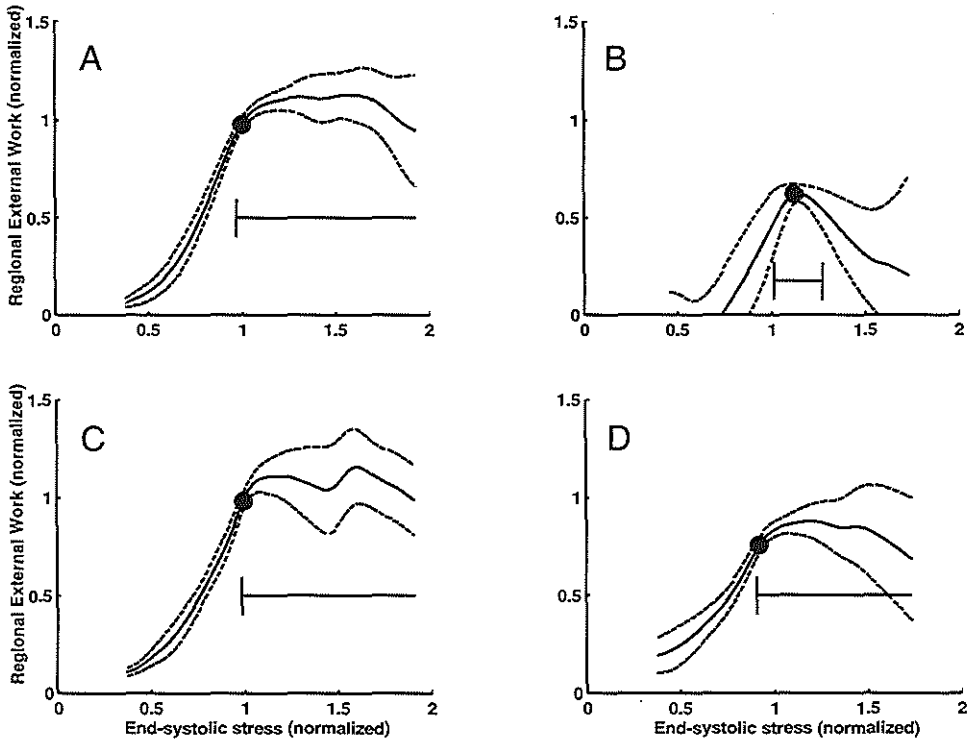


Fig. 2. Averaged curves of normalized EW- σ_{es} relationships. A: LADCA before stunning, B: LADCA after stunning, C: left circumflex coronary artery (LCXCA) before stunning, D: LCXCA after stunning. Solid curves are averaged curves, broken lines are 95% prediction intervals. The horizontal line denotes the part of the curve in which EW is not significantly decreased from EW at the working point. If this line extends to the end of the data, no significant decrease in EW was found. See text for details.

(-0.11-0.27, $P > 0.05$ vs. zero) and ΔEW decreased to 0.07 (0.01-0.13, $P < 0.05$ vs. zero). In addition, the σ_{es} -coordinate of the maximum showed a tendency to decrease by 11% (to $13.7 (8.37-19.0) \cdot 10^3 \text{ N/m}^2$, $P = 0.09$) and the EW-coordinate of the maximum of the EW- σ_{es} curve decreased by 39% to $8.65 (3.16-14.1) \cdot 10^2 \text{ J/m}^3$. For the LCXCA region the ANOVA showed a significant change in the curve due to LADCA stunning (Fig. 2D). However, only EW_{max} decreased by 22% to $9.11 (5.11-13.1) \cdot 10^2 \text{ J/m}^3$ at an unchanged σ_{es} of $13.1 (11.1-15.1) \cdot 10^3 \text{ N/m}^2$. The slopes of the curve at the left significance-border and the right non-significant maximum also remained unchanged at 1.68 (0.27-3.08) and -0.76 (-1.49 to -0.01), respectively.

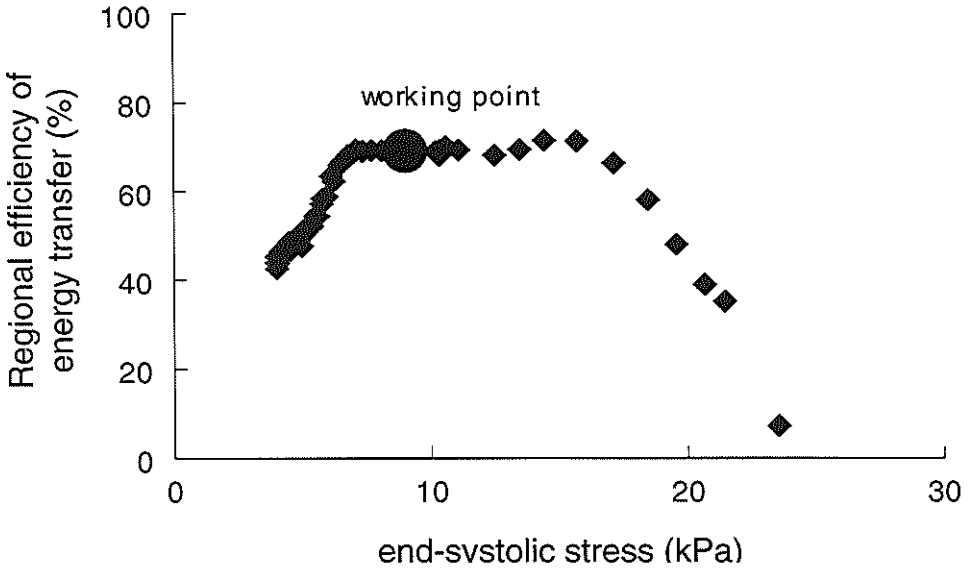


Fig. 3. Example of an EET- σ_{es} relationship of the LADCA perfusion area before stunning of the LADCA perfusion area. See text for details. EET, efficiency of energy transfer.

EET- σ_{es} relationships

The individual EET- σ_{es} relationships displayed a maximum in EET of 78 (74–83)% at an σ_{es} of 10.8 (7.56–14.0)·10³ N/m² (LADCA, before stunning, Fig. 3) and of 74 (69–79)% also at an σ_{es} of 10.8 (6.89–14.6)·10³ N/m² (LCXCA, before stunning) after changing σ_{es} over a large range of values. There was no significant difference between the two curves. The normalized average curves of both the LADCA and LCXCA regions displayed a flat profile over a relatively large range of σ_{es} values. (Fig. 4, A and C). Outside this region EET decreased more sharply. Therefore, a 25% (LADCA) and 38% (LCXCA) reduction in σ_{es} was necessary to induce a significant decrease in EET. Also, a 3% (LADCA) or 34% (LCXCA) increase in σ_{es} resulted in a significant decline in EET. The slopes of the curves at the left significance border were 0.54 (0.07–1.02) (LADCA) and 1.01 (-0.15–2.17) (LCXCA). The slopes at the right significance border were -0.10 (-1.09–0.89) and -0.79 (-1.32 to -0.26), respectively. $\Delta\sigma_{EET}$ was not significantly different from zero, at -0.04 (-0.11–0.04) (LADCA) and -0.04 (-0.17–0.10) (LCXCA). Although

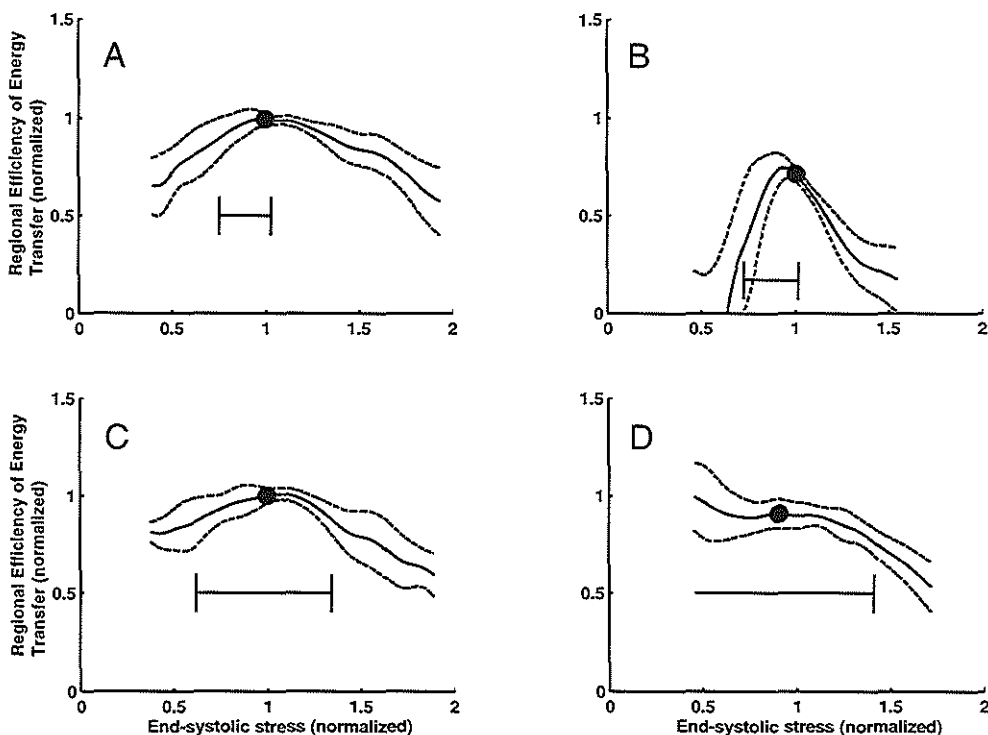


Fig. 4. Averaged curves of normalized EET- σ_{es} relationships. A: LADCA before stunning, B: LADCA after stunning, C: LCXCA before stunning, D: LCXCA after stunning. Solid curves are averaged curves, broken lines are 95% prediction interval. The horizontal line denotes the part of the curve in which EET is not significantly decreased from EET at the working point. If this line extends to the end of the data, no significant decrease in EET was found. See text for details.

the EET-coordinates of the working point were different from the maximum ($P < 0.05$), ΔEET was only 0.04 (0.02–0.06) (LADCA) and 0.08 (0.04–0.13) (LCXCA).

Stunning the LADCA region changed the shape of the EET- σ_{es} curve and shifted it downward (Fig. 4B). The curve now displayed a maximum at 58.9 (45.7–72.2)% (a decrease of 24%, $P < 0.05$ vs. before stunning), at an σ_{es} of 10.8 (6.46–15.2) $\cdot 10^3$ N/m² ($P > 0.05$ vs. before stunning). Still, a 29% decrease in σ_{es} and a 1% increase in σ_{es} caused EET to decrease significantly. The shape of the EET- σ_{es} curve changed in such a way that EET became more sensitive to both increments and decrements in σ_{es} , as the slope of the EET- σ_{es} relationship at the left significance-border increased five-fold to 3.33 (1.33–5.34) and the negative slope at the right significance-border increased nineteen-fold to -1.87 (-3.87–0.12). $\Delta\sigma_{EET}$ and ΔEET remained unaffected at -0.05 (-0.11–0.01) and 0.07 (0.03–0.12), however. In the LCXCA region, stunning had no significant effect on the

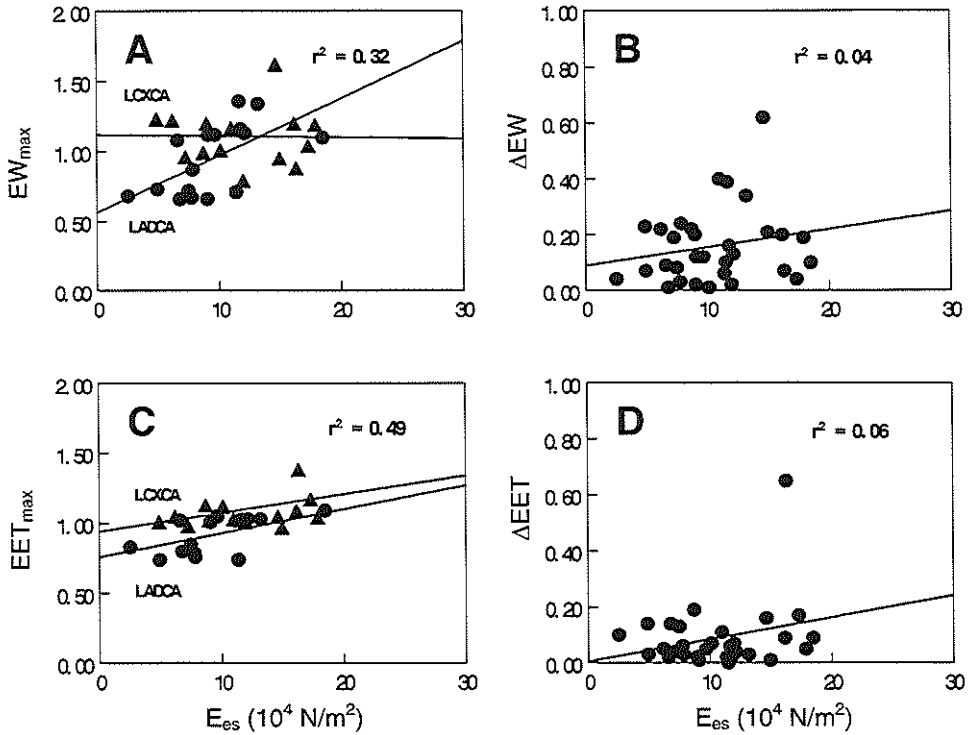


Fig. 5. Relationships between end-systolic elastance (E_{es}) and EW_{max} (A), ΔEW (B), EET_{max} (C), and ΔEET (D). Data from before and after stunning and from the LADCA and LCXCA perfusion areas are pooled. For A and C only, ● = LADCA, ▲ = LCXCA; for B and D, all data are presented by the same symbol (●). EW_{max} , maximal regional EW; ΔEW , difference between maximal regional EW and regional EW at the working point; EET_{max} , maximal regional efficiency of energy transfer; and ΔEET , difference between maximal regional efficiency of energy transfer and regional efficiency of energy transfer at the working point. See text for details.

$EET-\sigma_{es}$ curve (Fig. 4D). The curve displayed a maximum in EET at 76.6 (66.9–86.4)% with an σ_{es} -coordinate of 7.86 (5.04–10.7) $\cdot 10^3$ N/m². A decrease in σ_{es} did not cause a significant decrease in EET , but a 0.6% increase in σ_{es} caused a significant decrease in EET . The slope at the left non-significant minimum was 1.26 (-3.78–6.30) and the slope at the right significance border was 0.07 (-3.07–3.22).

Relationship with contractility

In the regression between E_{es} and the parameters EW_{max} , EET_{max} , ΔEW , and ΔEET , only EW_{max} and EET_{max} showed a significant positive relationship with E_{es} (Fig. 5). Further analysis revealed that both the relationships between EW_{max} and E_{es} and between EET_{max} and E_{es} were different for the LADCA and LCXCA perfusion areas.

Discussion

Normal myocardium

Our first aim was to evaluate whether regional EET and regional EW displayed a maximum in relation to regional afterload, defined as regional σ_{es} . In a strict sense, only EET displayed a maximum in the LADCA and LCXCA perfusion areas, as the relationship between regional EW and afterload showed an increase in EW without a subsequent decrease after increments in afterload. These findings are therefore partly in accordance with earlier studies (5, 7), in which, both global EW and EET displayed a maximum and decreased with increasing afterload. A possible explanation for this discrepancy is that in the present *in vivo* experiments, increments in afterload are accompanied by increments in preload. We investigated the effect of this possible pitfall by dividing EW at the working point and EW at the highest σ_{es} by their respective end-diastolic strains, a measure of regional preload. However, due to the small increments in strain (1.4%), we still could not find a significant decrease in EW at the highest σ_{es} . Therefore, we have to conclude that in the present settings the relationship between EW and afterload increased to a plateau when afterload was increased.

The increase in EW with increasing afterload was 18-20% of the EW at the working point, also when EW was corrected for preload changes. In contrast, maximal EET was only 4-8% different from the EET at the working point, while the two σ_{es} values were not different. Therefore, we conclude that in our experiments normal myocardium operated at maximal EET, rather than at maximal EW.

There is no consensus on whether global left ventricular power is maximal under physiological conditions. For instance, in a modeling-study based on data of intact, conscious dogs, Burkhoff et al., predicted that power is likely to be sub-maximal (5). However, if they used data from anesthetized, open-chest dogs, a maximization of power was predicted. In the present study measurements were performed in anesthetized, open-chest swine and we therefore expected a maximization of power. However, in anesthetized patients undergoing abdominal surgery, Kadoi et al. found a ventriculo-arterial coupling ratio in agreement with sub-maximal power. (13). In the same study, patients undergoing coronary artery bypass surgery with a low ejection fraction had a ventriculo-arterial coupling ratio suggesting maximization of power. Consequently, these results indicate that, apart from myocardial dysfunction, species differences may play an important role. To our knowledge, in swine ventriculo-arterial coupling has only been studied in the normal right ventricle, also suggesting sub-maximal power (3).

Stunned myocardium

Regional stunning of the LADCA perfusion area decreased contractility in accordance with former studies (14). In addition, end-systolic ϵ_0 increased by 10%. In a

former study, we have shown that stunning causes increases in left ventricular volume at zero pressure, independent of inotropic interventions (15). The increase in ϵ_0 may therefore be attributed to a decrease in elastic restoring forces, probably induced by alterations in the extracellular collagen matrix and/or the cytoskeleton.

After stunning the LADCA perfusion area, both EW and EET displayed maxima in relation to σ_{es} . In accordance with decrements in EW and EET at the working point, the maxima in EW and EET were decreased in comparison to normal myocardium. The maximum of the EW- σ_{es} relationship also tended to shift to the left, but this change was not significant ($P=0.09$). Maximal EW was now only 7% higher than EW at the working point, and $\sigma_{es,EWmax}$ was no longer different from $\sigma_{es,wp}$ at the working point. As a consequence, the working point was now similar to maximal EW. To the best of our knowledge, only relative changes in ventriculo-arterial coupling ratio have been reported after regional stunning (30). From these data it cannot be concluded whether or not power was maximized before or after stunning.

A second effect of stunning was that both EW and EET became more sensitive to increments in afterload. This is in agreement with our former study, in which we showed that both EW and EET deduced from pressure-segment length relationships, decreased more with increasing afterload after myocardial stunning (9). As EET also became more sensitive to decrements in σ_{es} , afterload regulation became more critical in stunned myocardium. Changes in preload did not influence this difference, as preload maximally increased by 4% before stunning and 4.5% after stunning ($P=0.41$). In the LCXCA perfusion area, however, the relationship between EW at the working point and maximal EW remained unchanged. So if we augment global afterload, EW will increase in the LCXCA perfusion area and decrease in the LADCA perfusion area. Consequently, global afterload will not simultaneously maximize EW in both myocardial regions. As EET at the working point does not change in relation to maximal EET, both regions still operate at maximal EET. However, small changes in afterload will immediately decrease EET in the stunned LADCA perfusion area. From these findings, we conclude that EW and EET are regulated separately in the two myocardial regions and the LCXCA region does, at least in porcine myocardium, not adapt itself to compensate for the LADCA region.

In accordance with the oxygen consumption paradox of stunned myocardium (8), steady-state myocardial oxygen consumption was unchanged after myocardial stunning. In a former study we showed that two periods of 10 min of ischemia caused ATP, ADP and total adenine nucleotides to decrease by 34%, 37%, and 33%, respectively, while energy charge [defined as $(ATP+0.5\cdot ADP)\cdot(ATP+ADP+AMP)^{-1}$], remained unchanged (17). This suggests an adequate ATP-turnover, despite a decrease in the concentrations of each high-energy phosphate.

Relationship with contractility

We studied the relationship between E_{cs} and EW_{max} , EET_{max} , ΔEW , and ΔEET in the LADCA perfusion area. Although ΔEW was decreased in stunned myocardium, we could not show a positive relationship between ΔEW and E_{cs} . A possible explanation might be that the range in ΔEW was too small, because we did find a positive relationship between E_{cs} and EW_{max} . This latter result was to be expected, because, apart from ΔEW , EW_{wp} also decreased with myocardial stunning, in accordance with former results (16). In that particular study, we also showed a positive non-linear relationship between EET_{wp} and E_{cs} .

Underlying mechanism

It is well accepted that myocardial stunning is the result of disturbances in excitation-contraction coupling. As a consequence, E_{cs} is decreased in stunned myocardium. Due to the positive relationship between E_{cs} and EW_{max} , the decrease in E_{cs} caused a reduction in EW_{max} . EW_{wp} , however, is not only dependent on contractility but also on the regional afterload, characterized by $\sigma_{cs,wp}$. Because regional afterload did not decrease, due to a compensatory increase in systemic vascular resistance (Table 1), EW_{wp} decreased less than EW_{max} , causing the reduction in ΔEW .

Limitations

The present study is based on the time-varying elastance concept, a single elastance changing over time as a model for the myocardium. Hence, visco-elastic properties, kinetic energy and the history-effect (4, 6, 18) are not accounted for. Although the effect of these properties is considered small under physiological circumstances, their contribution in stunned myocardium is presently unknown. In this respect, the results of this study should be interpreted with caution.

In our in vivo model, we were not able to change preload and afterload independently. Decreasing global left ventricular preload decreases not only regional preload but also regional afterload, as both regional wall-thickness and curvature increase. On the other hand, increasing global left ventricular afterload by inflating an intra-aortic balloon decreases cardiac output and therefore increases preload for the next beat. However, changes in preload were small and correcting for these increments in preload did not change our results significantly.

We used the posterior-anterior diameter to calculate regional stress in both the LADCA and LCXCA perfusion areas, which is not completely correct for the LCXCA perfusion area, especially after stunning. This diameter may increase after stunning, due to stretch of the LADCA perfusion area. Consequently, applying the curvature changes to the LCXCA perfusion area may not be fully correct. However, as σ_{cs} was unchanged after

myocardial stunning in both perfusion areas and E_{es} did not change in the LCXCA perfusion area, the error introduced was probably negligible.

We assumed that the myocardial volume between the LADCA crystals remained constant before and after induction of stunning. However, Jennings et al. showed that stunning causes about 8% increase in myocardial cell volume due to increased water content (12). If we assume that in our preparation myocardial volume between the crystals increased by 8% as well, real wall thickness may have increased by 2%. If so, we underestimated stress, E_{es} and EW before stunning by 2%. However, $\sigma_{es,wp}$ showed a non-significant increase due to myocardial stunning, which may be overestimated due to this limitation. Also, the significant decrease in E_{es} and EW due to myocardial stunning may be underestimated. Therefore, this limitation does not seem to affect the reported alterations caused by myocardial stunning.

As we measured regional MVO_2 by sampling the great cardiac vein, this measurement only reflected tissue MVO_2 during steady-state conditions, not allowing us to study the relationship between myocardial efficiency (EW_{wp}/MVO_2) and regional afterload on a beat-to-beat basis. Therefore, it remains unresolved whether or not in our study the myocardium operated at maximal myocardial efficiency.

This study was performed in pentobarbital-anesthetized swine. Because pentobarbital is known to decrease baseline myocardial contractility and to attenuate cardiovascular reflexes, caution is therefore warranted when the present results are extrapolated to the awake animal.

Conclusions

In this study, regional myocardium before stunning operated at maximal EET rather than at maximal EW, partially in accordance with findings in the global left ventricle. As a consequence, recruitment of EW was possible by increasing regional afterload. After myocardial stunning, the myocardium operated both at maximal EW and at maximal EET. In addition, both EW and EET became more sensitive to afterload. The reduced contractility of stunned myocardium is thought to have an important effect on these relationships.

Acknowledgements

The technical assistance of Mr. Jan R. van Meegeen and Mr. Rob H. van Bremen is gratefully acknowledged.

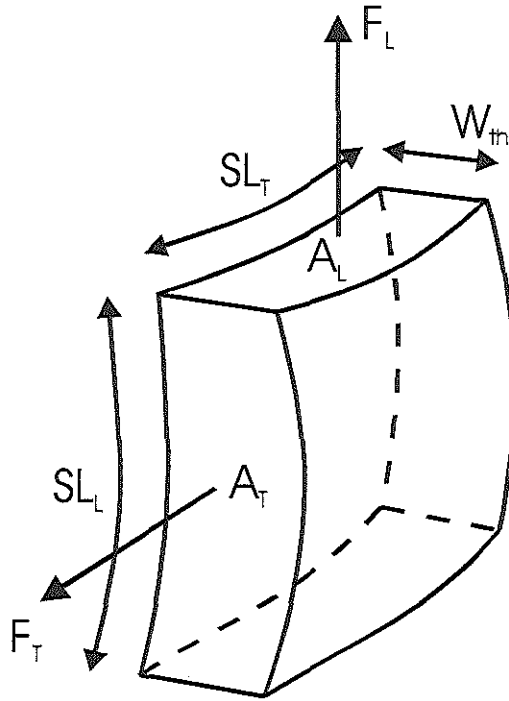


Fig 6. Schematic representation of the forces working on a block of myocardial tissue. SL_T , transversal segment length, SL_L , longitudinal segment length, W_{th} , wall thickness, A_T , transversal segment area, A_L , longitudinal segment area, F_T , transversal force, F_L , longitudinal force. For calculations see Appendix.

Appendix

To calculate regional stress and regional strain we used the following approach. We assumed a concentric spherical geometry of both the regional endocardium and epicardium. Wall tension (T) for a sphere, according to Laplace, is:

$$T = \frac{P \cdot r}{2} \quad (1)$$

in which P is the cavity pressure and r is the radius of the left ventricle. For a rectangular block of tissue in the ventricular wall between two perpendicularly oriented pairs of crystals, a longitudinal segment length (SL_L , which is in a plane through the long axis of the left ventricle), a transversal segment length (SL_T , perpendicular to SL_L), a force oriented parallel to SL_L (F_L) and a force oriented parallel to SL_T (F_T) are defined (Fig. 6). The equations for the two forces are then:

$$F_L = T \cdot SL_T = \frac{P \cdot r \cdot SL_T}{2} \quad (2)$$

and

$$F_T = T \cdot SL_L = \frac{P \cdot r \cdot SL_L}{2} \quad (3)$$

Dividing these forces by the respective areas A_L and A_T delivers the wall stresses in both directions. As the number of fibers producing the forces F_L and F_T being present in the areas A_L or A_T will not change over the cardiac cycle, normalization to fiber stress would not be affected by the changes in the respective areas. We therefore defined a reference state on which all subsequent stress calculations were based. In formula:

$$A_{L,ref} = SL_{T,ref} \cdot Wth_{ref} \quad (4)$$

and

$$A_{T,ref} = SL_{L,ref} \cdot Wth_{ref} \quad (5)$$

in which Wth_{ref} is the reference wall thickness. As the volume of the block of tissue (V_{ref}) remains constant during the cardiac cycle, Wth_{ref} can also be written as:

$$Wth_{ref} = \frac{V_{ref}}{SL_{T,ref} \cdot SL_{L,ref}} \quad (6)$$

Dividing Eq. 2 by Eq. 4 and Eq. 3 by Eq. 5, and combining with Eq. 6 gives us:

$$\sigma_L = \frac{P \cdot r \cdot SL_T \cdot SL_{L,ref}}{2 \cdot V_{ref}} \quad (7)$$

and:

$$\sigma_T = \frac{P \cdot r \cdot SL_L \cdot SL_{T,ref}}{2 \cdot V_{ref}} \quad (8)$$

in which σ_L and σ_T are the longitudinal and transversal wall stress, respectively. Mean average wall stress was defined as the geometric mean (29) according to:

$$\sigma_{mean} = \sqrt{\sigma_L \cdot \sigma_T} = \frac{P \cdot r}{2 \cdot V_{ref}} \cdot \sqrt{SL_{L,ref} \cdot SL_{T,ref}} \cdot \sqrt{SL_T \cdot SL_L} \quad (9)$$

Similarly, mean regional strain (ε) was derived from the geometric mean according to:

$$\varepsilon = \frac{\sqrt{SL_T \cdot SL_L}}{\sqrt{SL_{T,ref} \cdot SL_{L,ref}}} \quad (10)$$

References

1. Aversano, T., W. L. Maughan, W. C. Hunter, D. Kass, and L. C. Becker. End-systolic measures of regional ventricular performance. *Circulation* 73: 938-950, 1986.
2. Bier, J., B. Sharaf, and H. Gewirtz. Origin of anterior interventricular vein blood in domestic swine. *Am J Physiol* 260: H1732-1736, 1991.
3. Bolliger, C., P. Fourie, and A. Coetzee. The effect of prostaglandin E1 on acute pulmonary artery hypertension during oleic acid-induced respiratory dysfunction. *Chest* 99: 1501-1506, 1991.
4. Burkhoff, D., P. P. De Tombe, and W. C. Hunter. Impact of ejection on magnitude and time course of ventricular pressure-generating capacity. *Am J Physiol* 265: H899-909, 1993.
5. Burkhoff, D., and K. Sagawa. Ventricular efficiency predicted by an analytical model. *Am J Physiol* 250: R1021-1027, 1986.
6. Crozatier, B. Stretch-induced modifications of myocardial performance: from ventricular function to cellular and molecular mechanisms. *Cardiovasc Res* 32: 25-37, 1996.
7. De Tombe, P. P., S. Jones, D. Burkhoff, W. C. Hunter, and D. A. Kass. Ventricular stroke work and efficiency both remain nearly optimal despite altered vascular loading. *Am J Physiol* 264: H1817-1824, 1993.
8. Dean, E. N., M. Shlafer, and J. M. Nicklas. The oxygen consumption paradox of "stunned myocardium" in dogs. *Basic Res Cardiol* 85: 120-131, 1990.
9. Fan, D., L. K. Soei, L. M. Sassen, R. Krams, and P. D. Verdouw. Mechanical efficiency of stunned myocardium is modulated by increased afterload dependency. *Cardiovasc Res* 29: 428-437, 1995.
10. Goto, Y., H. Suga, O. Yamada, Y. Igarashi, M. Saito, and K. Hiramori. Left ventricular regional work from wall tension-area loop in canine heart. *Am J Physiol* 250: H151-158, 1986.
11. Ishihara, H., M. Yokota, T. Sobue, and H. Saito. Relation between ventriculoarterial coupling and myocardial energetics in patients with idiopathic dilated cardiomyopathy. *J Am Coll Cardiol* 23: 406-416, 1994.
12. Jennings, R. B., J. Schaper, M. L. Hill, C. Steenbergen, Jr., and K. A. Reimer. Effect of reperfusion late in the phase of reversible ischemic injury. Changes in cell volume, electrolytes, metabolites, and ultrastructure. *Circ Res* 56: 262-278, 1985.
13. Kadoi, Y., H. Kawahara, and N. Fujita. The end-systolic pressure-volume relationship and ventriculoarterial coupling in patients undergoing coronary artery bypass graft surgery. *Acta Anaesthesiol Scand* 42: 369-375, 1998.
14. Krams, R., D. J. Duncker, E. O. McFalls, A. Hogendoorn, and P. D. Verdouw. Dobutamine restores the reduced efficiency of energy transfer from total mechanical work to external mechanical work in stunned porcine myocardium. *Cardiovasc Res* 27: 740-747, 1993.
15. Krams, R., M. Janssen, C. Van der Lee, J. Van Meegen, J. W. De Jong, C. J. Slager, and P. D. Verdouw. Loss of elastic recoil in postischemic myocardium induces rightward shift of the systolic pressure-volume relationship. *Am J Physiol* 267: H1557-1564, 1994.
16. Krams, R., L. K. Soei, E. O. McFalls, E. A. Winkler Prins, L. M. Sassen, and P. D. Verdouw. End-systolic pressure length relations of stunned right and left ventricles after inotropic stimulation. *Am J Physiol* 265: H2099-2109, 1993.
17. Lamers, J. M., D. J. Duncker, K. Bezstarosti, E. O. McFalls, L. M. Sassen, and P. D. Verdouw. Increased activity of the sarcoplasmic reticular calcium pump in porcine stunned myocardium. *Cardiovasc Res* 27: 520-524, 1993.
18. Milnor, W. R. Ventricular Work. In: *Hemodynamics* (2nd ed.). Baltimore: Williams & Wilkins, 1989, p. 282-290.
19. Morris, J. J. r., G. L. Pellom, C. E. Murphy, D. R. Salter, J. P. Goldstein, and A. S. Wechsler. Quantification of the contractile response to injury: assessment of the work-length relationship in the intact heart. *Circulation* 76: 717-727, 1987.
20. Myhre, E. S., A. Johansen, J. Bjornstad, and H. Piene. The effect of contractility and preload on matching between the canine left ventricle and afterload. *Circulation* 73: 161-171, 1986.
21. Nichols, W. W., and C. J. Pepine. Ventricular/vascular interaction in health and heart failure. *Compr Ther* 18: 12-19, 1992.

22. **Sagawa, K., L. Maughan, H. Suga, and K. Sunagawa.** Energetics of the heart. In: *Cardiac contraction and the pressure-volume relationship*. New York: Oxford University Press, 1988, p. 171-231.
23. **Sagawa, K., L. Maughan, H. Suga, and K. Sunagawa.** Experimental search for time-varying elastance concept. In: *Cardiac contraction and the pressure-volume relationship*. New York: Oxford University Press, 1988, p. 55-69.
24. **Suga, H., R. Hisano, S. Hirata, T. Hayashi, O. Yamada, and I. Ninomiya.** Heart rate-independent energetics and systolic pressure-volume area in dog heart. *Am J Physiol* 244: H206-214, 1983.
25. **Toorop, G. P., G. J. Van den Horn, G. Elzinga, and N. Westerhof.** Matching between feline left ventricle and arterial load: optimal external power or efficiency. *Am J Physiol* 254: H279-285, 1988.
26. **van der Velde, E. T., D. Burkhoff, P. Steendijk, J. Karsdon, K. Sagawa, and J. Baan.** Nonlinearity and load sensitivity of end-systolic pressure-volume relation of canine left ventricle in vivo. *Circulation* 83: 315-327, 1991.
27. **Verdouw, P. D., M. A. van den Doel, S. de Zeeuw, and D. J. Duncker.** Animal models in the study of myocardial ischaemia and ischaemic syndromes. *Cardiovasc Res* 39: 121-135, 1998.
28. **Vinten-Johansen, J., P. A. Gayheart, W. E. Johnston, J. S. Julian, and A. R. Cordell.** Regional function, blood flow, and oxygen utilization relations in repetitively occluded-reperfused canine myocardium. *Am J Physiol* 261: H538-547, 1991.
29. **Weast, R. C., M. J. Astle, and W. H. Beyer.** CRC Handbook of Chemistry and Physics. (66 ed.). Boca Raton, Florida, USA: CRC Press, Inc., 1985, p. F-83.
30. **Yokoyama, Y., D. Novitzky, M. T. Deal, and T. R. Snow.** Facilitated recovery of cardiac performance by triiodothyronine following a transient ischemic insult. *Cardiology* 81: 34-45, 1992.

Chapter 5

Oxygen wastage of stunned myocardium

Introduction - We studied whether an increased oxygen cost of contractility and/or a decreased myofibrillar efficiency contribute to oxygen wastage of stunned myocardium. Because Ca^{2+} -sensitizers may increase myofibrillar Ca^{2+} -sensitivity without increasing cross-bridge cycling, we also investigated whether EMD 60263 restores myofibrillar efficiency and/or the oxygen cost of contractility.

Methods - Regional fiber stress and strain were calculated from mesomyocardially implanted ultrasound crystals and left ventricular pressure in anesthetized pigs (n=18). Regional myocardial oxygen consumption (MVO_2) was measured before contractility (end-systolic elastance, E_{es}) and total myofibrillar work (stress-strain area, SSA) were determined from stress-strain relationships. Atrial pacing at three heart rates and two doses of dobutamine were used to vary SSA and E_{es} , respectively. After stunning (two times 10 min ischemia followed by 30 min reperfusion), measurements were repeated following infusion of saline (n=8) or EMD 60263 (1.5 mg·kg⁻¹ i.v., n=10). Linear regression was performed using $\text{MVO}_2 = \alpha \cdot \text{SSA} + \beta \cdot E_{\text{es}} + \gamma \cdot \text{HR}^{-1}$ (α^{-1} =myofibrillar efficiency, β =oxygen cost of contractility, and γ =basal metabolism/min).

Results - Stunning decreased SSA by 57% and E_{es} by 64%, without affecting MVO_2 , while increasing α by 71% and β by 134%, without affecting γ . From the wasted oxygen, 72% was used for myofibrillar work and 18% for excitation-contraction coupling. EMD 60263 restored both α and β .

Conclusions - Oxygen wastage in stunning is predominantly caused by a decreased myofibrillar efficiency and to a lesser extent by an increased oxygen cost of contractility. Considering that EMD 60263 reversed both causes of oxygen wastage, it is most likely that this drug increases myofibrillar Ca^{2+} -sensitivity without increasing myofibrillar cross-bridge cycling.

Serge A.I.P. Trines, Cornelis J. Slager, Tessa A.M. Onderwater, Jos M.J. Lamers, Pieter D. Verdouw, and Rob Krams. Oxygen wastage of stunned myocardium in vivo is due to an increased oxygen cost of contractility and a decreased myofibrillar efficiency. *Cardiovasc Res, In Press.*

Introduction

Despite the decreased contractile function, myocardial oxygen consumption (MVO_2) of stunned myocardium has been reported to be relatively high (14). The underlying mechanism of this "oxygen wastage" is presently unclear.

During physiological conditions, MVO_2 is used for basal metabolism, excitation-contraction coupling and myofibrillar work (27) (Fig. 1). Although contractility (E_{es} , Fig. 1,2) is decreased in stunned myocardium (13), calcium transients remain unchanged (3, 6). Hence, while 80-90% of intracellular calcium is taken up by the sarcoplasmic reticulum (SR) (1, 18) and at least 70% of VO_2 for excitation-contraction coupling is consumed by the SR Ca^{2+} -ATPase (29), unchanged calcium transients may imply an unchanged VO_2 for excitation-contraction coupling ($\beta \cdot E_{es}$, Fig. 1). In accordance with these arguments, Ohgoshi et al. (19) observed in isolated stunned dog hearts that the oxygen cost of contractility (β , Fig. 1), i.e. the amount of non-myofibrillar VO_2 used per unit of contractility, was increased. These authors also showed that, the increase in β is not only due to a decreased myofibrillar calcium sensitivity, but also due to inefficient calcium cycling and the existence of futile cycles (15).

However, in normal myocardium VO_2 for excitation-contraction coupling comprises only up to 20%-30% of total MVO_2 (21), and it seems therefore likely that at least a part of the excess MVO_2 in stunned myocardium is also caused by a decreased efficiency of the myofibrils, which consume 60-70% of total MVO_2 in normal myocardium. Hence, we postulate that the amount of myofibrillar VO_2 consumed per unit of myofibrillar work (α ; Fig. 1) is also increased in stunned myocardium, while VO_2 for myofibrillar work remains unchanged ($\alpha \cdot SSA$). However, studies on myofibrillar efficiency of stunned myocardium are equivocal (Fig. 1:1/ α) (19, 23), showing both a decrease and an increase in efficiency.

A drawback of the aforementioned studies is that they have been performed in isolated hearts beating isovolumically or at a constant stroke volume. Although α and β can be determined in isolated hearts, the individual contribution of α and β to total MVO_2 consumed during normal working conditions can only be determined in the *in vivo* situation. Moreover, as SSA is highly load-dependent and isolated hearts lack normal loading conditions, the change in the contributions of α and β to total MVO_2 in stunning is presently unknown. Consequently, it remains unclear to what extent the oxygen wastage of *in vivo*-stunned myocardium can be explained by VO_2 for excitation-contraction coupling or by VO_2 for myofibrillar work. The first aim was therefore to study the oxygen cost of contractility and myofibrillar efficiency of stunned myocardium *in vivo*.

Ca^{2+} -sensitizers restore the decreased myofibrillar Ca^{2+} -sensitivity of stunned myocardium (30). These drugs decrease oxygen cost of contractility (17, 20) and have

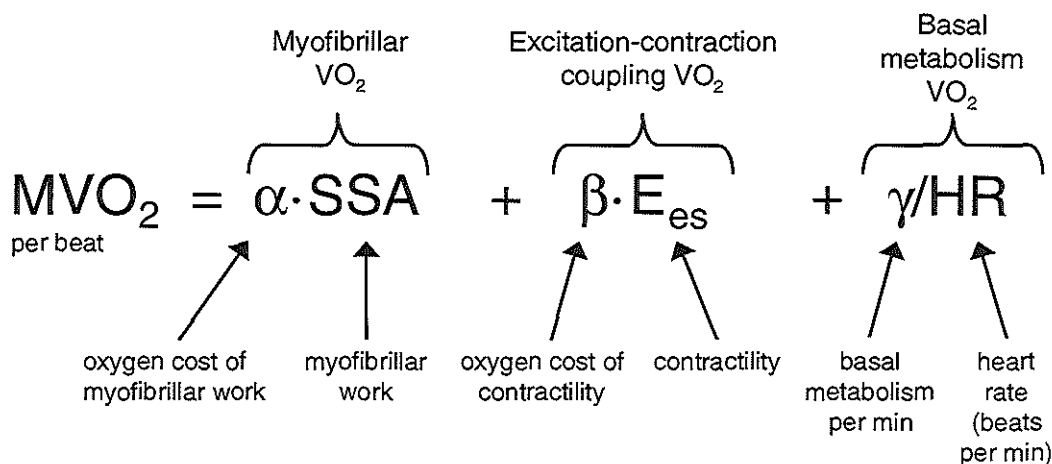


Fig. 1 Myocardial oxygen consumption (MVO_2) per beat is comprised of three components: $\alpha \cdot \text{SSA}$ is related to myofibrillar cross-bridge cycling through the production of myofibrillar work (SSA); $\beta \cdot E_{es}$ is consumed by the (calcium) pumps and depends on contractility (E_{es}); γ/HR is the basal metabolism per beat. As basal metabolism is constant per minute, the basal metabolism per minute (γ) is divided by heart rate (HR). See text for further details about the calculation of MVO_2 , SSA, and E_{es} .

therefore an energetic advantage over drugs that restore function by increasing Ca^{2+} transients. However, if a decreased myofibrillar efficiency also contributes to the oxygen wastage of stunned myocardium, Ca^{2+} -sensitizers will only partly reverse the oxygen wastage, unless they also restore myofibrillar efficiency. This is not unlikely, as Ca^{2+} -sensitizers may act by slowing down the dissociation of the actin-myosin cross-bridges or even by increasing their force rather than by increasing the number of formed cross-bridges (30). Some *in vitro* studies have shown an unchanged myofibrillar efficiency for Ca^{2+} -sensitizers (25, 32), but these findings are constrained by the above-presented arguments. Consequently, we also investigated whether EMD 60263, which does not have a 3',5'-cyclic monophosphate (cAMP)-mediated effect (2, 11), normalizes the increased oxygen cost of contractility and the myofibrillar efficiency in stunned myocardium.

Methods

All experiments were performed in accordance with the "Guide for the Care and Use of Laboratory Animals" as published by the US National Institutes of Health (NIH Publication No. 85-23, revised 1996).

Instrumentation

Crossbred Yorkshire-Landrace pigs (29-43 kg, $n=18$) were anesthetized, intubated and ventilated with a mixture of oxygen and nitrogen, before instrumentation for infusion

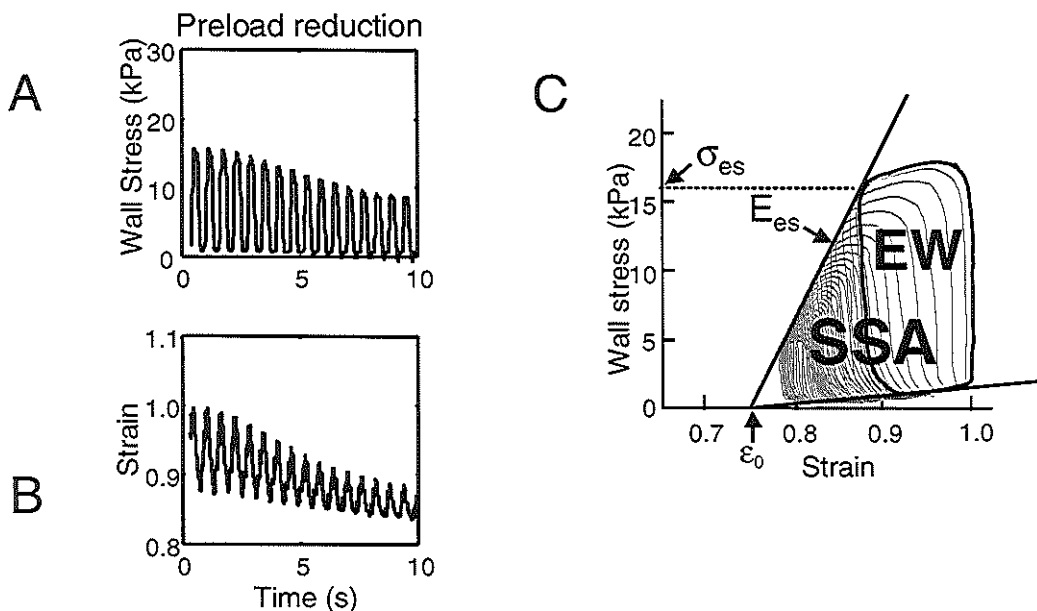


Fig. 2 Determination of regional stress-strain relationships. Reduction in left ventricular preload induces reductions in regional myocardial wall stress (A) and regional strain (B). After relating myocardial strain to myocardial stress during the reduction in preload, regional stress-strain relationships may be evaluated (C). σ_{es} = end-systolic stress, E_{es} = end-systolic elastance, the slope of the end-systolic stress-strain relationship, EW = external work, SSA = stress-strain area.

of 10-15 mg·kg⁻¹·h⁻¹ sodium pentobarbital, saline, EMD 60263 (courtesy of Prof. P. Schelling, E. Merck) and the negative chronotropic agent zatebradine (courtesy of Dr. J.W. Dämmgen, Dr. Karl Thomae) and measurement of aortic blood pressure and left ventricular (LV) pressure (Braun Medical BV, The Netherlands) (31). A balloon catheter was positioned in the inferior caval vein to transiently reduce left ventricular preload.

After a midsternal thoracotomy, electromagnetic flow probes (Skalar, Delft, The Netherlands) were placed around the ascending aorta and the proximal part of the left anterior descending coronary artery (LADCA). Distal to the flow probe, the LADCA was dissected for placement of an atraumatic clamp. To obtain local coronary venous blood samples, a cannula was inserted into the great cardiac vein. Pacing leads were attached to the right atrium and connected to a pacing stimulator (Grass S9). Rectal temperature was kept between 37°C and 38°C.

Segment areas and LV diameter were measured using ultrasound crystals as described before (31). Segment area crystals were implanted in the distribution area of the LADCA and left circumflex coronary artery (LCXCA) while LV diameter crystals were implanted in the LV anterior and posterior wall.

Experimental protocol

After 30-45 min of stabilization, heart rate (HR) was lowered below 70 beats·min⁻¹ by infusion of zatebradine. Then, either saline (control) or one out of two doses of dobutamine, increasing maximum LV pressure rise (LVdP/dt_{max}) to approximately 3000 (low dose, 0.7-2.5 μg·kg⁻¹·min⁻¹) and 4000 mmHg·s⁻¹ (high dose, 1.1-5.5 μg·kg⁻¹·min⁻¹), was infused in random order. During each infusion measurements of hemodynamics and wall function were made and blood samples (31) were taken at HR's of 70, 100 and 130 beats·min⁻¹ (in random order). With the ventilator turned off, LV preload was gradually reduced by inflating the balloon in the inferior caval vein (31). Stunning was produced by two 10 min LADCA occlusions separated by 10 min of reperfusion (31). Thirty min after the second occlusion, animals received either 1.5 mg·kg⁻¹ of EMD 60263 (n=10) or saline (n=8). Ten min later, in all animals the saline, low and high dose dobutamine infusions and measurements were repeated. In a time control group (n=3), all interventions described above with the same time protocol were performed, except that these hearts were not subjected to the occlusion intervention.

Data acquisition and analysis

Hemodynamic and segment area signals were digitized and stored on disk for off-line analysis. Systolic area shortening (SAS, in %) was calculated as (end-diastolic area – end-systolic area) / end-diastolic area * 100%. Left ventricular wall stress (σ , in N·m⁻²) and strain (ϵ , dimensionless) were calculated off-line (31) and end-systolic stress-strain (σ_{es} - ϵ_{es}) relationships were determined from the preload changes. The slope of this relationship, E_{es} (end-systolic elastance), was calculated at a constant stress corresponding to a LV pressure of 50 mmHg at baseline and taken as a measure of contractility (31) (Fig. 2). A pressure of 50 mmHg was chosen to include stunning-induced changes from convex to concave of the non-linear stress-strain relationships (13). The area enclosed by the LV stress-strain loop during a single heartbeat was determined as an index for regional external myocardial work (EW, in J·m⁻³, Fig. 2) (9). The stress-strain area (SSA), an index of total regional myocardial work, was calculated as the area enclosed by the end-systolic and end-diastolic relations and the systolic trajectory of the stress-strain loop (28). Oxygen consumption of the LADCA region was calculated as the product of LADCA-flow and the arterial-coronary venous oxygen difference divided by the mass of the LADCA region (31). The energy consumption per ml of O₂ was set at 20 J; this equivalence is independent of the substrate (22).

Statistics

To assess the effect of the various interventions on global hemodynamics and regional contractile and energetic parameters, two general linear models (GLM) for

repeated measures were applied (SPSS, version 9.0, SPSS Inc.). One GLM tested the effect of HR, dobutamine dose and stunning in the baseline and stunning data, the other GLM tested the effect of HR, dobutamine dose and EMD 60263 in the stunning data without or with subsequent infusion of EMD 60263.

To calculate the VO_2 for myofibrillar work, the VO_2 for excitation-contraction coupling, and the VO_2 for basal metabolism, multiple linear regression was performed on the pooled LADCA data of all animals using: $MVO_2 \cdot HR = \alpha \cdot SSA \cdot HR + \beta \cdot E_{cs} \cdot HR + \gamma$. To this end, animals were encoded using dummy-variables. Subsequently, the two conditions of stunning and stunning after administration of EMD 60263 were encoded separately as dummy-variables, which were multiplied with SSA and E_{cs} to create new dummies for differences in α and β , caused by stunning or stunning with EMD 60263. For each of these dummies, an F-test was performed to evaluate their individual contribution to the entire regression model. Two data points with high leverage values out of 305 data points were removed from the analysis.

The oxygen wastage in stunned myocardium was calculated by subtracting the predicted "normal" MVO_2 from the "stunned" MVO_2 . The predicted "normal" MVO_2 was calculated applying the baseline α , β and γ to the stunning SSA and E_{cs} . The "stunned" MVO_2 was calculated applying the stunning α , β and γ to the stunning SSA and E_{cs} . The individual contribution of myofibrillar work, excitation-contraction coupling and basal metabolism to the oxygen wastage of stunned myocardium was expressed as a percentage of the total oxygen wastage.

P-values below 0.05 were considered significant. Only significant changes are mentioned in the Results-section, unless stated otherwise.

Results

Systemic Hemodynamics (Table 1)

Before stunning - Raising HR from 70 to 130 beats·min⁻¹ significantly increased MAP and CO (both 21%), independent of the dobutamine dose, and decreased LVP_{ed} (44%), while $LVdP/dt_{max}$ remained unchanged. Infusion of dobutamine increased $LVdP/dt_{max}$ (164% for the highest dose) and CO (33%), while SVR decreased (13%).

After stunning - Induction of stunning decreased $LVdP/dt_{max}$ (23%), thereby causing a 30% decrease in MAP and an 18% decrease in CO while LVP_{ed} increased (26%). Moreover, stunning decreased the positive effect of dobutamine on $LVdP/dt_{max}$ to 122% at the highest dose.

Infusion of EMD 60263 - EMD 60263 restored the effect of dobutamine on $LVdP/dt_{max}$ to a maximum of 209% at the highest dose and reversed the positive effect of HR on CO to a decrease of 17%.

Table 1. Systemic Hemodynamics.

	Heart rate (beats·min ⁻¹)	Baseline (n=18)			Stunning (n=8)			Stunning + EMD 60263 (n=10)		
		Δ from control			Δ from control at baseline			Δ from control at baseline		
		control	dobutamine		control	dobutamine		control	dobutamine	
		low dose	high dose		low dose	high dose		low dose	high dose	
MAP (mmHg)	70	82±3	10±3	12±3	-10±3	-6±6	-6±6	-2±4	-5±3	-4±3
Test 1: *‡	100	96±3	4±3	4±3	-29±3	-16±3	-16±3	-14±4	-7±2	-8±3
Test 2:	130	99±3	3±3	4±2	-25±4	-17±3	-18±3	-16±4	-12±3	-12±4
LVdP/dt _{max} (mmHg·s ⁻¹)	70	1310±90	1220±110	2150±120	-210±130	370±260	1070±310	-310±90	830±190	1780±190
Test 1: †‡1	100	1460±80	1350±110	2430±140	-330±60	360±190	1050±200	-350±80	910±160	1730±150
Test 2: †§2	130	1470±80	1290±120	2420±170	-270±70	280±160	920±230	-240±100	750±160	1840±130
LVP _{ed} (mmHg)	70	14.1±1.2	-1.8±0.6	-1.5±0.8	2.1±0.6	1.5±0.5	1.5±1.0	-1.5±2.0	-4.2±1.3	-4.6±0.9
Test 1: *‡	100	11.2±1.0	-1.7±0.6	-2.3±0.8	0.5±1.2	0.3±1.3	-0.4±0.9	-0.9±0.9	-1.1±0.9	-1.6±0.6
Test 2: *†	130	8.9±0.9	-1.4±0.4	-1.8±0.5	2.3±0.7	1.2±1.1	0.8±0.9	-1.1±0.6	-1.5±0.6	-1.7±0.9
CO (l·min ⁻¹)	70	2.4±0.2	0.5±0.1	0.8±0.1	-0.2±0.1	0.2±0.1	0.5±0.1	-0.1±0.3	0.2±0.3	0.4±0.4
Test 1: *†‡	100	2.8±0.2	0.3±0.1	0.6±0.1	-0.5±0.1	-0.1±0.1	0.2±0.1	-0.7±0.2	-0.1±0.2	0.1±0.2
Test 2: *†#	130	2.9±0.2	0.3±0.1	0.6±0.1	-0.5±0.1	-0.1±0.1	0.1±0.2	-1.0±0.2	-0.5±0.2	-0.1±0.3
SVR (mmHg·min·l ⁻¹)	70	38±3	-2±1	-5±1	-1±1	-7±3	-11±1	1±2	-1±2	-2±3
Test 1: *†	100	38±3	-3±1	-5±2	2±6	-6±2	-9±3	4±2	-1±2	-1±2
Test 2: †#	130	37±3	-3±1	-5±2	-1±4	-2±5	-7±4	7±3	1±2	-1±2

Values are mean and standard error of the mean. MAP, mean arterial pressure; LVdP/dt_{max}, maximal left ventricular pressure rise; LVP_{ed}, left ventricular end-diastolic pressure; CO, cardiac output; SVR, systemic vascular resistance. Test 1: Effect of HR, dobutamine and stunning. Test 2: Effect of HR, dobutamine, and EMD 60263 in stunning. * effect of HR $P<0.05$; † effect of dobutamine $P<0.05$; ‡ effect of stunning $P<0.05$; § effect of EMD 60263 $P<0.05$; || Interaction between HR and dobutamine effect $P<0.05$; ¶ interaction between HR and stunning effect $P<0.05$; # interaction between HR and EMD 60263 $P<0.05$; 1 interaction between dobutamine and stunning $P<0.05$; 2 interaction between dobutamine and EMD 60263 $P<0.05$; 3 interaction between stunning and EMD 60263 $P<0.05$.

*Regional contractile and energetic parameters**LADCA region (Table 2)*

Before stunning - SAS (32%), SSA (40%), EW (40%), and MVO_2 (39%) decreased significantly when HR was raised from 70 to 130 beats·min⁻¹. Dobutamine infusion increased SAS (30%), E_{es} (198%), EW (50%), and MVO_2 (65%). Dobutamine also augmented the HR-induced decreases in SSA (from 20% during control to 40% during the high dose of dobutamine).

After stunning - Stunning decreased SAS (89%) and E_{es} (60%), while it increased ϵ_0 (13%). The decrease in E_{es} caused a reduction in SSA (57%) and EW (77%). The positive effect of dobutamine on E_{es} was increased due to LADCA stunning (to 371%). Stunning did not affect MVO_2 . In the control group, however, E_{es} , SSA and MVO_2 were unaffected.

Infusion of EMD 60263 - EMD 60263 increased SAS (267%) and EW (135%), and decreased ϵ_0 (9%). Moreover, EMD 60263 induced a positive effect of HR on E_{es} (16%) and enhanced the negative effect of HR on SAS (to 56%) and SSA (42%) and decreased the negative HR effect on EW (48%). EMD 60263 also decreased the effect of dobutamine on MVO_2 (now up to 23%).

LCXCA region (Table 3)

Before stunning - Increasing HR from 70-130 beats·min⁻¹ decreased SAS (43%). Dobutamine increased EW (47-74%) and SAS (42-78%). The increase in E_{es} was not significant ($P=0.139$).

After stunning - Induction of LADCA-stunning did not decrease E_{es} of the LCXCA region. However, SSA and EW were significantly decreased (59% and 63%, respectively). In addition, stunning increased the positive effect of dobutamine on EW (to 143%).

Infusion of EMD 60263 - Subsequent infusion of EMD 60263 increased SAS (33%) and σ_{cs} (16%), and decreased ϵ_0 (6%). Additionally, EMD 60263 decreased the negative effect of HR on SSA (to 38%) and EW (52%).

Table 2. Contractile and energetic parameters of the LADCA region.

	Heart rate (beats·min ⁻¹)	Baseline (n=18)			Stunning (n=8)			Stunning + EMD 60263 (n=10)		
		Δ from control			Δ from control at baseline			Δ from control at baseline		
		control	dobutamine low dose	dobutamine high dose	control	dobutamine low dose	dobutamine high dose	control	dobutamine low dose	dobutamine high dose
SAS (%)	70	12.2±0.7	1.8±0.3	3.2±0.5	-8.4±0.4	-4.2±0.4	-1.7±0.4	-4.7±1.1	-1.7±1.1	-0.7±0.9
Test 1: *†‡	100	10.2±0.6	1.7±0.3	2.6±0.4	-7.8±0.7	-4.3±0.7	-1.3±0.9	-5.2±1.1	-2.0±0.8	-0.3±1.2
Test 2: *†§#	130	8.3±0.6	1.5±0.3	2.5±0.5	-7.4±0.7	-4.8±0.8	-2.5±1.0	-5.0±1.4	-1.1±1.2	-0.1±1.2
E _{es} (10 ⁴ N·m ⁻²)	70	14.1±1.9	11.4±2.1	15.9±2.6	-9.0±5.7	5.3±7.9	9.9±4.2	-6.1±2.2	2.4±2.4	13.5±4.0
Test 1: †‡¶	100	17.8±2.8	18.7±4.1	17.7±4.2	-10.7±5.8	-3.0±1.6	1.8±2.8	-9.2±1.8	12.3±3.7	17.8±4.3
Test 2: †#	130	16.7±2.1	33.5±8.1	33.1±6.4	-10.7±3.6	-5.2±1.7	2.8±2.9	-7.4±1.8	5.9±4.5	20.3±4.9
ε ₀	70	0.82±0.01	0.01±0.01	0.01±0.01	0.11±0.01	0.09±0.01	0.08±0.01	0.03±0.03	0.03±0.01	0.03±0.01
Test 1: ‡¶	100	0.82±0.01	0.01±0.01	-0.01±0.01	0.10±0.01	0.06±0.01	0.07±0.01	0.04±0.02	0.05±0.01	0.04±0.01
Test 2: †§#	130	0.83±0.01	-0.01±0.01	-0.01±0.01	0.08±0.01	0.06±0.01	0.06±0.01	0.04±0.01	0.04±0.01	0.03±0.01
σ _{es} (10 ³ N·m ⁻²)	70	11.6±0.6	0.5±0.4	0.3±0.4	1.6±0.5	1.0±0.8	0.5±1.0	1.1±1.5	-1.0±0.6	-1.5±0.5
Test 1:	100	12.8±0.8	-0.8±0.4	-1.6±0.5	-1.3±0.9	-1.0±0.7	-2.0±0.8	-0.6±0.6	-1.6±0.6	-1.8±0.6
Test 2: *†	130	12.3±0.8	-0.9±0.5	-1.4±0.5	-0.2±1.0	-0.2±0.7	-1.9±0.6	-0.5±0.5	-2.3±0.8	-1.9±0.8
SSA (10 ² J·m ⁻³)	70	19.3±1.5	4.2±1.0	6.9±1.3	-8.7±1.9	-4.6±1.6	-1.2±1.7	-1.4±4.4	-1.6±2.3	-1.7±2.0
Test 1: *‡	100	18.7±1.3	0.4±0.8	1.4±1.1	-10.6±1.3	-6.7±1.0	-4.9±1.4	-5.6±2.0	-4.2±1.8	-2.6±1.7
Test 2: *† #	130	15.4±1.3	-0.5±1.2	0.3±0.9	-7.1±1.3	-5.6±1.0	-5.8±1.0	-5.0±1.6	-4.2±2.3	-2.8±2.0
EW (10 ² J·m ⁻³)	70	15.7±1.4	4.6±0.9	7.8±1.3	-9.7±1.7	-5.0±1.8	-1.1±1.5	-4.0±2.7	-1.7±2.1	-1.3±1.9
Test 1: *†‡	100	14.2±1.1	2.2±0.6	3.4±0.9	-10.5±0.8	-5.9±0.9	-2.6±1.1	-6.2±1.6	-3.8±1.6	-1.5±1.8
Test 2: *†§#	130	11.2±1.0	1.6±0.9	2.8±0.8	-8.6±0.6	-6.0±0.8	-4.2±1.0	-5.1±1.4	-2.9±1.9	-1.3±1.7
MVO ₂ (10 ² J·m ⁻³ ·beat ⁻¹)	70	156±12	77±18	102±20	-32±18	71±28	133±26	8±25	-6±24	36±27
Test 1: *†	100	128±9	46±12	60±12	24±33	78±35	81±23	-19±18	-11±18	6±18
Test 2: *†‡	130	120±12	29±13	37±11	20±27	44±25	46±19	-30±20	-11±15	-9±16

Values are mean and standard error of the mean. SAS, systolic area shortening, E_{es}, end-systolic elastance, ε₀, strain at zero stress, σ_{es}, end-systolic stress, SSA, stress-strain area, EW, external work, MVO₂, myocardial (LADCA) oxygen consumption. For further explanation of tests and symbols see Table 1.

Table 3. Contractile and energetic parameters of the LCXCA region.

	Heartrate (beats·min ⁻¹)	Baseline (n=18)			Stunning (n=8)			Stunning + EMD 60263 (n=10)		
		Δ from control			Δ from control at baseline			Δ from control at baseline		
		control	dobutamine		control	dobutamine		control	dobutamine	
		low dose	high dose		low dose	high dose		low dose	high dose	
SAS (%)	70	10.3±0.8	2.4±0.4	4.3±0.4	-2.0±1.2	-0.1±1.2	1.9±0.8	0.4±1.1	1.3±0.9	2.3±1.3
Test 1: *†	100	8.6±0.6	2.4±0.3	4.2±0.4	-2.9±1.5	0.2±0.9	0.7±1.1	-1.0±1.0	2.2±1.1	2.0±1.2
Test 2: *†§#	130	5.9±0.7	2.7±0.5	4.6±0.6	-1.7±1.3	0.2±1.1	1.2±1.1	-0.6±0.8	1.3±1.0	3.0±1.0
E _{es} (10 ⁴ N·m ⁻²)	70	13.7±2.3	4.7±1.7	3.8±1.3	4.1±4.1	7.4±4.0	9.8±7.2	2.9±3.0	4.5±2.0	7.2±2.5
Test 1:	100	13.8±2.0	8.4±2.3	9.6±2.1	0.8±4.6	11.3±4.4	12.5±4.2	0.9±2.6	8.7±2.6	9.4±2.4
Test 2: †	130	12.4±2.2	13.0±3.0	19.0±4.8	3.2±5.7	9.2±5.9	17.0±4.8	1.7±3.3	9.1±3.5	11.4±4.4
ε ₀	70	0.82±0.01	-0.01±0.01	-0.02±0.01	0.03±0.02	0.03±0.02	0.02±0.02	0.01±0.01	-0.01±0.01	0.01±0.01
Test 1: †	100	0.82±0.01	-0.01±0.01	-0.01±0.01	0.07±0.02	0.04±0.01	0.04±0.01	0.02±0.02	0.01±0.02	0.01±0.01
Test 2: †§	130	0.83±0.01	0.01±0.01	-0.01±0.01	0.06±0.01	0.05±0.01	0.05±0.01	0.02±0.02	0.01±0.02	-0.01±0.02
σ _{es} (10 ³ N·m ⁻²)	70	10.1±0.8	0.4±0.3	0.4±0.3	-1.5±1.3	-0.4±0.9	-0.7±0.9	-0.7±0.6	-1.1±0.5	-1.7±0.4
Test 1:	100	11.4±1.2	-0.8±0.4	-1.7±0.6	-2.9±1.0	-1.8±0.4	-2.2±0.6	-1.5±0.5	-1.7±0.5	-1.8±0.5
Test 2: §	130	10.9±1.0	-0.9±0.5	-1.4±0.4	-1.8±0.8	-1.5±0.4	-2.6±0.6	-1.2±0.5	-1.9±0.6	-1.7±0.7
SSA (10 ² J·m ⁻³)	70	14.6±1.3	3.5±0.8	7.0±1.2	-4.9±1.5	-2.6±0.8	0.1±1.5	-2.2±1.8	-1.4±1.3	-1.0±1.5
Test 1: †	100	14.9±1.7	0.7±0.7	2.0±0.8	-8.8±2.6	-3.9±0.6	-4.6±1.8	-4.9±1.4	-2.5±1.4	-2.5±1.2
Test 2: *†#	130	11.7±1.3	-0.1±1.0	1.5±0.7	-5.6±1.9	-4.3±1.3	-5.0±1.6	-4.0±1.0	-3.7±1.3	-1.5±1.3
EW (10 ² J·m ⁻³)	70	11.0±1.1	4.2±0.7	8.1±1.1	-3.5±1.3	-0.3±1.1	2.5±1.4	-0.9±1.6	0.3±1.3	1.5±1.4
Test 1: †‡1	100	10.4±1.2	2.7±0.4	4.9±0.5	-6.5±2.6	-1.0±1.2	-0.9±1.4	-3.3±1.0	0.5±1.4	0.6±1.1
Test 2: *†#	130	7.1±0.9	2.4±0.6	4.6±0.6	-3.9±1.8	-1.3±1.3	-0.6±1.3	-2.3±0.7	-0.8±1.1	1.4±1.2

Values are mean and standard error of the mean. SAS, systolic area shortening, E_{es}, end-systolic elastance, ε₀, strain at zero stress, σ_{es}, end-systolic stress, SSA, stress-strain area, EW, external work. For further explanation of tests and symbols see Table 1.

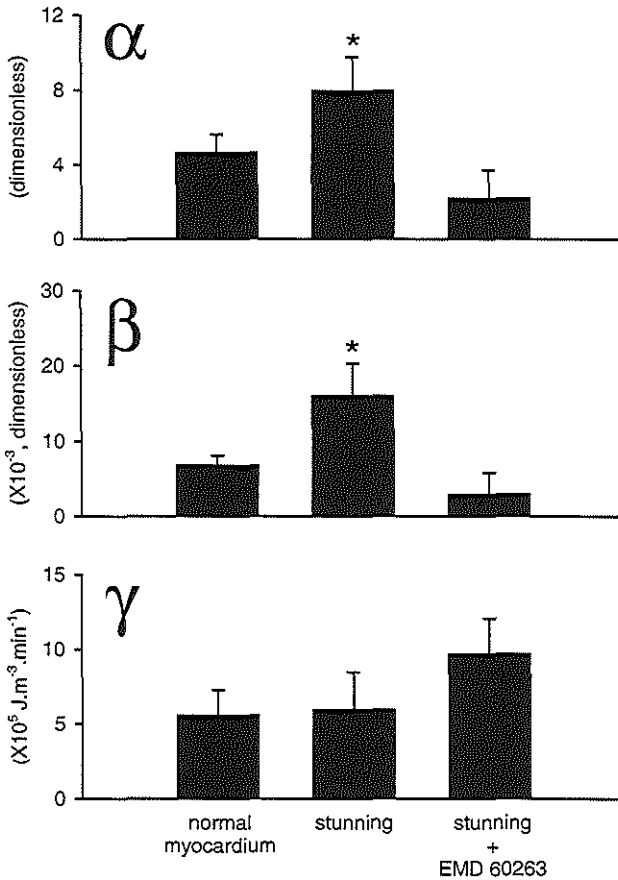


Fig. 3. Coefficients of the regression equation as described in Fig. 1. Top panel: α , middle panel: β , and bottom panel: γ . * $P < 0.05$ vs normal myocardium.

Myofibrillar work, excitation-contraction coupling and basal metabolism (Figure 3)

Normal myocardium - Before stunning, the regression $MVO_2 \cdot HR = \alpha \cdot SSA \cdot HR + \beta \cdot E_{cs} \cdot HR + \gamma$ yielded an α of 4.68 ± 0.97 (dimensionless, Fig. 3 top panel) with β $6.87 \pm 1.26 \cdot 10^{-3}$ (dimensionless, Fig. 3 middle panel) and γ $5.60 \pm 1.68 \cdot 10^5$ ($J \cdot m^{-3} \cdot min^{-1}$, Fig. 3 bottom panel), with $r^2 = 0.70$ for the total regression ($P < 0.001$). The three additional control experiments yielded an α of 3.36 ± 0.50 , with β $3.14 \pm 1.36 \cdot 10^{-3}$ and γ $3.86 \pm 1.79 \cdot 10^5$, with $r^2 = 0.81$ for the total regression ($P < 0.001$). These α , β and γ were not

significantly different from baseline α , β and γ mentioned above ($P=0.488$, $P=0.144$ and $P=0.748$, respectively).

Stunned myocardium - After stunning, α (71%, $P<0.001$) and β (134%, $P=0.019$) increased while γ remained unchanged ($P=0.969$, Fig. 3). Applying the baseline α , β and γ to the SSA and E_{es} of stunned myocardium, a "normal" MVO_2 was predicted that was significantly lower than the measured "stunned" MVO_2 . For example, $101\pm 4 \text{ J}\cdot\text{m}^{-3}\cdot\text{beat}^{-1}$ was predicted for a HR of $100 \text{ beats}\cdot\text{min}^{-1}$ without dobutamine, compared to the measured MVO_2 of $137\pm 34 \text{ J}\cdot\text{m}^{-3}\cdot\text{beat}^{-1}$. From the difference between predicted "normal" and predicted "stunned" MVO_2 , the "wasted" MVO_2 was for 72% myofibrillar VO_2 , for 18% excitation-contraction coupling VO_2 and for 10% basal metabolism VO_2 . In the three control experiments neither α (by -2%, $P=0.227$), β (by 31%, $P=0.738$) nor γ (by 18%, $P=0.832$) changed significantly.

Infusion of EMD 60263 - Compared to baseline, stunning with subsequent infusion of EMD 60263 yielded an unchanged α ($P=0.173$), β ($P=0.235$) and γ ($P=0.127$, Fig. 3). Compared to stunning alone, α and β were decreased ($P<0.001$ and $P=0.015$, respectively), while γ was unaltered ($P=0.349$).

Discussion

The major findings of the present study are that, in regionally stunned myocardium *in vivo*, i) the oxygen cost of contractility is increased, ii) the myofibrillar efficiency is decreased, iii) the relative contribution of both factors is such that oxygen wastage of stunned myocardium is caused mainly by an increased VO_2 for myofibrillar work and to a minor extent by an increased VO_2 for excitation-contraction coupling, and iv) infusion of a cAMP-independent Ca^{2+} -sensitizer EMD 60263 reversed both these changes.

Oxygen wastage of stunned myocardium may be caused by disturbances in energy generation or in energy consumption. Although an existing anaerobic metabolism has been denied by several studies (8), and energy generation is therefore thought to be constant per ml of O_2 , independent of the substrate (22), a decreased efficiency of the mitochondria could also explain part of the inefficient oxygen consumption of stunned myocardium. This could interfere with our results, as we did not directly measure ATP production. However, the efficiency of the mitochondrial ATP production is undiminished in stunned myocardium (33). We may therefore assume that oxygen consumption adequately reflects ATP production, both in the normal and in the stunned myocardium.

The increased oxygen cost of contractility in stunned myocardium is in accordance with observations in isolated dog hearts (19), but the interpretation of the subcellular processes underlying this observation is not obvious. The VO_2 consumed per unit of contractility (β) may be increased because of a decreased myofibrillar Ca^{2+} -sensitivity,

causing the myocardium to generate less force at maintained Ca^{2+} transients, but also because of a decreased efficiency of the SR Ca^{2+} -uptake, causing the SR to consume more oxygen for unchanged Ca^{2+} transients, or both. In addition, an energetically unfavorable redistribution of calcium cycling towards sarcolemmal calcium cycling and the existence of futile cycles may also contribute (15).

However, the extensive mathematical modeling underlying these latter two hypotheses rely upon the *in vitro* finding that the efficiency of the myofibrils remains unchanged (15). The present study provides evidence that in stunned myocardium, myofibrillar inefficiency is the major cause of the oxygen wastage, despite the increase of the oxygen cost of contractility. This is plausible because myofibrillar ATP consumption per cardiac cycle is 60-70% of total energy consumption, while excitation-contraction coupling comprises only 20-30%. In contrast to earlier studies, we determined the relative contribution of myofibrillar efficiency at normal working conditions. The decreased myofibrillar efficiency implies that myofibrillar ATP utilization is less reduced than the generation of force, which is consistent with the *in vitro* findings of Bezstarosti et al. (2).

EMD 60263, at a dose restoring systolic shortening in stunned myocardium (24), reversed the increased oxygen cost of contractility in this study. Likewise, oxygen cost of contractility decreased in excised cross-circulated dog hearts and in human hearts *in vivo* with MCI-154 (17, 20), but was unchanged in excised cross-circulated dog hearts with DPI 201-106 (5), pimobendan (10) and EMD 53998 (4), which is the racemic mixture of the Ca^{2+} -sensitizer EMD 57033 and the phosphodiesterase inhibitor EMD 57439. The unchanged oxygen cost of contractility for pimobendan and EMD 53998 may be explained by their combination of adenosine cAMP-mediated and Ca^{2+} -sensitizing effects (20). However, DPI 201-106 is not cAMP-dependent and the unchanged oxygen cost of contractility for this drug remains unexplained.

EMD 60263 also restored the decreased myofibrillar efficiency of the stunned myocardium, which supports the hypothesis that EMD 60263 may slow down the dissociation of the actin-myosin cross-bridges or increase their force rather than increase the number of cross-bridges formed, as has been shown for other Ca^{2+} -sensitizing drugs (30). An increased efficiency between force production and Ca^{2+} -ATPase activity has also been shown for EMD 53998 (16), but not for EMD 57033 alone (25, 32). As far as we know, a restored myofibrillar efficiency caused by EMD 60263 has not been reported before for this drug. It is clear that a drug showing increased myofibrillar efficiency has energetic advantages over drugs that do not increase myofibrillar efficiency.

Limitations

In this study, we calculated regional stress applying an adaptation from the validated method of Goto et al. (9) as described before (31). In our formula we used global LV pressure, as pressure is the same for the whole ventricle and actually drops to

zero at the epicardium in open-chest pigs, and regional wall thickness, calculated from area changes assuming a constant regional volume. In addition, we calculated regional curvature of the LADCA region from the regional posterior-anterior diameter, assuming a local spherical geometry. This assumption may underestimate regional stress in an absolute sense as the actual regional longitudinal wall radius may be larger than the measured transversal one. However, as we studied regional stress in the same way for all animals in all conditions, we think that the relative changes in stress and energetics, on which our conclusions are based, will not be seriously affected by this assumption. Subsequently, we used the posterior-anterior diameter to calculate regional stress in the LCXCA region, which may not be completely correct, as the diameter may increase after stunning the LADCA-perfused territory, due to stretch of the LADCA region. However, as LADCA stunning increased the diameter by only 4.8% (data not shown) and stunning did not affect E_{es} and σ_{es} of the LCXCA region, the error introduced was probably small.

Myofibrillar efficiency and oxygen cost of contractility were estimated *in vivo* and we were therefore unable to change contractility and myocardial work completely independent of each other. However, in the statistical analysis, the correlation coefficient between SSA and E_{es} was only 0.20, which does not pose problems of multicollinearity (7).

Dobutamine was used to increase excitation-contraction coupling. However, dobutamine decreases the Ca^{2+} -sensitivity of the myofibrils (12, 26) and this may influence the values of α and β . To evaluate this effect, we performed a sub-analysis after excluding the dobutamine-data from the regression. Although β could not be accurately determined due to the smaller changes in E_{es} , α remained unchanged at 3.367 ± 1.192 for normal myocardium, while it was still increased to 6.569 ± 2.107 for stunned myocardium. Therefore, the decreased myofibrillar efficiency in myocardial stunning appears to be independent of dobutamine infusion.

Conclusions

In this study, regionally stunned myocardium *in vivo* showed both a decrease in myofibrillar efficiency and an increase in oxygen cost of contractility. Although both changes contributed to the relatively high oxygen consumption, this "oxygen wastage" was mainly caused by the decreased myofibrillar efficiency. EMD 60263, a cAMP-independent Ca^{2+} -sensitizing drug, reversed both these effects. Therefore, this drug does not only increase myofibrillar Ca^{2+} -sensitivity, but probably without increasing myofibrillar cross-bridge cycling.

References

1. Banijamali, H. S., W. D. Gao, B. R. MacIntosh, and H. E. ter Keurs. Force-interval relations of twitches and cold contractures in rat cardiac trabeculae. Effect of ryanodine. *Circ Res* 69: 937-948, 1991.
2. Bezstarosti, K., L. K. Soei, R. Krams, F. J. Ten Cate, P. D. Verdouw, and J. M. Lamers. The effect of a thiaziazinone derived Ca^{2+} sensitizer on the responsiveness of Mg^{2+} -ATPase to Ca^{2+} in myofibrils isolated from stunned and nonstunned porcine and human myocardium. *Biochem Pharmacol* 51: 1211-1220, 1996.
3. Carrozza, J. P., Jr., L. A. Bentivegna, C. P. Williams, R. E. Kuntz, W. Grossman, and J. P. Morgan. Decreased myofilament responsiveness in myocardial stunning follows transient calcium overload during ischemia and reperfusion. *Circ Res* 71: 1334-1340, 1992.
4. De Tombe, P. P., D. Burkhoff, and W. C. Hunter. Effects of calcium and EMD-53998 on oxygen consumption in isolated canine hearts. *Circulation* 86: 1945-1954, 1992.
5. Futaki, S., Y. Goto, Y. Ohgoshi, H. Yaku, and H. Suga. Similar oxygen cost of myocardial contractility between DPI 201-106 and epinephrine despite different subcellular mechanisms of action in dog hearts. *Heart Vessels* 7: 8-17, 1992.
6. Gao, W. D., D. Atar, P. H. Backx, and E. Marban. Relationship between intracellular calcium and contractile force in stunned myocardium. Direct evidence for decreased myofilament Ca^{2+} responsiveness and altered diastolic function in intact ventricular muscle. *Circ Res* 76: 1036-1048, 1995.
7. Glantz, S. A., and B. K. Slinker. Multicollinearity and what to do about it. In: *Primer of Applied Regression and Analysis of Variance* McGraw-Hill, Inc., 1990, p. 181-238.
8. Gorge, G., I. Papageorgiou, and R. Lerch. Epinephrine-stimulated contractile and metabolic reserve in postischemic rat myocardium. *Basic Res Cardiol* 85: 595-605, 1990.
9. Goto, Y., Y. Igarashi, Y. Yasumura, T. Nozawa, S. Futaki, K. Hiramori, and H. Suga. Integrated regional work equals total left ventricular work in regionally ischemic canine heart. *Am J Physiol* 254: H894-904, 1988.
10. Hata, K., Y. Goto, S. Futaki, Y. Ohgoshi, H. Yaku, O. Kawaguchi, T. Takasago, A. Saeki, T. W. Taylor, T. Nishioka, and et al. Mechanoenergetic effects of pimobendan in canine left ventricles. Comparison with dobutamine. *Circulation* 86: 1291-1301, 1992.
11. Himmel, H. M., G. J. Amos, E. Wettwer, and U. Ravens. Effects of the calcium sensitizer [+-]EMD 60263 and its enantiomer [-]-EMD 60264 on cardiac ionic currents of guinea pig and rat ventricular myocytes. *J Cardiovasc Pharmacol* 33: 301-308, 1999.
12. Keane, N. E., P. G. Quirk, Y. Gao, V. B. Patchell, S. V. Perry, and B. A. Levine. The ordered phosphorylation of cardiac troponin I by the cAMP-dependent protein kinase--structural consequences and functional implications. *Eur J Biochem* 248: 329-337, 1997.
13. Krams, R., L. K. Soei, E. O. McFalls, E. A. Winkler Prins, L. M. Sassen, and P. D. Verdouw. End-systolic pressure length relations of stunned right and left ventricles after inotropic stimulation. *Am J Physiol* 265: H2099-2109, 1993.
14. Krukenkamp, I. B., N. A. Silverman, D. Sorlie, A. Pridjian, H. Feinberg, and S. Levitsky. Characterization of postischemic myocardial oxygen utilization. *Circulation* 74: III125-129, 1986.
15. Lee, S., J. Araki, T. Imaoka, M. Maesako, G. Iribe, K. Miyaji, S. Mohri, J. Shimizu, M. Harada, T. Ohe, M. Hirakawa, and H. Suga. Energy-wasteful total Ca^{2+} handling underlies increased O_2 cost of contractility in canine stunned heart. *Am J Physiol Heart Circ Physiol* 278: H1464-1472, 2000.
16. Leijendekker, W. J., and J. W. Herzig. Reduction of myocardial cross-bridge turnover rate in presence of EMD 53998, a novel Ca^{2+} -sensitizing agent. *Pflugers Arch* 421: 388-390, 1992.
17. Mori, M., M. Takeuchi, H. Takaoka, K. Hata, Y. Hayashi, H. Yamakawa, and M. Yokoyama. Oxygen-saving effect of a new cardiogenic agent, MCI-154, in diseased human hearts. *J Am Coll Cardiol* 29: 613-622, 1997.
18. Negretti, N., S. C. O'Neill, and D. A. Eisner. The relative contributions of different intracellular and sarcolemmal systems to relaxation in rat ventricular myocytes. *Cardiovasc Res* 27: 1826-1830, 1993.
19. Ohgoshi, Y., Y. Goto, S. Futaki, H. Taku, O. Kawaguchi, and H. Suga. Increased oxygen cost of contractility in stunned myocardium of dog. *Circ Res* 69: 975-988, 1991.

20. Onishi, K., K. Sekioka, R. Ishisu, Y. Abe, H. Tanaka, M. Nakamura, Y. Ueda, and T. Nakano. MCL-154, a Ca^{2+} sensitizer, decreases the oxygen cost of contractility in isolated canine hearts. *Am J Physiol* 273: H1688-1695, 1997.
21. Opie, L. H. Energy for ion fluxes. In: *The Heart, physiology from cell to circulation* (3d ed.). Philadelphia: Lippincot-Raven Publishers, 1998, p. 110.
22. Sagawa, K., L. Maughan, H. Suga, and K. Sunagawa. Energetics of the heart. In: *Cardiac contraction and the pressure-volume relationship*. New York: Oxford University Press, 1988. p. 171-231.
23. Schipke, J. D., U. Sunderdiek, B. Korbmacher, U. Schwanke, and G. Arnold. Utilization of oxygen by the contractile apparatus is disturbed during reperfusion of post-ischaemic myocardium. *Eur Heart J* 16: 1476-1481, 1995.
24. Soei, L. K., L. M. Sassen, D. S. Fan, T. van Veen, R. Krams, and P. D. Verdouw. Myofibrillar Ca^{2+} sensitization predominantly enhances function and mechanical efficiency of stunned myocardium. *Circulation* 90: 959-969, 1994.
25. Solaro, R. J., G. Gambassi, D. M. Warshaw, M. R. Keller, H. A. Spurgeon, N. Beier, and E. G. Lakatta. Stereoselective actions of thiazidinones on canine cardiac myocytes and myofilaments. *Circ Res* 73: 981-990, 1993.
26. Solaro, R. J., A. J. Moir, and S. V. Perry. Phosphorylation of troponin I and the inotropic effect of adrenaline in the perfused rabbit heart. *Nature* 262: 615-617, 1976.
27. Suga, H. Ventricular energetics. *Physiol Rev* 70: 247-277, 1990.
28. Suga, H., R. Hisano, S. Hirata, T. Hayashi, O. Yamada, and I. Ninomiya. Heart rate-independent energetics and systolic pressure-volume area in dog heart. *Am J Physiol* 244: H206-214, 1983.
29. Takaki, M., H. Kohzuki, Y. Kawatani, A. Yoshida, H. Ishidate, and H. Suga. Sarcoplasmic reticulum Ca^{2+} pump blockade decreases O_2 use of unloaded contracting rat heart slices: thapsigargin and cyclopiazonic acid. *J Mol Cell Cardiol* 30: 649-659, 1998.
30. Teramura, S., and T. Yamakado. Calcium sensitizers in chronic heart failure: inotropic interventions-reservation to preservation. *Cardiologia* 43: 375-385, 1998.
31. Trines, S. A., C. J. Slager, J. van der Moer, P. D. Verdouw, and R. Krams. Efficiency of energy transfer, but not external work, is maximized in stunned myocardium. *Am J Physiol Heart Circ Physiol* 279: H1264-1273, 2000.
32. Vannier, C., V. Lakomkine, and G. Vassort. Tension response of the cardiotonic agent (+)-EMD-57033 at the single cell level. *Am J Physiol* 272: C1586-1593, 1997.
33. Zuurbier, C. J., and J. H. van Beek. Undiminished mitochondrial function during stunning in rabbit heart at 28 degrees C. *Cardiovasc Res* 35: 113-119, 1997.

Chapter 6

Cardiovascular profile of EMD 57033

Introduction - Ca^{2+} sensitizers enhance systolic function, but impair relaxation in vitro; these effects may differ in stunned and normal myocardium. We therefore studied the effect of EMD 57033 on systolic and diastolic function of normal and stunned porcine myocardium in vivo.

Methods and Results - Myocardial stunning by 15 min coronary occlusion and 30 min reperfusion abolished systolic shortening (SS) (baseline 13 ± 1 %) and decreased end-systolic elastance (E_{es}) from 67 ± 7 to 47 ± 5 mmHg \cdot mm $^{-1}$ (both $P < 0.05$). Maximum rate of fall of myocardial elastance (dE/dt_{min}) decreased from -850 ± 100 to -320 ± 30 mmHg \cdot mm $^{-1}\cdot$ s $^{-1}$, while the time constant τ_e of the decay of elastance increased from 58 ± 3 to 68 ± 6 ms (both $P < 0.05$). End-diastolic elastance (E_{ed}) was unchanged although the zero pressure intercept ($L_{0,\text{ed}}$) had increased. In the stunned region, EMD 57033 (0.2 mg \cdot kg $^{-1}\cdot$ min $^{-1}$ for 60 min, i.v., $n=7$) increased SS to 19 ± 2 %, E_{es} to 287 ± 40 mmHg \cdot mm $^{-1}$, dE/dt_{min} to -3630 ± 640 mmHg \cdot mm $^{-1}\cdot$ s $^{-1}$ and decreased τ_e to 50 ± 3 ms, while E_{ed} remained unchanged. In the normal region, EMD 57033 increased SS from 14 ± 2 to 18 ± 3 %, E_{es} from 59 ± 4 to 263 ± 23 mmHg \cdot mm $^{-1}$, dE/dt_{min} from -480 ± 70 to -2280 ± 700 mmHg \cdot mm $^{-1}\cdot$ s $^{-1}$ and decreased τ_e from 91 ± 12 to 61 ± 3 ms (all $P < 0.05$), while E_{ed} remained unchanged. These responses were minimally affected by adrenoceptor blockade ($n=7$). Vehicle ($n=7$) had no effect on either region. EMD 57033 increased cardiac output (up to 27 ± 8 %) and LVdP/dt $_{\text{max}}$ (86 ± 19 %). Mean aortic pressure decreased (19 ± 7 %) due to systemic vasodilation that was not amenable to blockade of adrenoceptors or NO synthesis.

Conclusions - EMD 57033 restored systolic and diastolic function of stunned myocardium, and produced similar improvements in systolic and diastolic function in normal myocardium.

Sandra de Zeeuw, Serge A.I.P Trines, Rob Krams, Dirk J. Duncker, Pieter D. Verdouw.
Cardiovascular profile of the calcium sensitizer EMD 57033 in open-chest anesthetized pigs with regionally stunned myocardium. *Br J Pharmacol* 129: 1413-1422, 2000.

Introduction

Stunned myocardium is characterized by both a depressed systolic and diastolic function (3, 4, 8). Since a decreased responsiveness of the myofilaments to calcium (Ca^{2+}) has been implicated in the mechanism underlying stunning, several groups of investigators have successfully employed “ Ca^{2+} -sensitizing agents” to restore systolic function of stunned myocardium in a variety of *in vivo* (1, 24) and *in vitro* (14-16) models. It has been suggested that the inotropic response to Ca^{2+} -sensitizers may differ between stunned and normal myocardium. For instance, we have shown that the EMD 60263-induced increase in regional systolic shortening in stunned myocardium of anesthetized pigs was much more pronounced than that in normal myocardium (24). However, systolic shortening is strongly load-dependent, even more so in stunned myocardium, and does not necessarily reflect myocardial contractility (9). That also the lusitropic response to Ca^{2+} -sensitizers in stunned and normal myocardium may differ was suggested by Korbmacher et al. (16), who showed that in response to high doses of EMD 60263 global diastolic function deteriorated more in normal than in globally stunned isolated rabbit hearts. However, data on diastolic functional responses of stunned myocardium to Ca^{2+} -sensitizing agents *in vivo* are currently lacking.

In view of these considerations, we studied the effects of EMD 57033 on regional systolic and diastolic function in an *in vivo* porcine model of stunned and normal myocardium. EMD 57033 was chosen because it is a thiazadiazinone derivative, that lacks the inhibitory action on the delayed rectifier inward current that is exhibited by EMD 60263 and which may potentially modify systolic and diastolic responses by prolongation of the action potential duration (22). However, EMD 57033 possesses phosphodiesterase III inhibiting properties (which EMD 60263 lacks) that could act to enhance systolic and diastolic function (22). Therefore, we also studied EMD 57033 in the presence of α - and β -adrenergic receptor blockade. To circumvent the problem of load-dependency of systolic shortening, we employed, in analogy to the time-varying elastance concept, regional LV end-systolic pressure-segment length relations to obtain a more load-independent measure of regional myocardial contractility (2). Also based on the time-varying elastance concept we determined regional LV end-diastolic pressure-segment length relations to describe diastolic function. Since the latter is a measure of late diastolic function, we also determined the maximum rate of fall (dE/dt_{\min}) and the time constant (τ_e) of the decay of myocardial elastance to describe early diastolic function.

Methods

Animal care

All experiments were performed in accordance with the “Guiding Principles for the

Care and Use of Laboratory Animals” as approved by the American Physiological Society and with prior approval of the Animal Care Committee of the Erasmus University Rotterdam.

Animal preparation

Cross-bred Landrace x Yorkshire pigs of either sex (28-36 kg) were sedated with ketamine i.m. (20-30 mg·kg⁻¹, Apharmo, Huizen, The Netherlands) and anesthetized with sodium pentobarbital i.v. (20 mg·kg⁻¹, Sanofi, Paris, France), before they were intubated and connected to a respirator for intermittent positive pressure ventilation with a mixture (1:2 vol%) of oxygen and nitrogen. Arterial blood gas values were kept within the normal range (pH: 7.35-7.45; pCO₂: 35-45 mmHg; pO₂: 100-150 mmHg) by adjusting respiratory rate and tidal volume. Fluid-filled catheters were placed in the superior caval vein for administration of sodium pentobarbital (5-10 mg·kg⁻¹·h⁻¹) to keep a constant depth of anesthesia and for administration of Haemaccel (Behringwerke A.G., Marburg, Germany) to maintain fluid balance. A fluid-filled catheter was positioned in the descending aorta to monitor arterial blood pressure, while a micromanometer-tipped catheter (B. Braun Medical B.V., Uden, The Netherlands) was advanced into the left ventricle to measure LV blood pressure and its first derivative (LVdP/dt). In order to construct the LV pressure-segment length relations a balloon catheter was positioned in the inferior caval vein for varying LV preload.

After administration of pancuronium bromide (4 mg, Organon Teknika, Oss, The Netherlands) a midsternal thoracotomy was performed and the heart suspended in a pericardial cradle. Then, an electromagnetic flow probe (Skalar, Delft, The Netherlands) was placed around the ascending aorta to measure ascending aortic blood flow (cardiac output). A proximal segment of the left anterior descending coronary artery (LADCA) was dissected free for placement of a Doppler flow probe (Crystal Biotech, Northboro, MA, USA) to measure coronary blood velocity and for placement of an atraumatic clamp for occlusion of the artery. The vein accompanying the LADCA was cannulated for collection of blood samples for determination of coronary venous O₂ content.

Regional myocardial function was measured using sonomicrometry (Triton Technology Inc., San Diego, CA, USA) by placing one pair of ultrasound crystals in the distribution area of the LADCA and one pair in the distribution area of the left circumflex coronary artery (LCXCA). Each pair was implanted in the midmyocardial layer approximately 10 mm apart and parallel to the fiber direction.

Experimental protocols

After a 30-45 min stabilization period, baseline data of systemic hemodynamics and regional myocardial function were recorded, while arterial and coronary venous blood samples were collected. Preload was transiently reduced (< 12 s) (2) by inflation of the

balloon in the inferior caval vein for determination of the LV pressure-segment length relations. Subsequently, the LADCA was occluded for 15 min and after 15 min of reperfusion the 21 animals were randomly allocated to one of three groups. The first two groups received either intravenous $0.5 \text{ ml}\cdot\text{min}^{-1}$ propylene glycol ($n=7$) or $0.2 \text{ mg}\cdot\text{kg}^{-1}\cdot\text{min}^{-1}$ EMD 57033 ($n=7$) during 60 min. In 5 animals of the latter group blood samples were collected at 15 min intervals and the plasma stored at -25°C until determination of plasma levels of EMD 57033. Tissue samples were collected from various organs in two animals at the end of the experiment for determination of EMD 57033 levels. The third group ($n=7$) received EMD 57033 after adrenoceptor blockade to eliminate the putative dependency on adrenergic activity of the EMD 57033-induced changes. For this purpose, the α - and β -adrenoceptors were blocked after 15 min of reperfusion, i.e. 15 min before administration of EMD 57033 by intravenous infusion of $1 \text{ mg}\cdot\text{kg}^{-1}$ phentolamine and $0.5 \text{ mg}\cdot\text{kg}^{-1}$ propranolol (followed by $0.5 \text{ mg}\cdot\text{kg}^{-1}\cdot\text{h}^{-1}$), respectively. The adequacy of the doses of phentolamine and propranolol has been demonstrated previously (7, 28). Since we observed that the systemic vasodilation produced by EMD 57033 was unmitigated in the presence of combined α - and β -adrenoceptor blockade, we added a fourth group of pigs ($n=4$) in which EMD 57033 ($0.2 \text{ mg}\cdot\text{kg}^{-1}\cdot\text{min}^{-1}$ i.v.) was infused after 30 min of reperfusion in the presence of α - and β -adrenoceptor blockade and blockade of NO synthesis (20). NO synthesis was inhibited with N^ω -nitro-L-arginine ($20 \text{ mg}\cdot\text{kg}^{-1}$, i.v.) (5).

In the first three groups of animals, regional myocardial blood flows were determined by intra-atrial injection of $1\text{-}2\times 10^6$ radioactive microspheres [$15\pm 1 \mu\text{m}$ (s.d.) in diameter] labelled with either ^{46}Sc , ^{95}Nb , ^{103}Ru , ^{113}Sn or ^{141}Ce (NEN Company, Dreieich, Germany), using the arterial reference sampling technique (6). At the end of each experiment, the LADCA was ligated at the site of occlusion and the area perfused by the LADCA was identified by intracoronary injection of patent blue violet (Sigma Chemical Co., St. Louis, USA). Immediately thereafter, the animals were killed with an overdose of pentobarbital and the heart excised and handled as described earlier in order to obtain regional myocardial blood flow data in the LADCA and non-LADCA regions (6, 23).

Data acquisition and analysis

Systolic and post-systolic shortening. All segment length data were normalized to an end-diastolic length (EDL) of 10 mm at baseline to correct for variability in the implantation distance between the crystals. Systolic shortening (SS) was computed as $100\% \cdot (\text{EDL}-\text{ESL})/\text{EDL}$, in which EDL and ESL (end-systolic length) are the segment length at the onset of the rapid increase in LV pressure ($\text{LVdP}/\text{dt} = 250 \text{ mmHg}\cdot\text{s}^{-1}$) and at the end of LV ejection, respectively. Post-systolic segment shortening (PSS) was

calculated as $100\% \cdot (ESL - L_{\min}) / EDL$, in which L_{\min} is the minimum segment length after closure of the aortic valves.

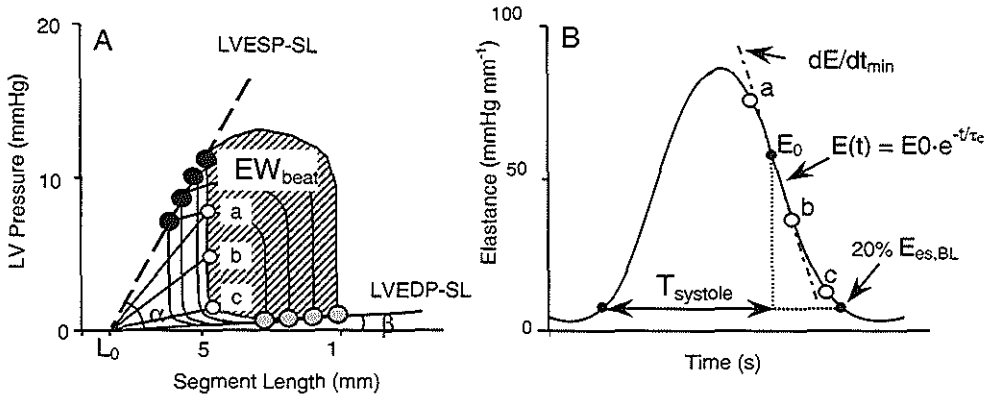


Fig. 1 Left ventricular (LV) pressure-segment length relations during transient decrease of preload (A). External work (EW_{beat}) was determined by integrating the area enclosed by the pressure-segment length loop over a full cardiac cycle. Regional end-systolic (E_{es}) and end-diastolic (E_{ed}) elastance were defined as the slopes ($\tan \alpha$ and $\tan \beta$) of the LV end-systolic pressure-segment length (LVESP-SL) and LV end-diastolic pressure-segment length (LVEDP-SL) relations, respectively. From the time-elastance curve the duration of systole (T_{systole}) and the maximum rate of fall of elastance (dE/dt_{min}) were determined (B). The time constant (τ_c) of the elastance decay between the occurrence of the maximum rate of fall of regional myocardial elastance (dE/dt_{min}) and the time point at which regional elastance had decreased to 20% of the peak systolic elastance at baseline was determined by fitting the decay in elastance to $E(t) = E_0 \cdot e^{-t/\tau_c}$ where E is elastance, t is time, and E_0 is the elastance at dE/dt_{min} .

Regional myocardial elastance using the LV pressure-segment length relations.

Regional myocardial end-systolic and end-diastolic elastance were determined from the LV pressure-segment length relations which were obtained by varying preload (Fig. 1A). Using linear regression analysis, end-systolic elastance (E_{es}) and the segment length at zero pressure intercept ($L_{0,\text{es}}$) were obtained applying the iterative method described by Van der Velde et al. (27), while end-diastolic elastance (E_{ed}) and the segment length at zero pressure intercept ($L_{0,\text{ed}}$) were determined using the time point at which $LVdP/dt$ had increased to $250 \text{ mmHg} \cdot \text{s}^{-1}$.

To describe early diastolic function in the LADCA and LCXCA regions we determined the time course of instantaneous regional elastance using the corresponding $L_{0,\text{es}}$ of the LADCA and LCXCA regions, obtained during the preload reduction (Fig. 1B). From the time course of elastance (in analogy to the global LV indices of relaxation) we determined the time constant (τ_c) of the elastance decay between the occurrence of the maximum rate of fall of regional myocardial elastance (dE/dt_{min}) and the time point at

which regional elastance had decreased to 20% of the peak systolic elastance at baseline. For this purpose the decay in elastance was fitted to $E(t) = E_0 e^{-t/\tau_e}$ where $E(t)$ is the instantaneous elastance at time point t , and E_0 is the elastance at dE/dt_{\min} . Finally, to study alterations in the onset of relaxation, we measured the duration of regional myocardial systole in the LADCA ($T_{\text{systole, LADCA}}$) and LCXCA ($T_{\text{systole, LCXCA}}$) perfused regions, which was defined as the time interval between the onset of the rapid increase in regional elastance and the occurrence of dE/dt_{\min} , in analogy to the determination of the duration of global LV systole.

To complement these regional myocardial measurements we also determined the time constant of global LV pressure decay (τ_{LVP}) during the time-interval between the occurrence of $LVdP/dt_{\min}$ and the timepoint when LVP had reached 5 mmHg above LV end-diastolic pressure (12). The duration of global LV systole ($T_{\text{systole, LV}}$) was defined as the time interval between the onset of the rapid increase in LV pressure ($LVdP/dt = 250 \text{ mmHg}\cdot\text{s}^{-1}$) and end-ejection.

Myocardial oxygen consumption, external work and mechanical efficiency. Myocardial oxygen consumption (MVO_2) of the perfusion territory of the LADCA was calculated as the product of local transmural myocardial blood flow and the difference in the oxygen contents of the arterial and local coronary venous blood. The area inside the LV pressure-segment length loop (Fig. 1) was taken as an index of external work per beat (EW_{beat}) (17, 19, 29), while mechanical efficiency was defined as the ratio of EW_{beat} and MVO_2_{beat} . Because EW reflects mechanical work but does not have the dimensions of work, the changes in mechanical efficiency have been expressed as percentage of baseline.

Determination of plasma and tissue concentrations of EMD 57033

To 600 μl of plasma or homogenized tissue 500 μl of water saturated ethylether was added and mixed. After the organic and aqueous phases were separated in an Eppendorff table centrifuge, the organic top layer was removed and collected in an Eppendorff vial. This extraction procedure was repeated five times and the ether phases were collected separately. Thereafter the ether was evaporated in a speed vac centrifuge and the residuals were resuspended and dissolved in 300 μl acetonitril. The amount of EMD 57033 in a given plasma or tissue sample was determined on a HPLC system. To this end, 30 μl of the acetonitril solutions was injected on a LiChrosorb RP 8 (5 μm) RT 125-4 column (Merck KGaA), which was equipped with a Hibar LiChroCart 4-4 precolumn (Merck KGaA). The column was equilibrated and developed in a buffer composed of 35% acetonitril and 65% 0.1 M sodium phosphate, pH 6.0 at a flow rate of 1 $\text{ml}\cdot\text{min}^{-1}$. The elution was monitored at a wavelength of 320 nm. The concentration of EMD 57033 was determined from the area of the peaks eluting at the appropriate time from the column by

comparison with the values determined for identically treated standard samples. The plasma concentration of a given blood or tissue sample was determined by adding the peak areas of the ether extraction samples.

Statistical analysis

All data have been presented as mean \pm standard error of the mean. Statistical significance ($P < 0.05$, two-tailed) of the changes within each group was tested using one-way analysis of variance for repeated measures followed by Dunnett's test. Comparison between the changes produced by the different interventions was assessed by two-way analysis of variance for repeated measures.

Drugs

EMD 57033 (the (+) enantiomer of 5-[1-(3,4-dimethoxybenzoyl)-1,2,3,4-tetrahydro-6-quinolyl]-6-methyl-3,6-dihydro-2H-1,3,4-thiadiazin-2-one; E. Merck KGaA, Darmstadt, Germany) was dissolved in propylene glycol so that an infusion rate of $0.5 \text{ ml} \cdot \text{min}^{-1}$ corresponded to $0.2 \text{ mg} \cdot \text{kg}^{-1} \cdot \text{min}^{-1}$ EMD 57033. Propranolol hydrochloride (ICI-Pharma, Rotterdam, The Netherlands) and phentolamine-methanesulfonide (CIBA-Geigy, Basel, Switzerland) were dissolved in saline. N^{ω} -nitro-L-arginine (Sigma Chemical Co., St Louis, USA) was dissolved in deionized water. Fresh solutions were prepared on the day of each experiment.

Results

Systemic hemodynamics

During the 15 min LADCA occlusion, mean arterial pressure had decreased from $100 \pm 2 \text{ mmHg}$ at baseline to $92 \pm 2 \text{ mmHg}$ ($n=21$, $P < 0.05$). Since the decrease in mean arterial pressure was accompanied by a similar fall in cardiac output, it follows that systemic vascular resistance had remained unchanged. $\text{LVdP/dt}_{\text{max}}$ decreased by $14 \pm 3 \%$, but T_{systole} was not affected. However, $\text{LVdP/dt}_{\text{min}}$ decreased from -2000 ± 70 to $-1590 \pm 70 \text{ mmHg} \cdot \text{s}^{-1}$ ($P < 0.05$), while τ_{LVP} and LV end-diastolic pressure increased (Table 1). After 15 min of reperfusion there was no recovery in any of the hemodynamic variables, except for LV end-diastolic pressure which had returned to baseline values. In the following 15 min the changes were negligible in the 14 animals which were left untreated, but in the other seven animals adrenergic blockade caused marked decreases in mean arterial pressure, heart rate, cardiac output, $\text{LVdP/dt}_{\text{max}}$ and $\text{LVdP/dt}_{\text{min}}$ (to $-1340 \pm 140 \text{ mmHg} \cdot \text{s}^{-1}$, $P < 0.05$), and caused a further increase in τ_{LVP} , while T_{systole} was maintained.

Infusion of the vehicle had minimal effects on systemic hemodynamics and global LV relaxation parameters (Table 1). In contrast, infusion of EMD 57033 caused a marked decrease in mean arterial pressure due to a decrease in systemic vascular resistance. LV

Table 1 Effect of EMD 57033 on Systemic Hemodynamics in Anesthetized Pigs with Stunned Myocardium.

	Baseline (n=21)	15 min Occlusion (n=21)	15 min Reperfusion (n=21)	Adrenergic Blockade	30 min Reperfusion	Infusion	Δ_{stun} by Infusion	
							30 min	60 min
MAP mmHg	100±2	92±2*	91±3*	-	94±4	PG	5±3	1±3
				+	68±6 [†]	EMD	2±6	-18±7 ^{†¶}
						EMD	11±3 [‡]	-3±2
CO l·min ⁻¹	2.7±0.1	2.4±0.1*	2.5±0.1*	-	2.5±0.1	PG	0.2±0.1 [‡]	0.2±0.1 [‡]
				+	2.0±0.1 [†]	EMD	0.6±0.1 ^{¶¶}	0.3±0.2 [‡]
						EMD	0.9±0.1 ^{¶¶}	0.9±0.2 ^{¶¶§}
SVR mmHg·min·l ⁻¹	37±1	39±1	37±2	-	39±1	PG	1.1±1.5	-2.8±1.2
				+	33±1	EMD	-7.5±3.0 [‡]	-11.6±3.0 ^{¶¶}
						EMD	-5.9±0.8 ^{¶¶}	-11.3±0.9 ^{¶¶}
HR Bpm	117±4	21±4	124±5	-	119±6	PG	-7±2	-8±4
				+	89±7 [†]	EMD	6±4 [†]	16±8 [†]
						EMD	11±2 ^{¶¶}	19±4 ^{¶¶}
LVSP mmHg	114±2	105±2*	104±3*	-	108±4	PG	7±3	3±3
				+	84±5	EMD	5±7	-14±6 ^{¶¶}
						EMD	6±3 ^{¶¶}	5±3 [§]
LVdP/dt _{max} mmHg·s ⁻¹	1850±90	1620±80*	1470±70*	-	1630±100	PG	-10±100	-130±90
				+	1060±80 [†]	EMD	760±140 ^{¶¶}	1230±200 ^{¶¶}
						EMD	880±110 ^{¶¶}	1380±210 ^{¶¶}
T _{isovole} ms	306±7	308±8	305±9	-	316±11	PG	20±3 [‡]	19±5 [‡]
				+	340±9 [†]	EMD	-16±7 ^{¶¶}	-27±14 ^{¶¶}
						EMD	-26±5 ^{¶¶}	-35±9 ^{¶¶}
τ_{LVP} ms	49±2	52±2*	50±2*	-	53±3	PG	2.3±0.7	2.3±1.4
				+	57±4 [†]	EMD	4.7±1.7	11.0±2.6 ^{¶¶}
						EMD	2.0±5.4	-6.3±5.1 [§]
LVEDP mmHg	6.8±0.6	10.1±0.7*	7.6±0.7*	-	7.2±0.8	PG	0.7±0.3	0.3±0.3
				+	9.0±1.2	EMD	-2.0±0.4 ^{¶¶}	-1.9±0.7 ^{¶¶}
						EMD	-2.5±0.6 ^{¶¶}	-3.9±0.7 ^{¶¶}

MAP, mean arterial pressure; HR, heart rate; CO, cardiac output; LVSP, left ventricular systolic pressure; LVdP/dt_{max}, maximal rate of rise in left ventricular pressure; LVEDP, left ventricular end-diastolic pressure; SVR, systemic vascular resistance; PG, propylene glycol (n=7); EMD, EMD 57033 (0.2 mg·kg⁻¹·min⁻¹, n=7 in each group); -, no α and β blockade; +, α and β blockade; Values are mean±s.e. mean; *P<0.05 vs. Baseline (only for 15 min Occlusion and 15 min Reperfusion); [†]P<0.05 vs. corresponding 15 min Rep (only for 30 min Reperfusion); [‡]P<0.05 vs. 30 min Reperfusion; [¶]P<0.05 vs. change in vehicle group; [§]P<0.05 vs. EMD 57033-induced change in animals without adrenoceptor blockade.

systolic pressure did not change during the first 30 min (113±8 mmHg), but fell to 94±7 mmHg during the following 30 min. There was a gradual increase in LVdP/dt_{max} up to 186±19 % of its stunning value (thereby exceeding the baseline value), which reflected an increase in global contractility as preload (LV end-diastolic pressure) and afterload (LV systolic pressure) both decreased. LVdP/dt_{min} and τ_{LVP} remained unchanged initially, but after 60 min LVdP/dt_{min} became less negative by 430±190 mmHg·s⁻¹ and τ_{LVP} had

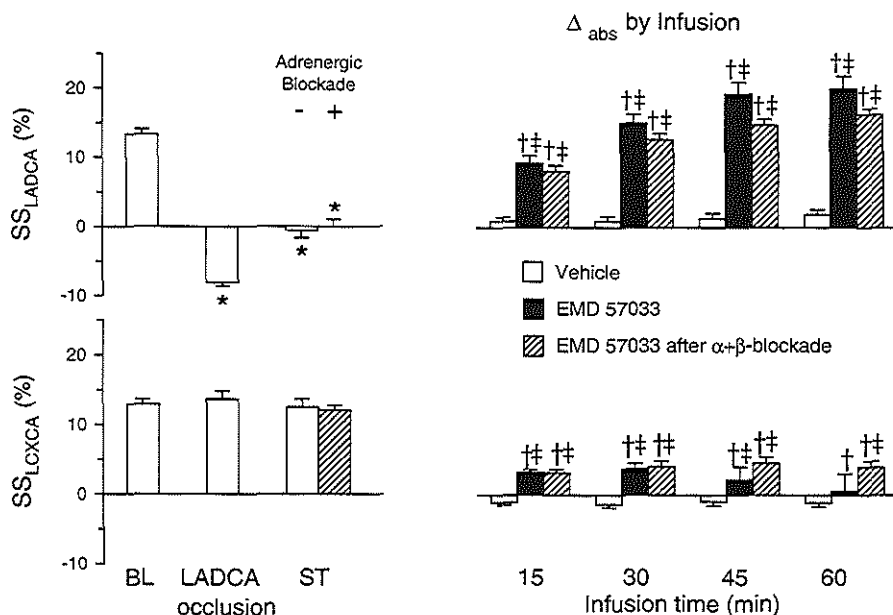


Fig. 2 Effect of EMD 57033 ($0.2 \text{ mg}\cdot\text{kg}^{-1}\cdot\text{min}^{-1}$, i.v.) on regional systolic shortening (SS) in the area perfused by the LADCA and the area perfused by the LCXCA. Absolute values are shown at baseline (BL, $n=21$), during ischemia (after 15 min LADCA occlusion, $n=21$), and during stunning (ST) in the absence ($n=14$) and in the presence ($n=7$) of $\alpha+\beta$ -adrenoceptor blockade. The effects of the infusions of vehicle ($n=7$) and EMD 57033 ($n=7$ in both groups) have been presented as absolute changes (Δ_{abs}) from their respective stunning values. Data are mean \pm s.e. mean; * $P<0.05$ stunning vs. baseline, † $P<0.05$ vs. stunning, ‡ $P<0.05$ vs. change in vehicle group, ‡‡ $P<0.05$ vs. EMD 57033-induced change in animals without adrenoceptor blockade.

increased by $19\pm 4\%$ ($P<0.05$ vs. vehicle) at a time when heart rate had increased and LV systolic pressure had decreased slightly. The increase in heart rate was also likely to be responsible for the decrease in T_{systole} . The effects of EMD 57033 did not depend on the activity of the adrenergic system, as the increases in heart rate and $\text{LVdP}/\text{dt}_{\text{max}}$ and the decrease in systemic vascular resistance were not affected when EMD 57033 was administered in the presence of adrenoceptor blockade. $\text{LVdP}/\text{dt}_{\text{min}}$, however, became more negative initially by $-430\pm 110 \text{ mmHg}\cdot\text{s}^{-1}$ ($P<0.05$), but had returned to stunning values at 60 min of infusion, possibly because LV systolic pressure was maintained during the infusion. Finally, τ_{LVP} remained unchanged.

Additional blockade of NO synthesis by N^{ω} -nitro-L-arginine, resulted in an elevated systemic vascular resistance ($52\pm 8 \text{ mmHg}\cdot\text{min}\cdot\text{l}^{-1}$) compared to adrenoceptor blockade alone ($33\pm 1 \text{ mmHg}\cdot\text{min}\cdot\text{l}^{-1}$, $P<0.05$). However, NO was not involved in the vasodilating actions of EMD 57033 as the decrease in systemic vascular resistance (-14 ± 5

mmHg·min⁻¹) was unmitigated at 60 min of infusion of EMD 57033. Similarly, additional blockade of NO also did not modify the responses of the other hemodynamic variables to EMD 57033 (not shown).

Regional systolic function

Systolic shortening After production of stunning, there was a complete loss of SS, and the appearance of a pronounced PSS (9.0±0.5 % vs. 1.5±0.3 % at baseline) in the distribution area of the LADCA, while SS of the normal myocardium remained unchanged (Fig. 2). Infusion of vehicle had a negligible effect on SS and PSS of both normal and stunned myocardium. During infusion of EMD 57033, SS in the stunned myocardium increased up to 19±2 %, while PSS disappeared. In the normal myocardium, SS increased from 14±2 % to 18±3 % ($P<0.05$). Adrenoceptor blockade did not modify the responses to EMD 57033 of regional wall motion in either stunned or normal myocardium.

End-systolic elastance Stunning produced a rightward shift of the LV end-systolic pressure-segment length relation in the LADCA area with an 18±7 % decrease in E_{es} ($P<0.05$, $n=14$; Fig. 3; Table 2). Infusion of vehicle had no effect on this relation, but EMD 57033 produced a leftward shift with a progressive increase in E_{es} to four times above its stunning values (both $P<0.05$). Adrenoceptor blockade blunted the EMD 57033-induced increase in E_{es} .

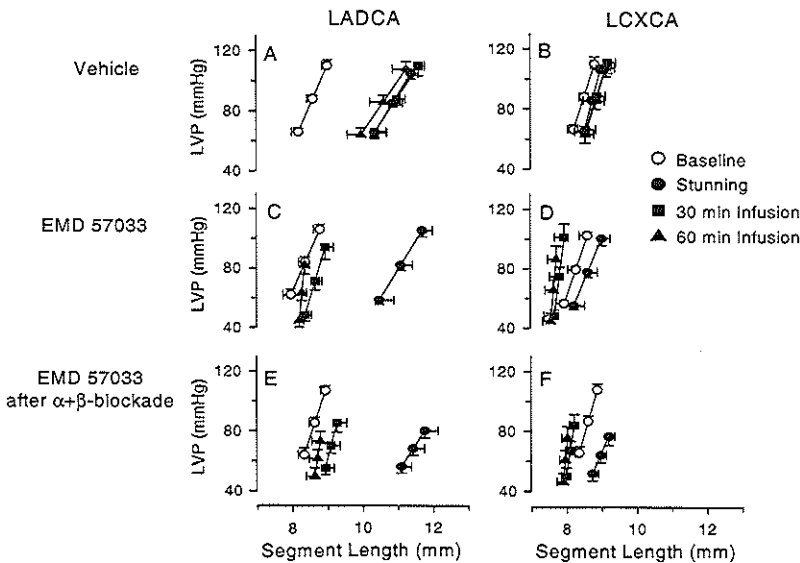


Fig. 3 LV end-systolic pressure-segment length relations in the LADCA (left panels) and LCXCA (right panels) perfusion territories at baseline, during stunning and after 30 min and 60 min of infusion of vehicle (A and B), or EMD 57033 (0.2 mg·kg⁻¹·min⁻¹, i.v.) in the absence (C and D) and in the presence (E and F) of adrenoceptor blockade. LVP, left ventricular pressure. For statistical analysis see Table 2.

In the LCXCA area, stunning and the subsequent infusion of vehicle had no effect on the LV end-systolic pressure-segment length relation. Infusion of EMD 57033 caused a tripling of E_{es} without a change in $L_{0,es}$. Adrenoceptor blockade had no effect on the responses of E_{es} and $L_{0,es}$ to EMD 57033.

Regional diastolic function

Onset of relaxation Stunning did not alter the onset of relaxation as the duration of regional LV systole in either LADCA ($T_{systole, LADCA}$) or LCXCA ($T_{systole, LCXCA}$) perfused myocardium remained unchanged (Fig. 4). The small decrease in heart rate that occurred during infusion of the vehicle was associated with small increases in $T_{systole, LADCA}$ and $T_{systole, LCXCA}$. Conversely, the EMD 57033-induced increase in heart rate resulted in reductions of $T_{systole, LADCA}$ and $T_{systole, LCXCA}$, that reached levels of statistical significance in the presence of adrenoceptor blockade.

Table 2 Effect of EMD 57033 on Regional Left Ventricular End-Systolic Elastance in Anaesthetised Pigs with Stunned Myocardium.

	Baseline (n=21)	Reperfusion		Δ_{abs} by Infusion	
		Adrenergic blockade	30 min	30 min	60 min
LADCA perfusion territory					
E_{es} , mmHg·mm ⁻¹	67±7	-	46±5*	PG EMD	-7±4 100±52
		+	49±11	EMD	60±23 ^{†‡}
$L_{0,es}$, mm	7.0±0.2	-	8.9±0.4*	PG EMD	-0.2±0.3 -1.2±0.5 [†]
		+	9.7±0.3*	EMD	-1.3±0.4 [†]
LCXCA perfusion territory					
E_{es} , mmHg·mm ⁻¹	80±7	-	76±7	PG EMD	-18±7 165±49 ^{†‡}
		+	52±6*	EMD	119±26 ^{†‡}
$L_{0,es}$, mm	7.4±0.1	-	7.5±0.2*	PG EMD	-0.2±0.1 0.1±0.1
		+	7.8±0.1	EMD	-0.1±0.1

LADCA, left anterior descending coronary artery; LCXCA, left circumflex coronary artery; E_{es} , end-systolic elastance; $L_{0,es}$, intercept at zero pressure of the LV end-systolic pressure-segment length relation; PG, propylene glycol (n=7); EMD, EMD 57033 (0.2 mg·kg⁻¹·min⁻¹, i.v., n=7 in each group); -, in the absence of α - and β -blockade; +, in the presence of α - and β -blockade; Values are mean± s.e. mean; * P <0.05 vs. Baseline (only for 30 min Reperfusion); [†] P <0.05 vs. 30 min Reperfusion; [‡] P <0.05 vs. change in vehicle group; [§] P <0.05 vs. EMD 57033-induced in animals without adrenoceptor blockade.

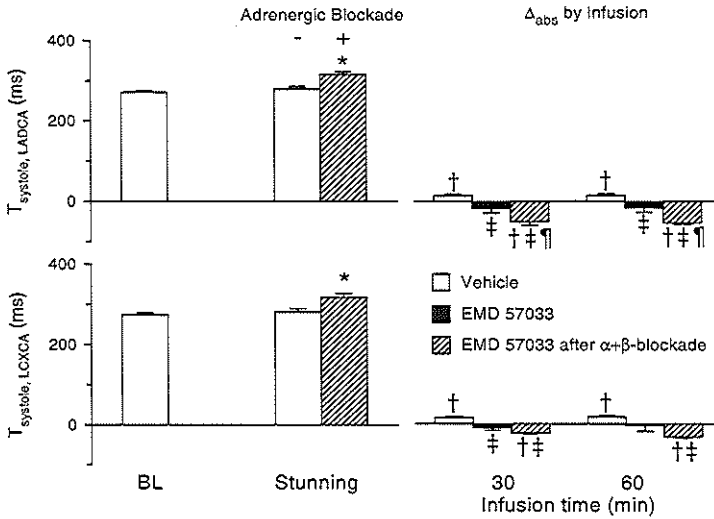


Fig. 4 The effect of EMD 57033 ($0.2 \text{ mg}\cdot\text{kg}^{-1}\cdot\text{min}^{-1}$, i.v.) on the duration of systole ($T_{systole}$) in the LADCA (top) and the LCXCA (bottom) perfusion territories. Absolute values are shown at baseline (BL, $n=21$), and during stunning (ST) in the absence ($n=14$) and in the presence ($n=7$) of $\alpha+\beta$ -adrenoceptor blockade. The effects of the infusions of vehicle ($n=7$) and EMD 57033 ($n=7$ in both groups) have been presented as absolute changes (Δ_{abs}) from their respective stunning values. Data are mean \pm s.e. mean; * $P<0.05$ stunning vs. baseline, † $P<0.05$ vs. stunning, ‡ $P<0.05$ vs. change in vehicle group, § $P<0.05$ vs. EMD 57033-induced change in animals without adrenoceptor blockade.

Maximum rate of fall of elastance and time constant of decay of elastance Stunning resulted in a less negative dE/dt_{min} (from $-850\pm 100 \text{ mmHg}\cdot\text{mm}^{-1}\cdot\text{s}^{-1}$ at baseline to $-280\pm 20 \text{ mmHg}\cdot\text{mm}^{-1}\cdot\text{s}^{-1}$) of the LADCA perfused area, but had no effect on dE/dt_{min} of the LCXCA perfused area ($-890\pm 80 \text{ mmHg}\cdot\text{mm}^{-1}\cdot\text{s}^{-1}$ at baseline). Vehicle had no effect on dE/dt_{min} in either region but in the presence of EMD 57033, dE/dt_{min} became more negative by $3380\pm 640 \text{ mmHg}\cdot\text{mm}^{-1}\cdot\text{s}^{-1}$ and $1800\pm 650 \text{ mmHg}\cdot\text{mm}^{-1}\cdot\text{s}^{-1}$ in the LADCA and LCXCA areas, respectively. Although adrenoceptor blockade tended to blunt the effects of EMD 57033, this did not reach levels of statistical significance (not shown).

In view of the dependency of dE/dt_{min} on maximum elastance (E_{cs}), we also determined the time constants of regional myocardial elastance decay (τ_e , Fig. 5). Stunning increased τ_e in the LADCA area, but had no effect on τ_e in the LCXCA area. Vehicle had no effect on τ_e of either area, while EMD 57033 decreased τ_e in both areas ($P<0.05$). Adrenoceptor blockade blunted the EMD 57033-induced decrease in both stunned and normal myocardium.

End-diastolic elastance In the LADCA area stunning had no effect on E_{ed} , but increased $L_{0,ed}$ from 8.7 ± 0.3 to $9.9\pm 0.4 \text{ mm}$ (Table 3, Fig. 6). Vehicle had no effect on E_{ed} or $L_{0,ed}$. In contrast, EMD 57033, which had also no effect on E_{ed} , tended to decrease $L_{0,ed}$

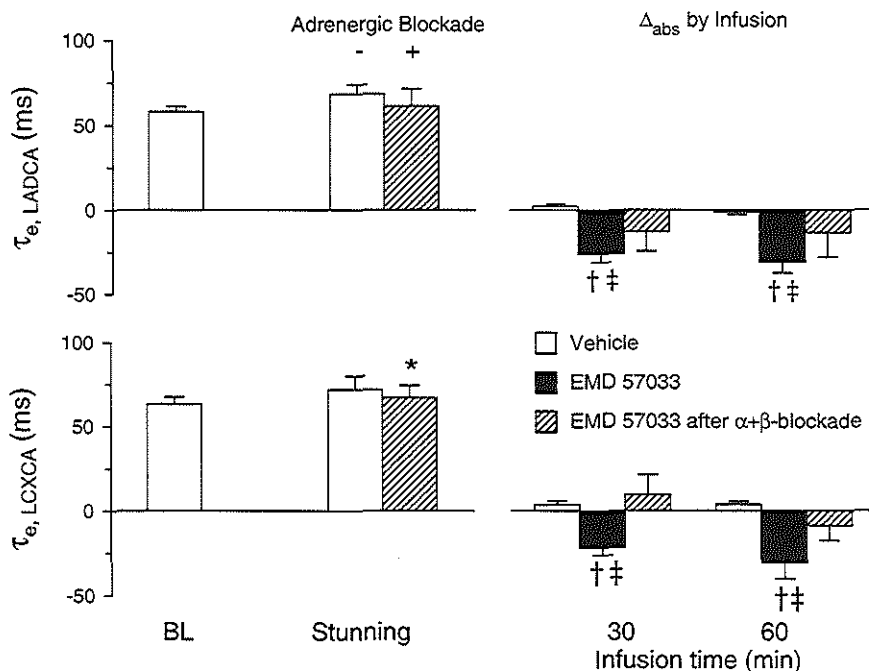


Fig. 5 From top to bottom are shown the time constants of decay of regional elastance (τ_e) during early diastole of the LADCA ($\tau_{e, LADCA}$) and LCXCA ($\tau_{e, LCXCA}$) perfusion territories. Absolute values are shown at baseline (BL, $n=21$) and during stunning in the absence ($n=14$) and in the presence ($n=7$) of $\alpha+\beta$ -adrenoceptor blockade. The effects of the infusions of vehicle ($n=7$) and EMD 57033 ($0.2 \text{ mg}\cdot\text{kg}^{-1}\cdot\text{min}^{-1}$, i.v., $n=7$ in both groups) have been presented as absolute changes (Δ_{abs}) from their respective stunning values. Data are mean \pm s.e. mean; * $P < 0.05$ stunning vs. baseline, † $P < 0.05$ vs. stunning, ‡ $P < 0.05$ vs. change in vehicle group, ¶ $P < 0.05$ vs. EMD 57033-induced change in animals without adrenoceptor blockade.

($P=0.098$). Adrenoceptor blockade had no significant effect on the responses of E_{ed} to EMD 57033, but prevented the decrease in $L_{0,ed}$.

In the adjacent LCXCA area, the stunning protocol and subsequent infusion of vehicle had no effect on the LV end-diastolic pressure-segment length relation (Table 3, Fig. 6). Infusion of EMD 57033 also had no effect on E_{ed} , but caused a leftward shift of the LV end-diastolic pressure-segment relation. Adrenoceptor blockade did not modify the responses of E_{ed} to EMD 57033, but blunted the decrease in $L_{0,ed}$.

Mechanical efficiency of the stunned myocardium

Stunning caused a 68 ± 5 % decrease ($P < 0.05$) in EW_{beat} but only a 12 ± 6 % decrease in the MVO_2_{beat} of the LADCA-perfused myocardium, so that mechanical efficiency (EW_{beat}/MVO_2_{beat}) decreased by 66 ± 6 % (Fig. 7). Infusion of vehicle had no effect on mechanical efficiency as both EW_{beat} and MVO_2_{beat} remained unchanged. However, during infusion of EMD 57033 both EW_{beat} and MVO_2_{beat} returned to baseline values and

consequently also mechanical efficiency was normalized. The increase in MVO_2 was accompanied by an equivalent increase in myocardial blood flow, so that myocardial O_2 extraction ($62 \pm 6\%$ at stunning and $62 \pm 6\%$ at 60 min of infusion) and coronary venous PO_2 (27 ± 3 mmHg at stunning and 28 ± 3 mmHg at 60 min of infusion) remained unchanged. In the pigs in which EMD 57033 was infused in the presence of adrenoceptor blockade, the responses of EW_{beat} , $MVO_{2\ beat}$, mechanical efficiency, and coronary venous PO_2 were not different from the responses to EMD 57033 in the absence of adrenoceptor blockade.

Table 3 *Effect of EMD 57033 on Regional Left Ventricular End-Diastolic Elastance in Anesthetized Pigs with Stunned Myocardium.*

	Baseline (n=21)	Reperfusion		Δ_{obs} by Infusion		
		Adrenergic blockade	30 min	30 min	60 min	
LADCA perfusion territory						
E_{cd} , mmHg·mm ⁻¹	4.2±0.4	-	3.9±0.4	PG	-0.4±0.5	-0.7±0.5
		+	4.4±0.4	EMD	-0.7±0.6	-0.6±1.3
				EMD	-0.8±0.5	-1.0±0.9
$L_{0,ed}$, mm						
	8.7±0.3	-	9.9±0.4*	PG	0.0±0.1	-0.3±0.2
		+	9.8±0.9*	EMD	-0.3±0.4	-1.9±1.4
				EMD	-0.4±0.2	-0.6±0.3
LCXCA perfusion territory						
E_{cd} , mmHg·mm ⁻¹	3.7±0.2	-	4.6±0.4*	PG	0.4±0.4	0.5±0.5
		+	6.2±1.1	EMD	-0.6±1.3	1.9±2.1
				EMD	-1.9±0.8 [†]	-2.3±1.5
$L_{0,ed}$, mm						
	9.1±0.4	-	9.6±0.7*	PG	0.2±0.2	0.1±0.2
		+	10.1±0.8*	EMD	-2.3±1.8 [†]	-2.8±1.5 [†]
				EMD	-0.5±0.1 ^{†‡}	-0.7±0.2 ^{†‡}

LADCA, left anterior descending coronary artery; LCXCA, left circumflex coronary artery; E_{cd} , end-diastolic elastance; $L_{0,ed}$, intercept at zero pressure of the LV end-diastolic pressure-segment length relation; PG, propylene glycol (n=7); EMD, EMD 57033 (0.2 mg·kg⁻¹·min⁻¹, i.v., n=7 in each group); -, in the absence of α - and β -blockade; +, in the presence of α - and β -blockade; Values are mean±s.e. mean; * $P < 0.05$ vs. Baseline (only for 30 min Reperfusion); [†] $P < 0.05$ vs. 30 min Reperfusion; [‡] $P < 0.05$ vs. change in vehicle group; ^{†‡} $P < 0.05$ vs. EMD 57033-induced change in animals without adrenoceptor blockade.

Plasma and tissue levels of EMD 57033

EMD 57033 could not be detected in the pre-drug samples. During EMD 57033 infusion, the plasma levels increased time-dependently to 3.54 ± 0.13 , 5.03 ± 0.63 , 6.53 ± 0.74 and 7.23 ± 0.67 $\mu\text{g}\cdot\text{ml}^{-1}$ at 15, 30, 45 and 60 min, respectively. In two of these experiments it was shown that at the end of the 60 min infusion EMD 57033 had accumulated in the left ventricle (26.6 and 29.5 μg per g of wet weight) and the liver (29.4 and 26.2 $\mu\text{g}\cdot\text{g}^{-1}$), while tissue levels in the stomach (6.7 and 6.6 $\mu\text{g}\cdot\text{g}^{-1}$) and skeletal muscle (13.5 and 5.3 $\mu\text{g}\cdot\text{g}^{-1}$) were in the range of the plasma concentrations. EMD 57033 concentrations in the cerebellum (4.3 and 4.2 $\mu\text{g}\cdot\text{g}^{-1}$) and cerebrum (4.4 and 5.3 $\mu\text{g}\cdot\text{g}^{-1}$) were below plasma levels, possibly due to the blood-brain barrier.

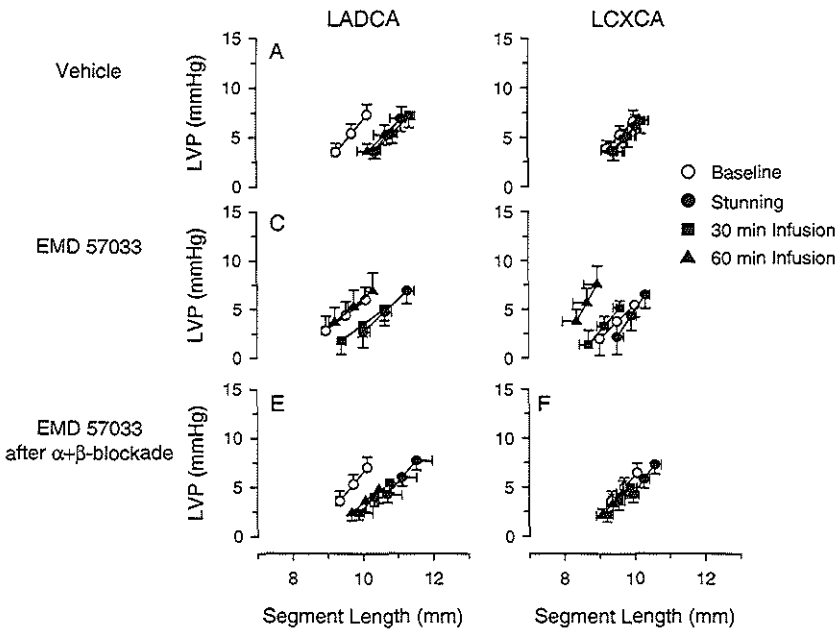


Fig. 6 LV end-diastolic pressure-segment length relations in the LADCA (left panels) and LCXCA (right panels) perfusion territories at baseline, during stunning and after 30 min and 60 min of infusion of vehicle (A and B), or EMD 57033 ($0.2 \text{ mg}\cdot\text{kg}^{-1}\cdot\text{min}^{-1}$, i.v.) in the absence (C and D) and in presence (E and F) of adrenoceptor blockade. LVP = left ventricular pressure. For statistical analysis see Table 3.

Discussion

The major findings in this *in vivo* porcine model of regional myocardial stunning are (i) EMD 57033 increased systolic shortening in stunned myocardium more than in the adjacent normal myocardium; (ii) EMD 57033 also increased end-systolic elastance in normal and stunned myocardium, but with similar responses in both regions; (iii) EMD 57033 did not delay the onset of relaxation, but improved the maximum rate of fall of regional myocardial elastance and decreased the time constant of early diastolic regional myocardial elastance decay; EMD 57033 had no effect on end-diastolic elastance in either normal and stunned myocardium; (iv) EMD 57033 restored mechanical efficiency of the stunned myocardium; (v) the effects on regional systolic and diastolic function were only slightly modified by pretreatment with α - and β -adrenoceptor blockade, indicating that at the dose used, phosphodiesterase III inhibition contributes only minimally to the actions of EMD 57033; (vi) finally, the EMD-induced systemic vasodilation was not amenable to either adrenoceptor blockade or additional inhibition of NO synthesis.

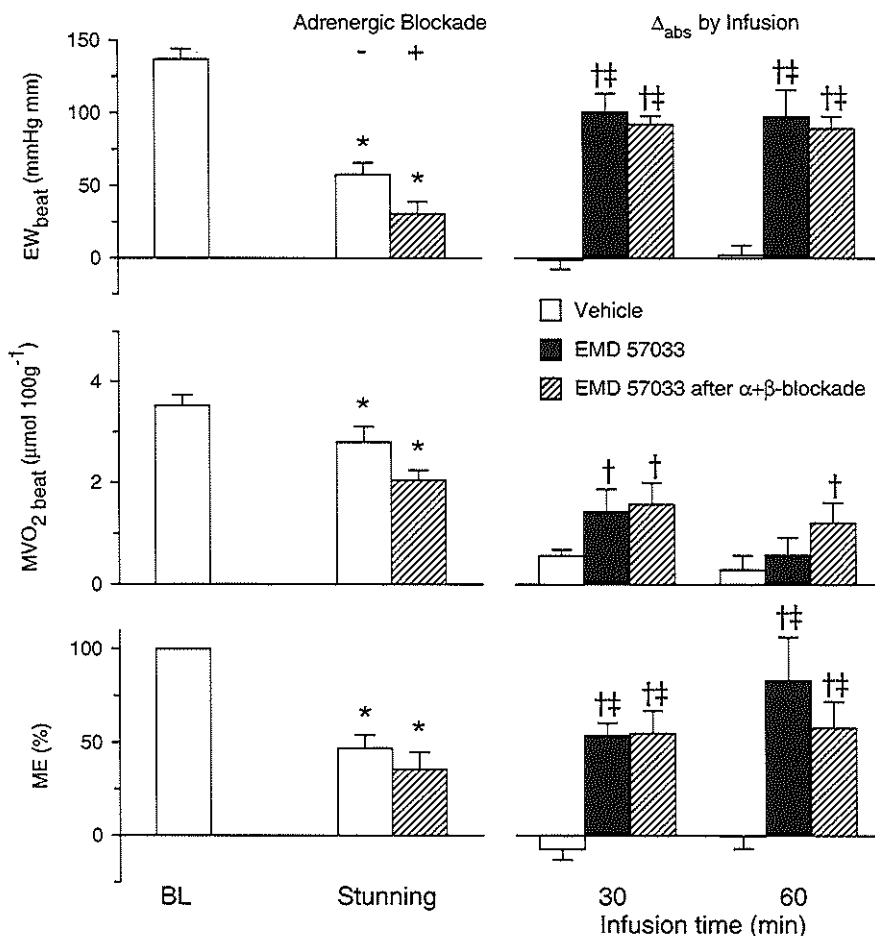


Fig. 7 EW_{beat} , $MVO_{2\ beat}$ and mechanical efficiency (ME) of the LADCA perfused area. Absolute values are shown at baseline (BL, $n=21$), and during stunning in the absence ($n=14$) and in the presence ($n=7$) of α - and β -adrenoceptor blockade. The effects of vehicle ($n=7$) and EMD 57033 ($0.2\text{ mg}\cdot\text{kg}^{-1}\cdot\text{min}^{-1}$, i.v.) in the absence ($n=7$) or presence ($n=7$) of adrenoceptor blockade have been presented as absolute changes (Δ_{abs}) from their respective stunning values. Data are mean \pm s.e. mean; * $P<0.05$ stunning vs. baseline, † $P<0.05$ vs. stunning, ‡ $P<0.05$ vs. change in vehicle group, ‡‡ $P<0.05$ vs. EMD 57033-induced change in animals without adrenoceptor blockade.

Systolic function

EMD 57033 resulted in a time-dependent (i.e. plasma concentration-dependent) restoration of SS in stunned myocardium, while producing only a small increase in SS in the remote normal region. This finding is in accordance with previous observations in our laboratory with EMD 60263 in a similar model of myocardial stunning in the in vivo pig heart (24). These studies could be interpreted to suggest a relatively preferential effect of

Ca^{2+} -sensitizing drugs on systolic function of stunned myocardium. However, SS is a load-sensitive index of systolic function and does not necessarily reflect the contractile state of the myocardium (17), particularly under conditions of stunning when its load-dependency is even greater (9). Indeed, EMD 57033 produced similar increments in E_{es} in stunned and normal myocardium. This suggests that the greater increase in SS in stunned myocardium resulted principally from a greater sensitivity for positive inotropic interventions of regions with a lower E_{es} . This is supported by the observation that the β -adrenoceptor agonist dobutamine also produces a preferential increase in systolic shortening of stunned myocardium, whereas E_{es} responses were similar in the normal and stunned region (9, 18). Similar to the present study, Korbmacher et al. (16) observed that EMD 60263 at an optimal dose of 3 μM produced similar increments in $\text{LVdP/dt}_{\text{max}}$ in normal (from 1415 to 1885 $\text{mmHg}\cdot\text{s}^{-1}$) and globally stunned (from 845 to 1300 $\text{mmHg}\cdot\text{s}^{-1}$) isolated rabbit hearts in which afterload was held constant. Also with EMD 57033, these authors reported similar increments in LV systolic pressure in stunned and normal isolated rabbit hearts at constant afterload. Interestingly, we observed that the increase in E_{es} in the stunned myocardium was time-dependent, whereas the E_{es} in normal myocardium at 30 min of infusion of EMD 57033 did not increase further after 60 min of infusion. In view of the progressive increase in plasma levels over time, this observation suggests that the maximum effect in normal myocardium was reached at a lower dose than that in stunned myocardium. Indeed, Korbmacher et al. (16) observed in their *in vitro* study that a further increase in dose of EMD 57033 to 10 μM did not further increase $\text{LVdP/dt}_{\text{max}}$ in stunned hearts, while it slightly decreased $\text{LVdP/dt}_{\text{max}}$ in normal myocardium. These findings suggest that the normal myocardium is more sensitive to adverse effects on systolic function than stunned myocardium, in which the Ca^{2+} responsiveness is lower (3).

It has been proposed that *in vitro* EMD 57033 exerts, besides its Ca^{2+} -sensitizing effects, phosphodiesterase inhibiting actions (22, 25). In the present study, blockade of α - and β -adrenoceptors did not modulate the inotropic responses to EMD 57033 in normal myocardium *in vivo*. Thus, the increase in E_{es} produced by EMD 57033 in normal myocardium was not altered by adrenoceptor blockade, while the index of global LV contractility, $\text{LVdP/dt}_{\text{max}}$, was also unmitigated in the presence of adrenoceptor blockade. Hence the EMD 57033-induced actions appeared to be primarily the result of an increase in Ca^{2+} responsiveness, which is in accordance with previous studies in awake pigs from our laboratory (26). However, there was a slight blunting of the increase in E_{es} in stunned myocardium, which is difficult to explain by a phosphodiesterase III inhibitory action, as it seems unlikely that a pharmacological property such as phosphodiesterase III inhibition could differ in the stunned from normal myocardium. Moreover, the duration of global LV systole, $T_{\text{systolic, LADCA}}$, and $T_{\text{systolic, LCXCA}}$, which were not altered by EMD 57033 in the presence of intact adrenoceptor activity, were not increased but were slightly shortened by

EMD 57033 in the presence of adrenoceptor blockade. Taken together, the present study suggests that the EMD 57033-induced systolic actions *in vivo* are not the result of phosphodiesterase III inhibition.

Stunning reduced mechanical efficiency, likely due to a decrease in E_{cs} which not only decreases external work but also increases potential work, resulting in a relatively high MVO_2 (17). EMD 57033 restored external work while producing only a small increase in MVO_2 , thereby restoring efficiency of stunned myocardium. This favorable effect is most likely the result of positive inotropism, rather than a unique feature of EMD 57033, because we previously observed a similar restoration of mechanical efficiency of stunned myocardium during infusion of the β -adrenoceptor agonist dobutamine (18).

Diastolic function

It has been suggested that increased Ca^{2+} responsiveness can lead to maintained contraction at Ca^{2+} levels at which normally relaxation occurs (21). In rat skinned right ventricular trabeculae, these authors have shown that EMD 57033 can even cause contraction in the absence of Ca^{2+} . Consequently, contraction could be prolonged thereby delaying the onset of relaxation (22, 25), the rate of relaxation could be attenuated (11, 16) and end-diastolic stiffness could be increased (11, 13), even when Ca^{2+} concentrations are normal.

Early diastolic function appeared to be well preserved during EMD 57033 infusion in the present study. $T_{systole}$ slightly decreased in both normal and stunned myocardium and in the left ventricle as a whole, possibly due to the small increase in heart rate. Thus, the onset of relaxation was not delayed by EMD 57033 either in the presence or absence of intact adrenoceptor activity, indicating that phosphodiesterase III inhibition did not mask the potential contraction prolongation produced by the Ca^{2+} -sensitizing actions of EMD 57033. $LVdP/dt_{min}$ is often used as an index of global early LV relaxation, despite its dependency on, in particular, LV systolic pressure (10, 30). In the present study, $LVdP/dt_{min}$ improved slightly during the first 30 min of EMD 57033 infusion but fell to 75% of the value at stunning during the following 30 min. The decrease in $LVdP/dt_{min}$ may have been due to the 20% reduction of LV systolic pressure, and does not necessarily reflect an impairment of global LV relaxation. This is even more so, as in the adrenoceptor blocked animals, both $LVdP/dt_{min}$ and LV systolic pressure were not affected by EMD 57033. This strongly suggests that phosphodiesterase III inhibition did not contribute significantly to the maintenance of $LVdP/dt_{min}$. Inspection of the less load-sensitive time constant τ_{LVP} supports this notion. Nevertheless, both indexes are global variables and do not discriminate between the effects of EMD 57033 on normal and stunned myocardium, which is also why regional indexes of ventricular relaxation were employed. In both stunned and normal myocardial regions, the maximum rate of fall of regional myocardial elastance (dE/dt_{min}) increased, which is not surprising in view of the

marked increments in E_{cs} . However, even after correction for the contractility-dependence of dE/dt_{min} , i.e. by calculating the time constant of elastance decay τ_e , the data indicated no untoward effects of EMD 57033 on early diastolic function. Importantly, even in the presence of adrenoceptor blockade, EMD 57033 did not exert detrimental actions on dE/dt_{min} or the relaxation time constants, suggesting that the lack of adverse effects were not the result of masking of untoward effects of Ca^{2+} -sensitization by concomitant phosphodiesterase III inhibitory effects of the compound. In the present study we also failed to find evidence of a negative effect of EMD 57033 on late diastolic function, as E_{cd} was maintained during EMD 57033 infusion, even in the presence of adrenoceptor blockade.

The importance of abnormalities in diastolic function is that these could compromise systolic pump function via reduced LV filling and via impairment of myocardial perfusion by reducing the effective diastolic perfusion time of the coronary bed. However, in the present study EMD 57033, either with or without adrenoceptor blockade, restored regional systolic shortening, external work and mechanical efficiency, while myocardial oxygen supply was unimpeded.

Conclusions

The Ca^{2+} -sensitizing agent EMD 57033, at a dose of $0.2 \text{ mg}\cdot\text{kg}^{-1}\cdot\text{min}^{-1}$, restored regional systolic and diastolic function of stunned myocardium in the in vivo porcine heart. In normal myocardium, quantitatively similar improvements in systolic and diastolic function were observed. Phosphodiesterase III inhibition contributed minimally to these actions. The results of the present study suggest that Ca^{2+} -sensitizing agents are prime candidates for complementing the current inodilator therapeutic arsenal in the clinical setting for acute states of heart failure, because they are powerful enhancers of systolic performance in vivo at doses that do not appear to exert adverse effects on diastolic function.

Acknowledgements

This study has been made possible by a grant from Merck KgaA, Darmstadt, Germany. The research of Dr. D.J. Duncker is supported by a fellowship of the Royal Netherlands Academy of Arts and Sciences. The authors gratefully acknowledge the technical assistance of J. van Meegeen and R.H. van Bremen.

References

1. Abe, Y., Y. Kitada, and A. Narimatsu. Effect of a calcium-sensitizing positive inotropic agent MCI-154 and its combined use with enalapril on posts ischemic contractile dysfunction of dog hearts. *J Cardiovasc Pharmacol* 26: 653-659, 1995.
2. Aversano, T., W. L. Maughan, W. C. Hunter, D. Kass, and L. C. Becker. End-systolic measures of regional ventricular performance. *Circulation* 73: 938-950, 1986.

3. **Bolli, R., and E. Marban.** Molecular and cellular mechanisms of myocardial stunning. *Physiol Rev* 79: 609-634, 1999.
4. **Charlat, M. L., P. G. O'Neill, C. J. Hartley, R. Roberts, and R. Bolli.** Prolonged abnormalities of left ventricular diastolic wall thinning in the "stunned" myocardium in conscious dogs: time course and relation to systolic function. *J Am Coll Cardiol* 13: 185-194, 1989.
5. **Duncker, D., R. Stubenitsky, and P. Verdouw.** Endogenous nitric oxide contributes to coronary vasodilation but does not modify myocardial O₂ consumption in awake swine at rest and during treadmill exercise. *Circulation* 96: I-73, 1997.
6. **Duncker, D. J., J. Heiligers, E. J. Mylecharane, P. R. Saxena, and P. D. Verdouw.** Nimodipine-induced changes in the distribution of carotid blood flow and cardiac output in pentobarbitone-anaesthetized pigs. *Br J Pharmacol* 89: 35-46, 1986.
7. **Duncker, D. J., P. R. Saxena, and P. D. Verdouw.** Systemic haemodynamic and beta-adrenoceptor antagonistic effects of bisoprolol in conscious pigs: a comparison with propranolol. *Arch Int Pharmacodyn Ther* 290: 54-63, 1987.
8. **Ehring, T., R. Schulz, J. D. Schipke, and G. Heusch.** Diastolic dysfunction of stunned myocardium. *Am J Cardiovasc Pathol* 4: 358-366, 1993.
9. **Fan, D., L. K. Soei, L. M. Sassen, R. Krams, and P. D. Verdouw.** Mechanical efficiency of stunned myocardium is modulated by increased afterload dependency. *Cardiovasc Res* 29: 428-437, 1995.
10. **Gaasch, W. H., J. D. Carroll, A. S. Blaustein, and O. H. Bing.** Myocardial relaxation: effects of preload on the time course of isovolumetric relaxation. *Circulation* 73: 1037-1041, 1986.
11. **Hajjar, R. J., U. Schmidt, P. Helm, and J. K. Gwathmey.** Ca⁺⁺ sensitizers impair cardiac relaxation in failing human myocardium. *J Pharmacol Exp Ther* 280: 247-254, 1997.
12. **Harkin, C. P., P. S. Pagel, J. P. Tessmer, and D. C. Warltier.** Systemic and coronary hemodynamic actions and left ventricular functional effects of levosimendan in conscious dogs. *J Cardiovasc Pharmacol* 26: 179-188, 1995.
13. **Hgashiyama, A., M. W. Watkins, Z. Chen, and M. M. LeWinter.** Effects of EMD 57033 on contraction and relaxation in isolated rabbit hearts. *Circulation* 92: 3094-3104, 1995.
14. **Korbmacher, B., U. Sunderdiek, G. Arnold, H. D. Schulte, and J. D. Schipke.** Improved ventricular function by enhancing the Ca⁺⁺ sensitivity in normal and stunned myocardium of isolated rabbit hearts. *Basic Res Cardiol* 89: 549-562, 1994.
15. **Korbmacher, B., U. Sunderdiek, H. D. Schulte, G. Arnold, and J. D. Schipke.** Comparison between the effects of a novel Ca⁺⁺ sensitizer and a phosphodiesterase inhibitor on stunned myocardium. *J Pharmacol Exp Ther* 275: 1433-1441, 1995.
16. **Korbmacher, B., U. Sunderdiek, G. Selcan, G. Arnold, and J. D. Schipke.** Different responses of non-ischemic and post-ischemic myocardium towards Ca²⁺ sensitization. *J Mol Cell Cardiol* 29: 2053-2066, 1997.
17. **Krams, R., D. J. Duncker, E. O. McFalls, A. Hogendoorn, and P. D. Verdouw.** Dobutamine restores the reduced efficiency of energy transfer from total mechanical work to external mechanical work in stunned porcine myocardium. *Cardiovasc Res* 27: 740-747, 1993.
18. **McFalls, E. O., D. J. Duncker, R. Krams, L. M. Sassen, A. Hoogendoorn, and P. D. Verdouw.** Recruitment of myocardial work and metabolism in regionally stunned porcine myocardium. *Am J Physiol* 263: H1724-1731, 1992.
19. **Morris, J. J. d., G. L. Pellom, C. E. Murphy, D. R. Salter, J. P. Goldstein, and A. S. Wechsler.** Quantification of the contractile response to injury: assessment of the work-length relationship in the intact heart. *Circulation* 76: 717-727, 1987.
20. **Nankervis, R., I. Lues, and L. Brown.** Calcium sensitization as a positive inotropic mechanism in diseased rat and human heart. *J Cardiovasc Pharmacol* 24: 612-617, 1994.
21. **Palmer, S., and J. C. Kentish.** Differential effects of the Ca²⁺ sensitizers caffeine and CGP 48506 on the relaxation rate of rat skinned cardiac trabeculae. *Circ Res* 80: 682-687, 1997.
22. **Ravens, U., H. M. Himmel, M. Fluss, K. Davia, and S. E. Harding.** Phosphodiesterase inhibition and Ca²⁺ sensitization. *Mol Cell Biochem* 157: 245-249, 1996.
23. **Sassen, L. M., L. K. Soei, M. M. Koning, and P. D. Verdouw.** The central and regional cardiovascular responses to intravenous and intracoronary administration of the phenylidihydropyridine elgodipine in anaesthetized pigs. *Br J Pharmacol* 99: 355-363, 1990.
24. **Soei, L. K., L. M. Sassen, D. S. Fan, T. van Veen, R. Krams, and P. D. Verdouw.** Myofibrillar Ca²⁺ sensitization predominantly enhances function and mechanical efficiency of stunned myocardium. *Circulation* 90: 959-969, 1994.

25. Solaro, R. J., G. Gambassi, D. M. Warshaw, M. R. Keller, H. A. Spurgeon, N. Beier, and E. G. Lakatta. Stereoselective actions of thiazidiazinones on canine cardiac myocytes and myofilaments. *Circ Res* 73: 981-990, 1993.
26. Stubenitsky, R., R. W. van der Weerd, D. B. Haitzma, P. D. Verdouw, and D. J. Duncker. Cardiovascular effects of the novel Ca^{2+} -sensitizer EMD 57033 in pigs at rest and during treadmill exercise. *Br J Pharmacol* 122: 1257-1270, 1997.
27. van der Velde, E. T., D. Burkhoff, P. Steendijk, J. Karsdon, K. Sagawa, and J. Baan. Nonlinearity and load sensitivity of end-systolic pressure-volume relation of canine left ventricle in vivo. *Circulation* 83: 315-327, 1991.
28. Verdouw, P. D., D. J. Duncker, and P. R. Saxena. Poor vasoconstrictor response to adrenergic stimulation in the arteriovenous anastomoses present in the carotid vascular bed of young Yorkshire pigs. *Arch Int Pharmacodyn Ther* 272: 56-70, 1984.
29. Vinten-Johansen, J., P. A. Gayheart, W. E. Johnston, J. S. Julian, and A. R. Cordell. Regional function, blood flow, and oxygen utilization relations in repetitively occluded-reperfused canine myocardium. *Am J Physiol* 261: H538-547, 1991.
30. Weisfeldt, M. L., H. E. Scully, J. Frederiksen, J. J. Rubenstein, G. M. Pohost, E. Beierholm, A. G. Bello, and W. M. Daggett. Hemodynamic determinants of maximum negative dP-dt and periods of diastole. *Am J Physiol* 227: 613-621, 1974.

Chapter 7

EMD 57033 and Ca^{2+} -responsiveness

Background - Despite ample in vitro evidence that myofilament Ca^{2+} -responsiveness of stunned myocardium is decreased, in vivo data are inconclusive. Conversely, while Ca^{2+} -sensitizing agents increase myofilament Ca^{2+} -responsiveness in vitro, it has been questioned whether this also occurs in vivo. We therefore tested in open-chest anesthetized pigs whether EMD 57033 (the (+) enantiomer of 5-[1-(3,4-dimethoxybenzoyl)-1,2,3,4-tetrahydro-6-quinolyl]-6-methyl-3,6-dihydro-2H-1,3,4-thiadiazin-2-one) increases responsiveness to Ca^{2+} of non-stunned myocardium and restores function of stunned myocardium by normalizing the responsiveness to Ca^{2+} .

Methods and Results - Studies were performed under β -adrenoceptor blockade to minimize the contribution of the phosphodiesterase-III inhibitory actions of EMD 57033. Consecutive intracoronary Ca^{2+} infusions were used to evaluate the contractile response (assessed by the left ventricular end-systolic elastance, E_{es}) to added Ca^{2+} of non-stunned myocardium and myocardium stunned by 15 min coronary artery occlusion and 30 min reperfusion. In non-stunned propranolol-treated myocardium, the Ca^{2+} infusions doubled E_{es} (baseline 6.9 ± 0.9 mmHg \cdot mm $^{-2}$, $n=8$). Following Ca^{2+} -washout, subsequent EMD 57033 infusion (0.1 mg \cdot kg $^{-1}$ \cdot min $^{-1}$, i.v.) tripled E_{es} ($P<0.05$) and potentiated the Ca^{2+} -induced increase in E_{es} to 55.7 ± 10.0 mmHg \cdot mm $^{-2}$ ($P<0.05$). Stunning ($n=7$) decreased E_{es} to 5.3 ± 0.6 mmHg \cdot mm $^{-2}$ ($P>0.10$) and attenuated the Ca^{2+} -induced increase in E_{es} ($P<0.05$). Subsequent infusion of EMD 57033 increased E_{es} to 6.8 ± 1.8 mmHg \cdot mm $^{-2}$ ($P<0.05$) and restored responsiveness to added Ca^{2+} .

Conclusions - These in vivo findings are consistent with the in vitro observations that myofilament Ca^{2+} -responsiveness of stunned myocardium is reduced and that EMD 57033 increases contractility by enhancing myofilament Ca^{2+} -responsiveness.

Sandra de Zeeuw, Serge A.I.P. Trines, Rob Krams, Dirk J. Duncker, Pieter D. Verdouw. In vivo evidence that EMD 57033 restores myocardial responsiveness to intracoronary Ca^{2+} in stunned myocardium. *Eur J Pharmacol* 103: 99-109, 2000

Introduction

It has been shown in *in vitro* models that a reduced responsiveness of the myofilaments to Ca^{2+} underlies the mechanism of myocardial stunning (14), but evidence that this mechanism is also operative *in vivo* is lacking (4). For instance, Ito et al. (20) observed that in an *in vivo* canine model of regional myocardial stunning maximum systolic shortening attainable with intracoronary Ca^{2+} infusions was not different for stunned and normal myocardium. In addition, Heusch et al. (18) also failed to find evidence for a decreased Ca^{2+} responsiveness as assessed by the response of a regional work index to intracoronary Ca^{2+} in *in vivo* porcine myocardium, stunned by a 90-min flow reduction that decreased the local myocardial work index by 60%, a protocol that produced stunning without necrosis. A complicating factor in explaining the discrepancies between the *in vitro* and the *in vivo* results, is that in the *in vivo* studies contractile function was estimated using indices that display considerable load-dependency and of which it is known that their load-dependency increases with stunning (12). Thus, Hofmann et al. (19) showed under well controlled *in vitro* conditions that pCa for half maximal activation of tension was decreased, compared to baseline, in single cell-sized preparations from porcine myocardium stunned *in vivo* by a 45-min period of 60% coronary flow reduction and 30 min of reperfusion. We have shown earlier that EMD 60263, a thiadiazinone derivative, which has been demonstrated to possess Ca^{2+} -sensitizing properties *in vitro* (3, 31), is capable of restoring systolic shortening of regionally stunned myocardium *in vivo* (33). The beneficial effects of a number of Ca^{2+} -sensitizing agents on systolic function of stunned myocardium have now been confirmed in several isolated and intact heart studies (1, 8, 22), but in none of these studies it was actually shown that during stunning, the responsiveness to Ca^{2+} was altered and that subsequent administration of the Ca^{2+} -sensitizing agents restored the responsiveness to Ca^{2+} .

Therefore, the aims of the present *in vivo* study were to determine whether administration of a Ca^{2+} -sensitizing agent alters the myocardial responsiveness to added Ca^{2+} in non-stunned myocardium and whether this agent restores function of stunned myocardium by normalization of the myocardial responsiveness to Ca^{2+} . As a Ca^{2+} -sensitizing agent we used EMD 57033 (the (+) enantiomer of 5-[1-(3,4-dimethoxybenzoyl)-1,2,3,4-tetrahydro-6-quinolyl]-6-methyl-3,6-dihydro-2H-1,3,4-thiadiazin-2-one), because we have shown that this agent, in a dose of $0.2 \text{ mg}\cdot\text{kg}^{-1}\cdot\text{min}^{-1}$, is capable of restoring systolic function of regionally stunned myocardium, without adversely affecting diastolic function (8), a potential concern with this class of agents (17, 32). Because EMD 57033 possesses minor phosphodiesterase-III (PDE-III) inhibitory properties (31, 39), the effect of EMD 57033 was evaluated in the presence of the β -adrenoceptor antagonist propranolol to minimize tonic and stimulated cAMP production,

thereby keeping the contribution of PDE-III inhibition to the actions of EMD 57033 to a minimum. The myocardial responsiveness to added Ca^{2+} was determined using intracoronary infusions to prevent that changes in systemic hemodynamics act as confounding factors. Finally, to further minimize the influence of changes in loading conditions, we used, in analogy to the left ventricular end-systolic pressure (LVESP)-volume (36) and LVESP-segment length (2, 12) relations, the LVESP-segment area relation to evaluate the contractile response to Ca^{2+} .

Methods

Experiments were performed in accordance with the "Guiding Principles for the Care and Use of Animals" of the Council of the American Physiological Society and under the regulations of the Erasmus University Rotterdam.

Animal preparation

Fifteen with ketamine (20-30 mg·kg⁻¹ i.m.) sedated cross-bred Landrace-Yorkshire pigs (25-35 kg) were anesthetized with sodium pentobarbital (20 mg·kg⁻¹, i.v.), intubated and ventilated with oxygen-enriched air (8, 32). Fluid-filled catheters were inserted for intravenous administration of sodium pentobarbital (5-10 mg·kg⁻¹·h⁻¹) and fluids, and for measurement of arterial blood pressure. A micromanometer-tipped catheter (B. Braun Medical) was inserted for monitoring left ventricular blood pressure. A balloon catheter was positioned in the inferior caval vein to transiently decrease left ventricular preload. After administration of pancuronium bromide (4 mg, i.v.), a midsternal thoracotomy was performed and an electromagnetic flow probe (Skalar) was placed around the ascending aorta, while a Doppler flow probe (Triton Technology) was placed proximally on the left anterior descending coronary artery (LADCA). Distal to the flow probe, the LADCA was dissected free for placement of an atraumatic clamp and cannulated for local infusion of Ca^{2+} . Segment area was measured using sonomicrometry (Triton Technology) by placing ultrasound crystals in the midmyocardial layer approximately 10 mm apart in the distribution areas of the LADCA and the left circumflex coronary artery (LCXCA). To minimize the influence of malalignment of a single crystal pair with the fiber direction, two pairs of crystals were implanted in each region: one pair parallel and another pair perpendicular to the myocardial fiber direction.

Experimental protocols

Propranolol-treated pigs with non-stunned myocardium

To evaluate the effect of EMD 57033 on the responsiveness to intracoronary Ca^{2+} of non-stunned myocardium, 8 pigs received propranolol (0.5 mg·kg⁻¹ + 0.5 mg·kg⁻¹·h⁻¹, a

dose that inhibits the isoproterenol-induced increases in heart rate and left ventricular dP/dt_{max} by more than 90% in pigs (40)), after which hemodynamic variables were recorded and LVESP-segment area relations were constructed by transiently reducing preload (8). Then, 3 consecutive 5-min infusions of Ca^{2+} ($CaCl_2 \cdot 2H_2O$ dissolved in saline) were administered into the LADCA at rates of 0.25, 0.50 and 0.75 ml/min (corresponding to 18, 36 and 54 $\mu\text{mol} \cdot \text{min}^{-1}$, respectively). At the end of each infusion step, measurements were repeated (Fig. 1). Following Ca^{2+} -washout, the EMD 57033 infusion (0.1 $\text{mg}/\text{kg} \cdot \text{min}^{-1}$, i.v.) was started and after 30 min the Ca^{2+} infusions were repeated.

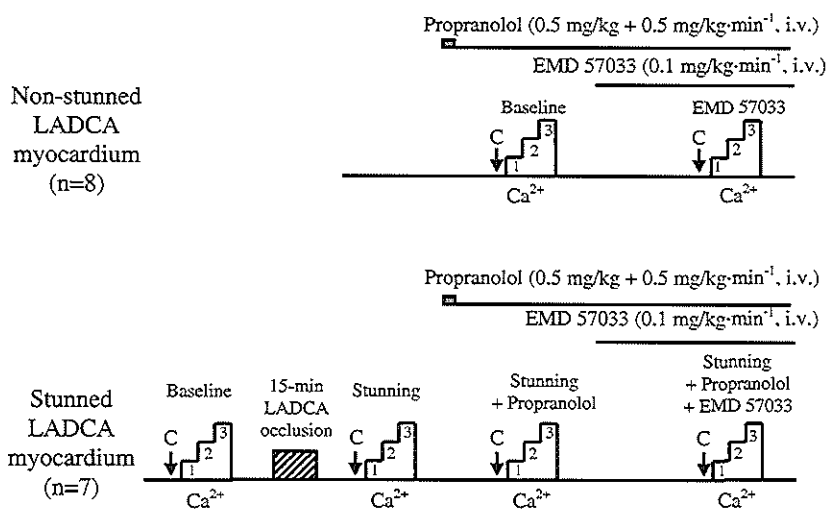


Fig. 1 Experimental protocols for propranolol-treated pigs with non-stunned myocardium and pigs with regionally stunned myocardium. Stunning was produced by a 15-min left anterior descending coronary artery occlusion (LADCA) and 30 min of reperfusion. Three consecutive Ca^{2+} infusions into the left anterior descending coronary artery were administered for 5 min each at rates of 18, 36 and 54 $\mu\text{mol} \cdot \text{min}^{-1}$, respectively. The arrows indicate the Control (C) measurements before the start of the Ca^{2+} infusions (Tables 1 and 2).

Pigs with stunned myocardium

To evaluate the effect of EMD 57033 on the myocardial responsiveness to intracoronary Ca^{2+} during stunning, seven pigs received the intracoronary Ca^{2+} infusions before (baseline) and 30 min after a 15-min LADCA occlusion (stunning; Fig. 1). Subsequently, the β -adrenoceptors were blocked by propranolol and after repeating the Ca^{2+} infusions (stunning + propranolol), the EMD 57033 infusion was started and 30 min later, the myocardial responsiveness to intracoronary Ca^{2+} was again determined (stunning + propranolol + EMD 57033).

Data analysis

All data were digitized and stored for off-line analysis (8). Segment length data were normalized to an end-diastolic length of 10 mm at baseline to correct for variability in the implantation distance between the various crystal pairs in the different animals. Regional left ventricular end-systolic elastance (E_{es}) was assessed using LVESP-segment area relations obtained from the relation between left ventricular pressure and the segment area encompassed by the two pairs of crystals. The slope of the LVESP-segment area relations (end-systolic elastance, E_{es}) and the zero pressure-area intercept (A_0) were determined via linear regression analysis of the LVESP-segment area data points (Fig. 2) which were obtained using an iterative method (38). Data are mean \pm standard error of the mean (S.E.M.). Statistical significance ($P < 0.05$, two-tailed) of changes was determined using one-way or two-way analysis of variance. Post-hoc testing was performed using Dunnett's test.

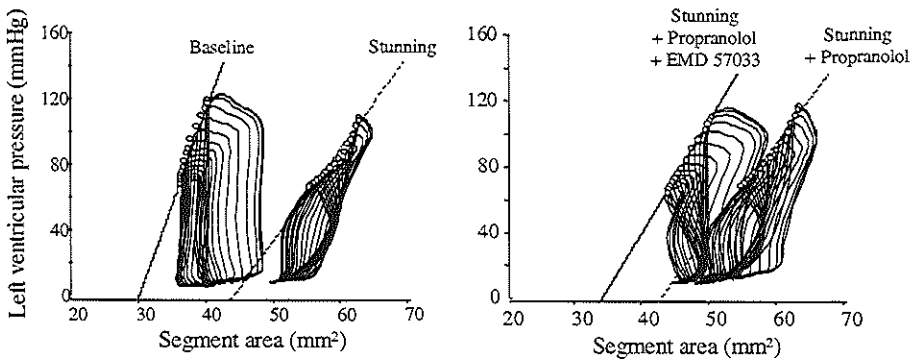


Fig. 2 Example of LVESP-segment area relations during Baseline, Stunning, Stunning + Propranolol and Stunning + Propranolol + EMD 57033 in an individual pig in which the myocardium was stunned by a 15-min occlusion of the LADCA.

Results

Hemodynamics

Propranolol-treated pigs with non-stunned myocardium

In the propranolol-treated pigs there were no changes in any of the hemodynamic parameters during the intracoronary Ca^{2+} infusions (not shown), except for a dose-dependent increase in left ventricular dP/dt_{max} up to $17 \pm 4\%$ ($P < 0.05$). The infusion of EMD 57033, which was started after recovery from the Ca^{2+} infusions, increased left ventricular dP/dt_{max} by $28 \pm 8\%$ and heart rate by $7 \pm 3\%$ (both $P < 0.05$; Table 1). The subsequent intracoronary Ca^{2+} infusions had again no hemodynamic effects (not shown),

except for the increase in left ventricular dP/dt_{\max} by $27\pm 5\%$ ($P<0.05$).

Pigs with stunned myocardium

When the β -adrenoceptors were still unblocked, the intracoronary Ca^{2+} infusions only increased left ventricular dP/dt_{\max} (up to $17\pm 4\%$, $P<0.05$). Production of myocardial stunning after recovery from the Ca^{2+} infusions, was accompanied by decreases in mean arterial blood pressure ($9\pm 3\%$), cardiac output ($13\pm 5\%$) and left ventricular dP/dt_{\max} ($18\pm 5\%$), while heart rate and systemic vascular resistance remained unchanged (Table 1). Similar to the non-stunned myocardium, the intracoronary Ca^{2+} infusions increased left ventricular dP/dt_{\max} dose-dependently by up to $13\pm 5\%$, while the other parameters were not affected. In the presence of propranolol, infusion of Ca^{2+} into the stunned myocardium again affected only left ventricular dP/dt_{\max} ($24\pm 5\%$). The subsequent infusion of EMD 57033 increased heart rate ($4\pm 2\%$), cardiac output ($21\pm 8\%$) and left ventricular dP/dt_{\max} ($30\pm 10\%$), while left ventricular end-diastolic pressure decreased slightly (all $P<0.05$). In the presence of EMD 57033 the only effects of the intracoronary Ca^{2+} infusions on hemodynamics were an increase in left ventricular dP/dt_{\max} ($27\pm 3\%$, $P<0.05$) and a small decrease ($12\pm 2\%$, $P<0.05$) in mean arterial pressure.

Table 1. *Effect of EMD 57033 on control values of global hemodynamics of propranolol-treated pigs with non-stunned myocardium and of pigs with stunned myocardium.*

	Propranolol-treated pigs with non-stunned myocardium (n=8)		Pigs with stunned myocardium (n=7)			
	Baseline	EMD 57033	Baseline	Stunning	Stunning + Propranolol	Stunning + Propranolol + EMD 57033
HR (bpm)	101±7	107±6 ^a	106±6	109±5	91±5 ^c	94±4 ^d
MAP (mmHg)	86±4	83±6	94±4	85±4 ^b	70±5 ^c	76±4
CO (L/min)	2.7±0.2	2.9±0.3	3.3±0.3	2.8±0.3 ^b	2.6±0.3	3.1±0.3 ^d
SVR (mmHg·min ⁻¹)	33±3	31±3	30±3	32±3	28±3 ^c	25±2
LVdP/dt _{max} (mmHg/s)	1360±80	1720±100 ^a	1610±80	1320±70 ^b	1010±100 ^c	1270±90 ^d
LVEDP (mmHg)	3.3±0.8	2.1±0.8	4.4±1.3	6.9±1.4 ^b	7.3±1.5	5.0±1.5 ^d
CBF (mL/min)	28±4	32±3	22±2	20±3	20±3	36±6 ^d

HR, heart rate; MAP, mean arterial blood pressure; CO, cardiac output; SVR, systemic vascular resistance; LVdP/dt_{max} maximal rate of rise in left ventricular pressure; LVEDP, left ventricular end diastolic pressure; CBF, coronary blood flow. Values are mean±S.E.M., ^a $P<0.05$ EMD 57033 vs. Baseline; ^b $P<0.05$ Stunning vs. Baseline; ^c $P<0.05$ Stunning + Propranolol vs. Stunning; ^d $P<0.05$ Stunning + Propranolol + EMD 57033 vs. Stunning + Propranolol.

Left ventricular end-systolic pressure-segment area relations

Propranolol-treated pigs with non-stunned myocardium

Infusion of Ca^{2+} caused a dose-dependent counter clockwise rotation of the LVESP-segment area relation of the myocardium perfused by the LADCA (Fig. 3A), thereby almost doubling E_{es} (Fig. 4A), without affecting A_o (27 ± 3 and 29 ± 2 mm² during control and during the highest Ca^{2+} infusion rate, respectively). After recovery from the Ca^{2+}

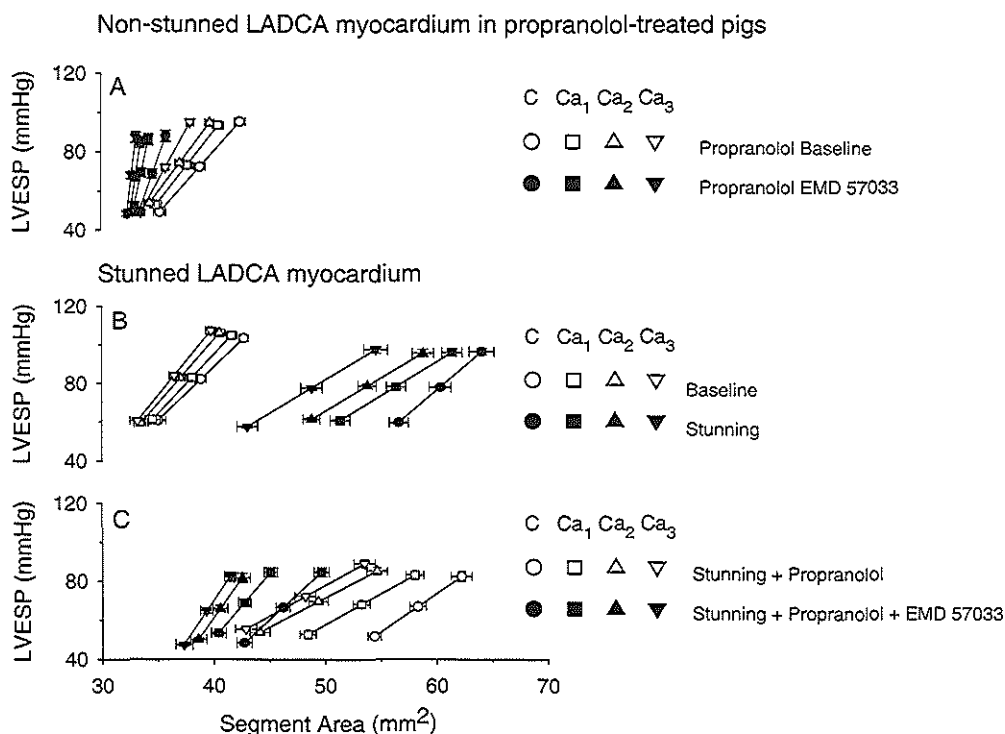


Fig. 3 Effect of EMD 57033 ($0.1 \text{ mg}\cdot\text{kg}^{-1}\cdot\text{min}^{-1}$ i.v.) on the response to 3 Ca^{2+} infusions into the left anterior descending coronary artery (LADCA) of the left ventricular end-systolic pressure (LVESP)-segment area relation in the distribution area of the left anterior descending coronary artery of non-stunned (panel A) and stunned (panels B and C) in vivo porcine myocardium. The 3 data points in each curve were derived from the linear left ventricular end-systolic pressure-segment area relation by computing left ventricular end-systolic pressure at 3 segment areas within the range of actual measurements (minimum, maximum and [minimum + maximum] /2) for each animal. C = Control; Ca_1 , Ca_2 and Ca_3 refer to the 3 Ca^{2+} infusion rates of 18, 36 and $54 \mu\text{mol}\cdot\text{min}^{-1}$, respectively.

infusions, the subsequent infusion of EMD 57033 more than doubled E_{es} (Table 2) and enhanced the Ca^{2+} -induced increments in E_{es} (Fig. 3A and 4A) without affecting A_o (30 ± 1 and $31 \pm 1 \text{ mm}^2$ during control and during the highest Ca^{2+} infusion rate, respectively).

The intravenous administration of EMD 57033 also caused a doubling of E_{es} in the myocardium perfused by the LCXCA (Table 2). However, in this segment the Ca^{2+} infusions into the LADCA before or during the EMD 57033 infusions altered neither E_{es} ($P = 0.28$ and $P = 0.09$; Fig. 4B) nor A_o ($P = 0.47$ and $P = 0.79$, not shown). These results

Non-stunned LADCA myocardium in propranolol-treated pigs

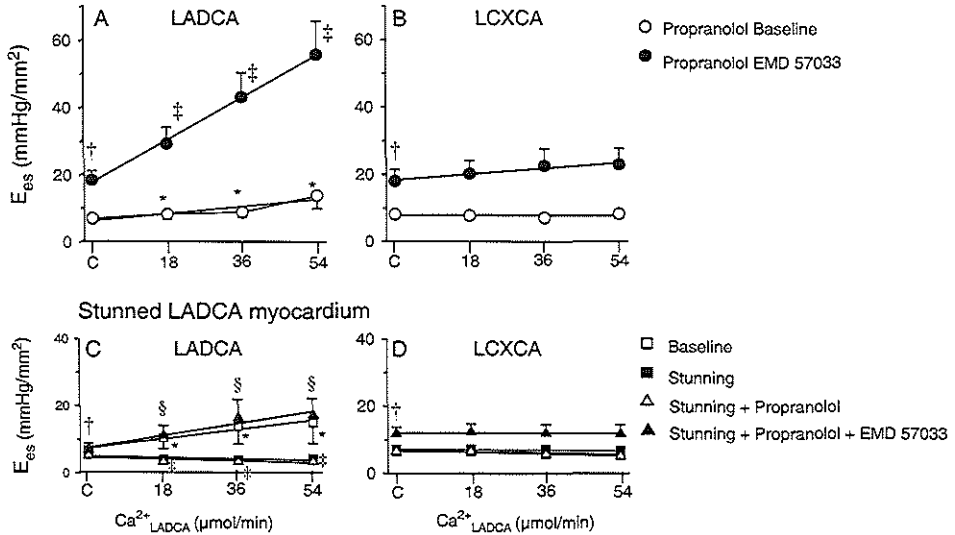


Fig. 4 Effect of EMD 57033 ($0.1 \text{ mg}\cdot\text{kg}^{-1}\cdot\text{min}^{-1}$ i.v.) on the response to 3 Ca^{2+} infusions into the left anterior descending coronary artery (LADCA) of E_{es} in the distribution areas of the left anterior descending coronary artery and the left circumflex coronary artery (LCXCA) of non-stunned (top panels) and stunned (bottom panels) in vivo porcine myocardium. C = Control; * $P < 0.05$ Ca^{2+} vs. Control (only for Baseline); † $P < 0.05$ EMD 57033 vs. Baseline (only for Control) or Stunning + Propranolol + EMD 57033 vs. Stunning + Propranolol (only for Control); ‡ $P < 0.05$ Ca^{2+} -response significantly different from Ca^{2+} -response during Baseline; § $P < 0.05$ Ca^{2+} -response significantly different from Ca^{2+} -response during Stunning + Propranolol.

indicate that the Ca^{2+} infusions into the LADCA did not lead to a spillover of Ca^{2+} in the distribution area of the LCXCA and that the ongoing infusion of EMD 57033 itself did not further increase contractility during the Ca^{2+} infusions.

Pigs with stunned myocardium

Infusion of Ca^{2+} during baseline also caused a counter clockwise rotation of the LVESP-segment area relation (Fig. 3B), thereby more than doubling E_{es} of the myocardium perfused by the LADCA (Fig. 4C) without affecting A_0 (not shown). Myocardial stunning lowered E_{es} from 6.6 ± 1.2 to $5.3 \pm 0.6 \text{ mmHg}\cdot\text{mm}^{-2}$ ($P > 0.10$), and caused a rightward shift of the LVESP-segment area relation reflected by the increase in A_0 from 24 ± 4 to $44 \pm 2 \text{ mm}^2$ ($P < 0.05$; Table 2). The Ca^{2+} infusions in the stunned myocardium caused a leftward shift of the LVESP-segment area relation (Fig. 3C) reflected by a recovery of A_0 to $26 \pm 4 \text{ mm}^2$ ($P < 0.05$). E_{es} was not significantly affected in the tested dose range of Ca^{2+} . The response of the LVESP-segment area relation of the stunned myocardium to the Ca^{2+} infusions was not modified by propranolol (Fig. 3C and 4C). During the subsequent

infusion of EMD 57033, E_{es} returned to baseline values, while A_0 recovered partly (Table 2). Importantly, the response of E_{es} to the Ca^{2+} infusions was restored to control levels (Fig. 4C). In the adjacent myocardium perfused by the LCXCA, neither E_{es} nor A_0 responded to the Ca^{2+} infusions into the LADCA before or after stunning the perfusion territory of the LADCA (Fig. 4D), while E_{es} almost doubled during intravenous infusion of EMD 57033 (Table 2).

Table 2. Effect of EMD 57033 on control values of E_{es} and A_0 of propranolol-treated pigs with non-stunned myocardium and of pigs with stunned myocardium.

	Propranolol-treated pigs with non-stunned myocardium (n=8)		Pigs with stunned myocardium (n=7)			
	Baseline	EMD 57033	Baseline	Stunning	Stunning + Propranolol	Stunning + Propranolol + EMD 57033
$E_{es, LADCA}$ (mmHg/mm ²)	6.9±0.9	18.3±2.8 ^a	6.6±1.2	5.3±0.6	5.0±0.9	6.8±1.8 ^d
$A_{0, LADCA}$ (mm ²)	27±3	30±1	24±4	44±2 ^b	41±3	33±3 ^d
$E_{es, LCXCA}$ (mmHg/mm ²)	8.1±1.2	18.0±3.5 ^a	6.5±0.8	7.1±1.2	6.6±1.4	11.8±2.0 ^d
$A_{0, LCXCA}$ (mm ²)	30±3	32±2	27±3	28±2	30±2	32±1

E_{es} , end-systolic elastance; A_0 , area intercept at zero pressure of the LVESP-segment area relation. Values are mean±S.E.M., ^a $P<0.05$ EMD 57033 vs. Baseline; ^b $P<0.05$ Stunning vs. Baseline; ^c $P<0.05$ Stunning + Propranolol vs. Stunning; ^d $P<0.05$ Stunning + Propranolol + EMD 57033 vs. Stunning + Propranolol.

Discussion

In vivo assessment of myocardial responsiveness to Ca^{2+}

In analogy to the time varying elastance concept (36), we employed the slope E_{es} of the LVESP-segment area relation to obtain a load-insensitive index of regional contractile function. A basic assumption for the determination of E_{es} is that during the preload reduction myocardial contractility (end-systolic stiffness of the myocardial tissue) does not change. For this reason, the preload reductions can only be studied during a period lasting no longer than 6-7 s (2) to avoid hypotension-induced reflex-mediated autonomic nervous system activity alterations. Consequently, the range over which the LVESP-segment area can be determined is limited. At a given level of contractility, the LVESP-segment area relation reflects that particular contractile state independent of whether the relation is constructed via alterations in pre- or afterload. In other words, LVESP and end-systolic area are not independent but interrelated and their relation is determined by the contractile state of the myocardium. Although alterations in diastolic function can modulate the diastolic elastance (and therefore, the left ventricular end-diastolic pressure-segment area relation), this should not affect the position of the LVESP-segment area

relation, provided contractility is unchanged. However, we have previously noted that alterations in diastolic function (i.e. a decrease in end-diastolic segment length) can produce translations in the LVESP-segment length relation. Thus, atrial pacing (which produces a decrease in end-diastolic segment length) also produces a leftward translation of the LVESP-segment length relation with no change in E_{es} (24). Similarly, the Ca^{2+} infusions in the present study also produced a leftward translation of the LVESP-segment area relation. These observations are difficult to explain but may be due to methodological limitations of the LVESP-regional segment area relations, which do not take into account the local left ventricular curvature (and hence, the radius) and wall thickness. For instance, at smaller segment areas, the wall thickness increases and radius decreases, which causes a decrease in regional wall stress that is larger than the decrease in left ventricular pressure. Consequently, it is possible that stress-strain relations would not show such a leftward shift.

Intracoronary Ca^{2+} infusions were employed to evaluate the myocardial responsiveness to added Ca^{2+} . As pointed out by Heusch et al. (18), in *in vivo* experiments, the intracoronary infusion rates cannot be directly translated into myocardial intracellular Ca^{2+} concentrations. We chose to present the response of E_{es} as a function of Ca^{2+} infusion rates rather than added Ca^{2+} concentrations in the blood. Using added blood concentrations would have yielded identical conclusions, because firstly, coronary blood flows were very similar under control conditions and following stunning, while in the presence of EMD 57033, blood flows were higher. These higher blood flows would result in lower Ca^{2+} concentrations and, hence, the effect of EMD 57033 on Ca^{2+} -responsiveness may have been slightly underestimated. Another potential concern is that intracoronary Ca^{2+} infusions may recruit different amounts of cytosolic Ca^{2+} (Ca^{2+} -induced Ca^{2+} release) in non-stunned myocardium under control conditions and in the presence of EMD 57033, or in stunned myocardium. However, *in vitro* studies have shown that EMD 57033 increases contractile force (28) without an effect on Ca^{2+} transients, indicating that the compound does not modulate activator Ca^{2+} , sarcoplasmic reticulum function or Ca^{2+} -induced Ca^{2+} release (13, 39). Also, several groups of authors have shown that the capacity of the sarcoplasmic reticulum for Ca^{2+} uptake and Ca^{2+} release is preserved in stunned myocardium (4, 10, 21, 26), and that, consequently, the Ca^{2+} -transients in stunned myocardium are not different from those in normal trabeculae (6, 14). Moreover, increases in the $[Ca^{2+}]_{out}$ produced identical increases in peak-systolic $[Ca^{2+}]_{in}$ in stunned and normal myocardial trabeculae (14), lending further support to the concept that Ca^{2+} -induced Ca^{2+} release and sarcoplasmic reticulum function are unperturbed in stunned myocardium. Similar to other *in vivo* studies (5, 7, 18), maximal Ca^{2+} -activated force could not be determined, because of the occurrence of arrhythmias and contracture-like phenomena (evidenced by marked reductions in end-diastolic segment length) and post- Ca^{2+} infusion loss of regional contractile function at higher concentrations of

intracoronary Ca^{2+} , which we observed in pilot experiments. In the present study, we used slightly lower Ca^{2+} concentrations as compared to previous studies (5, 7, 18, 20), to facilitate detection of the putative Ca^{2+} -sensitizing properties of EMD 57033. Nevertheless, we observed in the normal myocardium that the intracoronary Ca^{2+} infusions, in the dose-range tested, elicited relative increases in left ventricular $\text{dP/dt}_{\text{max}}$ (10-20%) and segment shortening (13%, not presented) that were similar to the 15% increases in wall thickening (5, 20), external work (18), segment shortening (7), and the 10-15% increases in left ventricular $\text{dP/dt}_{\text{max}}$ (5, 7, 18, 20) found in earlier studies.

Rationale for the dose of EMD 57033

To allow evaluation of the effect of EMD 57033 on the contractile response to the three 5-min intracoronary Ca^{2+} infusions, a steady state of hemodynamics and contractile function is mandatory during infusion of EMD 57033. In a previous study (8), we observed that systolic shortening, as well as E_{cs} , continued to increase throughout the 60 min infusion period of EMD 57033 at a rate of $0.2 \text{ mg}\cdot\text{kg}^{-1}\cdot\text{min}^{-1}$. Consequently, we selected a lower dose ($0.1 \text{ mg}\cdot\text{kg}^{-1}\cdot\text{min}^{-1}$) and observed in the initial experiments that this dose was still effective as E_{cs} in the myocardium perfused by the LCXCA increased from 8.1 ± 1.2 to $18.0\pm 3.5 \text{ mmHg}\cdot\text{mm}^{-2}$ after 30 min of infusion, but did not further increase during the subsequent Ca^{2+} infusions into the LADCA (Fig. 4), while the intravenous EMD 57033 infusion was continued. The latter observation precludes the necessity of a control group, in which Ca^{2+} infusions are replaced by vehicle to exclude the possibility that increases in E_{cs} during the intracoronary Ca^{2+} infusions were caused by a progressive increase in contractility secondary to the continuous infusion of EMD 57033.

Effect of EMD 57033 on Ca^{2+} -responsiveness of non-stunned myocardium

Calcium-sensitizing agents are a heterogeneous class of drugs (11, 16, 37). Thus, several of these agents have been shown to increase Ca^{2+} -sensitivity of the myofilaments *in vitro* by modifying the interaction between Ca^{2+} and Troponin C (e.g. sulmazole, levosimendan, pimobendan, MCI-154 and EMD 60263), by modifying the interaction between the various components of the thin filaments (e.g pimobendan, and MCI 154) or by altering actin-myosin crossbridge kinetics (EMD 57033). In addition to the Ca^{2+} -sensitizing properties, most of these agents also produce considerable PDE-III inhibitory activity (sulmazole, pimobendan, levosimendan and MCI-154). The exact mechanism by which EMD 57033 increases the Ca^{2+} sensitivity is still debated (27). Solaro et al. (34) proposed that EMD 57033 principally acts at the actin-myosin site, where the compound reverses the inhibition of actin-myosin interactions by troponin-tropomyosin and may also promote transition of crossbridges from weak to strong force-generating states. On the other hand, Pan and Johnson (30) observed in an *in vitro* model of pure recombinant human cardiac troponin C (TnC) that EMD 57033 binds to the $\text{Ca}^{2+}/\text{Mg}^{2+}$ sites of TnC.

In the present study, $0.1 \text{ mg}\cdot\text{kg}^{-1}\cdot\text{min}^{-1}$ EMD 57033 not only increased E_{es} but also enhanced the myocardial response to added Ca^{2+} . Thus, while E_{es} doubled (from 6.9 ± 0.9 to $13.8\pm 3.8 \text{ mmHg}\cdot\text{mm}^{-2}$) during the intracoronary Ca^{2+} infusions in the absence of EMD 57033, E_{es} tripled (from 18.3 ± 2.8 to $55.7\pm 10.0 \text{ mmHg}\cdot\text{mm}^{-2}$) during the Ca^{2+} infusions in the presence of EMD 57033, despite the higher control value during infusion of EMD 57033.

Several lines of evidence suggest that in the present in vivo study, the EMD 57033-induced systolic actions are principally the result of Ca^{2+} -sensitization, with a negligible contribution of PDE-III inhibition. In in vitro studies, varying dosages of EMD 57033 have been used. For instance, Grandis et al. (15) found in Langendorff-perfused rat hearts that a dose of only $2 \mu\text{M}$ could already increase contractility without a significant change in MVO_2 . Furthermore, Korbmacher et al. (22) used $30 \mu\text{M}$ EMD 57033 in isolated rabbit hearts and showed that at that concentration, EMD 57033 exerts its effect by both Ca^{2+} -sensitizing and PDE-III inhibitory properties. On the other hand, White et al. (39), who used EMD 57033 in a dose range of $0.1\text{--}20 \mu\text{M}$ in isolated ferret cardiac muscle, reported that EMD 57033 acts predominantly by increasing myofilament Ca^{2+} -sensitivity. Taken together, these in vitro studies suggest that PDE-III inhibition occurs principally at concentrations of EMD 57033 in excess of $20 \mu\text{M}$. In our previous study (8) with EMD 57033 ($0.2 \text{ mg}\cdot\text{kg}^{-1}\cdot\text{min}^{-1}$), plasma levels increased time-dependently to 8, 12, 15 and $17 \mu\text{M}$ at 15, 30, 45 and 60 min infusion, respectively, which is below the in vitro PDE-III inhibiting threshold concentration of $20 \mu\text{M}$. Since in the present study we infused $0.1 \text{ mg}\cdot\text{kg}^{-1}\cdot\text{min}^{-1}$, this dose would therefore also not be expected to produce PDE-III inhibition. This is supported by the finding that the increases in both E_{es} and left ventricular $\text{dP}/\text{dt}_{\text{max}}$ produced by $0.2 \text{ mg}\cdot\text{kg}^{-1}\cdot\text{min}^{-1}$ EMD 57033 (maximal plasma levels $17 \mu\text{M}$) in normal myocardium were not altered by propranolol, suggesting minimal contribution of PDE-III inhibition to the positive inotropic actions of EMD 57033. In contrast, we have previously shown that the same dose of propranolol virtually abolished the inotropic actions of the phosphodiesterase inhibitor / Ca^{2+} -sensitizer pimobendan (9). Moreover, the duration of both global and regional left ventricular systole were not altered by EMD 57033 in the study by De Zeeuw et al. (8), independent of the presence of propranolol, indicating that a positive lusitropic effect of PDE-III inhibition was also unlikely. Taken together, the in vivo observation of an enhancement by EMD 57033 of the Ca^{2+} -induced increase in E_{es} is highly consistent with the in vitro observation that EMD 57033 increases myocardial contractile force via an increase in myofilament Ca^{2+} responsiveness.

Effect of EMD 57033 on Ca^{2+} -responsiveness of stunned myocardium

Myocardial stunning was characterized by a trend towards a decrease in E_{es} and a marked rightward shift of the LVESP-segment area relation. At first glance, this appears

to be a surprising finding as most studies (including some from our own laboratory) have reported both a decrease in E_{es} and a rightward shift, although some studies have also reported a rightward shift as the most prominent feature of stunning (25, 35). The reason for the differences is unclear, but may be related to the range of pressures over which the LVESP-segment area relation was constructed. It is well known that the LVESP-segment length relation may be curvilinear and that the curvilinearity increases at higher end-systolic pressures that are obtained when increases in afterload are used (29). For this reason, we used preload reductions to yield a pressure range of 40 mmHg over which good linearity was observed. A rightward shift of the LVESP-segment area relation is compatible with a decrease of elastic-restoring forces, probably induced by alterations in structural non-contractile elements, such as the extracellular collagen matrix and/or the cytoskeleton. However, as outlined under section “*In vivo assessment of myocardial responsiveness to Ca^{2+}* ”, the use of LVESP-segment area relations, rather than of left ventricular end-systolic stress-strain relations, may also have contributed to the marked rightward shift.

It is now generally accepted that the mechanism underlying myocardial stunning does not involve a decreased Ca^{2+} availability (4, 14, 21, 26), but a decreased responsiveness of the myofilaments to Ca^{2+} (4, 14). However, experimental support for this hypothesis is derived from studies in isolated muscle preparations, whereas evidence obtained in *in vivo* experiments is lacking. Thus, several groups of investigators have shown that in stunned myocardium, the response of systolic wall thickening (20), segment shortening (5), or external work (18) to intracoronary Ca^{2+} infusions is not impaired. In two of these studies, Ca^{2+} infusions were used that produced maximal levels of systolic shortening (5) and external work (18) during control conditions, but whether these concentrations also resulted in maximum responses in stunned myocardium was not determined. Only Ito et al. (20) used Ca^{2+} doses that resulted in maximum responses of systolic shortening in both normal and stunned myocardium, and demonstrated an unperturbed maximum wall thickening in response to Ca^{2+} following stunning. Consistent with previous studies, we observed a similar Ca^{2+} -induced increase in area reduction in normal and stunned myocardium. In contrast, however, in the dose-range tested, the Ca^{2+} -induced increases in E_{es} were depressed following stunning. These findings can be explained by a rightward shift of the $[Ca^{2+}]$ -contractile force relations, i.e. a decrease in Ca^{2+} -sensitivity. A decrease in Ca^{2+} -sensitivity is supported by the study of Hofmann et al. (19) who showed a rightward shift of the $[Ca^{2+}]$ -force relation with a maintained maximum Ca^{2+} -activated force. In addition, a decrease in maximum Ca^{2+} -activated force may also have contributed to the decreased Ca^{2+} responsiveness (14).

An interesting observation in the present study was that the increase in E_{es} produced by EMD 57033 in stunned myocardium was less than in non-stunned myocardium. In our previous study, we also observed that at lower concentrations (12 μ M), the effect of EMD

57033 on E_{cs} was more pronounced in non-stunned than in stunned myocardium (8), while at higher concentrations (17 μM) the E_{cs} of non-stunned and stunned myocardium were no longer different. However, interpretation of these observations is difficult, because stunned myocardium perfused by the LADCA was compared to non-stunned myocardium perfused by the LCXCA, and hence, regional differences in contractile responses cannot be excluded. In the present study, we directly compared stunned myocardium to non-stunned myocardium of the same distribution area, which points, indeed, towards a reduced sensitivity of stunned myocardium to the actions of EMD 57033. This is also supported by observations by Korbmacher et al. (23) who found that non-stunned isolated rabbit hearts were also more sensitive to the Ca^{2+} -sensitizing effects of EMD 60263 than stunned hearts.

Both the response of E_{cs} to EMD 57033 as well as the response of E_{cs} to the Ca^{2+} infusions in the presence of EMD 57033 were less in stunned than in non-stunned LADCA perfused myocardium. However, infusion of $0.1 \text{ mg}\cdot\text{kg}^{-1}\cdot\text{min}^{-1}$ of EMD 57033 not only increased E_{cs} of stunned myocardium (from 5.0 ± 0.9 vs. $6.9\pm 0.9 \text{ mmHg}\cdot\text{mm}^{-2}$), but also restored its response to the Ca^{2+} infusions to baseline levels. These findings are consistent with a decreased myofilament Ca^{2+} responsiveness of stunned myocardium, and a restoration of myofilament Ca^{2+} responsiveness by EMD 57033. It is very well possible that the use of a higher dose of EMD 57033 in stunned myocardium that would have resulted in an increase in E_{cs} comparable to the level of E_{cs} produced by $0.1 \text{ mg}\cdot\text{kg}^{-1}\cdot\text{min}^{-1}$ in non-stunned myocardium (i.e. $18.3\pm 2.8 \text{ mmHg}\cdot\text{mm}^{-2}$) would also result in comparable responses to intracoronary Ca^{2+} .

Conclusions

EMD 57033 enhanced the myocardial responsiveness to intracoronary added Ca^{2+} in non-stunned and stunned myocardium which supports the concept, based on in vitro observations, that EMD 57033 increases myocardial contractility via an increase in myofilament Ca^{2+} -responsiveness, and that myofilament Ca^{2+} -responsiveness of stunned myocardium is decreased, but can be restored by EMD 57033.

References

1. Abe, Y., Y. Kitada, and A. Narimatsu. Effect of a calcium-sensitizing positive inotropic agent MCI-154 and its combined use with enalapril on posts ischemic contractile dysfunction of dog hearts. *J Cardiovasc Pharmacol* 26: 653-659, 1995.
2. Aversano, T., W. L. Maughan, W. C. Hunter, D. Kass, and L. C. Becker. End-systolic measures of regional ventricular performance. *Circulation* 73: 938-950, 1986.
3. Bezstarosti, K., L. K. Soei, P. D. Verdouw, and J. M. Lamers. Phosphorylation by protein kinase C and the responsiveness of $\text{Mg}(2+)\text{-ATPase}$ to Ca^{2+} of myofibrils isolated from stunned and non-stunned porcine myocardium. *Mol Cell Biochem* 176: 211-218, 1997.
4. Bolli, R., and E. Marban. Molecular and cellular mechanisms of myocardial stunning. *Physiol Rev* 79: 609-634, 1999.
5. Buffington, C. W., and K. P. Rothfield. Effects of intracoronary calcium chloride on the

- postschismic heart in pigs. *Ann Thorac Surg* 59: 1448-1455, 1995.
6. Carrozza, J. P., Jr., L. A. Bentivegna, C. P. Williams, R. E. Kuntz, W. Grossman, and J. P. Morgan. Decreased myofilament responsiveness in myocardial stunning follows transient calcium overload during ischemia and reperfusion. *Circ Res* 71: 1334-1340, 1992.
 7. Crystal, G. J., and X. Zhou. Nitric oxide does not modulate the increases in blood flow, O₂ consumption, or contractility during CaCl₂ administration in canine hearts. *Cardiovasc Res* 42: 232-239, 1999.
 8. de Zeeuw, S., S. A. Trines, R. Krams, P. D. Verdouw, and D. J. Duncker. Cardiovascular profile of the calcium sensitizer EMD 57033 in open-chest anaesthetized pigs with regionally stunned myocardium. *Br J Pharmacol* 129: 1413-1422, 2000.
 9. Duncker, D. J., J. M. Hartog, L. Levinsky, and P. D. Verdouw. Systemic haemodynamic actions of pimobendan (UD-CG 115 BS) and its O-demethylmetabolite UD-CG 212 Cl in the conscious pig. *Br J Pharmacol* 91: 609-615, 1987.
 10. Duncker, D. J., R. Schulz, R. Ferrari, D. Garcia-Dorado, C. Guarnieri, G. Heusch, and P. D. Verdouw. "Myocardial stunning" remaining questions. *Cardiovasc Res* 38: 549-558, 1998.
 11. Endoh, M. Changes in intracellular Ca²⁺ mobilization and Ca²⁺ sensitization as mechanisms of action of physiological interventions and inotropic agents in intact myocardial cells. *Jpn Heart J* 39: 1-44, 1998.
 12. Fan, D., L. K. Soei, L. M. Sassen, R. Krams, and P. D. Verdouw. Mechanical efficiency of stunned myocardium is modulated by increased afterload dependency. *Cardiovasc Res* 29: 428-437, 1995.
 13. Ferroni, C., O. Hano, C. Ventura, E. G. Lakatta, M. Klockow, H. Spurgeon, and M. C. Capogrossi. A novel positive inotropic substance enhances contractility without increasing the Ca²⁺ transient in rat myocardium. *J Mol Cell Cardiol* 23: 325-331, 1991.
 14. Gao, W. D., D. Atar, P. H. Backx, and E. Marban. Relationship between intracellular calcium and contractile force in stunned myocardium. Direct evidence for decreased myofilament Ca²⁺ responsiveness and altered diastolic function in intact ventricular muscle. *Circ Res* 76: 1036-1048, 1995.
 15. Grandis, D. J., P. J. DelNido, and A. P. Koretsky. Functional and energetic effects of the inotropic agents EMD-57033 and BAPTA on the isolated rat heart. *Am J Physiol* 269: C472-479, 1995.
 16. Haikala, H., and I. B. Linden. Mechanisms of action of calcium-sensitizing drugs. *J Cardiovasc Pharmacol* 26: S10-19, 1995.
 17. Hajjar, R. J., and J. K. Gwathmey. Calcium-sensitizing inotropic agents in the treatment of heart failure: a critical view. *Cardiovasc Drugs Ther* 5: 961-965, 1991.
 18. Heusch, G., J. Rose, A. Skyschally, H. Post, and R. Schulz. Calcium responsiveness in regional myocardial short-term hibernation and stunning in the in situ porcine heart. Inotropic responses to postextrasystolic potentiation and intracoronary calcium. *Circulation* 93: 1556-1566, 1996.
 19. Hofmann, P. A., W. P. Miller, and R. L. Moss. Altered calcium sensitivity of isometric tension in myocyte-sized preparations of porcine postschismic stunned myocardium. *Circ Res* 72: 50-56, 1993.
 20. Ito, B. R., H. Tate, M. Kobayashi, and W. Schaper. Reversibly injured, postschismic canine myocardium retains normal contractile reserve. *Circ Res* 61: 834-846, 1987.
 21. Kaplan, P., M. Hendrikx, M. Mattheussen, K. Mubagwa, and W. Flameng. Effect of ischemia and reperfusion on sarcoplasmic reticulum calcium uptake. *Circ Res* 71: 1123-1130, 1992.
 22. Korbmacher, B., U. Sunderdiek, G. Arnold, H. D. Schulte, and J. D. Schipke. Improved ventricular function by enhancing the Ca⁺⁺ sensitivity in normal and stunned myocardium of isolated rabbit hearts. *Basic Res Cardiol* 89: 549-562, 1994.
 23. Korbmacher, B., U. Sunderdiek, G. Selcan, G. Arnold, and J. D. Schipke. Different responses of non-ischemic and post-ischemic myocardium towards Ca²⁺ sensitization. *J Mol Cell Cardiol* 29: 2053-2066, 1997.
 24. Krams, R., D. J. Duncker, E. O. McFalls, A. Hogendoorn, and P. D. Verdouw. Dobutamine restores the reduced efficiency of energy transfer from total mechanical work to external mechanical work in stunned porcine myocardium. *Cardiovasc Res* 27: 740-747, 1993.
 25. Krams, R., M. Janssen, C. Van der Lee, J. Van Meegen, J. W. De Jong, C. J. Slager, and P. D. Verdouw. Loss of elastic recoil in postschismic myocardium induces rightward shift of the

- systolic pressure-volume relationship. *Am J Physiol* 267: H1557-1564, 1994.
26. Lamers, J. M., D. J. Duncker, K. Bezstarosti, E. O. McFalls, L. M. Sassen, and P. D. Verdouw. Increased activity of the sarcoplasmic reticular calcium pump in porcine stunned myocardium. *Cardiovasc Res* 27: 520-524, 1993.
 27. Lee, J. A., and D. G. Allen. Calcium sensitizers: mechanisms of action and potential usefulness as inotropes. *Cardiovasc Res* 36: 10-20, 1997.
 28. Lues, L., N. Beier, R. Jonas, M. Klockow, and G. Haesler. The two mechanisms of action of racemic cardiotoxic EMD 53998, calcium sensitization and phosphodiesterase inhibition, reside in different enantiomers. *J Cardiovasc Pharmacol* 21: 883-892, 1993.
 29. Miller, W. P. Effect of altered contractility on the linearity of regional left ventricular end-systolic relations in intact hearts. *Am Heart J* 128: 114-123, 1994.
 30. Pan, B. S., and R. G. Johnson, Jr. Interaction of cardiotoxic thiaziazinone derivatives with cardiac troponin C [published erratum appears in *J Biol Chem* 1996 Aug 9;271(32):19632]. *J Biol Chem* 271: 817-823, 1996.
 31. Ravens, U., H. M. Himmel, M. Fluss, K. Davia, and S. E. Harding. Phosphodiesterase inhibition and Ca²⁺ sensitization. *Mol Cell Biochem* 157: 245-249, 1996.
 32. Soei, L. K., S. de Zeeuw, R. Krams, D. J. Duncker, and P. D. Verdouw. Ca(2+) sensitization and diastolic function of normal and stunned porcine myocardium. *Eur J Pharmacol* 386: 55-67, 1999.
 33. Soei, L. K., L. M. Sassen, D. S. Fan, T. van Veen, R. Krams, and P. D. Verdouw. Myofibrillar Ca²⁺ sensitization predominantly enhances function and mechanical efficiency of stunned myocardium. *Circulation* 90: 959-969, 1994.
 34. Solaro, R. J., G. Gambassi, D. M. Warshaw, M. R. Keller, H. A. Spurgeon, N. Beier, and E. G. Lakatta. Stereoselective actions of thiaziazinones on canine cardiac myocytes and myofilaments. *Circ Res* 73: 981-990, 1993.
 35. Stahl, L. D., T. R. Aversano, and L. C. Becker. Selective enhancement of function of stunned myocardium by increased flow. *Circulation* 74: 843-851, 1986.
 36. Suga, H. Ventricular energetics. *Physiol Rev* 70: 247-277, 1990.
 37. Teramura, S., and T. Yamakado. Calcium sensitizers in chronic heart failure: inotropic interventions- reseration to preservation. *Cardiologia* 43: 375-385, 1998.
 38. van der Velde, E. T., D. Burkhoff, P. Steendijk, J. Karsdon, K. Sagawa, and J. Baan. Nonlinearity and load sensitivity of end-systolic pressure-volume relation of canine left ventricle in vivo. *Circulation* 83: 315-327, 1991.
 39. White, J., J. A. Lee, N. Shah, and C. H. Orchard. Differential effects of the optical isomers of EMD 53998 on contraction and cytoplasmic Ca²⁺ in isolated ferret cardiac muscle. *Circ Res* 73: 61-70, 1993.
 40. Wolfenbittel, B. H., and P. D. Verdouw. Nifedipine and myocardial performance in the presence and absence of beta-blockade with propranolol. *Arch Int Pharmacodyn Ther* 266: 83-92, 1983.

Chapter 8

Comparison of calcium sensitization and adrenoceptor stimulation

Introduction - Myocardial stunning is associated with a reduced external work (EW), efficiency of energy transfer (EET) and mechanical efficiency (ME). In this study we evaluated whether these energetic changes were a consequence of the decreased contractile function or a result of a specific underlying mechanism of stunning.

Methods - To that end, stunning was induced in 11 open-chest pigs by two cycles of 10 min of LADCA occlusion followed by 30 min of reperfusion. Preload and afterload changes were induced before and during stunning to construct regional stress-strain relationships, from which contractility (E_{cs} , $N \cdot m^{-2}$), EW at the working-point (EW_{wp} , $J \cdot \text{beat}^{-1} \cdot m^{-3}$), maximal EW (EW_{max}), EET at the working-point (EET_{wp} , %), and maximal EET (EET_{max}) were determined. MVO_2 ($J \cdot \text{beat}^{-1} \cdot m^{-3}$) was calculated from the difference of arterial and coronary venous oxygen content and LADCA flow. ME was determined as $EW/MVO_2 \cdot 100\%$. Dobutamine (0.5 , 1 and $2 \mu g \cdot kg^{-1} \cdot \text{min}^{-1}$), and EMD 57033 (0.05 , 0.1 , and $0.2 \text{ mg} \cdot kg^{-1} \cdot \text{min}^{-1}$) were given after the second stress-strain relationship was determined. Subsequently, stress-strain relationships were determined at each dose of each agent. To compare the effects of dobutamine and EMD 57033, changes in the different parameters were related to contractility using linear regression.

Results - Myocardial stunning decreased E_{cs} by 30%, EW_{wp} by 56%, EW_{max} by 63%, EET_{wp} by 34%, and EET_{max} by 33%. ME decreased by 55%, while MVO_2 was unaffected. EW_{wp} , EW_{max} , EET_{wp} , and EET_{max} were increased similarly with dobutamine and EMD 57033. In contrast, MVO_2 increased only after dobutamine. Consequently, ME increased linearly after raising contractility with EMD 57033, and remained constant with dobutamine.

Conclusions - Decrements of EW and EET in stunned myocardium are a mechanical response to the decrements in contractility. In contrast, decrements in ME respond differently to dobutamine and to EMD 57033 implying that this parameter reflects merely a disturbance related to the energy conversion of the stunned myofibril.

Serge A.I.P. Trines, Carlo A.G. Smits, Joost van der Moer, Cornelis J. Slager, Pieter D. Verdouw, and Rob Krams. Calcium sensitization, but not adrenoceptor stimulation, increases mechanical efficiency in stunned myocardium. *Submitted*

Introduction

In stunned myocardium, decrements in regional end-systolic elastance, a load-independent index of contractility, are accompanied by decrements in regional external work (EW) and by a shift in the partitioning of EW to total work, towards a reduced efficiency of energy transfer (EET) (7, 13). Furthermore, despite decreases in EW, myocardial oxygen consumption (MVO_2) remains relatively high, leading to a lowered mechanical efficiency (ME) (7).

In normal hearts, left ventricular EW and EET are not only dependent on contractility, but also on afterload (4). Therefore, we evaluated in an earlier study how and to what degree stunning affected the relationship between regional EW, EET and regional afterload. Indeed, it could be shown that stunning increased the afterload-dependency of regional EW and EET in stunned myocardium (23). Therefore, to adjust for afterload-dependency of EW and EET, we calculated the maxima of the EW- and EET-afterload relationships (EW_{max} , EET_{max}) as they are independent of afterload. In that study (23), a linear relationship between EW_{max} , EET_{max} and the degree of contractile dysfunction was suggested, implying that contractility is the main factor underlying these changes.

However, as stunning was the only factor influencing contractility in the previous study, it was impossible to separate the effect of contractility from the effect of a decreased calcium cycling or myofibrillar calcium sensitivity on EW_{max} and EET_{max} . In addition, while EW may depend largely upon contractile function, myocardial oxygen consumption (MVO_2) and therefore ME depend to a minor extent upon contractility (20). Based on these arguments it remains undecided whether the decreases in EW_{max} , EET_{max} , and ME of stunned myocardium are a mechanical response to the decreased contractility or are related to either decreases in calcium cycling or decreases in myofibrillar calcium sensitivity.

In the present study, we therefore tested whether the changes in EW_{max} , EET_{max} , and ME are related to the proposed underlying mechanism of myocardial stunning. To that end, we restored contractility in regional myocardial stunning by increasing calcium sensitivity with the calcium-sensitizer EMD 57033 and by increasing calcium cycling with dobutamine. If the observed changes in myocardial stunning are a mechanical response to the decreased contractility, both inotropic interventions will reverse the effects of stunning on EW_{max} , EET_{max} , and ME to a similar extent, but if the changes are specific for myocardial stunning, we expect a different response between EMD 57033 and dobutamine.

Methods

General

All experiments were performed in accordance with the "Guiding principles for the care and use of animals" as approved by the Council of the American Physiological Society and under the regulations of the Animal Care Committee of the Erasmus Medical Center Rotterdam.

Instrumentation

Crossbred Yorkshire-Landrace pigs ($n=11$) were anesthetized with 15-20 mg·kg⁻¹ sodium pentobarbital i.v., intubated and connected to a ventilator for intermittent positive pressure ventilation. Arterial oxygen content and blood gases were kept within the normal range. Fluid filled catheters were placed in the superior caval veins for continuous infusion of sodium pentobarbital (10-15 mg·kg⁻¹·h⁻¹), saline, dobutamine or the calcium sensitizer EMD 57033, and the administration of the specific negative chronotropic agent zatebradine. Depth of the anesthesia was continuously checked throughout the experiment by the absence of corneal reflexes and reaction to pain stimuli. Central aortic blood pressure was monitored via an 8 F catheter positioned in the thoracic descending aorta, while left ventricular pressure was obtained with a 7 F micromanometer-tipped catheter. A latex balloon mounted on a 7 F fluid-filled catheter was positioned in the inferior caval vein just above the diaphragm for transient reduction of LV preload. A latex Fogarty balloon mounted on a 7 F catheter was positioned in the ascending aorta for transiently increasing afterload of the left ventricle.

Following a midline sternotomy the heart was suspended in a pericardial cradle. An electromagnetic flow probe was placed around the ascending aorta for measurement of cardiac output. A small segment of the proximal part of the left anterior descending coronary artery (LADCA) was dissected free for placement of an electromagnetic flow probe (Skalar, Delft, The Netherlands) and an atraumatic clamp to occlude the LADCA. To obtain local coronary venous blood samples, a cannula was inserted into the great cardiac vein which drains specifically the LADCA perfusion area (3). Pacing leads were attached to the right atrial appendage and connected to a pacing stimulator (Grass S9, Quincy, Mass., USA). Rectal temperature was maintained between 37°C and 38°C throughout the experiment by heating the infused saline and applying external heating pads.

To measure regional myocardial area, two perpendicularly oriented pairs of ultrasound crystals (diameter 2.5 mm, 7.5 MHz, Triton Inc., USA) were implanted in the midmyocardium of the distribution area of the LADCA approximately at one-third of the distance from apex to base, each pair at 10 mm distance between the crystals. Similarly, two pairs of crystals were implanted in the midmyocardium of the distribution area of the

left circumflex coronary artery (LCXCA), approximately at half the distance from apex to base. To determine the diameter of the ventricle, one ultrasound crystal (diameter 6 mm; 5 MHz; Triton) was positioned in the midmyocardium of the anterior left ventricular wall, close to the LADCA segment length crystals, while another crystal was positioned in the midmyocardium of the posterior wall and directed to optimize signal quality. The midmyocardial position of the crystals was verified at the end of the experiment.

Drugs

Zatebradine (UL-FS 49) was a gift from Dr. J.W. Dämmgen (Dr. Karl Thomae, Boehringer Ingelheim KG, Biberach a/d Riss, Germany). Dobutamine was obtained from Dagra Pharma B.V., Diemen, The Netherlands and P. Schelling (E. Merck; Darmstadt, Germany) generously supplied EMD 57033.

Experimental protocol

After a 30-45 min stabilization period, heart rate was lowered below 70 beats·min⁻¹ by infusion of zatebradine and subsequently raised to 100 beats·min⁻¹ using an external pacemaker. Steady-state recordings of hemodynamic variables and regional myocardial function were recorded during a period of 10 respiratory cycles after which global arterial and regional myocardial venous blood samples were collected. Subsequently, the balloon located in the inferior caval vein was inflated over a period of 15 s to create a series of 20-25 beats resulting in a gradual reduction of left ventricular pressure (1). During the inflation of the balloon the respirator was switched off. After hemodynamic variables had resumed pre-inflation values, the balloon located in the ascending aorta was gradually inflated over a period of 10 s to create a series of 10-20 beats with a maximal increase in end-systolic left ventricular pressure of approximately 30-40 mmHg. The respirator was switched off during this procedure. The order of inflating the two balloons was randomized for each measurement.

Next, stunning was produced by two coronary LADCA occlusions of 10 min separated by 10 min of reperfusion. This model provides a stable degree of stunning for at least 6 hours (9). Thirty minutes after the second occlusion, the blood samples, the steady-state measurements and the balloon inflations as mentioned above were repeated.

Following this, dobutamine was infused intravenously at increasing rates of 0.5, 1, and 2 µg·kg⁻¹·min⁻¹, with a duration of 15 min per dose. Intravenous infusion was preferred above intracoronary infusion to minimize the effect of changes in interventricular interaction (8). After recovery of the hemodynamic variables, EMD 57033 was infused at increasing rates of 0.05, 0.1, and 0.2 mg·kg⁻¹·min⁻¹, each rate lasting 15 min. The order of drug infusion was not randomized as unpublished data of our department showed that contractility and work did not return to pre-infusion levels after 60 min of EMD 57033 washout. At the end of each experiment, methylene blue was

infused in the LADCA coronary artery and the myocardium perfused by the LADCA was dissected and weighed. In addition, also the myocardium enclosed by the segment crystals in both LADCA and LCXCA regions was dissected and weighed.

Data acquisition and analysis

All hemodynamic variables and regional segment length signals were digitized (sampling frequency 125 Hz per channel; 12 bits AD converter; Windaq, USA) and stored on disk for off-line analysis. Myocardial oxygen consumption of the LADCA perfusion area (MVO_2 , in $J \cdot \text{beat}^{-1} \cdot \text{m}^{-3}$) was calculated as the product of coronary blood flow and the difference in arterial and venous oxygen content divided by the heart rate and the mass of the LADCA perfusion area and converted to Joules ($1 \text{ ml } O_2 \equiv 20 \text{ J}$ (16)). Regional wall stress (σ , in $N \cdot \text{m}^{-2}$) and strain (ϵ , dimensionless) were calculated off-line as described before (23). End-systolic stress-strain relationships were determined from the combined pre- and afterload changes (Fig. 1). To determine the end-systolic points, a linear relationship was applied in which elastance was defined as $\sigma/(\epsilon - \epsilon_0)$, in which ϵ_0 is the strain at zero wall stress. End-systolic stress-strain points were determined for each heart beat at maximal elastance. The stress and strain at these points were defined as end-systolic stress (σ_{es}) and end-systolic strain.

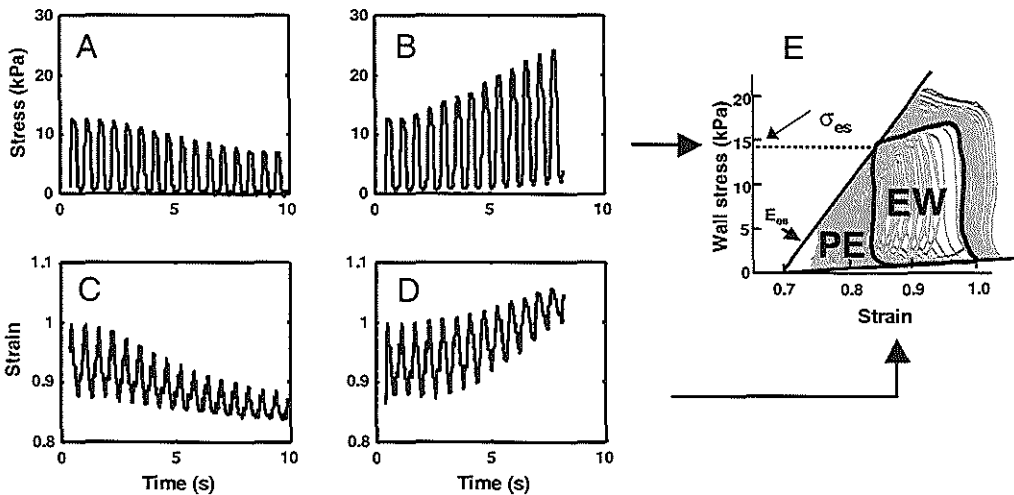


Fig. 1 Example of the determination of regional stress-strain relationships. Changes in loading conditions induce changes in regional wall stress (Fig. 1A and B) and regional myocardial strain (Fig. 1C and D). As myocardial strain is related to myocardial stress during the changes in loading conditions, regional stress-strain relationships may be evaluated (Fig. 1E). σ_{es} , end-systolic stress, E_{es} , end-systolic elastance, EW, external work, PE, Potential Energy.

As the end-systolic stress-strain relationship was often curvilinear, the end-systolic points were also fitted to a second order polynomial regression equation (13, 24). If the second order term was not significantly different from zero ($P \geq 0.05$), the linear equation was selected. The second order polynomial was selected if it was concave to the strain-axis. If it was convex to the strain-axis and the fitted curve did not intersect the strain-axis, the data were fitted to a third order polynomial. End-systolic elastance (E_{es} , in $N \cdot m^{-2}$) was used as an index of contractility (Fig. 1). As this slope is not constant for a second or third order polynomial, E_{es} was calculated as the local slope at a stress corresponding to a left ventricular end-systolic pressure of 70 mmHg at baseline. The area enclosed by the regional stress-strain loop during a single heart beat was determined as an index for regional myocardial external work (EW, in $J \cdot \text{beat}^{-1} \cdot m^{-3}$), normalized per unit of volume (Fig. 1) (10, 14, 25). Stress-strain area (SSA, in $J \cdot \text{beat}^{-1} \cdot m^{-3}$), the regional equivalent of the pressure-volume area, an index of total ventricular work, was calculated as the area enclosed by the end-systolic and end-diastolic relations and the systolic trajectory of stress-strain loop (13, 21). Potential energy (PE, in $J \cdot \text{beat}^{-1} \cdot m^{-3}$) was calculated by subtracting EW from SSA. The regional efficiency of energy transfer (EET, in %) was calculated as $(EW/SSA) \cdot 100\%$. The situation before pre- and afterload changes was called the working-point, and σ_{es} , SSA, EW, PE and EET at the working-point were called $\sigma_{es,wp}$, SSA_{wp} , EW_{wp} , PE_{wp} and EET_{wp} . Mechanical efficiency was calculated as $(EW_{wp}/MVO_2) \cdot 100\%$.

Subsequently for each animal, EW and EET were plotted against σ_{es} and maximal EW and EET (EW_{max} , EET_{max}) were determined (Fig. 2).

Statistics

To evaluate the effect of infusion of dobutamine and the effect of infusion of EMD 57033, two different one-way ANOVA for repeated measurements were performed followed by Dunnett's post-hoc tests for multiple comparisons. The effect of stunning was evaluated with a paired t-test. The effect of dobutamine and EMD 57033 on EW_{wp} , EW_{max} , EET_{wp} , EET_{max} , MVO_2 , and ME was evaluated by regression analyses on these variables for dobutamine and EMD 57033 separately with E_{es} as independent variable. As EMD 57033 increased E_{es} more than dobutamine did, the data-points in which EMD 57033 caused E_{es} to increase above the maximum E_{es} during dobutamine were excluded from the analyses. The animals were encoded using dummy variables (17). All data have been expressed as mean and standard error of the mean. P -values below 0.05 were considered significant. Only significant changes are mentioned in the Results-section, unless stated otherwise.

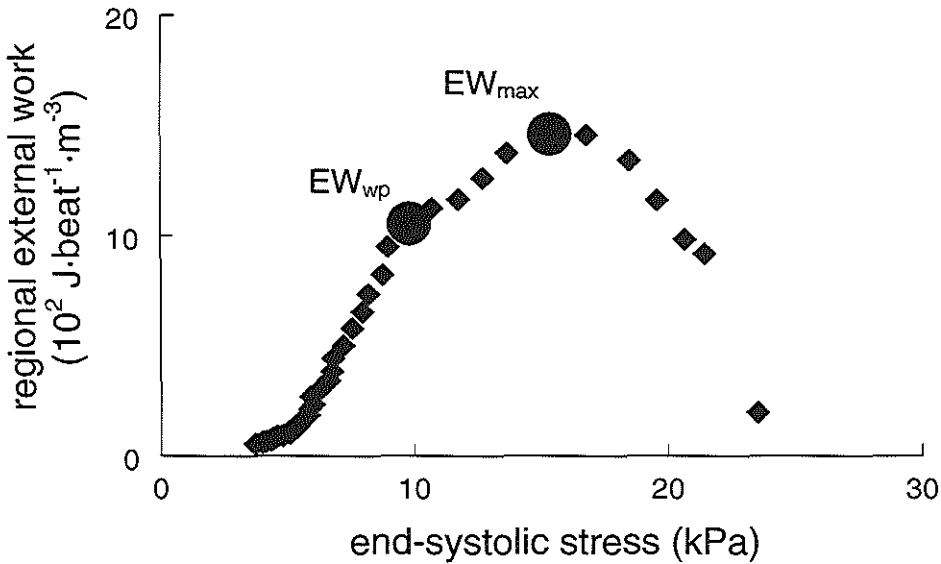


Fig. 2. Example of an $EW-\sigma_{es}$ relationship of the left anterior descending coronary artery (LADCA) perfusion area before stunning, showing external work at the working-point (EW_{wp}) and maximal EW (EW_{max}).

Results

Systemic hemodynamics (Table 1)

Myocardial stunning decreased mean arterial pressure by 12% and maximum rate of left ventricular pressure rise by 20%. This decrease in pressure was accompanied by a decrease in cardiac output of 25%. Consequently, systemic arterial resistance increased by 21% (Table 1). End-diastolic left ventricular pressure remained unchanged.

Infusion of dobutamine produced dose-dependent increments in maximum rate of left ventricular pressure rise (up to 157%) and consequently mean arterial pressure (12%) and cardiac output (25%).

After recovery from dobutamine, the subsequent infusion of EMD 57033 induced dose-dependent increments in maximum rate of left ventricular pressure rise (up to 70%) and decreases in systemic vascular resistance (18%). As a consequence of both changes, cardiac output increased (up to 21%), while end-diastolic left ventricular pressure remained unchanged.

Table 1. Systemic hemodynamics before and after LADCA stunning and during dobutamine and EMD 57033 infusion at 100 beats·min⁻¹ (n=11).

	Baseline	Stunning	Dobutamine ($\mu\text{g}\cdot\text{kg}^{-1}\cdot\text{min}^{-1}$) Δ from stunning			EMD 57033 ($\text{mg}\cdot\text{kg}^{-1}\cdot\text{min}^{-1}$) Δ from stunning		
			0.5	1	2	0.05	0.1	0.2
Mean arterial pressure (mmHg)	89±4	78±4*	5±3	10±3 [†]	9±2 [†]	6±4	8±3 [†]	-3±3
Maximum rate of left ventricular pressure rise (mmHg·s ⁻¹)	1440±80	1160±120*	370±100	830±130 [†]	1650±230 [†]	20±50	160±60	720±170 [†]
End-diastolic left ventricular pressure (mmHg)	10.5±1.2	12.0±1.2	-1.3±1.1	-1.0±0.6	-1.2±0.7	0.3±0.6	-0.5±0.8	-0.1±0.6
Cardiac output (l·min ⁻¹)	2.8±0.2	2.1±0.2 [†]	0.2±0.1	0.5±0.1 [†]	0.5±0.2 [†]	0.1±0.1	0.3±0.1	0.4±0.2 [†]
Systemic arterial resistance (mmHg·min·l ⁻¹)	33±3	40±3*	-1±2	-3±1	-2±4	3±2	-1±2	-7±2 [†]

Values are mean and standard error of the mean. * $P<0.05$ vs. baseline, [†] $P<0.05$ vs. stunning.

Regional contractile and energetic parameters

LADCA perfusion area (Table 2)

Induction of myocardial stunning decreased E_{es} by 30% and increased ϵ_0 by 13% (Table 2). Consequently, EW_{wp} decreased by 56%, while PE_{wp} remained unchanged. As a result, SSA_{wp} [= $\text{EW}_{\text{wp}} / (\text{EW}_{\text{wp}} + \text{PE}_{\text{wp}})$] decreased by 31% and EET_{wp} (= $\text{EW}_{\text{wp}} / \text{SSA}_{\text{wp}}$) decreased by 34%. Furthermore, EW_{max} decreased by 63%, while EET_{max} decreased by 33%. As EW_{wp} decreased and MVO_2 remained unchanged, ME decreased by 55%. $\sigma_{\text{es,wp}}$ remained unchanged.

Infusion of dobutamine increased E_{es} dose-dependently (up to 175%, Table 2). This was accompanied by dose-dependent increments in EW_{wp} (by 114%) and EW_{max} (161%), while PE tended to decrease. Again as a consequence, EET_{wp} (70%) and EET_{max} (68%) increased. Furthermore, because MVO_2 (37%) and EW both increased significantly, ME remained unchanged (Table 2). Although systemic vascular resistance (global afterload) was unaltered, $\sigma_{\text{es,wp}}$ (regional afterload) decreased slightly (by 10%). The other contractile and energetic parameters were not influenced by dobutamine.

Infusion of EMD 57033 raised E_{es} (up to 418%) and lowered ϵ_0 (up to 7%). Due to these inotropic changes, PE_{wp} decreased by 60% while EW_{max} (143%), EET_{wp} (109%), and EET_{max} (95%) increased and EW_{wp} tended to increase ($P=0.079$). In agreement with systemic vascular resistance, EMD 57033 decreased regional $\sigma_{\text{es,wp}}$ (up to 34%). As EMD

57033 did not affect MVO_2 while EW_{wp} tended to increase, ME increased significantly (by 89%). SSA was unaffected by EMD 57033.

Table 2. Regional contractile and energetic parameters of the LADCA region before and after LADCA stunning and during dobutamine and EMD 57033 infusion at 100 beats·min⁻¹ (n=11).

	Baseline	Stunning	Dobutamine ($\mu\text{g}\cdot\text{kg}^{-1}\cdot\text{min}^{-1}$)			EMD 57033 ($\text{mg}\cdot\text{kg}^{-1}\cdot\text{min}^{-1}$)		
			Δ from stunning			Δ from stunning		
			0.5	1	2	0.05	0.1	0.2
E_{cs} ($10^4 \text{ N}\cdot\text{m}^{-2}$)	12.2±1.4	8.5±1.2*	5.1±1.2	9.8±4.5*	13.1±5.0†	3.8±0.8	6.2±1.4	26.2±8.1†
ϵ_0	0.80±0.01	0.90±0.01*	-0.01±0.01	-0.02±0.01	-0.03±0.01†	-0.02±0.01	-0.04±0.02	-0.06±0.02†
$\sigma_{cs,wp}$ ($10^3 \text{ N}\cdot\text{m}^{-2}$)	13.5±2.2	15.1±2.7	-0.3±0.6	-0.9±0.7	-1.6±0.6†	-0.1±0.7	-1.1±0.5	-5.5±1.3†
SSA_{wp} ($10^2 \text{ J}\cdot\text{beat}^{-1}\cdot\text{m}^{-3}$)	19.6±4.1	13.5±3.3*	0.8±1.0	1.7±1.8	4.2±2.0	-0.5±1.3	1.5±1.6	-1.3±2.5
EW_{wp} ($10^2 \text{ J}\cdot\text{beat}^{-1}\cdot\text{m}^{-3}$)	13.2±2.2	5.8±1.3*	1.1±0.6	2.9±1.0	6.1±1.6†	0.3±1.3	3.4±1.3	4.4±2.7
EW_{max} ($10^2 \text{ J}\cdot\text{beat}^{-1}\cdot\text{m}^{-3}$)	16.9±3.5	6.3±1.4*	1.3±0.6	3.8±0.9†	9.1±1.8*	0.6±1.2	4.3±1.4	9.1±4.5†
PE_{wp} ($10^2 \text{ J}\cdot\text{beat}^{-1}\cdot\text{m}^{-3}$)	6.5±2.1	7.7±2.3	-0.3±0.7	-1.2±1.0	-1.9±0.9	-0.8±1.0	-1.9±0.7	-5.7±1.4†
EET_{wp} (%)	72.1±3.2	47.5±5.5*	8.0±3.4	16.7±5.3†	24.2±6.1†	7.7±6.7	20.6±4.7†	35.8±7.2†
EET_{max} (%)	77.5±1.9	52.2±6.2*	7.1±3.7	18.8±6.0†	26.9±6.3†	6.5±5.0	21.1±5.7†	34.0±6.9†
MVO_2 ($10^2 \text{ J}\cdot\text{beat}^{-1}\cdot\text{m}^{-3}$)	161±28	154±31	-10±10	18±12	51±16†	20±17	17±17	12±17
ME (%)	11±3	5±1*	2±1	2±1	4±2	1±1	3±2	5±3†

Values are mean and standard error of the mean. E_{cs} , end systolic elastance; ϵ_0 , strain at zero stress; $\sigma_{cs,wp}$, end-systolic stress at the working-point; SSA_{wp} , stress-strain area at the working-point; EW_{wp} , external work at the working-point; EW_{max} , maximal EW; PE_{wp} , potential energy at the working-point; EET_{wp} , efficiency of energy transfer at the working-point; EET_{max} , maximal EET; MVO_2 , myocardial oxygen consumption; ME, mechanical efficiency. * $P<0.05$ vs. baseline. † $P<0.05$ vs. stunning.

LCXCA perfusion area (Table 3)

Myocardial stunning did not change any of the contractile and energetic parameters of the LCXCA perfusion area, except ϵ_0 , which increased slightly (by 4%). Both infusion of dobutamine and infusion of EMD 57033 increased E_{cs} dose-dependently (up to 79% and 158%, Table 3). Furthermore, dobutamine increased EW_{wp} (up to 58%), EW_{max} (83%), EET_{wp} (26%), and EET_{max} (19%) while after EMD 57033, PE was decreased (up to 80%) and both EET_{wp} and EET_{max} were increased (by 37% and 33%, respectively), while EW_{wp} and EW_{max} remained unchanged. In accordance with systemic vascular resistance, EMD 57033 also decreased $\sigma_{cs,wp}$ (up to 26%). No other effects on the

contractile and energetic parameters of the LCXCA perfusion area for dobutamine and EMD 57033 were identified.

Table 3. Regional contractile and energetic parameters of the LCXCA region before and after LADCA stunning and during dobutamine and EMD 57033 infusion at 100 beats·min⁻¹ (n=11).

	Baseline	Stunning	Dobutamine ($\mu\text{g}\cdot\text{kg}^{-1}\cdot\text{min}^{-1}$) Δ from stunning			EMD 57033 ($\text{mg}\cdot\text{kg}^{-1}\cdot\text{min}^{-1}$) Δ from stunning		
			0.5	1	2	0.05	0.1	0.2
E_{cs} ($10^4 \text{ N}\cdot\text{m}^{-2}$)	12.2±1.4	15.0±2.3	1.5±0.9	4.8±2.8	9.7±2.8 [†]	-1.4±3.0	2.6±2.6	16.8±8.5 [†]
ϵ_0	0.82±0.02	0.85±0.02*	0.01±0.01	0.01±0.01	-0.01±0.01	0.01±0.01	0.01±0.01	0.01±0.01
$\sigma_{\text{cs,wp}}$ ($10^3 \text{ N}\cdot\text{m}^{-2}$)	12.5±1.8	11.9±1.8	0.2±0.4	-0.1±0.4	-0.2±0.3	0.4±0.7	-0.2±0.5	-3.1±0.6 [†]
SSA_{wp} ($10^2 \text{ J}\cdot\text{beat}^{-1}\cdot\text{m}^{-3}$)	15.9±2.4	12.8±2.2	0.2±1.0	1.2±1.4	2.7±1.6	-0.3±1.2	0.3±1.5	-3.6±1.9
EW_{wp} ($10^2 \text{ J}\cdot\text{beat}^{-1}\cdot\text{m}^{-3}$)	10.7±1.5	8.3±1.3	1.0±0.7	2.3±1.0	4.2±1.5 [†]	0.1±0.7	0.8±1.1	-0.1±1.7
EW_{max} ($10^2 \text{ J}\cdot\text{beat}^{-1}\cdot\text{m}^{-3}$)	12.7±1.7	9.6±1.4	1.7±0.7	3.8±1.0 [†]	7.2±1.4 [†]	0.3±0.9	2.7±0.9	2.2±2.4
PE_{wp} ($10^2 \text{ J}\cdot\text{beat}^{-1}\cdot\text{m}^{-3}$)	5.1±1.0	4.5±1.0	-0.8±0.4	2.4±2.2	1.8±1.7	-0.4±0.5	-0.6±0.9	-3.6±0.6 [†]
EET_{wp} (%)	68.8±1.7	65.5±2.4	7.0±1.8	12.4±6.2 [†]	15.6±5.8 [†]	1.6±2.6	3.8±6.0	23.4±1.6 [†]
EET_{max} (%)	72.7±2.0	73.4±3.9	6.3±2.2	11.3±4.1 [†]	12.4±5.8 [†]	2.5±2.8	4.4±5.7	22.8±2.4 [†]

Values are mean and standard error of the mean. E_{cs} , end systolic elastance; ϵ_0 , strain at zero stress; $\sigma_{\text{cs,wp}}$, end-systolic stress at the working-point; SSA_{wp} , stress-strain area at the working-point; EW_{wp} , external work at the working-point; EW_{max} , maximal EW; PE_{wp} , potential energy at the working-point; EET_{wp} , efficiency of energy transfer at the working-point; EET_{max} , maximal EET. * $P<0.05$ vs. baseline. [†] $P<0.05$ vs. stunning.

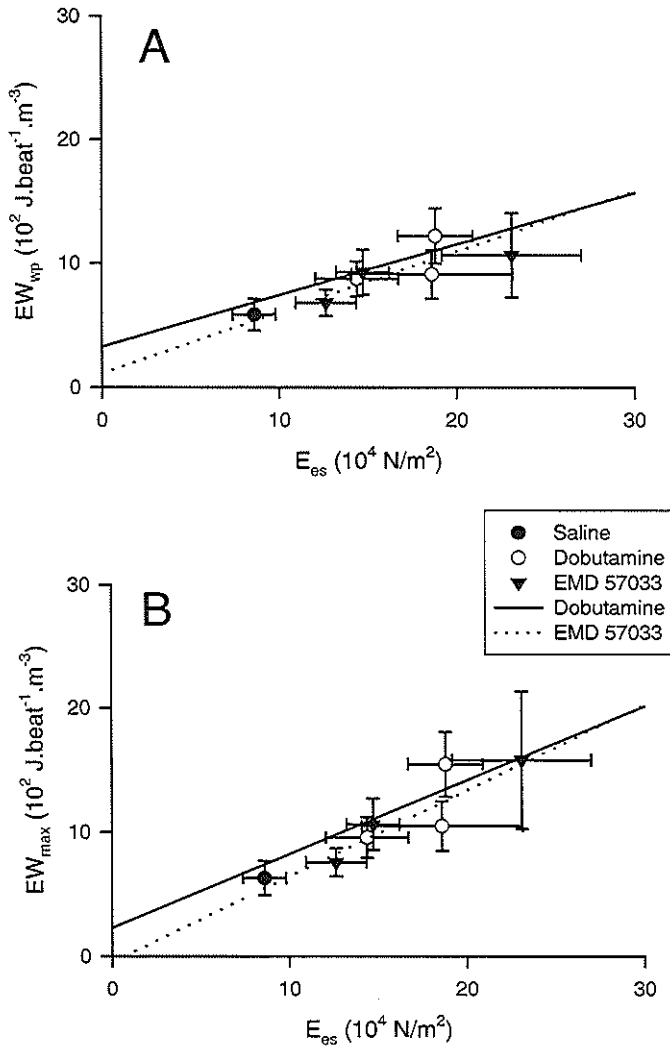


Fig 3. Relationship between E_{es} and EW_{wp} (A) and EW_{max} (B) for dobutamine and EMD 57033. Data for the plots were averaged per drug dose, while regression lines were calculated on the individual data. For regression equations see text.

Comparison between Dobutamine and EMD 57033 (Fig. 3-5)

In order to correct for the different inotropic range of both agents, all parameters of interest were related to contractility. The EW_{wp} - E_{es} relationship was similar for dobutamine ($EW_{wp} = 4.14 \cdot 10^{-3} \cdot E_{es} + 324, P < 0.001$) and EMD 57033 ($EW_{wp} = 4.92 \cdot 10^{-3} \cdot E_{es} + 111, P = 0.02$, Fig. 3A), when both responses were evaluated over the

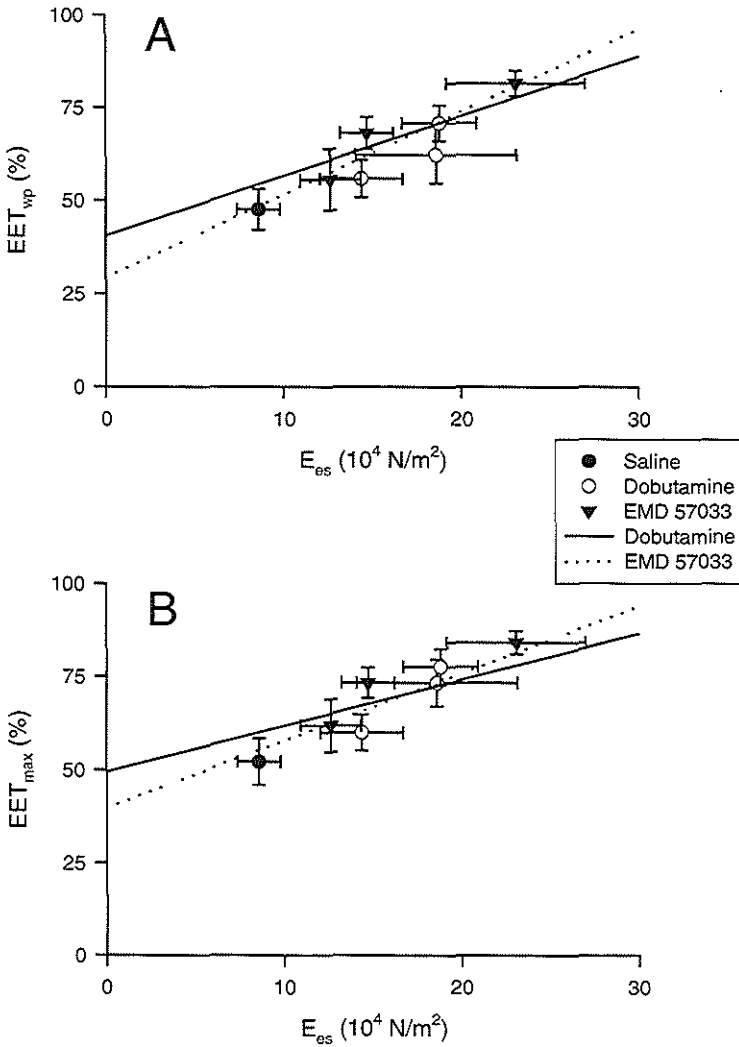


Fig 4. Relationship between E_{es} and EET_{wp} (A) and EET_{max} (B) for dobutamine and EMD 57033. Data for the plots were averaged per drug dose, while regression lines were calculated on the individual data. For regression equations see text.

same range of contractilities. This similarity could not be explained on basis of a balancing effect of inotropy and loading condition because the relationship between EW_{max} and E_{es} was also similar during dobutamine ($EW_{max} = 5.94 \cdot 10^{-3} \cdot E_{es} + 229$, $P < 0.01$) and EMD 57033 infusion ($EW_{max} = 6.91 \cdot 10^{-3} \cdot E_{es} - 47.9$, $P = 0.049$, Fig. 3B). Because PE_{wp} and PE_{max} responded in the same fashion as EW_{wp} and EW_{max} (data not shown), EET_{wp}

and EET_{max} displayed similar relationships for dobutamine ($EET_{wp} = 1.61 \cdot 10^{-4} \cdot E_{cs} + 40.5$ and $EET_{max} = 1.24 \cdot 10^{-4} \cdot E_{cs} + 49.5$, both $P < 0.01$) and EMD 57033 ($EET_{wp} = 2.23 \cdot 10^{-4} \cdot E_{cs} + 29.2$ and $EET_{max} = 1.80 \cdot 10^{-4} \cdot E_{cs} + 39.8$, $P = 0.02$ and $P < 0.01$, respectively, Fig. 4).

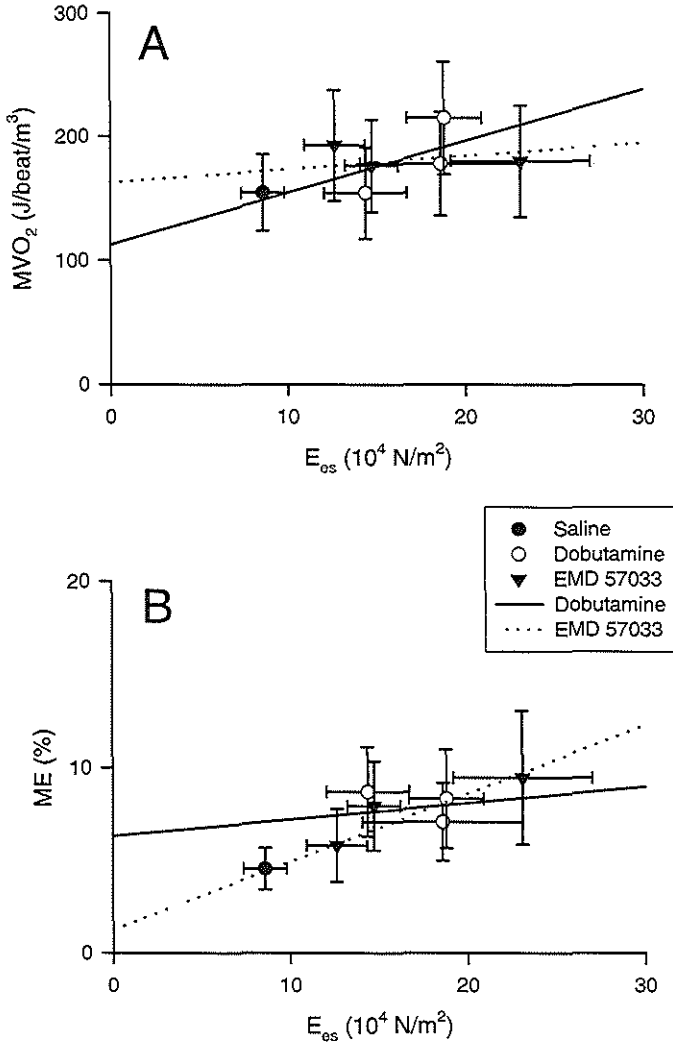


Fig 5. Relationship between E_{cs} and MVO_2 (A) and ME (B) for dobutamine and EMD 57033. Data for the plots were averaged per drug dose, while regression lines were calculated on the individual data. For regression equations see text.

In contrast, MVO_2 did not increase when contractility was increased with EMD 57033 ($MVO_2 = 1.08 \cdot 10^{-2} \cdot E_{cs} + 16.3 \cdot 10^3$, $P=0.61$), while it increased during dobutamine ($MVO_2 = 4.21 \cdot 10^{-2} \cdot E_{cs} + 11.2 \cdot 10^3$, $P<0.01$, Fig. 5A). Consequently, because EW_{wp} behaved similarly after both interventions, ME (i.e. EW_{wp}/MVO_2) increased after increasing contractility with EMD 57033 ($ME = 3.67 \cdot 10^{-5} \cdot E_{cs} + 1.25$ $P<0.01$) but was not affected by dobutamine ($ME = 8.85 \cdot 10^{-6} \cdot E_{cs} + 6.32$, $P=0.29$, Fig. 5B).

Discussion

In the present analysis, we evaluated whether the decreases in EW, EET, and ME in myocardial stunning were related to a specific underlying mechanism of stunning or just a mechanical consequence of the decrease in contractility. We specifically studied EW, EET, and ME as it has been shown that these parameters play a significant role in the process of oxygen wastage in myocardial stunning (7, 13, 22) and because these parameters become very sensitive to changes in afterload at low levels of contractility (7, 23). As expected, both increasing calcium cycling with dobutamine and increasing calcium sensitivity with EMD 57033 restored regional contractility and work in stunned myocardium. Despite the fact that both agents induced similar effects on the mechanical parameters EW_{wp} , EW_{max} , EET_{wp} , and EET_{max} , dobutamine increased MVO_2 , while EMD 57033 did not affect MVO_2 . Consequently, ME was only improved by EMD 57033. The present data suggest that the decreases in EW and EET are a consequence of the decrements in regional contractility rather than the result of a specific underlying mechanism. However, the decrements in ME found during stunning may be related to the underlying mechanism.

Dobutamine and EMD 57033 have been studied before in stunned myocardium, applying more load-dependent indices of contractility and work (5, 13, 15). However, as both agents exert peripheral vascular effects, the degree of recruitment of contractile function by these agents may have been affected by the load-dependency of the applied parameters. In the present study a load-independent index of contractility and an afterload-independent index of work were used and therefore the direct inotropic effect of both drugs could be compared. It could be shown that both agents exerted a clear dose-response of contractility and of the energetic parameters EW_{max} and EET_{max} . Furthermore, the responses of EW_{max} and EET_{max} , when studied over a similar range of contractilities, were similar for both agents. The latter observation may indicate that the decreases in EW and EET in stunned myocardium are not related to calcium cycling or myofibrillar calcium sensitivity, but merely a mechanical consequence of the decreased contractility.

Stunned myocardium displays relatively high oxygen consumption ('oxygen wastage'). The underlying mechanism is presently unknown, but a favorable effect of calcium sensitizing agents has been reported (11, 18, 22), suggesting that the inefficiency was located in the myofibrils. The present study confirms and extends these studies by

showing that the increase in ME is related to the increments in contractility for EMD 57033, but not for dobutamine. Furthermore, because the decrease in EW was merely a mechanical response to the decreased contractility, the different response of ME is solely due to differences in MVO_2 . As dobutamine mainly increases calcium cycling, while EMD 57033 predominantly affects myofibrillar calcium sensitization, the present data are in accordance with a decreased ME of stunned myocardium which is mainly located in the myofibrils.

Limitations

In the present study dobutamine and EMD 57033 were used to increase calcium cycling and myofibrillar calcium sensitivity, respectively. Although we did not measure calcium cycling and myofibrillar calcium sensitivity directly, it has been shown that EMD 57033 acts primarily on the myofibrils (12). We have earlier evaluated the putative phosphodiesterase inhibiting properties of EMD 57033 in the same dose range as used in the present study (5, 19). Based on the results of those studies, we may conclude that in the present study we have evaluated primarily the calcium sensitizing properties of EMD 57033 (2). While it is known that dobutamine also affects the myofibrils (6), it predominantly increases calcium cycling. Moreover, dobutamine decreases rather than increases myofibrillar calcium sensitivity.

Conclusions

In this study we showed that the stunning-induced decreases in external work and efficiency of energy transfer are merely a consequence of the decrease in myocardial contractility. On the other hand, the decreased ME of stunned myocardium is only increased after calcium sensitization, which strongly suggests that in stunned myocardium there is an energetic disturbance, which is located in the myofibrils.

References

1. **Aversano, T., W. L. Maughan, W. C. Hunter, D. Kass, and L. C. Becker.** End-systolic measures of regional ventricular performance. *Circulation* 73: 938-950, 1986.
2. **Bezstarosti, K., L. K. Soei, R. Krams, F. J. Ten Cate, P. D. Verdouw, and J. M. Lamers.** The effect of a thiadiazinone derived Ca^{2+} sensitizer on the responsiveness of Mg^{2+} -ATPase to Ca^{2+} in myofibrils isolated from stunned and nonstunned porcine and human myocardium. *Biochem Pharmacol* 51: 1211-1220, 1996.
3. **Bier, J., B. Sharaf, and H. Gewirtz.** Origin of anterior interventricular vein blood in domestic swine. *Am J Physiol* 260: H1732-1736, 1991.
4. **De Tombe, P. P., S. Jones, D. Burkhoff, W. C. Hunter, and D. A. Kass.** Ventricular stroke work and efficiency both remain nearly optimal despite altered vascular loading. *Am J Physiol* 264: H1817-1824, 1993.
5. **de Zeeuw, S., S. A. Trines, R. Krams, P. D. Verdouw, and D. J. Duncker.** Cardiovascular profile of the calcium sensitizer EMD 57033 in open-chest anaesthetized pigs with regionally stunned myocardium. *Br J Pharmacol* 129: 1413-1422, 2000.

6. Endoh, M., and J. R. Blinks. Actions of sympathomimetic amines on the Ca²⁺ transients and contractions of rabbit myocardium: reciprocal changes in myofibrillar responsiveness to Ca²⁺ mediated through alpha- and beta-adrenoceptors. *Circ Res* 62: 247-265, 1988.
7. Fan, D., L. K. Soei, L. M. Sassen, R. Krams, and P. D. Verdouw. Mechanical efficiency of stunned myocardium is modulated by increased afterload dependency. *Cardiovasc Res* 29: 428-437, 1995.
8. Fan, D., L. K. Soei, R. Stubenitsky, E. Boersma, D. J. Duncker, P. D. Verdouw, and R. Krams. Contribution of asynchrony and nonuniformity to mechanical interaction in normal and stunned myocardium. *Am J Physiol* 273: H2146-2154, 1997.
9. Frass, O., H. S. Sharma, R. Knoll, D. J. Duncker, E. O. McFalls, P. D. Verdouw, and W. Schaper. Enhanced gene expression of calcium regulatory proteins in stunned porcine myocardium. *Cardiovasc Res* 27: 2037-2043, 1993.
10. Goto, Y., H. Suga, O. Yamada, Y. Igarashi, M. Saito, and K. Hiramori. Left ventricular regional work from wall tension-area loop in canine heart. *Am J Physiol* 250: H151-158, 1986.
11. Grandis, D. J., P. J. DelNido, and A. P. Koretsky. Functional and energetic effects of the inotropic agents EMD-57033 and BAPTA on the isolated rat heart. *Am J Physiol* 269: C472-479, 1995.
12. Gross, T., I. Lues, and J. Daut. A new cardiotoxic drug reduces the energy cost of active tension in cardiac muscle. *J Mol Cell Cardiol* 25: 239-244, 1993.
13. Krams, R., D. J. Duncker, E. O. McFalls, A. Hogendoorn, and P. D. Verdouw. Dobutamine restores the reduced efficiency of energy transfer from total mechanical work to external mechanical work in stunned porcine myocardium. *Cardiovasc Res* 27: 740-747, 1993.
14. Morris, J. J. r., G. L. Pellom, C. E. Murphy, D. R. Salter, J. P. Goldstein, and A. S. Wechsler. Quantification of the contractile response to injury: assessment of the work-length relationship in the intact heart. *Circulation* 76: 717-727, 1987.
15. Nozawa, T., Y. Yasumura, S. Futaki, N. Tanaka, M. Uenishi, and H. Suga. Efficiency of energy transfer from pressure-volume area to external mechanical work increases with contractile state and decreases with afterload in the left ventricle of the anesthetized closed-chest dog. *Circulation* 77: 1116-1124, 1988.
16. Sagawa, K., L. Maughan, H. Suga, and K. Sunagawa. Energetics of the heart. In: *Cardiac contraction and the pressure-volume relationship*. New York: Oxford University Press, 1988, p. 171-231.
17. Slinker, B. K., and S. A. Glantz. Missing data in two-way analysis of variance. *Am J Physiol* 258: R291-297, 1990.
18. Soei, L. K., L. M. Sassen, D. S. Fan, T. van Veen, R. Krams, and P. D. Verdouw. Myofibrillar Ca²⁺ sensitization predominantly enhances function and mechanical efficiency of stunned myocardium. *Circulation* 90: 959-969, 1994.
19. Stubenitsky, R., R. W. van der Weerd, D. B. Haitzma, P. D. Verdouw, and D. J. Duncker. Cardiovascular effects of the novel Ca²⁺-sensitizer EMD 57033 in pigs at rest and during treadmill exercise. *Br J Pharmacol* 122: 1257-1270, 1997.
20. Suga, H. Ventricular energetics. *Physiol Rev* 70: 247-277, 1990.
21. Suga, H., R. Hisano, S. Hirata, T. Hayashi, O. Yamada, and I. Ninomiya. Heart rate-independent energetics and systolic pressure-volume area in dog heart. *Am J Physiol* 244: H206-214, 1983.
22. Sunderdiak, U., B. Korbmayer, E. Gams, and J. D. Schipke. Myocardial efficiency in stunned myocardium. Comparison of Ca(2+)-sensitization and PDE III-inhibition on energy consumption. *Eur J Cardiothorac Surg* 18: 83-89, 2000.
23. Trines, S. A., C. J. Slager, J. van der Moer, P. D. Verdouw, and R. Krams. Efficiency of energy transfer, but not external work, is maximized in stunned myocardium. *Am J Physiol Heart Circ Physiol* 279: H1264-1273, 2000.
24. van der Velde, E. T., D. Burkhoff, P. Steendijk, J. Karsdon, K. Sagawa, and J. Baan. Nonlinearity and load sensitivity of end-systolic pressure-volume relation of canine left ventricle in vivo. *Circulation* 83: 315-327, 1991.
25. Vinten-Johansen, J., P. A. Gayheart, W. E. Johnston, J. S. Julian, and A. R. Cordell. Regional function, blood flow, and oxygen utilization relations in repetitively occluded-reperfused canine myocardium. *Am J Physiol* 261: H538-547, 1991.

Chapter 9

Geometry assessment of the left ventricle

Introduction - Regional wall stress is an important parameter in the prognosis of heart failure. In order to assess regional wall stress using echocardiography, a method has to be available to reconstruct the left ventricular inner and outer surfaces from a set of echo images and to calculate local values for the principal radii and wall thickness.

Methods - We describe a method to reconstruct the ventricular inner and outer surfaces from a set of ultrasound images, to subdivide this reconstruction in a standardized way in 10 sections and to calculate the principal radii and wall thickness. By simulating all measurements involved to derive these parameters on a realistic 3D model of a left ventricle, including the generation of 3D-ultrasound acquisition, the accuracy of this method was evaluated.

Results - The standard error of the estimate (SEE) for the regression between model and reconstruction of the 10 regional sections was found to be 0.50 mm for wall thickness and 0.34 mm for the combined principal radii.

Conclusions - We conclude that the described algorithm provides a quick and accurate way to assess the regional geometry and thereby wall stress.

J.A. Oomen, S.A.I.P. Trines, C.A.G. Smits, W.B. Vermeulen, R. Krams, and C.J. Slager. Geometry assessment of the Left Ventricle from 3D Ultrasound Images to Estimate Regional Wall Stress. *Submitted*

Introduction

Regional left ventricular wall stress is an important parameter in the prognosis of heart failure (3, 6, 7). Over the years, many techniques have been employed to assess this wall stress, either directly, using strain gauges on the ventricular wall (1, 4, 5) or by calculating the stress indirectly using a spherical model (10), or approximating the complete ventricle by an ellipsoid (9). However, while the first method using strain gauges is very invasive, the last two methods only produce an estimate of the global or average wall stress and are therefore of limited use if one is interested in regional variations in wall stress.

In order to assess wall stress locally we may use Laplace's equation $\sigma = P / (h \cdot (\kappa_1 + \kappa_2))$. Therefore, we have to compute or measure ventricular pressure (P), local wall thickness (h) and the sum of the local principal curvatures ($\kappa_1 + \kappa_2$). It is possible to compute the local wall thickness and principal curvatures if a true 3D reconstruction of the left ventricle is available and presently it is possible to achieve such a reconstruction through recently introduced ultrasound techniques, as well as by EBT or MRI. Although the imaging resolution of 3D ultrasound is less than that of the other modalities, ultrasound offers the possibility of imaging at the bedside, which will be an important prerequisite for a number of applications, e.g. post infarction studies.

In this paper we will describe: i) a method suitable for the reconstruction of the 3D surfaces of a left ventricle from a set of ultrasound images, acquired with an axially rotating echo probe, ii) methods for subdividing the ventricle in well-defined regional segments, and iii) the estimation of wall thickness and principal curvatures for those segments. Using a virtual 3D left ventricular reference model the method will be described and an estimate will be given of the accuracy of the parameters required for the wall stress estimation.

Methods

Constructing a virtual reference model

As a first step to test our methods, a virtual left ventricular reference was constructed as a description in VRML (Virtual Reality Modeling Language) of a real porcine heart. In order to build such a description, a pig heart was prepared by cutting the aortic valve open and fixating the heart with 4% formaldehyde under an aortic as well as left ventricular pressure of 100 mmHg. Two superficial cuts, running from base to apex, were carved in the epicardium to provide marks for later reconstruction and matching purposes. The left ventricle was cut in 4 millimeter thick slices, with the slices oriented parallel to the base plane.

Following this procedure, digital photographs were taken from both sides of each slice. Using these photographs, the epicardium and endocardium were subsequently traced using a custom-built program, developed in Delphi (Borland, Scotts Valley, California). Applying a MatLab[®] (The MathWorks Inc., Natick, Ma, USA) script, these tracings were subsequently combined to achieve a VRML representation of the left ventricle, henceforth called the 'reference model'. This reference model was used as the standard against which the reconstruction method and wall stress algorithms were tested. To allow a comparison between the reference model and the later-described 3D ultrasound reconstructed geometry, a thin artificial rod, running parallel to the XZ-plane, was added to the model, thus defining its circumferential orientation.

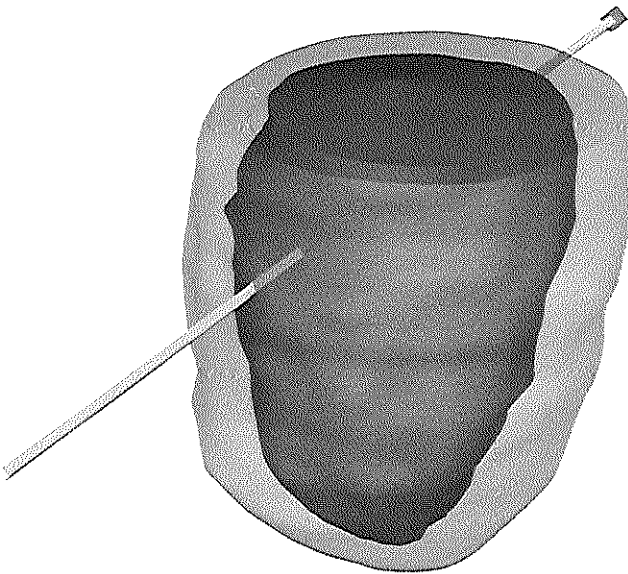


Fig. 1 A rendering of the virtual reference model, constructed from photographs of slices of a porcine heart.

Scanning the reference model

3D Studio Max[®] (Autodesk Inc) was used to make a surface rendering of the reference model, as shown in Fig. 1. Artificial echo images were constructed in the following way: the model, together with the rod, was tilted along two axes, to obtain a realistic position and orientation for the simulated ultrasound probe which was thought to be located at the Y-axis of the 3D Max coordinate system. Subsequently, using a Boolean intersection (3D Studio Max) of the reference model with a very thin slice, a cut-through of the model was acquired, which represented the ideal ultrasound cross sectional image

as would have been acquired with an ultrasound probe (Fig. 2). To acquire the subsequent images, as generated by the virtual rotating scanner, the slice was rotated around the Y-axis with increments of 6 degrees. In this way rotating over a total angle of 180 degrees, the reference model was scanned producing a total of 30 virtual ultrasound images (Fig. 3).

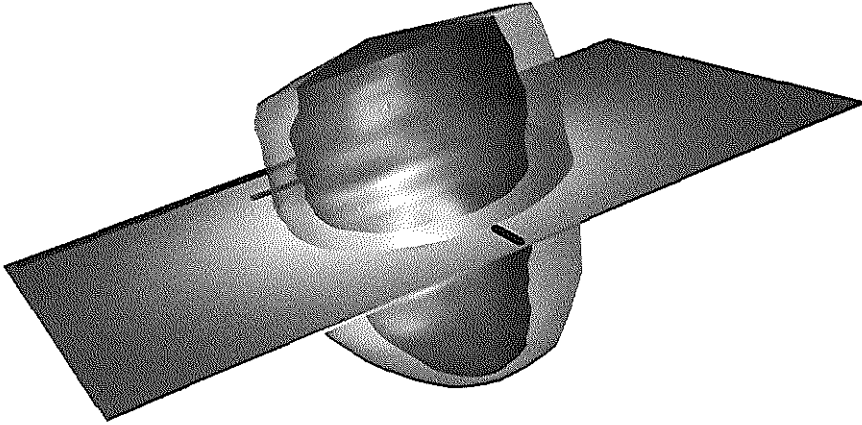


Fig. 2 Cutting the model by a thin slice to obtain virtual ultrasound images.

3D reconstruction from the ultrasound images

One of the virtual ultrasound images as rendered in 3D Max, is shown in Fig. 3. The intersection of the cut-plane with the reference model is clearly visible. For calibration purposes a horizontal line (top) was generated which corresponded to a length of 100 mm. The small vertical line (bottom) indicates the rotation axis of the ultrasound plane. A small dot marks the point where the cut plane intersects the artificial rod, thus enabling further algorithms to create a 3D reconstruction of the rod and thus to obtain the orientation of the ventricle in 3D space.

A complete set of these pictures was traced using a custom-built tracing program, which delivered tracings for each scan plane, representing points on the endocardial (S_1) and the epicardial (S_2) surface and a set of points along the rod. No tracing was performed in the region of the valvular plane, thus leaving the base open. Using the known acquisition angle of rotation for each scan plane, these tracings were combined into a 3D representation of the epicardium and the endocardium by applying the suitable rotation

matrix, using an algorithm written in MatLab[®]. This resulted in a surface mesh for endocardium and another for the epicardium (Fig. 4, left, only epicardial mesh visible).

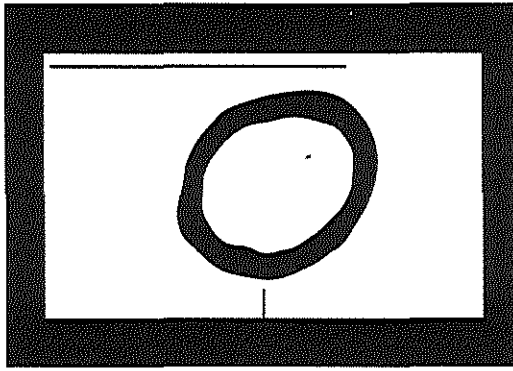


Fig. 3 Virtual ultrasound image acquired in 3D Studio Max.

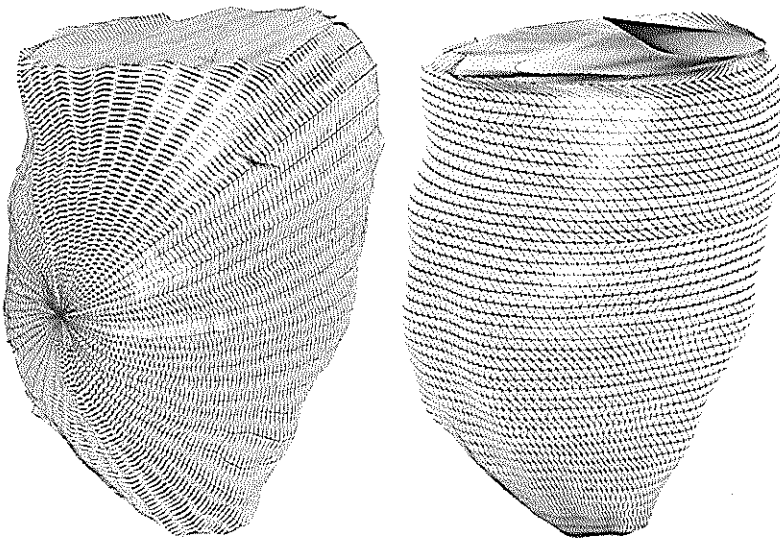


Fig. 4 The original mesh of S2 defined by the scan planes (left) and the same surface resampled in 70 horizontal planes (right).

The valvular base was defined by the end points of the open-ended contours, which we called ‘contour base points’. The base midpoint was defined as the point halfway between the maximum and minimum x, y and z-value of the set of contour base points.

Subsequently, the apex was defined as the endocardial point with the largest 3D distance to the base midpoint. The line connecting the apex with the midpoint of the base (i.e. the long axis) was aligned with the Z-axis, through rotation of the meshes defining the endocardium, epicardium and the rod. The orientation of the rod, derived from the known set of points, was used to rotate these meshes around the Z-axis in such a way that the XY-projection of the rod was parallel to the X-axis, thus obtaining a standard position in 3D space.

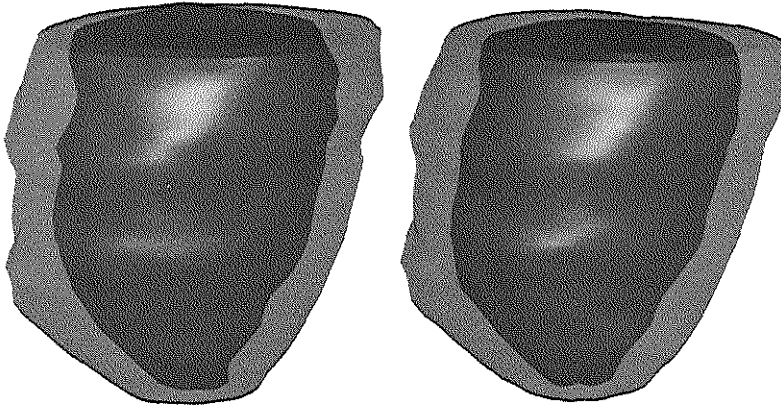


Fig. 5 The reference model (left) compared to the echo reconstructed model (right).

Because the ultrasound-originating surface meshes were based on the sequentially generated echo planes, these meshes became oblique (left in Fig. 4). Each surface mesh was therefore resampled at 70 equidistant planes parallel to the XY-plane, to construct a mesh more amenable to further subdivision in local ventricular regions. This resampling was done for the S_1 and S_2 surfaces separately, by dividing the ventricular long axis in 70 equidistant sections and defining perpendicular planes for each section. At each plane all points were determined where one of the edges of the model crossed this plane. The set of points thus found was converted into polar coordinates and transformed into a Fourier description. Restricting the number of Fourier components to 12 and transforming back to the polar coordinates resulted in circumferential filtering of the transversal contours and redistribution of all vertices into equal angular orientations. The surface mesh for endocardium and epicardium reconstructed from the virtual echo images compared well to the mesh of the reference model (Fig. 5).

Because this method caused the endocardial contour (S_1) and the epicardial contour (S_2) to be resampled at the same number of planes (70) and with the same number of vertices in each plane (120), corresponding points of the endocardium could be easily paired with points on the epicardium. Subsequently, a midmyocardial surface (S_m) could be defined as the collection of points midway between each of the pairs of endocardial and epicardial points.

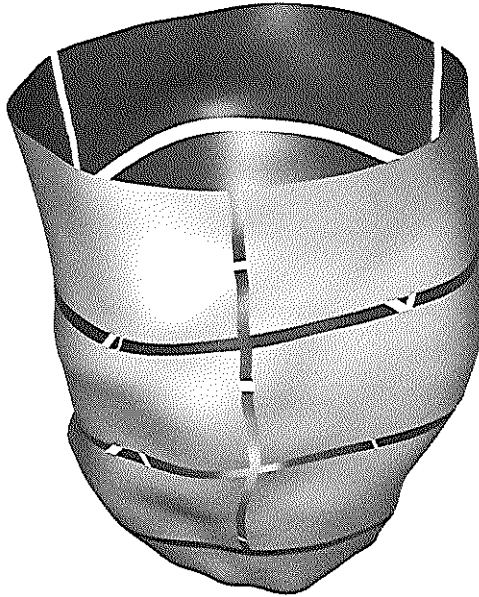


Fig. 6 The surface S_1 divided into 10 local regions.

Regions of interest

The surfaces S_1 and S_2 were each divided into 10 regions in the following manner. The complete surface was divided in 70 equidistant cross-sections oriented perpendicularly to the Z-axis. The apical region encompassed 10 sections while each of the other three regions encompassed 20 sections.

The apical sections contained all vertices from the first 10 apical planes (Fig. 6). The next 3 regions were each divided in 3 segments. Each segment spanned a 120 degree angle around the long axis. Since S_1 and S_2 were divided in the same manner, this resulted in the same number of paired vertices in the regions of S_1 and S_2 . Therefore the midmyocardial surface S_m was also divided in the same manner, because each midmyocardial region consisted of the set of vertices, which were located midway between the paired vertices from S_1 and S_2 .

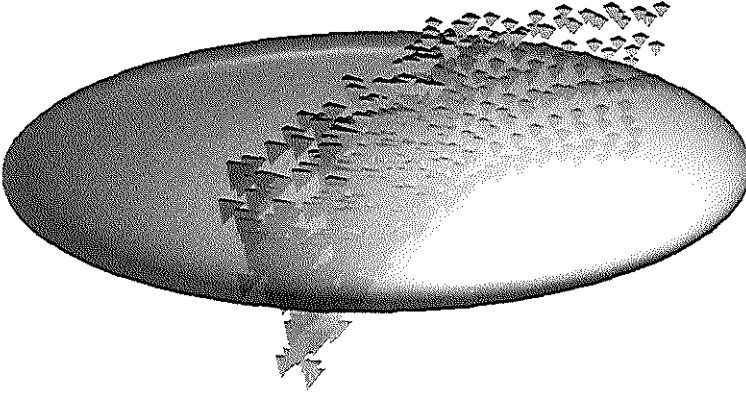


Fig. 7 Inadequate ellipsoid fit to points of a local region as a result of solving the quadric form

Ellipsoid Fitting

The principal curvatures for a local section were determined by fitting an ellipsoid to the corresponding midmyocardial surface and computing the principal radii of this ellipsoid at the point to be defined as the center of the local section. As each of the segments of S_m contained several hundred points, it seemed straightforward to compute the ellipsoid through these points by using the quadric form for the ellipsoid and solving the overdetermined system of linear equations given by:

$$\sum_{i=1}^N A \cdot (x_i^2 + y_i^2) + B \cdot z_i^2 + C \cdot x_i + D \cdot y_i + E \cdot z_i = 1 \quad \{1\}$$

for A, B, C, D and E, substituting x_i , y_i , z_i with all points of the segment under consideration. However, this approach did not necessarily lead to the correct estimate for the ellipsoid, as is demonstrated in Fig. 7. As all points of the ellipsoid's surface were considered candidates for the fitting process, this procedure can lead to an ellipsoid that has most of its surface, rather than only a part of one side, encompassed by the cloud of points.

So instead of solving the overdetermined set of equations {1}, we used an optimization method provided in MatLab which uses a simplex minimization algorithm to

arrive at an ellipsoid which achieves a minimum sum of algebraic distances between each of the S_m surface points and the ellipsoid surface. Because such a method is very sensitive to the initial conditions, in other words is prone to settle for a solution at an incorrect local minimum, it was important to start with a suitable first guess. The algorithm to arrive at a first estimate for the ellipsoid was adapted from the algorithm for ellipse fitting described by Fitzgibbon et al. (2). The ellipsoid to be found is expressed by the equation:

$$a \cdot (x^2 + y^2) + b \cdot z^2 + c \cdot x + d \cdot y + e \cdot z + f = 0 \tag{2}$$

which can be expressed in vector form as:

$$F = (\bar{\mathbf{a}}, \bar{\mathbf{x}}) \tag{3}$$

With $\bar{\mathbf{a}} = [a, b, c, d, e, f]$ and $\bar{\mathbf{x}} = [(x^2 + y^2), z^2, x, y, z]^T$

Our problem is then to find a minimization for {3} by a suitable choice for the vector π , given a suitable constraint on π . This minimum can be found by solving the rank-deficient eigenvalue problem:

$$D^T D \mathbf{a} = S \mathbf{a} = \lambda C \mathbf{a} \tag{4}$$

Where \mathbf{D} is called the design matrix constructed from the known 3D points of the regional surface, $\mathbf{S} = \mathbf{D}^T \mathbf{D}$ is called the scatter matrix, \mathbf{a} is the vector of polynomial coefficients to be estimated, and \mathbf{C} is the matrix that expresses the constraints.

Expression {2} has some freedom in the choice of a, b, c, d, e, and f. For instance they can all be normalized by setting f = 1. Following Fitzgibbon et al. (2) we used the normalization $-4ab = 0$, causing the constraint matrix C to be given by:

$$C = \begin{bmatrix} 0 & -2 & 0 & 0 & 0 & 0 \\ -2 & 0 & 0 & 0 & 0 & 0 \\ 0 & 0 & 0 & 0 & 0 & 0 \\ 0 & 0 & 0 & 0 & 0 & 0 \\ 0 & 0 & 0 & 0 & 0 & 0 \\ 0 & 0 & 0 & 0 & 0 & 0 \end{bmatrix} \tag{5}$$

First the design matrix $D = [(x+y)^2, z^2, x, y, z, 1]^T$ is computed, using the known x,y,z-values of all points of the region of the ventricle under consideration. The vector \mathbf{a} is given by the (as yet unknown) values [a b c d e f]. Now, using the standard MatLab function, the eigenvectors and eigenvalues for $S \mathbf{a} = \lambda C \mathbf{a}$ are computed and the eigenvector corresponding to the negative eigenvalue corresponds to the first estimate for [a b c d e f]. Hereafter the estimate is used as starting value for a simplex optimization procedure,

which is used to compute the final result. The error function, to be used with this optimization is given by:

$$E(R_1, R_2, X_0, Y_0, Z_0) = \sqrt{(R_1^2 + R_2^2)} \cdot \sum_N^{i=1} \sqrt{\left(\frac{(x_i - X_0)^2 + (y_i - Y_0)^2}{R_1^2} + \frac{(z_i - Z_0)^2}{R_2^2} - 1 \right)^2} / N \quad \{6\}$$

where R_1 and R_2 are the major and minor radii of the ellipsoid and X_0 , Y_0 and Z_0 are the coordinates of the center of the ellipsoid.

Note the first factor, where R_1 and R_2 are the major and minor axis of the ellipsoid. Without this factor the result of the cost function E is dimensionless and expresses the relative algebraic distances between the ellipsoid surface and each of the points to be fitted. Adding this factor turns the result of the cost function into an absolute distance, thereby disadvantaging ellipsoids with very large dimensions. This turned out to be beneficial because it prevented the ellipsoid from iterating in some cases to a paraboloid solution that did not converge.

Principal curvatures

The center of each midmyocardial region was defined as the point $M(X_m, Y_m, Z_m)$ where X_m , Y_m and Z_m are the mean values of respectively the X , Y and Z coordinates of the set of vertices defining the local region. We assumed that any midmyocardial region can be described as part of the surface of an ellipsoid. The coordinate system is now translated in such a way that the center of the ellipsoid is at the origin and the ellipsoid can now be described with spherical parameters:

$$\begin{aligned} X &= a \cdot \cos(\alpha) \cdot \cos(\beta) \\ Y &= a \cdot \cos(\alpha) \cdot \sin(\beta) \\ Z &= b \cdot \sin(\alpha) \end{aligned} \quad \{7\}$$

The point Q is now chosen as a point on the surface of the ellipsoid close to M . For any Q on the ellipsoid the curve of intersection of a plane containing the normal to the surface at Q and the surface itself has a curvature κ , which changes when the plane is rotated about the normal. Following Euler the direction for which the curvature is maximal is orthogonal to the direction where the curvature is minimal (8). The maximum and minimum curvatures at Q are henceforth called the principal curvatures. The principal curvatures in a point Q on an ellipsoid can be derived from the general formulas given in reference (8):

$$\kappa_{\min} = \frac{b}{a \cdot \sqrt{T}} \quad \text{and} \quad \kappa_{\max} = \frac{a \cdot b}{T^{3/2}} \quad \{8\}$$

with $T=a^2 \cdot \sin^2(\alpha)+b^2 \cdot \cos^2(\alpha)$.

Because the ellipsoid is a solid of revolution around the vertical Z-axis, all points with equal values of the Z-coordinate have the same curvature, and the principal curvatures in any point depend only on the angle α and not on β .

Wall thickness computation

To derive the average wall thickness of the segment S_m , we computed the volume between S_1 and S_2 and divided this volume by the surface area of S_m . The volume was calculated using the following approach. As described before, each of the surfaces is defined by resampled points on this surface. As the points on a surface define a mesh of bordering triangles, the sum of the areas of these triangles was taken as the area of the surface segment. Because the points on S_1 and S_2 were paired, each point on S_1 corresponded to a point on S_2 . These points could be connected to form prisms. The summed volume of these prisms, divided by the summed surface area of the corresponding triangles from S_m , was taken as the thickness of the segment.

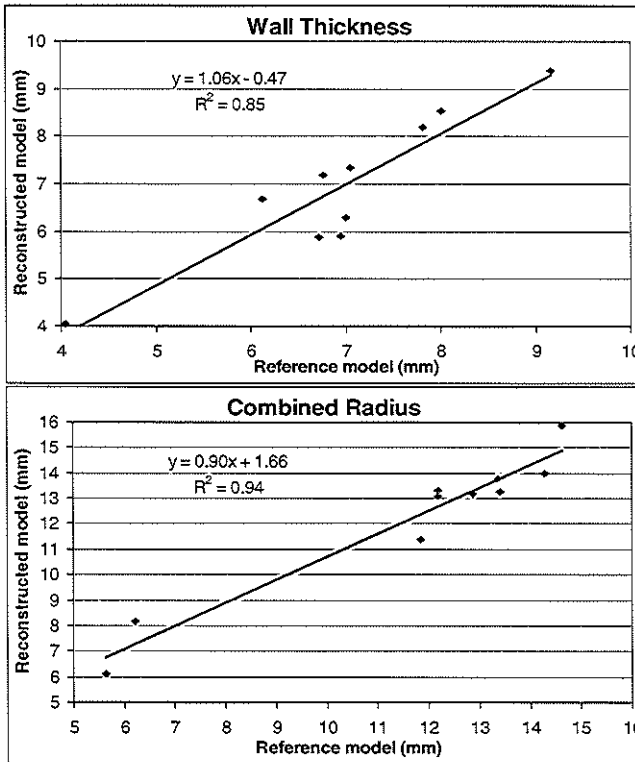


Fig. 8 Radius and wall thickness estimation for 10 local regions for the echo-reconstructed model, compared to the same estimation for the original VRML model.

Results

In order to check the validity of our algorithm it was applied to a mathematically constructed surface of two concentric spheres. These spheres, representing endocardium and epicardium were given a radius of 60 and 70 mm respectively, resulting in a midmyocardial radius of 65 mm. Summing the curvatures results in a combined radius of 32.5 mm. The wall thickness found when the algorithm was applied to these surfaces was 10 ± 0.19 mm and the (combined) radii were found to be 32.5 ± 4.10^{-4} (mean \pm SD).

The computations described above were applied to the reference model as well as to the 3D reconstructed echocardiographic model. The principal curvatures were summed and converted to radii, because a millimeter figure is easier to comprehend than a 1/millimeter curvature. Fig. 8 shows the relationship between the computed radius and wall thickness of the virtual model and the radius and wall thickness of the reconstructed echo model, computed by the same algorithm. The standard error of the estimate (SEE) for the radius was found to be 0.34 mm and the SEE for the wall thickness was 0.50 mm.

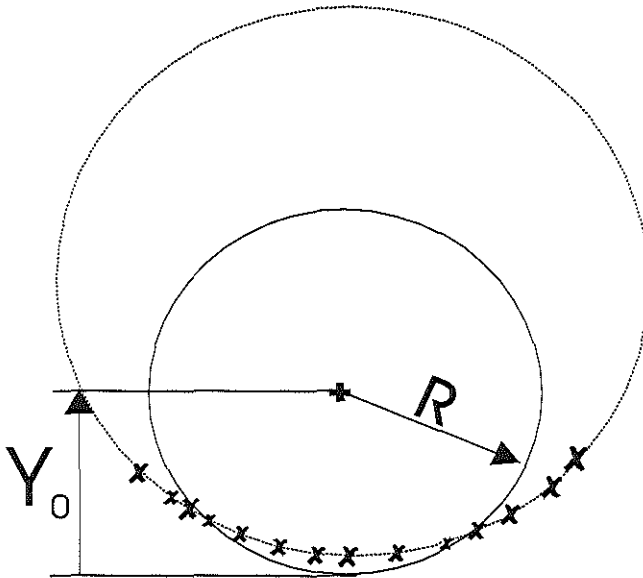


Fig. 9 Fitting a circle through a set of points.

Discussion

The results indicate that a useful estimate of regional principal radii can be found using the proposed algorithm. It is also found that the estimation of wall thickness is less accurate than the combined radius estimation. The absolute error for the radius has about the same magnitude ($SEE=0.34$ mm) as the absolute error for the wall thickness ($SEE=0.50$ mm), but because the radii are often much larger than the wall thickness, the relative error for the combined radius is less, resulting in a better correlation. We suppose that most of the error is due to the inaccuracy of defining the long axis and the subsequent procedure of reorientation and subdivision of the ventricle in regions. Mismatch in the orientation of the reference model and the reconstructed echo model leads to differences in the location of the local regions. Therefore, the local regions compared in our investigations are slightly different in size and location, resulting in the errors found.

The ellipsoid through the 3D points that define a local region of the midmyocardial wall is first estimated by solving expression {4}. However, the solution thus found is not the optimal one, because it tends to be biased towards low eccentricity. This is a favorable trait, because it avoids hyperbolic solutions. As a consequence however, further optimization by an iterative method is needed after this first estimate is found. The cost function {8}, used for this optimization, possesses some particular features that have to be taken into account, which can easily be demonstrated in the case of a circle (Fig. 9). The points shown in Fig. 9 fit on the dotted circle. The solid circle represents the present estimate. However, if the optimization starts at the solid circle, changing only the radius (R) or only the height (Y_0), will raise the value of the cost function as can be seen by inspection of Fig. 9. However, changing the value of Y_0 and R simultaneously in the right direction will slightly lower the value of the cost function E . This means that the partial derivatives $\delta E/\delta R$, $\delta E/\delta Y_0$ are very large and positive, while $\delta E^2/(\delta Y_0 \delta R)$ is small and negative. Consequently, if the method depends on the computation of partial derivatives, the matrix containing these derivatives will become ill-conditioned, due to the very high positive values for terms like $\delta E/\delta R$ and very small negative for terms like $\delta E^2/(\delta Y_0 \delta R)$. Therefore a simplex method was used for the optimization, which avoids the use of derivatives.

Conclusions

If the left ventricular pressure is known, knowledge of the regional wall thickness and regional curvature suffice to calculate the regional wall stress. The method described in this paper uses ellipsoid fitting to arrive at a realistic number for the local curvature and the ratio of local wall volume to local wall surface area as an estimate for local wall

thickness. It is shown that this method, in conjunction with a reconstruction algorithm for ultrasound images from a rotating echo probe, will deliver useful results.

References

1. **Burns, J. W., J. W. Covell, R. Myers, and J. Ross, Jr.** Comparison of directly measured left ventricular wall stress and stress calculated from geometric reference figures. *Circ Res* 28: 611-621., 1971.
2. **Fitzgibbon, A., M. Pilu, and R. B. Fisher.** Direct Least Square Fitting of Ellipses. *IEEE T Pattern Anal* 21: 476-480, 1999.
3. **Hara, Y., M. Hamada, and K. Hiwada.** Left ventricular end-systolic wall stress is a potent prognostic variable in patients with dilated cardiomyopathy. *Jpn Circ J* 63: 196-200., 1999.
4. **Hefner, L. L., L. T. Sheffield, G. C. Cobbs, and W. Klip.** Relation Between Mural Force and Pressure in the Left Ventricle of the Dog. *Circ Res* 11: 654-663. 1962.
5. **Huisman, R. M., G. Elzinga, N. Westerhof, and P. Sipkema.** Measurement of left ventricular wall stress. *Cardiovasc Res* 14: 142-153., 1980.
6. **James, M. A., T. J. MacConnell, and J. V. Jones.** Is ventricular wall stress rather than left ventricular hypertrophy an important contributory factor to sudden cardiac death? *Clin Cardiol* 18: 61-65., 1995.
7. **Percy, R. F., A. B. Miller, and D. A. Conetta.** Usefulness of left ventricular wall stress at rest and after exercise for outcome prediction in asymptomatic aortic regurgitation. *Am Heart J* 125: 151-155., 1993.
8. **Rogers, D. F., and J. A. Adams.** Ruled and developed surfaces. In: *Mathematical Elements for Computer Graphics* (2nd ed.). New York: McGraw-Hill, Inc., 1990, p. 417-422.
9. **Sandler, H., and H. T. Dodge.** Left Ventricular Tension and Stress in Man. *Circ Res* 13: 91-104, 1963.
10. **Woods, R. H.** A few applications for a physical theory to membranes in the human body in a state of tension. *J Anat Physiol* 26: 326-370. 1892.

Chapter 10

Discussion and Summary

Myocardial stunning is defined as the prolonged decrease in myocardial function after a single or multiple brief periods of ischemia, followed by complete reperfusion. This decreased function occurs in the absence of necrosis, and is totally reversible. The myocardium exhibits contractile reserve, i.e. it can be stimulated by inotropic drugs, or postextrasystolic potentiation. Although necrosis is absent, myocardial enzymes are released, signifying the reversible myocardial damage. In this thesis, we studied aspects of the underlying mechanism by evaluating in vivo parameters of calcium cycling in open-chest swine (chapter 2 and 3), we investigated changes in energetics and efficiencies (chapter 4 and 5), we studied the pharmacological modulation of stunning (chapter 6, 7, and 8), and we developed a new method for the calculation of regional left ventricular wall stress (chapter 9).

Calcium cycling in stunned myocardium (chapter 2 and 3)

In these chapters we concentrated on changes in calcium cycling as a possible cause for myocardial stunning. In the past, calcium transients were found to be unchanged in stunned hearts, but these transients were measured at heart rates far below the physiological heart rates for these species (10, 18). Since calcium transients, and therefore myocardial force, increase with increasing heart rate, the so-called “force-frequency effect” (FFE) (30, 34), possible stunning-induced decreases in calcium transients may have been masked by the low heart rate. In chapter 2 we studied the effect of stunning on the FFE in vivo (determined as the slope of end-systolic elastance, E_{es} , over heart rate), as this has never been studied before with the use of load-independent parameters. In addition, because of the recently proposed key role of the sarcoplasmic reticulum calcium ATPase (SERCA2)-phospholamban interaction in the FFE (21), we also modulated this interaction with dobutamine before and after stunning. We showed that myocardial stunning abolished the FFE in vivo. In addition, although dobutamine enhanced the FFE in stunned myocardium, the effect was significantly reduced compared to before stunning. In addition, a quantitative analysis of the literature on changes in sarcoplasmic reticulum (SR) Ca^{2+} -uptake showed a negative relationship between changes in Ca^{2+} -uptake and heart rate, again implying that SR function of stunned myocardium is

disturbed at higher heart rates. Therefore, we concluded that our findings suggest that calcium cycling is disturbed heart-rate dependently in stunned myocardium.

In chapter 3 we studied the FFE of stunned myocardium in more detail. Although we stated in the previous chapter that the absence of the FFE could be ascribed to a disturbed calcium cycling, a decreased myofibrillar calcium sensitivity could still contribute to this absence. Therefore, we studied whether the calcium sensitizer EMD 57033 was able to restore the FFE. To distinguish between disturbances in sarcolemmal (SL) Ca^{2+} fluxes and processes located in the interior of the cell, i.e. Ca^{2+} -induced Ca^{2+} -release (CICR), or SR Ca^{2+} -ATPase (SERCA2) function, we also investigated recirculation fraction (RF), a measure of the relative contribution of internal calcium cycling to total calcium cycling (14, 30, 34). To investigate a possible heart-rate dependent inhibition of SERCA2 function, we measured SR Ca^{2+} -uptake and phospholamban phosphorylation at Ser¹⁶ and Thr¹⁷ of the stunned and non-stunned myocardium in vitro, in samples taken from both the stunned (LADCA) and non-stunned (LCXCA) region at two different heart rates. Finally, we infused ryanodine, which specifically opens the SR Ca^{2+} -release channel (ryanodine receptor, RyR), as it has been suggested that the opening probability of the RyR may have decreased in stunning (33). As expected, we found that stunning abolished the FFE. Although EMD 57033 increased E_{cs} , the slope over heart rate (i.e. the FFE) was unaffected, both in normal and stunned myocardium, suggesting that the absence of the FFE is caused by a disturbance in calcium cycling and not by a decrease in myofibrillar calcium sensitivity. In addition, the RF was decreased heart rate-dependently, with the largest decrease at the highest heart rate, signifying a heart rate-dependent disturbance of CICR and/or SERCA2 function. However, neither stunning nor heart rate had an effect on SR Ca^{2+} -uptake or Ser¹⁶ and Thr¹⁷-phosphorylation of phospholamban in vitro. Additionally, in normal myocardium ryanodine mimicked the stunning-induced decrease in RF, suggesting an increased rather than a decreased opening-probability of the RyR. In contrast, ryanodine had no effect on the FFE of normal myocardium. Therefore, we concluded that a second disturbance in CICR, in addition to a possibly increased opening of the RyR, may underly the absence of the FFE in stunning.

Maximization of external work and efficiency of energy transfer (chapter 4)

In the past, several studies have addressed the relationship between power, external work (EW), or efficiency of energy transfer (EET = external work/total work·100%) and afterload in normal hearts and have found a maximization of power and EW (22, 32), but not of EET (6). In addition, as impairment of global left ventricular function causes the ventricle to deviate from the optimal situation (15, 23), it has been shown that myocardial stunning decreases both regional EW and EET (17, 35), and that both EW and EET were more sensitive to increasing afterload (9). In this chapter we studied therefore the

relationships of EW and EET in relation to regional afterload (end-systolic stress, σ_{es}). We showed that in normal myocardium both EET and EW displayed a maximum in relation to afterload, which is partially in accordance with findings in the global left ventricle. Additionally, the myocardium operated at maximal EET rather than at maximal EW. Therefore, additional EW could be recruited by increasing regional afterload. In stunned myocardium, this recruitment had disappeared, without affecting the maximization of EET. In addition, both EW and EET became more sensitive to changes in regional afterload. Finally, we showed a positive relationship between both maximal EW and EET and contractility (E_{cs}), suggesting that the stunning-induced changes in these parameters were caused by the decreased contractility of stunned myocardium.

Oxygen wastage of stunned myocardium (chapter 5)

As mentioned in the Introduction, stunned myocardium displays decreased contractile function in combination with an unchanged oxygen consumption (oxygen wastage). Although this oxygen wastage has been ascribed to a decreased efficiency of excitation-contraction coupling (increased oxygen cost of contractility) (24), VO_2 for excitation-contraction coupling comprises only 20-30% of total MVO_2 (26). It seems therefore possible that myofibrillar efficiency is decreased as well. In this chapter we studied both myofibrillar efficiency and oxygen cost of contractility in normal and in stunned myocardium, the latter also in the presence of the calcium sensitizer EMD 60263, because calcium sensitizers are known to decrease oxygen cost of contractility (19, 25) and may even increase myofibrillar efficiency (31). We showed that the stunning-induced oxygen wastage was mainly caused by a decreased myofibrillar efficiency and to a minor extent by an increased oxygen cost of contractility. Additionally, EMD 60263 reversed both these effects, suggesting that this drug increases myofibrillar calcium sensitivity without increasing myofibrillar cross-bridge cycling.

Pharmacological modulation of myocardial stunning (chapter 6, 7, and 8)

If stunning affects a large region of the left ventricle, cardiac function will be impaired to a level that inotropic therapy is needed. As discussed above, calcium sensitizers may have energetic advantages above β -adrenergic drugs as they do not increase calcium cycling. Because an adverse effect may be the impairment of diastolic function (8, 16), we studied in chapter 6 whether EMD 57033 exhibited negative lusitropic effects *in vivo*. In addition, we tested whether this drug had different effects on normal and on stunned myocardium. We showed that *in vivo* the calcium sensitizer EMD 57033 restored systolic function (E_{cs}) in stunned myocardium, while neither regional early diastolic function (as measured by the maximum rate of decay of elastance and the time constant of the decay), nor late diastolic function (as measured by end-diastolic elastance) were impaired. These effects were all similar in normal and in stunned

myocardium. Moreover, neither the phosphodiesterase III inhibiting properties of EMD 57033, nor adrenergic receptor stimulation contributed minimally to these actions, as α - and β -blockade had a minor influence. Therefore, we concluded that calcium sensitizers are promising candidates for complementing the current inotropic arsenal and that calcium sensitization does not cause a mandatory impairment of diastolic function.

As *in vitro* evidence is available that the sensitivity for calcium of the myofibrils is decreased in stunned myocardium (5, 10), and that calcium sensitizing drugs can increase this sensitivity again (3, 8), we studied in chapter 7 the *in vivo* responsiveness of normal and stunned myocardium to intracoronary calcium in the absence and presence of the calcium sensitizer EMD 57033. To minimize the phosphodiesterase III inhibiting properties of EMD 57033, we applied β -blockade by infusing propranolol. In normal myocardium, intracoronary calcium increased contractility (E_{es}), while in stunned myocardium this responsiveness had disappeared. Propranolol had no additional effect, but EMD 57033 restored the responsiveness to intracoronary calcium in stunned myocardium and enhanced the responsiveness in normal myocardium. Therefore, we concluded that these results are consistent with the *in vitro* findings that EMD 57033 increases myofibrillar calcium sensitivity, independent of its minor phosphodiesterase III inhibiting properties.

In chapter 4 and in earlier studies we showed that stunning decreases EW, EET, and mechanical efficiency (ME) (17). It remained unclear, however, whether these changes are secondary to the decreased contractility or that they are primarily caused by a specific underlying mechanism of stunning. In addition, since calcium sensitizers may exhibit energetic advantages above standard inotropic therapy (chapter 5), we compared in chapter 8 the effects of the calcium sensitizer EMD 57033 and dobutamine on the myocardial energetic parameters EW, EET and ME. To normalize for dose-dependent effects of these drugs, we studied the effect on the energetic parameters in relation to the effect on contractility (E_{es}). Both drugs restored EW and EET similarly, suggesting that the stunning-induced changes in these parameters are due to the decreased contractility and not to a specific underlying mechanism of stunning, as they were not preferentially influenced by either calcium sensitization or increasing calcium cycling. In contrast, the decreased ME was only restored by calcium sensitization, suggesting an energetic disturbance located in the myofibrils.

Geometry assessment of the left ventricle to estimate regional wall stress (chapter 9)

In the final chapter we introduced a new method to calculate regional myocardial wall stress from 3D ultrasound. This method was developed to overcome the limitations of our current method to calculate regional wall stress: the highly invasive nature of ultrasound crystals and the assumption of regional spherical geometry. We constructed algorithms for the reconstruction of 3D ventricular endocardial and epicardial surfaces

from 2D images as acquired by a rotating echo probe. These surfaces were divided in 10 sections and from each section wall thickness was assessed. Furthermore, a midplane was constructed between these surfaces from which the principal radii were calculated for each section. The radii and wall thickness were calculated for a left ventricular phantom and for a 3D reconstruction from virtual 2D images derived from this phantom. Comparison of these radii and wall thicknesses showed a good agreement between the two methods, signifying the accuracy of this method for the calculation of regional wall stress.

Suggestions for future research

The precise localization of the disturbance in excitation-contraction coupling in stunning is still not fully elucidated, especially *in vivo*. Measurement of calcium transients in stunned myocardium *in vivo* may aid in isolation of myofibrillar disturbances from disturbances in calcium cycling. The most widely used calcium indicators are chemical fluorescent probes because their signal is quite large for a given change in intracellular calcium (29). However, the possible pitfall in measuring calcium transients *in vivo* using these probes is the assessment of pathlength and 3D sample volume, since it is unclear to what depth the reflection of emitted light can still be detected. However, using ratiometric probes (the calcium concentration is dependent on the ratio of two wavelengths for excitation or emission) overcomes this problem as both the numerator and the denominator of the ratio are equally influenced (29). Nonetheless, the practical problem of excitation and measurement of the dye-loaded myocardium of a moving heart, and the possible difference between the epicardial myocardium (which will usually be measured) and the endocardial myocardium, remain to be solved. Using indicators with a high and indicators with a low affinity for calcium, cytosolic calcium and SR calcium can both be measured. Consequently, changes in calcium transients, SR calcium content and myofibrillar calcium sensitivity may be detected in stunned myocardium *in vivo*. Additionally, the effect of calcium sensitizing drugs on calcium transients and calcium sensitivity *in vivo* can possibly be assessed.

If further research discloses the specific localization of the disturbance in excitation-contraction coupling, drugs may be developed to reverse such a disturbance. If our suggestion of an increased opening of the RyR is correct, drugs that partially close this channel could have a beneficial effect. If sarcolemmal calcium cycling is affected, drugs could be produced that increase calcium-induced calcium release. It should be kept in mind, however, that stimulation of SR calcium cycling is preferred above stimulation of sarcolemmal calcium cycling, as the latter consumes the double amount of ATP per mol of calcium compared to the former (2).

Since increasing evidence is available that calcium sensitizers have energetic advantages above β -adrenergic drugs and may also be less arrhythmogenic due to the lack

of increases in systolic calcium, clinical research should be aimed at the therapeutic advantages and safety of calcium sensitizers. Although some clinical research has already been performed in patients with severe heart failure (28), especially the feasibility of application outside the hospital should be investigated, as the therapeutic arsenal for outpatient (oral) inotropic therapy is currently very limited.

If indeed myocardial stunning occurs repetitively following exercise in patients with stable angina pectoris (1), more research should be conducted to find out whether and when this repetitive stunning may lead to myocardial hibernation or cause irreversible damage to the myocardium. If irreversible damage does occur in patients who would otherwise not be candidates for revascularization therapy based on their clinical symptoms, early revascularization therapy could to some degree prevent irreversible decrements in left ventricular function.

The method we described to assess regional left ventricular wall stress from 3D echocardiography should first be validated *in vivo*. If this method appears to be accurate enough, measurement of regional end-systolic wall stress can aid the prognosis in a range of heart diseases, e.g. dilated cardiomyopathy (13) or aortic regurgitation (27). As wall stress is highly load-dependent, the next step will be to combine the stress measurements with the assessment of regional myocardial strain. Apart from strain measurements in magnetic resonance imaging, regional strain can also be derived from ultrasound, using the cross-correlation ("elastography") method or the velocity gradient ("tissue Doppler") method (7). The combination of stress and strain measurements at different loading conditions will enable the non-invasive investigation of regional end-systolic elastance (E_{es}), a load-independent parameter of contractility. Although some clinical studies have applied this parameter (4, 11, 12, 20), the clinical relevance of E_{es} in diagnosis, prognosis and the evaluation of therapy has for a large part still to be elucidated.

References

1. Ambrosio, G., S. Betocchi, L. Pace, M. A. Losi, P. Perrone-Filardi, A. Soricelli, F. Piscione, J. Taube, F. Squame, M. Salvatore, J. L. Weiss, and M. Chiariello. Prolonged impairment of regional contractile function after resolution of exercise-induced angina. Evidence of myocardial stunning in patients with coronary artery disease. *Circulation* 94: 2455-2464., 1996.
2. Barry, W. H., and J. H. Bridge. Intracellular calcium homeostasis in cardiac myocytes. *Circulation* 87: 1806-1815., 1993.
3. Bezstarosti, K., L. K. Soei, R. Krams, F. J. Ten Cate, P. D. Verdouw, and J. M. Lamers. The effect of a thiadiazinone derived Ca^{2+} sensitizer on the responsiveness of Mg^{2+} -ATPase to Ca^{2+} in myofibrils isolated from stunned and nonstunned porcine and human myocardium. *Biochem Pharmacol* 51: 1211-1220, 1996.
4. Brown, K. A., and R. V. Ditchey. Human right ventricular end-systolic pressure-volume relation defined by maximal elastance. *Circulation* 78: 81-91., 1988.
5. Carrozza, J. P., Jr., L. A. Bentivegna, C. P. Williams, R. E. Kuntz, W. Grossman, and J. P. Morgan. Decreased myofilament responsiveness in myocardial stunning follows transient calcium overload during ischemia and reperfusion. *Circ Res* 71: 1334-1340, 1992.

6. De Tombe, P. P., S. Jones, D. Burkhoff, W. C. Hunter, and D. A. Kass. Ventricular stroke work and efficiency both remain nearly optimal despite altered vascular loading. *Am J Physiol* 264: H1817-1824, 1993.
7. D'hooge, J., A. Heimdal, F. Jamal, T. Kukulski, B. Bijnens, F. Rademakers, L. Hatle, P. Suetens, and G. R. Sutherland. Regional Strain and Strain Rate Measurements by Cardiac Ultrasound: Principles, Implementation and Limitations. *Eur J Echocardiography* 1: 154-170, 2000.
8. Endoh, M. Changes in intracellular Ca^{2+} mobilization and Ca^{2+} sensitization as mechanisms of action of physiological interventions and inotropic agents in intact myocardial cells. *Jpn Heart J* 39: 1-44, 1998.
9. Fan, D., L. K. Soei, L. M. Sassen, R. Krams, and P. D. Verdouw. Mechanical efficiency of stunned myocardium is modulated by increased afterload dependency. *Cardiovasc Res* 29: 428-437, 1995.
10. Gao, W. D., D. Atar, P. H. Backx, and E. Marban. Relationship between intracellular calcium and contractile force in stunned myocardium. Direct evidence for decreased myofilament Ca^{2+} responsiveness and altered diastolic function in intact ventricular muscle. *Circ Res* 76: 1036-1048, 1995.
11. Goresan, J., A. M. Feldman, R. L. Kormos, W. A. Mandarino, A. J. Demetris, and R. J. Batista. Heterogeneous immediate effects of partial left ventriculectomy on cardiac performance. *Circulation* 97: 839-842., 1998.
12. Haber, H. L., C. L. Simek, J. D. Bergin, A. Sadun, L. W. Gimble, E. R. Powers, and M. D. Feldman. Bolus intravenous nitroglycerin predominantly reduces afterload in patients with excessive arterial elastance. *J Am Coll Cardiol* 22: 251-257., 1993.
13. Hara, Y., M. Hamada, and K. Hiwada. Left ventricular end-systolic wall stress is a potent prognostic variable in patients with dilated cardiomyopathy. *Jpn Circ J* 63: 196-200., 1999.
14. Hata, Y., J. Shimizu, S. Hosogi, H. Matsubara, J. Araki, T. Ohe, M. Takaki, T. Takasago, T. W. Taylor, and H. Suga. Ryanodine decreases internal Ca^{2+} recirculation fraction of the canine heart as studied by postextrasystolic transient alternans. *Jpn J Physiol* 47: 521-530, 1997.
15. Ishihara, H., M. Yokota, T. Sobue, and H. Saito. Relation between ventriculoarterial coupling and myocardial energetics in patients with idiopathic dilated cardiomyopathy. *J Am Coll Cardiol* 23: 406-416, 1994.
16. Korbmacher, B., U. Sunderdiek, G. Selcan, G. Arnold, and J. D. Schipke. Different responses of non-ischemic and post-ischemic myocardium towards Ca^{2+} sensitization. *J Mol Cell Cardiol* 29: 2053-2066, 1997.
17. Krams, R., D. J. Duncker, E. O. McFalls, A. Hogendoorn, and P. D. Verdouw. Dobutamine restores the reduced efficiency of energy transfer from total mechanical work to external mechanical work in stunned porcine myocardium. *Cardiovasc Res* 27: 740-747, 1993.
18. Kusuoka, H., Y. Koretsune, V. P. Chacko, M. L. Weisfeldt, and E. Marban. Excitation-contraction coupling in postischemic myocardium. Does failure of activator Ca^{2+} transients underlie stunning? *Circ Res* 66: 1268-1276, 1990.
19. Mori, M., M. Takeuchi, H. Takaoka, K. Hata, Y. Hayashi, H. Yamakawa, and M. Yokoyama. Oxygen-saving effect of a new cardiotonic agent, MCI-154, in diseased human hearts. *J Am Coll Cardiol* 29: 613-622, 1997.
20. Morita, S., R. L. Kormos, W. A. Mandarino, K. Eishi, A. Kawai, T. A. Gasior, L. G. Deneault, J. M. Armitage, R. L. Hardesty, and B. P. Griffith. Right ventricular/arterial coupling in the patient with left ventricular assistance. *Circulation* 86: II316-325., 1992.
21. Munch, G., B. Bolck, K. Brixius, H. Reuter, U. Mehlhorn, W. Bloch, and R. H. Schwinger. SERCA2a activity correlates with the force-frequency relationship in human myocardium. *Am J Physiol Heart Circ Physiol* 278: H1924-1932, 2000.
22. Myhre, E. S., A. Johansen, J. Bjornstad, and H. Piene. The effect of contractility and preload on matching between the canine left ventricle and afterload. *Circulation* 73: 161-171, 1986.
23. Nichols, W. W., and C. J. Pepine. Ventricular/vascular interaction in health and heart failure. *Compr Ther* 18: 12-19, 1992.
24. Ohgoshi, Y., Y. Goto, S. Futaki, H. Taku, O. Kawaguchi, and H. Suga. Increased oxygen cost of contractility in stunned myocardium of dog. *Circ Res* 69: 975-988, 1991.
25. Onishi, K., K. Sekioka, R. Ishisu, Y. Abe, H. Tanaka, M. Nakamura, Y. Ueda, and T. Nakano. MCI-154, a Ca^{2+} sensitizer, decreases the oxygen cost of contractility in isolated canine hearts. *Am J Physiol* 273: H1688-1695, 1997.

26. **Opie, L. H.** Energy for ion fluxes. In: *The Heart, physiology from cell to circulation* (3d ed.). Philadelphia: Lippincot-Raven Publishers, 1998, p. 110.
27. **Percy, R. F., A. B. Miller, and D. A. Conetta.** Usefulness of left ventricular wall stress at rest and after exercise for outcome prediction in asymptomatic aortic regurgitation. *Am Heart J* 125: 151-155., 1993.
28. **Slawsky, M. T., W. S. Colucci, S. S. Gottlieb, B. H. Greenberg, E. Haeusslein, J. Hare, S. Hutchins, C. V. Leier, T. H. LeJemtel, E. Loh, J. Nicklas, D. Ogilby, B. N. Singh, and W. Smith.** Acute hemodynamic and clinical effects of levosimendan in patients with severe heart failure. Study Investigators. *Circulation* 102: 2222-2227., 2000.
29. **Takahashi, A., P. Camacho, J. D. Lechleiter, and B. Herman.** Measurement of intracellular calcium. *Physiol Rev* 79: 1089-1125., 1999.
30. **Ter Keurs, H. E., W. D. Gao, H. Bosker, A. J. Drake-Holland, and M. I. Noble.** Characterisation of decay of frequency induced potentiation and post- extrasystolic potentiation. *Cardiovasc Res* 24: 903-910, 1990.
31. **Teramura, S., and T. Yamakado.** Calcium sensitizers in chronic heart failure: inotropic interventions-reservation to preservation. *Cardiologia* 43: 375-385, 1998.
32. **Toorop, G. P., G. J. Van den Horn, G. Elzinga, and N. Westerhof.** Matching between feline left ventricle and arterial load: optimal external power or efficiency. *Am J Physiol* 254: H279-285, 1988.
33. **Valdivia, C., J. O. Hegge, R. D. Lasley, H. H. Valdivia, and R. Mentzer.** Ryanodine receptor dysfunction in porcine stunned myocardium. *Am J Physiol* 273: H796-804, 1997.
34. **Wier, W. G., and D. T. Yue.** Intracellular calcium transients underlying the short-term force-interval relationship in ferret ventricular myocardium. *J Physiol (Lond)* 376: 507-530, 1986.
35. **Yokoyama, Y., D. Novitzky, M. T. Deal, and T. R. Snow.** Facilitated recovery of cardiac performance by triiodothyronine following a transient ischemic insult. *Cardiology* 81: 34-45, 1992.

Nederlandse samenvatting

Myocardstunning is gedefinieerd als de langdurige functieverstoring van het myocardweefsel, veroorzaakt door een of meer periodes van ischemie met een volledig herstel van de perfusie. De verstoorde functie vindt plaats zonder dat er sprake is van necrose en is volledig reversibel. Ondanks de verstoorde functie van het gestunnde myocardweefsel bezit het weefsel een contractiele reserve, d.w.z. het kan gestimuleerd worden door middel van inotrope farmaca of door postextrasystolische potentiatie. Hoewel er geen sprake is van necrose komen er wel myocardenzymen vrij, hetgeen de reversibele beschadiging van de hartspiercel aangeeft. In dit proefschrift zijn aspecten van het onderliggende mechanisme van stunning onderzocht door in vivo parameters voor calciumstromen te bestuderen (hoofdstuk 2 en 3), zijn veranderingen in energetica en efficiënties bestudeerd (hoofdstuk 4 en 5), is de farmacologische beïnvloeding van stunning onderzocht (hoofdstuk 6, 7 en 8) en is een nieuwe methode ontwikkeld voor de berekening van regionale linker ventrikel wandspanning (hoofdstuk 9).

Calciumstromen in gestunned myocardweefsel (hoofdstuk 2 en 3)

In deze hoofdstukken hebben we ons beziggehouden met veranderingen in calciumstromen als een mogelijke oorzaak van myocardstunning. In het verleden is gerapporteerd dat calciumstromen onveranderd waren in gestunnde harten, maar deze stromen werden gemeten bij hartfrequenties die ver onder de fysiologische hartfrequenties voor deze diersoorten lagen (10, 18). Vanwege het feit dat calciumstromen, en daardoor krachtopbouw in het myocardweefsel, toenemen met een toename in hartfrequentie, het zogenoemde "force-frequency effect" (FFE) (30, 34), kunnen mogelijke afnames in calciumstromen gemaskeerd zijn geweest door de lage hartfrequentie. In hoofdstuk 2 hebben we in vivo het effect van stunning op het FFE (gedefinieerd als de helling van eindsystolische elastantie, E_{es} , over hartfrequentie) bestudeerd, omdat dit nog niet eerder gedaan was met behulp van parameters die onafhankelijk van de belasting van het hart zijn. Omdat de interactie tussen de sarcoplasmatisch reticulum calcium-ATPase (SERCA2) en phospholamban een centrale rol speelt in het FFE (21), hebben we deze interactie ook nog beïnvloed met dobutamine, zowel voor als na de inductie van stunning. We hebben aangetoond dat myocardstunning in vivo het FFE opheft. Daarnaast hebben we laten zien dat, hoewel dobutamine het FFE weer doet toenemen in gestunned myocardweefsel, het effect significant kleiner was dan voor stunning. Een kwantitatieve analyse van de literatuur over veranderingen in sarcoplasmatisch reticulum (SR) calciumopname liet bovendien een negatieve relatie zien tussen verandering in calciumopname en hartfrequentie, opnieuw suggererend dat de

functie van het SR in gestunned myocardweefsel met name verstoord is bij hogere hartfrequenties. We hebben daarom geconcludeerd dat onze resultaten suggereren dat calciumstromen hartfrequentie-afhankelijk verstoord zijn in gestunned myocardweefsel.

In hoofdstuk 3 hebben we het FFE van gestunned myocardweefsel meer gedetailleerd onderzocht. Hoewel we in het vorige hoofdstuk stelden dat het verdwijnen van het FFE toegeschreven kan worden aan een verstoring van de calciumstromen, konden we niet helemaal uitsluiten dat een verminderde calciumgevoeligheid van de myofibrillen ook aan deze verdwijning bijdraagt. Daarom hebben we in dit hoofdstuk bestudeerd of de "calciumsensitizer" EMD 57033 het FFE kan herstellen. Om verder onderscheid te kunnen maken tussen verstoringen van de sarcolemmale (SL) calciumstromen en processen binnenin de cel, zoals calcium-geïnduceerde calciumafgifte (CICR) of SR Ca^{2+} -ATPase (SERCA2) functie, hebben we de recirculatie fractie (RF) onderzocht, een maat voor de relatieve bijdrage van de interne calciumstromen aan de totale calciumstromen (14, 30, 34). Om een mogelijke hartfrequentie-afhankelijke remming van SERCA2 functie te bestuderen, hebben we bovendien SR calciumopname en Ser¹⁶ en Thr¹⁷ phosphorylering van phospholamban gemeten in weefsel uit naaldbiopten die zowel uit het gestunnde als uit het normale gebied werden afgenomen bij twee verschillende hartfrequenties. Tenslotte hebben we ryanodine geïnfundeerd om het SR calciumafgiftekanaal (ryanodine receptor, RyR) selectief te openen, omdat in het verleden gesuggereerd is dat de openingswaarschijnlijkheid van dit kanaal mogelijk verlaagd is in stunning (33). Zoals te verwachten was vonden we dat stunning het FFE ophief. Hoewel EMD 57033 E_{cs} verhoogde, bleef de helling ten opzichte van de hartfrequentie (het FFE) onveranderd, zowel in normaal als in gestunned myocardweefsel, hetgeen suggereert dat de opheffing van het FFE veroorzaakt wordt door een verstoring van de calciumstromen en niet door een afname van de myofibrillaire calciumgevoeligheid. Ook de RF was hartfrequentieafhankelijk afgenomen, met de grootste afname bij de hoogste hartfrequentie, wijzend op een hartfrequentieafhankelijke verstoring van CICR en/of SERCA2 functie. Noch hartfrequentie, noch stunning had echter een effect op SR calciumopname of op Ser¹⁶ of Thr¹⁷ phosphorylering van phospholamban in vitro. In het normale myocardweefsel simuleerde ryanodine het effect van stunning op de RF, maar had geen effect op het FFE. Daarom concludeerden we dat in stunning een tweede verstoring van CICR, naast een waarschijnlijk toegenomen openingswaarschijnlijkheid van de RyR, ten grondslag ligt aan het verdwijnen van het FFE.

Maximalisatie van external work en efficiency of energy transfer (hoofdstuk 4)

In het verleden is in verschillende studies in normale harten de relatie tussen power, externe arbeid (external work, EW) en rendement van externe arbeid t.o.v. totale arbeid (efficiency of energy transfer, EET) versus nabelasting onderzocht; daarbij werd een

maximalisatie van power en EW gevonden (22, 32), maar niet van EET (6). Bovendien is aangetoond dat verstoring van de globale linker ventrikelfunctie de ventrikel doet afwijken van de optimale situatie (15, 23), terwijl myocardstunning zowel regionale EW als EET vermindert (17, 35), en deze parameters meer gevoelig maakt voor een toename in nabelasting (9). In dit hoofdstuk hebben we daarom de relaties tussen regionale EW en EET versus regionale nabelasting (eind-systolische stress, σ_{es}) onderzocht. We hebben laten zien dat in normaal myocardweefsel zowel EW als EET een maximum laten zien in relatie tot nabelasting, hetgeen gedeeltelijk in overeenstemming is met bevindingen in de globale linker ventrikel. Bovendien hebben we laten zien dat het myocardweefsel was ingesteld op maximale EET en niet op maximale EW. Dit betekent dat EW gerekruteerd kon worden door regionale nabelasting te verhogen. In gestunned myocardweefsel was deze rekrutering verdwenen, terwijl het myocardweefsel nog steeds op maximale EET opereerde. Tenslotte lieten we een positieve relatie tussen zowel maximale EW als EET en contractiliteit (E_{cs}) zien, hetgeen suggereert dat de door stunning geïnduceerde veranderingen veroorzaakt werden door de afname in contractiliteit van gestunned myocardweefsel.

“Oxygen wastage” van gestunned myocardweefsel (hoofdstuk 5)

Hoewel de contractiele functie van gestunned myocardweefsel verminderd is, is de zuurstofconsumptie onveranderd; dit wordt “oxygen wastage” genoemd. Hoewel deze oxygen wastage wordt toegeschreven aan een verminderde efficiëntie van excitatie-contractie koppeling (toegenomen “oxygen cost of contractility”) (24), is het O_2 -gebruik voor excitatie-contractie koppeling slechts 20-30% van het totale O_2 -gebruik (26). Het lijkt daarom aannemelijk dat in stunning ook de efficiëntie van de myofibrillen is afgenomen. In dit hoofdstuk hebben we zowel de myofibrillaire efficiëntie alsmede de oxygen cost of contractility bestudeerd in normaal en gestunned myocardweefsel. Bovendien hebben we deze efficiënties ook bestudeerd in gestunned myocardweefsel na toediening van de calciümsensitizer EMD 60263, omdat het bekend is dat calciümsensitizers de oxygen cost of contractility doen afnemen (19, 25) en misschien zelfs een toename in myofibrillaire efficiëntie kunnen veroorzaken (31). We hebben laten zien dat de door stunning veroorzaakte oxygen wastage voornamelijk veroorzaakt werd door een verminderde myofibrillaire efficiëntie en in mindere mate door een verhoogde oxygen cost of contractility. Bovendien werden beide veranderingen door EMD 60263 opgeheven, suggererend dat deze stof de myofibrillaire calciümevoeligheid doet toenemen zonder de vorming van myofibrillaire “cross-bridges” te verhogen.

Farmacologische beïnvloeding van myocardstunning (hoofdstuk 6, 7 en 8)

Als een groot deel van de linker ventrikel door stunning is aangedaan, zal de functie van het hart dermate aangetast worden dat inotrope therapie nodig is. Zoals we in het

vorige hoofdstuk besproken hebben zijn calciumsensitizers mogelijk energetisch voordeliger dan β -adrenerge stoffen, aangezien ze de calciumstromen niet verhogen. Omdat zij mogelijk als bijwerking hebben dat ze diastolische functie negatief beïnvloeden (8, 16), hebben we in hoofdstuk 6 onderzocht of EMD 57033 negatief lusitrope effecten vertoont in vivo. Bovendien hebben we bestudeerd of deze stof verschillende effecten heeft op normaal en gestunned myocardweefsel. We hebben laten zien dat de calciumsensitizer EMD 57033 systolische functie (E_{es}) herstelde in gestunned myocardweefsel in vivo, terwijl zowel vroegdiastolische functie (bepaald als maximale elastantieafname en de tijdconstante van deze afname) als laatdiastolische functie (einddiastolische elastantie) niet aangetast werden. Deze effecten waren vergelijkbaar in normaal en gestunned myocardweefsel. Zowel de phosphodiësterase III remmende eigenschappen van EMD 57033 als adrenerge receptor stimulatie hadden bovendien een minimale bijdrage, aangezien α - en β -blokkade nauwelijks effect hadden. We concludeerden daarom dat calciumsensitizers veelbelovende kandidaten zijn voor uitbreiding van het huidige arsenaal aan inotrope farmaca en dat calciumsensitatie niet noodzakelijkerwijs diastolische functie verslechtert.

Aangezien er in vitro bevindingen zijn dat de calciumgevoeligheid van de myofibrillen afgenomen is in gestunned myocardweefsel (5, 10), en dat calciumsensitizers deze calciumgevoeligheid weer kunnen laten toenemen (3, 8), hebben we in hoofdstuk 7 de in vivo respons van normaal en gestunned myocardweefsel op intracoronaire calciuminfusies onderzocht, zowel zonder als met infusie van de calciumsensitizer EMD 57033. Om de phosphodiësterase III remmende eigenschappen van EMD 57033 te minimaliseren werd β -blokkade toegepast met behulp van propranolol. In normaal myocardweefsel liet intracoronair calcium de contractiliteit (E_{es}) toenemen, terwijl in gestunned myocardweefsel deze respons verdwenen was. Propranolol had hier verder geen effect op, maar EMD 57033 herstelde deze respons in gestunned myocardweefsel en verhoogde de respons in normaal myocardweefsel. Daarom hebben we geconcludeerd dat deze resultaten consistent zijn met de in vitro bevindingen dat EMD 57033 de myofibrillaire calciumgevoeligheid verhoogt, onafhankelijk van zijn minimale phosphodiësterase III remmende eigenschappen.

In hoofdstuk 4 en in eerdere artikelen hebben we laten zien dat stunning een afname in EW, EET en mechanische efficiëntie (ME) veroorzaakt (17). Onduidelijk is echter of deze veranderingen secundair zijn aan de verlaagde contractiliteit of primair door een specifiek onderliggend mechanisme van stunning veroorzaakt worden. Omdat het bovendien zo is dat calciumsensitizers energetische voordelen kunnen hebben in vergelijking tot normale inotrope therapie (hoofdstuk 5), hebben we in hoofdstuk 8 de effecten van de calciumsensitizer EMD 57033 op EW, EET en ME vergeleken met die van dobutamine. Om te normaliseren voor de dosisafhankelijke effecten van deze stoffen, hebben we de effecten op deze energetische parameters bestudeerd in relatie tot het effect

op contractiliteit (E_{cs}). Beide stoffen herstelden EW en EET op vergelijkbare wijze, hetgeen suggereert dat de door stunning geïnduceerde veranderingen in deze parameters het gevolg zijn van de verlaging in contractiliteit en niet van een specifiek onderliggend mechanisme van stunning, aangezien ze niet specifiek beïnvloed werden door calciumsensitisatie dan wel door het verhogen van de calciumstromen. In tegenstelling tot deze resultaten werd ME echter alleen hersteld door calciumsensitisatie, suggererend dat een energetische verstoring plaatsvindt in de myofibrillen.

Bepaling van linker ventrikel geometrie ter berekening van regionale wandspanning (hoofdstuk 9)

In het laatste hoofdstuk introduceerden we een nieuwe methode ter berekening van regionale wandspanning in het myocardweefsel uit 3D ultrageluidbeelden. Deze methode hebben we ontwikkeld vanwege de beperkingen van onze huidige methode om regionale wandspanning te berekenen: het zeer invasieve karakter van de ultrageluidkristallen en de aanname van een regionale bolvormige geometrie. We hebben algoritmes geconstrueerd voor de reconstructie van 3D ventriculaire endocardiale en epicardiale oppervlaktes vanuit 2D beelden, zoals die verkregen worden van een ronddraaiende echoprobe. Deze oppervlaktes werden in 10 secties verdeeld en van elke sectie werd de wanddikte berekend. Verder werd een midvlak geconstrueerd tussen de beide oppervlaktes waarvan per sectie de principale radii berekend werden. De radii en wanddikte werden zowel berekend voor een linker ventrikelfantoom als voor een 3D reconstructie van virtuele 2D beelden afgeleid van dit fantoom. Vergelijking van deze radii en wanddiktes toonde een goede overeenkomst tussen de twee methodes, hetgeen aangeeft dat deze methode accuraat genoeg is voor de berekening van regionale wandspanning.

Suggesties voor verder onderzoek

De precieze lokalisatie van de verstoring van excitatie-contractie koppeling in stunning is nog steeds niet volledig opgehelderd, met name in vivo. Het meten van calciumstromen in gestunned myocardweefsel in vivo zou kunnen helpen om onderscheid te maken tussen verstoringen van de myofibrillen en van de calciumstromen. Fluorescente markers zijn de meest gebruikte calciumindicatoren, omdat hun signaal behoorlijk groot is bij een bepaalde verandering in intracellulair calcium (29). Het probleem met het meten van calciumstromen in vivo met deze markers is echter de bepaling van de padlengte van het signaal en het 3D meetvolume, aangezien het onduidelijk is tot welke diepte de reflectie van uitgezonden licht nog kan worden waargenomen. Het gebruik van ratiometrische markers (de calciumconcentratie hangt af van de ratio van twee golflengtes voor excitatie of emissie) voorkomt dit probleem echter omdat zowel de teller als de noemer van de ratio op dezelfde wijze hierdoor beïnvloed worden (29). Los hiervan moeten de praktische problemen van excitatie en meting van het met een marker geladen

myocardweefsel van een bewegend hart, en het mogelijke verschil tussen epicardiaal myocardweefsel (dat meestal bemonsterd zal worden) en endocardiaal myocardweefsel nog opgelost worden. Door gebruik te maken van markers met een hoge en markers met een lage affiniteit voor calcium kunnen zowel cytosolair als SR calcium gemeten worden. Daardoor kunnen veranderingen in calciumstromen, SR calciuminhoud en myofibrillaire calciumgevoeligheid gedetecteerd worden in gestunned myocardweefsel in vivo. Ook kunnen mogelijk de effecten van calciumsensitizers op calciumstromen en calciumgevoeligheid in vivo bestudeerd worden.

Wanneer in de toekomst de precieze lokalisatie van de verstoring van excitatie-contractie koppeling wordt vastgesteld, kunnen stoffen ontwikkeld worden om deze verstoring op te heffen. Als onze suggestie van een toegenomen openingswaarschijnlijkheid van de RyR correct blijkt te zijn, zouden farmaca die dit kanaal gedeeltelijk sluiten een gunstig effect kunnen hebben. Als sarcolemmale calciumstromen aangetast blijken te zijn, kunnen stoffen ontwikkeld worden die de calciumgeïnduceerde calciumafgifte stimuleren. Het is belangrijk om te beseffen dat stimulatie van SR calciumstromen te prefereren is boven stimulatie van sarcolemmale calciumstromen, omdat sarcolemmale calciumstromen de dubbele hoeveelheid ATP per mol calcium gebruiken (2).

Aangezien steeds meer aanwijzingen beschikbaar komen dat calciumsensitizers energetische voordelen hebben in vergelijking tot β -adrenerge stimulantia en ze misschien ook minder aanleiding geven tot ritmestoomissen doordat ze het systolisch calcium niet verhogen, zou klinisch onderzoek gericht moeten worden op de therapeutische voordelen en veiligheid van calciumsensitizers. Hoewel al enig onderzoek is verricht in patiënten met ernstig hartfalen (28), zou juist ook de toepasbaarheid buiten de klinische setting onderzocht moeten worden, omdat de therapeutische mogelijkheden voor (orale) inotrope therapie buiten het ziekenhuis momenteel zeer beperkt zijn.

Als myocardstunning na inspanning inderdaad herhaaldelijk voorkomt bij patiënten met stabiele angina pectoris (1), zou meer onderzoek gericht moeten worden op de vraag of en wanneer herhaalde episodes van stunning kunnen leiden tot "hibernation" van het myocardweefsel of zelfs tot irreversibele schade. Indien irreversibele schade inderdaad optreedt in patiënten die, gebaseerd op hun klachtenpatroon, normaal gesproken niet in aanmerking zouden komen voor revascularisatietherapie, zou vroege revascularisatie een irreversibele afname in linker ventrikelfunctie mogelijk gedeeltelijk kunnen voorkomen.

De methode die we beschreven hebben om regionale linker ventrikel wandspanning te bepalen met behulp van 3D echocardiografie moet eerst gevalideerd worden in vivo. Als dan blijkt dat deze methode nauwkeurig genoeg is, kan de bepaling van regionale eind-systolische wandspanning gebruikt worden bij het vaststellen van de prognose van verschillende hartziekten, onder andere gedilateerde cardiomyopathie (13) en aorta insufficiëntie (27). Omdat wandspanning zeer afhankelijk is van de belasting van het hart,

zal de volgende stap zijn om de stressmetingen te combineren met de bepaling van regionale vervorming ("strain"). Naast bepaling van strain met behulp van "magnetic resonance imaging" (MRI), kan regionale strain ook afgeleid worden van ultrageluid, gebruik makend van de "cross-correlation" (elastografie) methode of van de "velocity gradient" (tissue Doppler) methode (7). De combinatie van het meten van wandspanning en strain bij verschillende belastingen van het hart maken het mogelijk om niet-invasief eind-systolische elastantie (E_{es}) te berekenen, een belastingonafhankelijke parameter van contractiliteit. Hoewel sommige klinische studies deze parameter toegepast hebben (4, 11, 12, 20), moet de klinische relevantie van E_{es} in de diagnose, prognose en de evaluatie van therapie nog grotendeels ontrafeld worden.

Referenties

1. **Ambrosio, G., S. Betocchi, L. Pace, M. A. Losi, P. Perrone-Filardi, A. Soricelli, F. Piscione, J. Taube, F. Squame, M. Salvatore, J. L. Weiss, and M. Chiariello.** Prolonged impairment of regional contractile function after resolution of exercise-induced angina. Evidence of myocardial stunning in patients with coronary artery disease. *Circulation* 94: 2455-2464., 1996.
2. **Barry, W. H., and J. H. Bridge.** Intracellular calcium homeostasis in cardiac myocytes. *Circulation* 87: 1806-1815., 1993.
3. **Bezstarosti, K., L. K. Soei, R. Krams, F. J. Ten Cate, P. D. Verdouw, and J. M. Lamers.** The effect of a thiazidiazinone derived Ca^{2+} sensitizer on the responsiveness of Mg^{2+} -ATPase to Ca^{2+} in myofibrils isolated from stunned and nonstunned porcine and human myocardium. *Biochem Pharmacol* 51: 1211-1220, 1996.
4. **Brown, K. A., and R. V. Ditchey.** Human right ventricular end-systolic pressure-volume relation defined by maximal elastance. *Circulation* 78: 81-91., 1988.
5. **Carrozza, J. P., Jr., L. A. Bentivegna, C. P. Williams, R. E. Kuntz, W. Grossman, and J. P. Morgan.** Decreased myofilament responsiveness in myocardial stunning follows transient calcium overload during ischemia and reperfusion. *Circ Res* 71: 1334-1340, 1992.
6. **De Tombe, P. P., S. Jones, D. Burkhoff, W. C. Hunter, and D. A. Kass.** Ventricular stroke work and efficiency both remain nearly optimal despite altered vascular loading. *Am J Physiol* 264: H1817-1824, 1993.
7. **D'hooge, J., A. Heimdal, F. Jamal, T. Kukulski, B. Bijnens, F. Rademakers, L. Hatle, P. Suetens, and G. R. Sutherland.** Regional Strain and Strain Rate Measurements by Cardiac Ultrasound: Principles, Implementation and Limitations. *Eur J Echocardiography* 1: 154-170, 2000.
8. **Endoh, M.** Changes in intracellular Ca^{2+} mobilization and Ca^{2+} sensitization as mechanisms of action of physiological interventions and inotropic agents in intact myocardial cells. *Jpn Heart J* 39: 1-44, 1998.
9. **Fan, D., L. K. Soei, L. M. Sassen, R. Krams, and P. D. Verdouw.** Mechanical efficiency of stunned myocardium is modulated by increased afterload dependency. *Cardiovasc Res* 29: 428-437, 1995.
10. **Gao, W. D., D. Atar, P. H. Backx, and E. Marban.** Relationship between intracellular calcium and contractile force in stunned myocardium. Direct evidence for decreased myofilament Ca^{2+} responsiveness and altered diastolic function in intact ventricular muscle. *Circ Res* 76: 1036-1048, 1995.
11. **Gorcsan, J., A. M. Feldman, R. L. Kormos, W. A. Mandarino, A. J. Demetris, and R. J. Batista.** Heterogeneous immediate effects of partial left ventriculectomy on cardiac performance. *Circulation* 97: 839-842., 1998.
12. **Haber, H. L., C. L. Simek, J. D. Bergin, A. Sadun, L. W. Gimple, E. R. Powers, and M. D. Feldman.** Bolus intravenous nitroglycerin predominantly reduces afterload in patients with excessive arterial elastance. *J Am Coll Cardiol* 22: 251-257., 1993.
13. **Hara, Y., M. Hamada, and K. Hiwada.** Left ventricular end-systolic wall stress is a potent prognostic variable in patients with dilated cardiomyopathy. *Jpn Circ J* 63: 196-200., 1999.

14. Hata, Y., J. Shimizu, S. Hosogi, H. Matsubara, J. Araki, T. Ohe, M. Takaki, T. Takasago, T. W. Taylor, and H. Suga. Ryanodine decreases internal Ca^{2+} recirculation fraction of the canine heart as studied by postextrasystolic transient alternans. *Jpn J Physiol* 47: 521-530, 1997.
15. Ishihara, H., M. Yokota, T. Sobue, and H. Saito. Relation between ventriculoarterial coupling and myocardial energetics in patients with idiopathic dilated cardiomyopathy. *J Am Coll Cardiol* 23: 406-416, 1994.
16. Korbmacher, B., U. Sunderdiek, G. Selcan, G. Arnold, and J. D. Schipke. Different responses of non-ischemic and post-ischemic myocardium towards Ca^{2+} sensitization. *J Mol Cell Cardiol* 29: 2053-2066, 1997.
17. Krams, R., D. J. Duncker, E. O. McFalls, A. Hogendoorn, and P. D. Verdouw. Dobutamine restores the reduced efficiency of energy transfer from total mechanical work to external mechanical work in stunned porcine myocardium. *Cardiovasc Res* 27: 740-747, 1993.
18. Kusuoka, H., Y. Koretsune, V. P. Chacko, M. L. Weisfeldt, and E. Marban. Excitation-contraction coupling in posts ischemic myocardium. Does failure of activator Ca^{2+} transients underlie stunning? *Circ Res* 66: 1268-1276, 1990.
19. Mori, M., M. Takeuchi, H. Takaoka, K. Hata, Y. Hayashi, H. Yamakawa, and M. Yokoyama. Oxygen-saving effect of a new cardiogenic agent, MCI-154, in diseased human hearts. *J Am Coll Cardiol* 29: 613-622, 1997.
20. Morita, S., R. L. Kormos, W. A. Mandarino, K. Eishi, A. Kawai, T. A. Gasior, L. G. Deneault, J. M. Armitage, R. L. Hardesty, and B. P. Griffith. Right ventricular/arterial coupling in the patient with left ventricular assistance. *Circulation* 86: II316-325., 1992.
21. Munch, G., B. Bolck, K. Brixius, H. Reuter, U. Mehlhorn, W. Bloch, and R. H. Schwinger. SERCA2a activity correlates with the force-frequency relationship in human myocardium. *Am J Physiol Heart Circ Physiol* 278: H1924-1932, 2000.
22. Myhre, E. S., A. Johansen, J. Bjornstad, and H. Piene. The effect of contractility and preload on matching between the canine left ventricle and afterload. *Circulation* 73: 161-171, 1986.
23. Nichols, W. W., and C. J. Pepine. Ventricular/vascular interaction in health and heart failure. *Compr Ther* 18: 12-19, 1992.
24. Ohgoshi, Y., Y. Goto, S. Futaki, H. Taku, O. Kawaguchi, and H. Suga. Increased oxygen cost of contractility in stunned myocardium of dog. *Circ Res* 69: 975-988, 1991.
25. Onishi, K., K. Sekioka, R. Ishisu, Y. Abe, H. Tanaka, M. Nakamura, Y. Ueda, and T. Nakano. MCI-154, a Ca^{2+} sensitizer, decreases the oxygen cost of contractility in isolated canine hearts. *Am J Physiol* 273: H1688-1695, 1997.
26. Opie, L. H. Energy for ion fluxes. In: *The Heart, physiology from cell to circulation* (3d ed.). Philadelphia: Lippincot-Raven Publishers, 1998, p. 110.
27. Percy, R. F., A. B. Miller, and D. A. Conetta. Usefulness of left ventricular wall stress at rest and after exercise for outcome prediction in asymptomatic aortic regurgitation. *Am Heart J* 125: 151-155., 1993.
28. Slawsky, M. T., W. S. Colucci, S. S. Gottlieb, B. H. Greenberg, E. Haeusslein, J. Hare, S. Hutchins, C. V. Leier, T. H. LeJemtel, E. Loh, J. Nicklas, D. Ogilby, B. N. Singh, and W. Smith. Acute hemodynamic and clinical effects of levosimendan in patients with severe heart failure. Study Investigators. *Circulation* 102: 2222-2227., 2000.
29. Takahashi, A., P. Camacho, J. D. Lechleiter, and B. Herman. Measurement of intracellular calcium. *Physiol Rev* 79: 1089-1125., 1999.
30. Ter Keurs, H. E., W. D. Gao, H. Bosker, A. J. Drake-Holland, and M. I. Noble. Characterisation of decay of frequency induced potentiation and post- extrasystolic potentiation. *Cardiovasc Res* 24: 903-910, 1990.
31. Teramura, S., and T. Yamakado. Calcium sensitizers in chronic heart failure: inotropic interventions-reservation to preservation. *Cardiologia* 43: 375-385, 1998.
32. Toorop, G. P., G. J. Van den Horn, G. Elzinga, and N. Westerhof. Matching between feline left ventricle and arterial load: optimal external power or efficiency. *Am J Physiol* 254: H279-285, 1988.
33. Valdivia, C., J. O. Hegge, R. D. Lasley, H. H. Valdivia, and R. Mentzer. Ryanodine receptor dysfunction in porcine stunned myocardium. *Am J Physiol* 273: H796-804, 1997.
34. Wier, W. G., and D. T. Yue. Intracellular calcium transients underlying the short-term force-interval relationship in ferret ventricular myocardium. *J Physiol (Lond)* 376: 507-530, 1986.
35. Yokoyama, Y., D. Novitzky, M. T. Deal, and T. R. Snow. Facilitated recovery of cardiac performance by triiodothyronine following a transient ischemic insult. *Cardiology* 81: 34-45, 1992.

Dankwoord

Het is natuurlijk een dooddouner, maar dit proefschrift zou er niet zijn geweest zonder de hulp van velen. Ik zal ook vast wel iemand vergeten te bedanken, dat gebeurt nu eenmaal, mijn excuses daarvoor.

Van de mensen van de afdeling, Rob Krams, jou dan maar als eerste. Systematisch heb je mij gestimuleerd om kritisch naar de data te kijken en altijd de vraagstelling bovenaan te plaatsen. Rob, van jou heb ik geleerd wat wetenschappelijk onderzoek is, bedankt daarvoor.

Mijn promotor, prof. Piet Verdouw: bedankt voor de mogelijkheid om hier mijn promotieonderzoek te doen. Vele discussies hebben we gevoerd over voetbal en sport in het algemeen. Er komt een dag dat bewezen wordt dat duursport slecht voor een mens is, wacht maar!

Prof. Baan, prof. Lamers, dr. Van Mastrigt, dr. Slager, prof. Van der Wall en prof. Westerhof: bedankt voor uw bereidheid om het geheel door te lezen en in de promotiecommissie plaats te nemen.

De studenten die zo gek waren om tot 's avonds laat op het lab te experimenteren: Joost, Tessa, Wim en Carlo. Joost: zelfs voor Jan van Meegen werden de slechte grappen soms te erg, maar Ad Patat vraagt me nog regelmatig waar je bent gebleven. Tessa: Na die eerste discussie over studentenverenigingen zijn we niet meer opgehouden met discussiëren, wanneer gaan we nu eens samen de PvdA onveilig maken?. Wim: Welke reclame kwam er nu ook al weer het vaakst op Stadsradio Rotterdam? Carlo: Hmm, het eten past toch niet helemaal bij de wijn... Zonder jullie hulp had ik nooit al die late experimenten kunnen doen. Bedankt, ook voor de gezelligheid.

Degenen die zo gek waren om beroepsmatig, al dan niet vrijwillig, overdag en ook tot 's avonds laat op het lab te experimenteren: Jan, René, Elza, Sandra en Rob van Bremen. Jan: heel veel avonden hebben we daar doorgebracht, gaan we die voortzetten in het St. Franciscus? René: half elf klaar? Elza: heb je al een dartpijlje naar de wereldkaart gegooid voor de de volgende reisbestemming? Sandra: na het "Grote Sandra de Zeeuw lied" op jouw promotie moet ik nu zeker op het ergste voorbereid zijn? Rob: jij zal de reputatie van lekker eten alleen voort moeten zetten, vrees ik. Jullie allen bedankt.

Mijn trouwste lunchpartner: Carla, bedankt voor al het typewerk en de vele lunches waar al het wel en wee besproken werd. Veel succes verder op de afdeling!

De rest van de Experimentele Cardiologie: Heleen: hoe staat het met de vijfde positie? Ik hoop dat als je dit leest je inmiddels in het DSO speelt. Alisina, Amran, Babak, Birgit, Dalia, Daphne, David Haitzma, David Liem, Dirk, Dirk-Jan, Eric, Harald, Ilona, Jan-Willem, Jelger, Johan, Karim, Liz, Luc, Maarten, Miranda, Monique, Nadine, Reijer, Sacha, Sebastiaan, Shahla, Wim en Willem zijn ze dat allemaal? Bedankt!

De mensen van de Hemodynamiek: Kees, Jan, Jolanda en Hans. Kees, bedankt voor de vele nuttige discussies. Jan: jouw “stress” komt nog wel bij je regie-examen! Jolanda, bedankt voor de hulp bij mijn wiskundige problemen. Hans: Gaan we de curvatuursensor nog een keer uit de kast halen?

Mijn kamergenoten: Hans en Caroline. Hans: Ik hoop dat ik nu meer tijd krijg voor al die boeken die je mij leent en we gaan zeker binnenkort weer samen muziek maken. Caroline: jij neemt nu de fakkel over als AIO van Rob, succes en tot ziens op jouw promotie.

Van de afdelingen Biochemie en Farmacologie: Jos Lamers en Karel Bezstarosti: bedankt voor de analyses en discussies. Ik heb er veel van geleerd. Nu nog de proteomics op gestunned weefsel, wie weet. René de Vries, Jan Heiligers en Regien Schoemaker: bedankt voor de varkenshart en het paceapparaat, dat ze nuttig waren heb je ergens anders in dit proefschrift al kunnen lezen.

De mensen van de Experimentele Echo: Prof. Bom, Ayache, Charles, Chris, Corrie, Fermín, Frans, Frits, Jan, Marvin, Nico, Peggy, Peter, Stephane en Ton: bedankt voor het lenen van de echoapparatuur en benodigdheden en voor de computertips. Van *Latex* heb ik toch maar afgezien, de blauwe schermen zijn me te dierbaar.

Mijn ouders, broer en zussen: bedankt dat jullie altijd achter mij gestaan hebben, zowel moreel als financieel. Jullie hebben tenslotte de basis gelegd waarop ik deze promotie heb kunnen bouwen. Raoul, bedankt voor de nuttige adviezen (“Je moet gewoon nauwkeuriger meten, hoeveel meetpunten heb je eigenlijk rond dat maximum”).

En last but not least Renske: Ondanks dat ik het niet echt moeilijk had in vergelijking met jouw eigen situatie, heb je me toch voortdurend gesteund. Nog even en dan kunnen we weer volop leuke dingen gaan doen, ik verheug me er nu al op. Saya cintamu pacarku!

Curriculum Vitae

Serge Trines werd op 4 mei 1972 in Eindhoven geboren. In 1990 behaalde hij het VWO diploma op het St. Joriscollege in Eindhoven, waarna hij Geneeskunde ging studeren aan de Erasmus Universiteit Rotterdam. In 1994 werkte hij 10 maanden aan zijn afstudeerproject: "Fysiologische en biochemische benadering voor de contractiele dysfunctie van het gestunne hartweefsel: Zijn er mogelijkheden tot causale inotrope interventie?". Dit project werd uitgevoerd op de afdeling Experimentele Cardiologie van het Thoraxcentrum te Rotterdam, waarbij hij begeleid werd door Dr. R. Krams en Prof. Dr. P.D. Verdouw. Bovendien doorliep hij in dat jaar een Erasmus Elective stage op de Cardiologie afdeling van het Qasr-el-Aini ziekenhuis in Caïro, Egypte. Na zijn artsexamen in januari 1997 keerde hij terug naar de afdeling Experimentele Cardiologie als assistent in opleiding. Het onderzoek dat hij daar de afgelopen 4½ jaar verricht heeft leidde uiteindelijk tot dit proefschrift. Op 1 mei 2001 is hij begonnen aan de vooropleiding Interne Geneeskunde in het St. Franciscus Gasthuis te Rotterdam (opleider: Dr. H.S.L.M. Tjen) in het kader van de specialistenopleiding Cardiologie van het Leids Universitair Medisch Centrum (opleider: Prof. dr. E.E. van der Wall).

Publications

1. Dongsheng Fan, Loes MA Sassen, **Serge AIP Trines**, Loe Kie Soei, Rob Krams, and Pieter D Verdouw. Increasing the Ca^{2+} -sensitivity reverses the increased afterload dependency of external work and the efficiency of energy conversion of stunned myocardium. *Appl Card Path* 5: 63-72, 1994.
2. JA Oomen, **SAIP Trines**, WB Vermeulen, R Krams, JCH Schuurbijs, WB Vletter, JRTC Roelandt, and CJ Slager. Towards assessment of regional wall stress of the left ventricle using 3D ultrasound imaging. *Computers in Cardiology* 26: 129-132, 1999.
3. Sandra de Zeeuw, **Serge AIP Trines**, Rob Krams, Pieter D Verdouw, and Dirk J Ducker. Cardiovascular profile of the calcium sensitizer EMD 57033 in open-chest anaesthetized pigs with regionally stunned myocardium. *Br J Pharmacol* 129: 1413-1422, 2000.
4. Sandra de Zeeuw, **Serge AIP Trines**, Rob Krams, Dirk J Duncker, Pieter D Verdouw. In vivo evidence that EMD 57033 restores myocardial responsiveness to intracoronary Ca^{2+} in stunned myocardium. *Eur J Pharmacol* 403: 99-109, 2000.
5. **Serge AIP Trines**, Cornelis J Slager, Joost van der Moer, Pieter D Verdouw, and Rob Krams. Efficiency of energy transfer, but not external work, is maximized in stunned myocardium. *Am J Physiol* 279: H1264-H1273, 2000.
6. **Serge AIP Trines**, Cornelis J Slager, Tessa AM Onderwater, Jos MJ Lamers, Pieter D Verdouw and Rob Krams. Oxygen wastage of stunned myocardium in vivo is due to an increased oxygen cost of contractility and a decreased myofibrillar efficiency. *Cardiovasc Res*, *In press*.
7. **SAIP Trines**, CAG Smits, J van der Moer, CJ Slager, PD Verdouw, and R Krams. Calcium Sensitisation, but not Adrenoceptor Stimulation, increases Mechanical Efficiency in Stunned Myocardium. *Submitted*.
8. **SAIP Trines**, CAG Smits, TAM Onderwater, JmJ Lamers, PD Verdouw, CJ Slager, and R Krams. Myocardial Stunning is Associated With A Disturbed Regulation of the Force-Frequency Response. *Submitted*.

9. **SAIP Trines**, K Bezstarosti, CAG Smits, JMJ Lamers, CJ Slager, PD Verdouw, and R Krams. Absence of the Force-Frequency Effect in Stunned Myocardium: Evidence for a Disturbed Ca^{2+} -handling. *Submitted*.
10. JA Oomen, **SAIP Trines**, CAG Smits, WB Vermeulen, R Krams, and CJ Slager. Geometry assessment of the Left Ventricle from 3D Ultrasound Images to estimate Regional Wall Stress. *Submitted*.

Abstracts

1. Krams R, **SAIP Trines**, LK Soei, CJ Slager, JMJ Lamers and PD Verdouw. Reduced myocardial efficiency in stunned myocardium can be explained by a different partitioning of myocardial oxygen demand. *Eur Heart J* 16: 685, p 108, 1995.
2. Sandra de Zeeuw, Loekie Soei, Jan R van Meegen, **Serge AIP Trines**, Rob Krams, Dirk J Duncker, Pieter D Verdouw. Recovery of systolic function of stunned myocardium by the Ca^{2+} -sensitizer EMD 57033 is not accompanied by impairment of diastolic function. *Circulation* 96: 1109, p 200, 1997.
3. **Trines SAIP**, Van der Moer J, Krams R, Slager CJ, Van Meegen JR, Verdouw PD. Afterload for maximum regional myocardial work is reduced by stunning. *J Cardiovasc Diagn Proc* 15: PI 28, p 146, 1998.
4. **Serge AIP Trines**, Joost van der Moer, Rob Krams, Cees J Slager, Jan R van Meegen, Pieter D Verdouw. Loss of recruitment of myocardial work after stunning can be brought back by different inotropic interventions. *Cardiovasc Drug Ther* 13: 19, p 7, 1999.
5. Sandra de Zeeuw, Loekie Soei, Jan R van Meegen, **Serge AIP Trines**, Rob Krams, Dirk J Duncker, Pieter D Verdouw. EMD 57033 increases calcium responsiveness of normal and stunned myocardium in vivo. *Cardiovasc Drug Ther* 13: 23, p 8, 1999.
6. **Serge AIP Trines**, Joost van der Moer, Rob Krams, Cornelis J Slager, Jan R van Meegen, Pieter D Verdouw. External work recruitment can be restored in stunned myocardium without increasing oxygen consumption using EMD 57033, a calcium sensitizer. *Circulation* 100: 39, p I-8, 1999.

